5-7-2020

The Genetics of Floral Carotenoid Pigmentation in Monkeyflowers (Mimulus)

Lauren E. Stanley
University of Connecticut - Storrs, lauren.stanley@uconn.edu

The Genetics of Carotenoid Pigmentation in Monkeyflowers(Mimulus)

Lauren E. Stanley, PhD

University of Connecticut, 2020

Carotenoids are red, orange, and yellow pigments found in photosynthetic organisms that play vital roles in light capture and photoprotection. In flowering plants, carotenoids may also accumulate as secondary metabolites in non-photosynthetic tissues, contributing to the bright colors of many flowers and fruits. Because the main function of floral and fruit carotenoids is in the attraction of pollinators and seed dispersers, these pigments are crucial in the ecology and evolution of many angiosperms. In order to accumulate dispensable carotenoids, plants must activate the carotenoid biosynthesis pathway (CBP) genes and develop specialized storage organelles called chromoplasts. The genetic regulation of these processes during flower and fruit development determines when and where pigments are accumulated and leads to an incredible diversity of carotenoid pigmentation in natural species and horticultural varieties. However, very few regulatory genes controlling carotenoid biosynthesis and storage are known, particularly in flowers.

This dissertation investigates the genetic regulation of floral carotenoid biosynthesis and storage. Chapter 1 reviews current knowledge of CBP gene regulation at the transcriptional level, identifying knowledge gaps and challenges in the field. Chapters 2, 3, and 4 begin to fill these knowledge gaps, using a forward genetics approach to identify carotenoid regulators in a newly developed model system, monkeyflowers (*Mimulus*). Chapter 2 describes *Reduced Carotenoid Pigmentation 2* (*RCP2*), which encodes a tetratricopeptide repeat protein positively regulating CBP gene expression and chromoplast development. Chapter 3 investigates *Accumulation and Replication of Chloroplasts 6* (*ARC6*), a chloroplast division gene necessary for chromoplast

division and floral carotenoid accumulation. Chapter 4 characterizes *Dicer-like 4* (*DCL4*), which encodes a small-RNA-producing endoribonuclease that negatively regulates CBP genes to produce floral nectar guide patterns. These genes are among the first identified carotenoid regulators in flowers, advancing the study of carotenoid synthesis and storage and illustrating the importance of forward genetics approaches in diverse model systems.

The Genetics of Carotenoid Pigmentation in Monkeyflowers(*Mimulus*)

Lauren E. Stanley

B.S., University of Pittsburgh, 2014

A Dissertation Submitted in Partial Fulfillment of the

Requirements for the Degree of

Doctor of Philosophy

at the

University of Connecticut

2020

APPROVAL PAGE

Doctor of Philosophy Dissertation

The Genetics of Floral Carotenoid Pigmentation in Monkeyflowers(*Mimulus*)

Presented by

Lauren E. Stanley, B.S.

Major Advisor _____

Yao-Wu Yuan

Associate advisor_____

Pamela K. Diggle

Associate advisor_____

Elizabeth L. Jockusch

Associate advisor_____

Barbara G. Mellone

Associate advisor_____

Carl D. Schlichting

University of Connecticut
2020

Acknowledgements

Many people helped to make this dissertation possible. I would first like to thank my wonderful advisor, Yao-Wu Yuan, who has helped me develop so much as a scientist and a writer. It was an honor to be your first graduate student. I hope I proved you wrong at least once!

Second, I would like to thank my committee of brilliant scientists: Elizabeth Jockusch, Pam Diggle, Carl Schlichting, and Barbara Mellone. Your expertise and insight strengthened my work and helped me to see my science from different perspectives. I would also like to thank Bernard Goffinet, Louise Lewis, and Paul Lewis, my "teaching committee," for their mentorship and encouragement in my pedagogical pursuits.

Next, I would like to thank my past and present colleagues in the Yuan lab, especially Baoqing Ding, Connor Hill, Amy LaFountain, Qiaoshan Lin, Chang Liu, and Janelle Sagawa, for their contributions to my projects. I am also grateful to Maritza Abril and Xuanhao Sun from the BEML, who assisted me in electron microscopy.

Many thanks to the EEB department: the faculty, whose doors were always open; the office staff, who made my time as a graduate student run so smoothly; the greenhouse staff, who kept my plants alive; and the EEB graduate students, who were so generous and helpful. I would particularly like to thank the members of my extended "cohort": Kaitlin Gallagher, Kristen Nolting, Katie Taylor, Tanisha Williams, Nasim Rahmatpour, and Amy LaFountain.

Finally, thank you to Mike, Susan, Jessica, Wayne, and Kay Stanley for supporting me on my strange journey to become a flower color doctor. I love you.

TABLE OF CONTENTS

frontiers in Plant Science

REVIEW
published: 09 August 2019
doi: 10.3389/fpls.2019.01017

Transcriptional Regulation of Carotenoid Biosynthesis in Plants: So Many Regulators, So Little Consensus

Lauren Stanley and Yao-Wu Yuan**

Department of Ecology and Evolutionary Biology, University of Connecticut, Storrs, CT, United States

In plants, the carotenoid biosynthesis pathway (CBP) is essential for the production of photosynthetic and protective pigments, plant hormones, and visual/olfactory attractants for animal pollinators and seed dispersers. The regulation of carotenoid biosynthesis at the transcriptional level is vitally important for all of these functions and has been the subject of intensive research. Many putative transcriptional regulators, both direct and indirect, have been identified through conventional mutant analysis, transcriptome profiling, yeast one-hybrid screening, and candidate gene approaches. Despite this progress, our understanding of the transcriptional regulation of carotenoid biosynthesis remains fragmented and incomplete. Frequently, a stimulus or regulator is known, but the mechanism by which it affects transcription has not been elucidated. In other cases, mechanisms have been proposed (such as direct binding of a CBP gene promoter by a transcription factor), but function was tested only *in vitro* or in heterologous systems, making it unclear whether these proteins actually play a role in carotenoid regulation in their endogenous environments. Even in cases where the mechanism is relatively well understood, regulators are often studied in isolation, either in a single plant species or outside the context of other known regulators. This presents a conundrum: why so many candidate regulators but so little consensus? Here we summarize current knowledge on transcriptional regulation of the CBP, lay out the challenges contributing to this conundrum, identify remaining knowledge gaps, and suggest future research directions to address these challenges and knowledge gaps.

Keywords: carotenoid biosynthesis, transcriptional regulation, photosynthetic tissue, flowers, fruits, seeds, roots

OPEN ACCESS

Edited by:
Manuel Rodriguez-Concepcion, Centre for Research in Agricultural Genomics (CRAG), Spain

Reviewed by:
Gianfranco Diretto, Energy and Sustainable Economic Development (ENEA), Italy
Gabriela Toledo-Ortiz, Lancaster University, United Kingdom

****Correspondence:***
Lauren Stanley
lauren.stanley@uconn.edu
Yao–Wu Yuan
yuan.colreeze@gmail.com

Specialty section:
This article was submitted to Plant Metabolism and Chemodiversity, a section of the journal Frontiers in Plant Science

Received: *17 May 2019*
Accepted: *22 July 2019*
Published: *09 August 2019*

Citation:
Stanley L and Yuan Y-W (2019) Transcriptional Regulation of Carotenoid Biosynthesis in Plants: So Many Regulators, So Little Consensus. Front. Plant Sci. 10:1017. doi: 10.3389/fpls.2019.01017

INTRODUCTION

Carotenoids are red, orange, and yellow pigments produced by photoautotrophic organisms. In the green tissues of plants, carotenoids are essential for light capture, photoprotection, and stabilization of the photosynthetic apparatus (Frank and Cogdell, 1996; Hashimoto et al., 2016). Leaf carotenoids are therefore synthesized in tight coordination with chlorophylls, and their composition is remarkably conserved across higher plants (Goodwin and Britton, 1988; Meier et al., 2011). In addition to their integral roles in photosynthesis, carotenoids accumulate as secondary metabolites in many flowers and fruits to attract pollinators and seed dispersers. Due to their dispensable nature in non-green tissues, these pigments often differ drastically in composition and concentration between species or

even between varieties of the same species (Moehs et al., 2001; Bradshaw and Schemske, 2003; Nielsen et al., 2003; Giovannoni, 2007; Ha et al., 2007; Chiou et al., 2010; Yamagishi et al., 2010; Yamamizo et al., 2010; Zhang et al., 2015). Floral and fruit carotenoids can also be cleaved to produce volatile compounds (i.e., scents and flavors), which further enhance plant–animal interactions (Dudareva et al., 2006). Finally, carotenoids serve as precursors for the synthesis of the plant hormones abscisic acid (ABA) and strigolactones, as well as other apocarotenoids that are involved in many developmental processes and stress responses (Cutler et al., 2010; Hou et al., 2016; Jia et al., 2017).

Because of their critical importance in the physiology, development, ecology, and evolution of plants, carotenoid metabolism and function have been intensively studied. The highly conserved carotenoid biosynthesis pathway (CBP) has been characterized in many plants (reviewed in Ruiz-Sola and Rodríguez-Concepción, 2012). In recent years, attention has turned to the regulation of carotenoid accumulation at multiple levels: transcriptional, post-transcriptional, post-translational, storage/degradation, and feedback regulation by end products. This has led to the discovery of numerous carotenoid regulatory mechanisms such as the post-translational regulation of phytoene synthase (PSY) by Orange (Or) (Lu et al., 2006; Zhou et al., 2015), the catabolism of carotenoids by carotenoid cleavage dioxygenases (CCDs) and 9-cis-epoxycarotenoid dioxygenases (NCEDs) (e.g., Auldridge et al., 2006; Ohmiya et al., 2006; Vallabhaneni et al., 2010), and feedback regulation by apocarotenoid-derived signaling molecules (e.g., Avendaño-Vásquez et al., 2014).

In this review, we will focus on the transcriptional regulation of carotenoid biosynthesis genes. For other aspects of carotenoid regulation, we refer readers to several recent reviews (Cazzonelli and Pogson, 2010; Yuan et al., 2015; Nisar et al., 2015; Liu et al., 2015a; Hou et al., 2016; Li et al., 2016; Enfissi et al., 2017; Llorente et al., 2017; Sun et al., 2018a; Ohmiya et al., 2019). In this paper, "transcriptional regulation" of carotenoid biosynthesis genes simply refers to altered transcript abundance in response to a stimulus or as a result of the mutation, knockdown, or overexpression of another gene (e.g., transcription factor, chromatin remodeler). Additionally, we use the term "CBP genes" to refer to the core CBP, from *PSY* to *NSY* (see **Figure 1** for a schematic of the CBP). Upstream non-carotenoid specific genes [mevalonate (MVA) or methylerythritol phosphate (MEP) pathways], genes of the side branches leading to the production of hormones and apocarotenoids, and genes necessary for the production of uncommon carotenoids (e.g., capsanthin, capsorubin, astaxanthin), are not discussed in detail.

We have organized this review by tissue type because carotenoids serve unique functions in photosynthetic tissues, fruits, flowers, seeds, and roots and because the literature is already somewhat structured in this manner. For example, tomatoes are considered the model system for carotenoid biosynthesis in fruits, and *Arabidopsis* for that in leaves. Even in narrowing the scope to just transcriptional regulation, this review covers about 40 putative regulators of carotenoid biosynthesis genes (**Table S1**). However, there is little overlap of these numerous regulators between studies of different tissue types or different plant species. In other words, very few of these putative regulators seem to have a conserved function in the transcriptional control of carotenoid biosynthesis genes across tissue types or plant species. We lay out some of the challenges contributing to this conundrum, identify remaining knowledge gaps, and suggest research directions to address these challenges and knowledge gaps in the coming years.

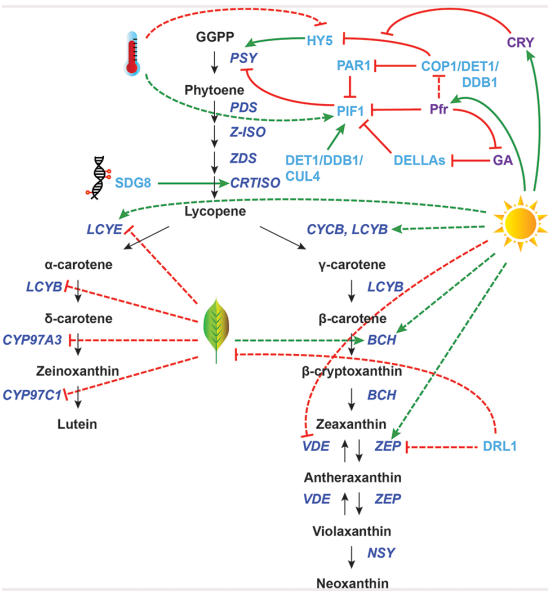

FIGURE 1 | Transcriptional regulation of carotenoid biosynthesis pathway (CBP) genes in photosynthetic tissues. The regulation of CBP genes in response to light (sun), senescence (leaf), and high temperature (thermometer) and by epigenetic controls (DNA) is shown. The carotenoid biosynthesis pathway is in black, with carotenoid biosynthesis genes indicated in dark blue. Carotenoid regulators discussed in the paper are shown in light blue, with other regulators in purple. Green arrows indicate positive regulation, while blunt red arrows indicate negative regulation. Solid lines show direct interactions, while dotted lines show indirect/unknown interactions. GGPP, geranylgeranyl pyrophosphate; *PSY*, phytoene synthase; *PDS*, phytoene desaturase; *Z-ISO*, 15-cis-zeta-carotene isomerase; *ZDS*, zeta-carotene desaturase; *CRTISO*, carotene isomerase; *LCYB*, lycopene beta-cyclase; *CYCB*, chromoplast-specific lycopene beta-cyclase; *BCH*, beta-carotene hydroxylase; *ZEP*, zeaxanthin epoxidase; *VDE*, violaxanthin deepoxidase; *NSY*, neoxanthin synthase; *LCYE*, lycopene epsilon-cyclase; *CYP97A3*, cytochrome P450–type beta-hydroxylase; *CYP97C1*, cytochrome P450–type epsilon-hydroxylase.

Photosynthetic Tissues

Carotenoids are an integral part of the light harvesting apparatus, capturing light energy and protecting the photosynthetic apparatus from damaging reactive oxygen species (ROS) formed during photosynthesis (Demmig-Adams and Adams, 1996; Pogson et al., 1998; Niyogi, 1999; Baroli and Niyogi, 2000; Dall'Osto et al., 2007). These pigments may also play an important role in temperature stress by scavenging ROS produced by photosystem II (PSII) in extreme temperatures and stabilizing thylakoid membranes (Havaux, 1998; Pospíšil, 2016).

Additionally, the developmental program for leaf senescence requires carotenoid precursors for the production of ABA and strigolactones (Nambara and Marion-Poll, 2005; Snowden et al., 2005; López-Ráez et al., 2008; Alder et al., 2012; Ueda and Kusaba, 2015). Transcriptional regulation of the CBP genes in photosynthetic tissues is therefore highly influenced by light, temperature, and developmental cues.

Light

The light signaling machinery of plants has been extensively characterized in *Arabidopsis* (e.g., Delker et al., 2014; Dong et al., 2014; reviewed in Jiao et al., 2007; Lau and Deng, 2012), and many key regulatory genes have been identified. One such gene, *Phytochrome Interacting Factor 1* (*PIF1*), is perhaps the best-understood transcriptional regulator of carotenoid biosynthesis. During seedling deetiolation, phytochromes are activated by red light and move from the cytoplasm into the nucleus to interact with signaling components. The bHLH transcription factor PIF1, which represses *AtPSY* expression in the dark, is phosphorylated by phytochromes upon photoactivation and subsequently degraded by the proteasome (Bae and Choi, 2008; Shen et al., 2008; Shin et al., 2009). This initiates the rapid de-repression of *AtPSY* as well as genes involved in chlorophyll biosynthesis and chloroplast development.

Toledo-Ortiz et al. (2010) showed that *Arabidopsis* PIF1 binds directly to a G-box element in the *AtPSY* promoter in both *in vitro* and *in vivo* assays and demonstrated that this binding leads to transcriptional repression. PIFs also contribute to the regulation of *AtPSY* in mature plants during their daily light/dark cycles. In fully deetiolated plants grown under short-day conditions, higher levels of carotenoids and *AtPSY* transcripts were found in *pif* mutants than in wild-type plants (Toledo-Ortiz et al., 2010).

Another important player in light signaling is the bZIP transcription factor Long Hypocotyl 5 (HY5), which acts antagonistically to PIF1 during photomorphogenesis. HY5 activates carotenoid and chlorophyll biosynthesis genes, as well as genes involved in chloroplast development and cotyledon expansion. Unlike PIF1, which is stabilized in the dark by the DET1/DDB1/CUL4 complex, HY5 is stabilized by light (the COP1/DDB1/CUL4 complex targets HY5 for degradation in the dark) (Shi et al., 2015; Zhu et al., 2015). Interestingly, HY5 and PIF1 bind to the same G-box element of the *AtPSY* promoter, which serves as a relatively simple switch to promote deetiolation upon illumination. This switch also functions in the daily light/dark cycles of mature plants (Toledo-Ortiz et al., 2014).

PIFs are also involved in shade-triggered reduction of carotenoid accumulation in *Arabidopsis* leaves, through an HY5-independent mechanism. When there is a low red/far red (R/FR) ratio of light in shade conditions, Phytochrome Rapidly Regulated 1 (PAR1), a bHLH co-factor, is upregulated and induces *AtPSY* expression by physically interacting with PIF1 and preventing it from sitting on the *AtPSY* promoter (Bou-Torrent et al., 2015).

Carotenoid biosynthesis is also induced when greening is de-repressed in the dark, which can be achieved through the blockage of gibberellic acid (GA) biosynthesis (Rodríguez-Villalón et al., 2009; Toledo-Ortiz et al., 2010). GA negatively regulates DELLA proteins, which in turn negatively regulate PIFs. In *Arabidopsis* GA biosynthesis mutants, *AtPSY* transcript levels in etiolated seedlings are elevated relative to the wild type. In "double" mutants lacking both GA and DELLAs, this response is repressed. Treatment of wild-type plants with a GA inhibitor reduced PIF1 binding to the G-box in the *AtPSY* promoter (Cheminant et al., 2011).

While the PIF1/HY5 regulatory mechanism is relatively well understood, there is still much to be learned about the transcriptional regulation of carotenoid biosynthesis during deetiolation. For instance, many other carotenoid biosynthesis genes are de-repressed during photomorphogenesis in *Arabidopsis*, such as *AtBCH2*, *AtZEP*, and *AtLCYE* (which are constitutively de-repressed in *pif* mutants). Of these, only *AtBCH2* has a G-box in its promoter, but this G-box is not bound by PIF1 (Toledo-Ortiz et al., 2010). Additionally, truncated *AtPSY* genes lacking G-boxes in Arabidopsis are still light responsive (Welsch et al., 2003), indicating that there are other factors involved in light responsiveness unrelated to the PIF pathway and/or that PIFs may bind other elements.

Indeed, a chromatin immunoprecipitation–microarray (ChIP–chip) analysis in *Arabidopsis* seeds showed that PIF1 binds to 748 sites, only 59% of which contain G-box elements (Oh et al., 2009); additionally, only a small fraction of G-box elements in the *Arabidopsis* genome have been shown to be bound by PIFs (Kim et al., 2016). PIF1 has been shown to bind PIF binding E-box (PBE) elements *in vitro*, though this interaction is relatively weak (Kim et al., 2008; Pfeiffer et al., 2014). PIF1-interacting transcription factors may facilitate the targeting of PIF1 to specific sites, particularly those containing multiple G-boxes and/or G-box coupling elements (GCEs) (Kim et al., 2016). Thus, non-canonical PIF binding sites may play a role in PIF1 regulation of other CBP genes.

Another thing to consider is that PIF1 is certainly not a specific carotenoid regulator: it has been shown to directly regulate the chlorophyll biosynthesis gene *AtPOR* by binding its promoter and to indirectly regulate other genes in that pathway (Moon et al., 2008). This may account in part for the tight coordination between chlorophyll and carotenoid biosynthesis in green tissues during photomorphogenesis. However, for PIF1 to function in chromoplast-containing tissues, the regulation of carotenoid and chlorophyll biosynthesis must be decoupled (see the "Fruits" section).

The intensity of light affects both carotenoid concentration and composition (Hirschberg, 2001). High light stress produces ROS such as triplet chlorophyll and singlet oxygen, which can be deactivated by carotenoids. Additionally, excess excitation energy in the photosystems can be effectively dissipated by carotenoids, particularly zeaxanthin (Dall'Osto et al., 2012; Jahns and Holzwarth, 2012). High light causes a rapid decrease in lumen pH, which increases violaxanthin deepoxidase (VDE) enzyme activity, converting violaxanthin to zeaxanthin (**Figure 1**). Although this interconversion between violaxanthin and zeaxanthin (i.e., the xanthophyll cycle) is regulated post-translationally by activation and inactivation of the VDE enzyme (Müller et al., 2001), high light does induce transcriptional changes of CBP genes as well. For example, the ratio of *LCYB* to *LCYE* transcripts increases fivefold in both *Arabidopsis* and tomato leaves in high light relative to low light (Hirschberg, 2001),

which channels metabolic flux through the branch of the CBP that produces zeaxanthin (**Figure 1**). *AtBCH2* transcription is also upregulated by high light treatment in *Arabidopsis* (Rossel et al., 2002), likely enhancing the metabolic flow towards xanthophylls as well. However, the transcription factors responsible for these CBP gene expression changes remain unknown.

Ultraviolet B (UV-B) light also triggers the production of carotenoids, which are directly linked to photoprotection of the photosynthetic apparatus (Middleton and Teramura, 1993). Irradiation of *Arabidopsis* plants with UV-B causes slight decreases in lutein and β-carotene content but a substantial increase in zeaxanthin. Correspondingly, the expression of *AtPSY, AtZDS*, and *AtBCH1/2* is enhanced. Loss-of-function *AtLYCE* (*LUT2)* mutants accumulate more β-carotene branch xanthophylls compared to the wild type and consequently show decreased DNA and oxidative damage under UV-B light (Emiliani et al., 2018). Interestingly, the UV-B response pathway and the photomorphogenesis pathway share several common components. For example, the active form of UV RESPONSE LOCUS 8 (UVR8), a UV-B–specific photoreceptor, directly interacts with COP1 and regulates *HY5* expression (Brown et al., 2005; Brown and Jenkins, 2008; Cloix and Jenkins, 2008; Favory et al., 2009; Rizzini et al., 2011). Therefore, it would not be surprising if the transcriptional regulators of the CBP genes downstream of *AtPSY* (e.g., *AtZDS*, *AtBCH1/2*) turned out to be the same for both UV-B response and photomorphogenesis.

Temperature

The PIF1/HY5 switch can also control *AtPSY* expression in response to temperature cues (Toledo-Ortiz et al., 2014). In addition to being stabilized by light, HY5 is stabilized by cold temperatures (Catalá et al., 2011). In a ChIP assay, both the *AtPSY* and *AtVDE* promoters were preferentially bound by HY5 at low compared to ambient temperatures. Furthermore, the rapid increase of HY5 and decrease of PIF1 protein levels when etiolated *Arabidopsis* seedlings were exposed to light was more robust at lower temperature (Toledo-Ortiz et al., 2014). This would lead to higher expression of *AtPSY* at lower temperatures. These findings are echoed by experiments in maize (*Zea mays*), which showed that *ZmPSY1* and *ZmPSY2* expression decreases at high temperatures in both light and dark conditions (Li et al., 2008a).

The sensitivity of *PSY* transcript levels to temperature cues indicates that transcriptional regulation of the CBP may be partially responsible for temperature stress responses. It makes sense that high light and low temperature responses would overlap, because the consequences of these stressors are similar: they both produce ROS and prevent the repair of PSII damage (reviewed in Szymańska et al., 2017). Thus, PIF1/HY5 regulation of *PSY* may be an important mechanism for increasing carotenoids to scavenge ROS. However, high temperature stress, which also produces damaging ROS, reduces the expression of *PSY*, indicating that transcriptional regulation of this gene is not responsible for high temperature stress response.

Senescence

Leaf senescence is a developmentally controlled process leading eventually to organ death. The breakdown and recycling of macromolecules from senescing leaves allow plants to reallocate resources to reproduction or new growth (Gan and Amasino, 1997; Lim et al., 2007). One of the most prominent phenotypes during senescence is leaf yellowing due to the breakdown of pigments in chloroplasts (Ougham et al., 2005). Although all photosynthetic pigments are eventually broken down, chlorophylls are usually lost more rapidly than carotenoids. There are also changes in the composition of carotenoids during senescence: while all decline, lutein remains at relatively stable levels compared to neoxanthin, violaxanthin, and antheraxanthin (Biswal, 1995; Britton and Young, 1989). This is perhaps due to the cleavage of β-carotene branch carotenoids for the production of strigolactones and ABA, which further promote leaf senescence (Yang et al., 2003; Ueda and Kusaba, 2015).

The transcription of CBP genes changes dramatically during leaf senescence. In an *Arabidopsis* microarray analysis of senescing leaves, *AtLCYE*, *AtCYP97C1*, and *AtCYP97A3* expression drops, reducing flux through the α-carotene branch of the pathway. This is followed by the induction of *AtBCH1*, which might be important for downstream hormone production (Breeze et al., 2011). Similar trends can also be seen in woody perennial plants: in aspen trees (*Populus tremula*), *PtBCH2* is significantly induced by autumn senescence (Andersson et al., 2004).

The only known potential regulator of CBP genes during leaf senescence is *DRL1* from grapevine (*Vitis vinifera*), encoding a NAC transcription factor. Overexpression of *DRL1* in tobacco has been shown to delay leaf senescence and decrease ABA levels. The expression of *NtZEP1* and carotenoid cleavage genes is reduced in these transgenic plants (Zhu et al., 2019). However, the endogenous function of *DRL1* in grapevine is yet to be reported.

Other CBP Regulators in Photosynthetic Tissues

Besides *ZEP*, two other CBP genes downstream of *PSY* have potential known regulators in photosynthetic tissues. In *Arabidopsis* leaves, the Ethylene Response Factor (ERF) transcription factor RELATED TO AP2 2 (RAP2.2) was shown to bind the *AtPSY* and *AtPDS* promoters *in vitro* (Welsch et al., 2007). However, overexpression of *AtRAP2.2* in *Arabidopsis* leaves did not result in higher *AtPSY* or *AtPDS* messenger RNA (mRNA) levels, nor a change in carotenoid concentration. A knockout mutant of *AtRAP2.2* was not available, probably due to lethality. These results leave the endogenous function of *AtRAP2.2* in carotenoid regulation ambiguous.

AtCRTISO is another CBP gene in photosynthetic tissues with an identified regulator: the histone methyltransferase Set Domain Group 8 (SDG8). *sdg8* mutants produce low levels of *CRTISO* mRNA, which correlates with reduced trimethyl-H3K4 and increased dimethyl-H3K4 around the *CRTISO* transcription start site (Cazzonelli et al., 2009). Although this mechanism is well understood, SDG8 is certainly not a specific carotenoid regulator: mutation in this gene downregulates 85 other genes and causes broad pleiotropic effects, including increased shoot branching, reduced fertility, and early flowering. It is currently

unknown whether the function of SDG8 in carotenoid biosynthesis is conserved across species.

As described above, only a few regulators of carotenoid biosynthesis in green tissues, such as PIF1 and HY5, have been well characterized and shown to directly regulate *PSY* in *Arabidopsis*. Additionally, their importance as regulators of photomorphogenesis, responses to daily light/dark cycles, and temperature has been established. However, we still know very little about what regulates most CBP genes downstream of *PSY* in green tissues.

Fruits

The ripening developmental program of fleshy fruits involves changes in texture (alteration of cell wall composition, reduction in turgor pressure), flavor and aroma (alteration of volatiles, sugar/starch, and acid metabolism), and color (alteration of chlorophyll, carotenoid, and flavonoid content) (Klee and Giovannoni, 2011). Many economically important fruits (e.g., tomato, orange, papaya) produce copious carotenoids during ripening, and therefore, the transcriptional control of CBP genes during fruit ripening has attracted considerable research efforts.

Tomatoes

The foremost model for carotenoid regulation during fruit ripening is tomato (*Solanum lycopersicum*) (**Figures 2**–**3**), which primarily accumulates lycopene in mature fruits. During tomato fruit development, transcription of the early CBP genes *SlPSY1* and *SlPDS* increases, while the transcription of *SlLCYE* and *SlLCYB*, which convert lycopene to other downstream products, decreases (Pecker et al., 1992; Giuliano et al., 1993; Fraser et al., 1994; Corona et al., 1996; Ronen et al., 1999; Alba et al., 2005). Tomato fruits are climacteric, and thus, ethylene biosynthesis and signaling are necessary for the onset and completion of ripening (reviewed in Liu et al., 2015b). CBP gene regulation is also tightly coupled with these processes, and many of the regulators that affect CBP gene expression also affect other aspects of ripening. These may therefore be considered general regulators of ripening, oftentimes functioning far upstream of the CBP genes.

Several MADS-box ripening regulators affect the expression of CBP genes in tomatoes, and a ripening model similar to the floral quartet model has been proposed (**Figure 2**). In this model, different combinations of MADS-box proteins bind different target genes (Bemer et al., 2012; Shima et al., 2013; Fujisawa et al., 2014). These "ripening quartet" regulators include Tomato AGAMOUS-LIKE1 (TAGL1), Ripening Inhibitor (RIN), FRUITFULL1 (FUL1), and FUL2. These transcription factors have both overlapping and individual (but never antagonistic) contributions to the expression of CBP genes, with the total effect being the positive regulation of *SlPSY1*, *SlPSY2*, *SlZDS*, *SlZ-ISO*, *SlCRTISO*, and *SlBCH*, and the negative regulation of *SlLCYB*, *SlLCYE*, and *SlCYCB* (the chromoplast-specific paralogue of *SlLCYB*) (Vrebalov et al., 2002; Ito et al., 2008; Itkin et al., 2009; Vrebalov et al., 2009; Giménez et al., 2010; Fujisawa et al., 2011; Fujisawa et al., 2012; Fujisawa et al., 2013; Fujisawa et al., 2014; Martel et al., 2011; Bemer et al., 2012; Qin et al., 2012; Shima et al., 2013; Zhong et al., 2013). For the effects of each individual regulator, see **Figure 2A**.

These MADS-box proteins exert their effects over CBP gene transcription both directly by binding the promoters of some genes and indirectly by unknown mechanisms. Various studies have shown the promoter of *SlLCYB* to be bound by all four regulators; the promoter of *SlPSY1* to be bound by TAGL1, RIN, and FUL1; the promoters of *SlZ-ISO*, *SlCRTISO*, and *SlZEP* by RIN, FUL1, and FUL2; the promoter of *SlBCH* by FUL1 and FUL2; the promoter of *SlCYCB* by TAGL1; and the promoter of *SlLCYE* by RIN (Ito et al., 2008; Itkin et al., 2009; Vrebalov et al., 2009; Giménez et al., 2010; Fujisawa et al., 2011; Fujisawa et al., 2012; Fujisawa et al., 2013; Fujisawa et al., 2014; Martel et al., 2011; Bemer et al., 2012; Qin et al., 2012; Shima et al., 2013; Zhong et al., 2013; see **Figure 2B** for a graphical summary).

It should be mentioned that ChIP studies assessing RIN binding to target gene promoters have produced inconsistent results. Some studies have shown that the *SlPSY1* promoter is bound by RIN (Martel et al., 2011; Zhong et al., 2013; Fujisawa et al., 2013), while others have not detected this interaction or had inconclusive results (Fujisawa et al., 2011; Fujisawa et al., 2012; Fujisawa et al., 2013). Also, though FUL1 has been shown to bind the promoter of *SlPSY1* and promote its expression (Shima et al., 2013; Fujisawa et al., 2014), one study in which *FUL1* and *FUL2* were silenced showed that fruits did not have altered expression of *SlPSY1* (Bemer et al., 2012). The loss of FUL1 function may have been compensated by RIN and TAGL1, and thus, its endogenous role in regulating carotenoid biosynthesis remains unclear.

Other CBP-regulating MADS-box genes in tomato that interact with or regulate the ripening quartet are *SlMADS1, SlFYFL*, and *SlCMB1* (**Figure 2**). SlMADS1 and SlFYFL are both negative regulators of carotenoid biosynthesis, suppressing *SlPSY1* expression (SlFYFL also suppresses *SlPDS* and *SlZDS*) (Dong et al., 2013; Xie et al., 2014). SlCMB1 promotes the expression of *SlPSY1* and *SlPDS*, while suppressing *SlCYCB*, *SlLCYB,* and *SlLCYE* transcription (Zhang et al., 2018a).

Many other regulators play a role in CBP gene regulation during fruit ripening, especially those involved in hormone synthesis and signaling. SlAP2a (an APETALA2/ERF protein) positively regulates fruit ripening, promoting the expression of *SlPSY1*, *SlCRTISO*, *SlBCH*, and *SlPDS1*, and repressing *SlZEP1* and *SlCYCB* (Chung et al., 2010; Karlova et al., 2011). The overexpression of *Tomato Ethylene Response Factor 1 (TERF1)* induces *SlZDS* expression, perhaps *via* plastid-to-nucleus retrograde signaling (Wu et al., 2019). Silencing *LeHB-1* (encoding an HD-Zip transcription factor) inhibits fruit ripening and lycopene production, most likely through inhibition of ethylene biosynthesis (Lin et al., 2008). However, the transcript levels of CBP genes were not assessed in the *LeHB-1* silenced lines.

NAC family transcription factors involved in ethylene biosynthesis also affect the transcription of CBP genes: SlNAC4 positively regulates *SlPSY1* and negatively regulates *SlCYCB*, *SlLCYB*, and *SlLCYE* (Zhu et al., 2014), while SlNAC1 has the opposite effect (Ma et al., 2014; Meng et al., 2016). SlNAC1 has been shown by yeast one-hybrid assay to interact with the

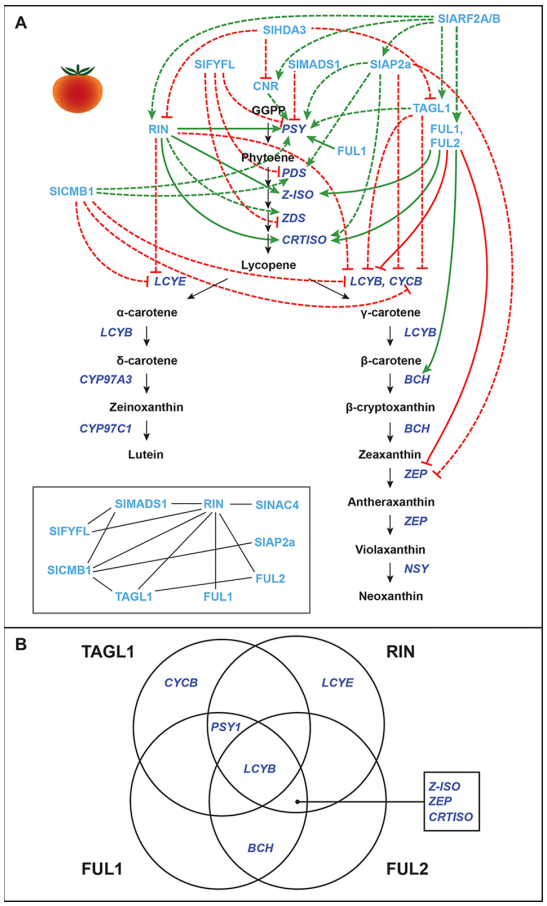

FIGURE 2 | Transcriptional regulation of CBP genes in tomato fruits: "ripening quartet"–related proteins. **(A)** The regulation of CBP genes in tomato fruits. The carotenoid biosynthesis pathway is in black, with carotenoid biosynthesis genes indicated in dark blue. Carotenoid regulators discussed in the paper are shown in light blue. Green arrows indicate positive regulation, while blunt red arrows indicate negative regulation. Solid lines show direct interactions, while dotted lines show indirect/unknown interactions. Inset: protein–protein interactions between "ripening quartet" regulators. **(B)** Venn diagram showing the direct binding of TAGL1, RIN, FUL1, and FUL2 to CBP gene promoters.

promoters of *SlPSY1* and ethylene biosynthesis genes (Ma et al., 2014).

Additionally, overexpression of *SlNAC1* increases the amount of ABA, potentially by providing the carotenoid precursors for its synthesis (Ma et al., 2014). In wild-type fruits, ABA production precedes ethylene production and may be an important trigger for ripening (Zhang et al., 2009). ABA application promotes several ripening processes, including carotenoid accumulation, by regulating transcription factors for ethylene biosynthesis and signaling (Mou et al., 2016). Another regulator related to ethylene–ABA is SlPti4 (also a member of the AP2/ERF superfamily). Silencing of *SlPti4* enhances ABA production while decreasing ethylene production, which induces the expression of *SlCYCB* and the consequent color change from red to orange (Sun et al., 2018b). Finally, the zinc finger transcription factor SlZFP2 inhibits fruit ripening by negatively regulating ABA biosynthesis (Weng et al., 2015). *SlZFP2*-overexpressing fruits accumulate more β-carotene and lycopene compared to the wild type, but it is unclear whether SlZFP2 actually regulates CBP gene expression, as the transcript levels of CBP genes were not reported in this study (Weng et al., 2015).

Besides ethylene and ABA, other plant hormones are also involved in tomato fruit ripening, with complex actions and interactions. Auxin acts antagonistically to ethylene, delaying ripening. Exogenous application of an auxin inhibitor to tomato fruits produces an effect similar to ethylene application, indicating that perhaps the presence vs. absence of auxin, not ethylene *per se*, determines ripening in tomato (Su et al., 2015). RNA interference (RNAi) mediated silencing of two paralogues of *Auxin Response Factor 2*, *SlARF2A* and *SlARF2B*, caused downregulation of *SlPSY1*, *SlPDS*, and *SlZDS* and upregulation of *SlLCYB1*, *SlLCYB2*, and *SlCYCB* (Hao et al., 2015). Several key ripening genes (e.g., *RIN*, *CNR*, *NOR*, *AP2a*, *TAGL1*, *FUL1/2*) were also downregulated in these RNAi lines, indicating that *SlARF2A/B* may regulate CBP gene expression through the ripening factors.

Brassinosteroid (BR) application to pericarp discs induces lycopene formation (Vardhini and Rao, 2002). Transgenic lines overexpressing *Brassinazole Resistant 1* (*BZR1*) have increased transcript levels of *SlPSY1* and *SlZDS* (Liu et al., 2014). Cytokinins (CKs) are also involved in ripening: SlIPT4, which catalyzes the rate-limiting step of CK biosynthesis, represses the expression of *SlPSY1* and *SlPDS*, while upregulating the expression of *SlZ-ISO* and *SlZDS* (Zhang et al., 2018b). Given that both BR and CK are isoprenoids synthesized using precursors from the MEP/MVA pathways, it is perhaps not too surprising that their biosynthesis and signaling affect carotenoid biosynthesis (Sakakibara, 2006; Andrade et al., 2017). Another hormone, jasmonic acid (JA), promotes lycopene accumulation and CBP gene expression, even in ethylene-insensitive mutants (Liu et al., 2012), but the mechanism is unknown.

Light is also an important regulator of CBP genes during tomato fruit development. Interestingly, the shading response seen in *Arabidopsis* leaves is utilized in tomatoes for fruit ripening. In an *in vivo* ChIP assay, SlPIF1a binds to a PBE-box located in the promoter of the tomato *SlPSY1* gene to repress its expression. This repression is only maintained when the R/FR light ratio is low. In an elegant experiment, Llorente et al. (2016) showed that the presence of chlorophyll in the immature green fruit pericarp acts as a self-shading mechanism, giving a low R/FR ratio. When developmentally triggered degradation of chlorophyll begins, the R/FR ratio increases, and *SlPSY* is de-repressed by phytochrome-mediated degradation of SlPIF1a.

Other light signaling components have been examined in tomato fruits. Mutations in the high pigment genes *HP1* (*DDB1*) and *HP2* (*DET1*) give increased amounts of chlorophyll in immature fruits and increased amounts of carotenoids in mature fruits (Mustilli et al., 1999; Levin et al., 2003; Lieberman et al., 2004). DDB1 and DET1, which are known to interact

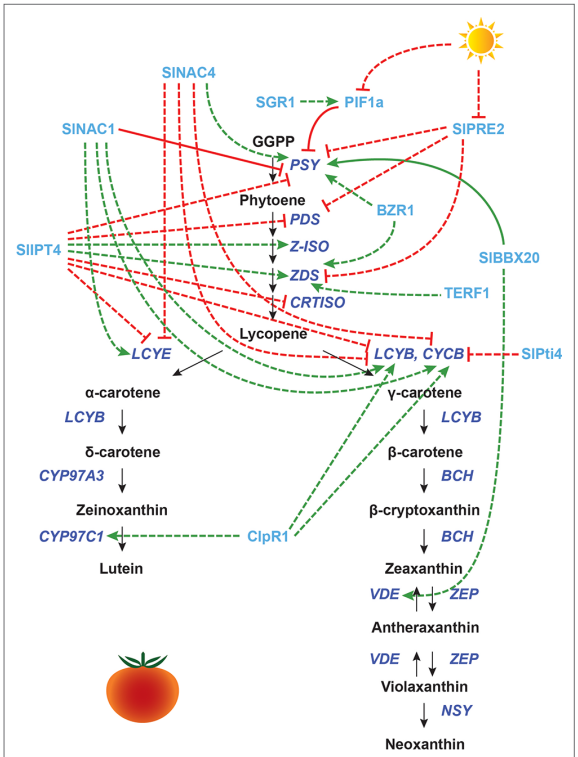

FIGURE 3 | Transcriptional regulation of CBP genes in tomato fruits: other proteins. The regulation of CBP genes in tomato fruits. The carotenoid biosynthesis pathway is shown in black, with carotenoid biosynthesis genes indicated in dark blue. Carotenoid regulators discussed in the paper are shown in light blue. Green arrows indicate positive regulation, while blunt red arrows indicate negative regulation. Solid lines show direct interactions, while dotted lines show indirect interactions.

with PIF1/HY5 and regulate their protein levels in *Arabidopsis* leaves, do not appear to strongly affect the expression of CBP genes in tomato fruits. The high pigment levels are probably due to changes in plastid size and/or number that increase the storage capacity of carotenoids. CBP gene expression has been shown to be slightly altered in tomato *det1* mutants compared to wild type: in a transcriptome study, *SlPSY1*, *SlPDS*, and *SlLCYB* transcript levels were all slightly elevated in immature fruits, while *SlCYCB* transcript levels were reduced. At the mature red stage, *SlPSY1*, *SlZDS*, and *SlCYCB* were upregulated, but carotenoid biosynthesis is not at peak levels in mature fruit, and thus, these differences may not be developmentally relevant (Kolotilin et al., 2007).

Another light-responsive CBP regulator in tomato is *SlPRE2,* an atypical bHLH transcription factor whose expression is repressed in high light. When *SlPRE2* is overexpressed, it alters the growth of stems and leaves, promotes hypocotyl elongation, and downregulates chlorophyll biosynthesis genes as well as *SlPSY1*, *SlPDS*, and *SlZDS.* Transcript levels of *HY5* are also reduced, which could explain the low level of *SlPSY1* transcripts (Zhu et al., 2017a).

Other proteins appear to indirectly affect the transcription of CBP genes through plastid processes. Overexpression of the B-box protein BBX20 increases the chlorophyll and carotenoid content in tomato leaves and fruits, inducing *SlPSY1* and *SlVDE* expression. BBX20 was found to bind to a G-box in the *SlPSY1* promoter *in vitro* and interacts with DET1. Carotenoid content is probably enhanced because of both the increase in *SlPSY1* expression and an increased number of chloroplasts. *BBX20* overexpression does not affect carotenoid accumulation or CBP transcription in flowers, indicating that distinct mechanisms operate in fruits and flowers (Xiong et al., 2019).

The Clp protease *ClpR1* enhances transcript levels of *SlLCYB*, *SlCYCB*, and *SlCYP97C11*. This gene probably affects the transcription of carotenoid biosynthesis genes through its contributions to the chloroplast-to-chromoplast transition (D'Andrea et al., 2018). The Stay Green 1 (SGR1) protein represses *SlPSY1* expression (although the effect appears minor). When *SGR1* is knocked down, fruits have lower *PIF1* expression and altered ethylene signal transduction. SGR1 also interacts directly with SlPSY1 protein, and knockdown of this gene induces early chloroplast-to-chromoplast transition, indicating that this gene has many regulatory functions (Luo et al., 2013).

Epigenetic regulation is also crucial to fruit ripening and carotenoid biosynthesis in tomato. Zhong et al. (2013) showed that about 1% of the tomato genome shows differential methylation during fruit ripening by chemically inhibiting methyltransferases. For a review on epigenetic controls in tomato fruit ripening, see Giovannoni et al., 2017; for a review on epigenetic control of carotenoid biosynthesis, see Arango et al., 2016.

Colorless non-ripening (Cnr) tomato mutants do not express *SlPSY1* (Thompson et al., 1999, Eriksson et al., 2004) and thus do not produce lycopene. The CNR locus was shown to be a *SQUAMOSA Promoter Binding Protein–like (SPL)* gene, with the causal mutation occurring in the promoter. This mutation was an epimutation, with increased methylation in mutants (Manning et al., 2006). When wild-type tomato fruits are treated with a methylation inhibitor, they produce early-ripening red sectors (which have unmethylated CNR promoters). The sectors that remain green also remain hypermethylated, suggesting that methylation of ripening genes acts as a developmental block. *SlPSY1* transcripts were isolated from early-ripening sectors, suggesting that this fruit ripening mechanism is upstream of carotenogenesis and other ripening processes (Zhong et al., 2013). The CNR *SPL* gene might be a conserved carotenoid regulator across species. Constitutive expression of *AtmiR156b* (which silences *AtSPL3*, a CNR *SPL* homologue; Wang et al., 2009) produces excess amounts of lutein and β-carotene in *Brassica napus* seeds, though CBP gene expression was not assessed (Gandikota et al., 2007; Wei et al., 2010; Arango et al., 2016). None of the CBP genes has a sequence complementary to AtmiR156b, so this increase in carotenoids is indirect (Wei et al., 2010), likely through the *SPL* gene.

Another epigenetic regulator, the tomato histone deacetylase gene *SlHDA3*, negatively regulates *SlPSY1* expression, while positively regulating *SlCYCB*, *SlLCYB*, and *SlLCYE*. Ethylene biosynthesis genes and cell wall metabolism genes were also negatively regulated by *SlHDA3*, as were *RIN*, *Cnr*, and *TAGL1* (Guo et al., 2018).

Other Climacteric Fruits

Putative transcriptional regulators have also been identified in other climacteric fruits (**Figure 4**). In papaya (*Carica papaya*), *in vitro* and dual luciferase assays in a heterologous host (i.e., tobacco) showed that the ethylene response protein CpEIN3a binds to and activates the promoters of *CpPDS4* and *CpBCH*. Further, its interacting partner CpNAC2 binds to and activates the promoters of *CpPDS2, CpPDS4, CpZDS*, *CpLCYE*, and *CpBCH*. The interaction between CpEIN3a and CpNAC2 increases activation of these genes (Fu et al., 2017). Also in papaya, the NAC family transcription factor CpNAC1 has been shown to bind to the *CpPDS2* and *CpPDS4* promoters *in vitro* and activate them in transient assays in tobacco (Fu et al., 2016). Two other papaya transcription factors, CpbHLH1 and CpbHLH2, bind to the promoters of *CpCYCB* and *CpLCYB in vitro* and in tobacco transient assays, with CpbHLH1 acting as a repressor and CpbHLH2 as an activator (Zhou et al., 2019). However, the endogenous functions of these papaya genes are unknown.

In kiwifruit (*Actinidia deliciosa)*, a promoter screen identified *AdMYB7* (among other MYBs) as a putative regulator of *AdLCYB*. The authors confirmed interaction between AdMYB7 and the *AdLCYB* promoter in a gel mobility shift assay. When *AdMYB7* was overexpressed in tobacco in a transient assay, the carotenoid content increased twofold. Stable overexpression of this gene in tobacco gave increased expression of *NbPSY*, *NbPDS*, *NbZDS*, *NbLCYB*, *NbLCYE*, and chlorophyll biosynthesis genes (Ampomah-Dwamena et al., 2019).

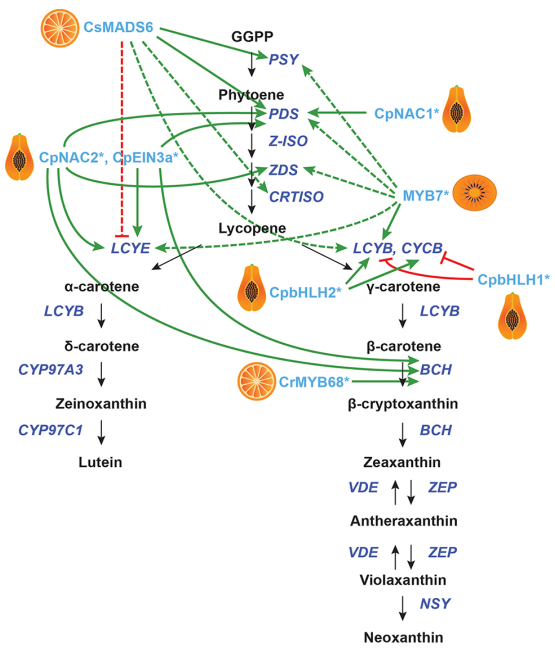

FIGURE 4 | Transcriptional regulation of CBP genes in other fruits. The regulation of CBP genes in citrus, peach, papaya, and orange kiwi. The carotenoid biosynthesis pathway is shown in black, with carotenoid biosynthesis genes indicated in dark blue. Carotenoid regulators discussed in the paper are shown in light blue. Green arrows indicate positive regulation, while blunt red arrows indicate negative regulation. Solid lines show direct interactions, while dotted lines show indirect/unknown interactions.

Non-Climacteric Fruits

Watermelon (*Citrullus lanatus*) fruits, like tomatoes, accumulate lycopene. However, they are non-climacteric, meaning that their ripening process is not concurrent with a spike of ethylene production and cellular respiration. The expression of watermelon homologues of *CNR*, *SlAP2a*, and *SlERF6* was correlated with ripening and carotenoid biosynthesis; however, that of *RIN*, *TAGL1*, *NAC-NOR*, *DET1*, *DDB1*, and *CUL4* was not (Grassi et al., 2013). This suggests that some regulators might be common to carotenoid-accumulating fruits, while others are potentially involved in other aspects of ripening, such as ethylene biosynthesis/perception and light sensing/plastid transition.

In citrus, a yeast one-hybrid screen using the promoters of *CsLCYB1* and *CsLYCB2* identified the MADS-box gene *CsMADS6* (a homologue of *TAGL1*), which is expressed in flowers and fruits. Overexpression of *CsMADS6* in citrus calli gave increased expression of *CsPSY*, *CsPDS*, *CsCRTISO*, *CsLCYB2*, and *CsBCH*, while transcription of *CsLCYE* was repressed. Additionally, the transcript levels of citrus *HY5* and *RAP2.2* homologues increased, while *PIF1* levels were reduced (*RIN* and *FUL* are not expressed in citrus calli). CsMADS6 can bind the promoters of *CsPSY* and *CsPDS in vitro* to activate them (Lu et al., 2018). Another citrus gene, the *R2R3-MYB CrMYB68*, has been shown to directly and negatively regulate *CrBCH2* by Electromobility Shift Assays and dual luciferase assays, but the endogenous function of this gene in citrus is unknown (Zhu et al., 2017b).

Flowers

The coordinated transcriptional regulation of CBP genes is largely responsible for the coloration of carotenoid-pigmented flowers (e.g., Corona et al., 1996; Moehs et al., 2001; Chiou et al., 2010; Dalal et al., 2010; Yamagishi et al., 2010; Yamamizo et al., 2010; Ohmiya, 2013; Zhang et al., 2015; Kishimoto et al., 2018; Wang and Yamagishi, 2019). However, very few genes regulating the transcription of CBP genes in flowers have been identified (**Figure 5**). Notably, none of the regulators involved in tomato fruit ripening dramatically affect flower petal color, even though tomatoes have carotenoid-pigmented flowers. This is probably because fruit and flower carotenoid biosynthesis are differentially regulated: while tomato fruits accumulate lycopene, the main carotenoid components in tomato flowers are the xanthophylls violaxanthin and neoxanthin (Galpaz et al., 2006). Most flowers

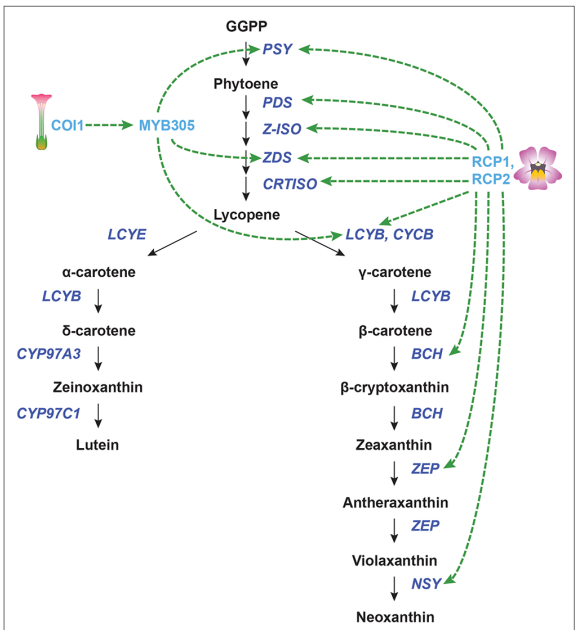

FIGURE 5 | Transcriptional regulation of CBP genes in flowers. The regulation of CBP genes in *Nicotiana tabacum* and *Mimulus* species. The carotenoid biosynthesis pathway is shown in black, with carotenoid biosynthesis genes indicated in dark blue. Carotenoid regulators discussed in the paper are shown in light blue. Green arrows indicate positive regulation, while blunt red arrows indicate negative regulation. Dotted lines show indirect/unknown interactions.

studied to date primarily store xanthophylls and/or β-carotene (Ohmiya, 2011).

The F-box protein CORONATINE INSENSITIVE 1 (COI1) is necessary for the perception of jasmonic acid JA. In addition to its many other functions, COI1-mediated JA signaling has been implicated in the production of floral and extrafloral nectar. Silencing of *COI1* in *Nicotiana tabacum* not only suppresses nectar production in flowers but also decreases the amount of β-carotene in the floral nectary. The expression of *NtPSY*, *NtZDS*, and *NtLCYB* was reduced in the *COI1*-silenced lines during carotenoid accumulation (and persisted throughout development for *NtPSY*). Silencing *COI1* also strongly downregulated the *R2R3-MYB* gene *MYB305* in floral nectaries, suggesting that COI1 works upstream of this gene (Wang et al., 2014). It was previously shown that RNAi knockdown of *MYB305* causes the loss of β-carotene in floral nectaries (though gene expression of the CBP genes was not analyzed) (Liu et al., 2009). MYB305, then, may mediate the transcriptional regulation of *NtPSY*, *NtZDS*, and *NtLCY*.

In the monkeyflower species *Mimulus lewisii*, an *R2R3-MYB* gene called *Reduced Carotenoid Pigmentation 1 (RCP1)* positively regulates all of the CBP genes expressed in flowers, contributing to the bright yellow coloration of the floral nectar guides (Sagawa et al., 2016). Although this seems like a promising global regulator for carotenoid biosynthesis in flowers, the DNA binding site/s of this transcription factor is/are yet to be determined. It is unknown whether RCP1 directly or indirectly activates transcription of the CBP genes. Another gene from monkeyflowers, *RCP2*, is also necessary for carotenoid biosynthesis in petals. *RCP2* codes for a tetratricopeptide repeat protein that promotes the expression of the entire CBP, apparently through the regulation of chromoplast formation (Stanley et al., 2017). It appears that chromoplast defects in *rcp2* mutants are somehow conveyed to the nucleus through retrograde signaling, which reduces transcription of all CBP genes. Again, the mechanism for this coordinated regulation of carotenoid biosynthesis genes is still unknown, and almost certainly indirect.

Seeds

Seed carotenoids are critical for ABA biosynthesis and seed dormancy, as well as protecting seeds from ROS damage. Therefore, carotenoids contribute to successful germination (Howitt and Pogson, 2006). In *Arabidopsis* and *Nicotiana plumbaginifolia*, it has been shown that *ZEP* transcript levels increase during seed development, peaking just before the accumulation of ABA (Audran et al., 1998; Audran et al., 2001).

Very few transcriptional regulators of seed carotenoid biosynthesis have been identified (**Figure 6**). In maize, the endosperm P-box and AACA motif regulatory sequences are

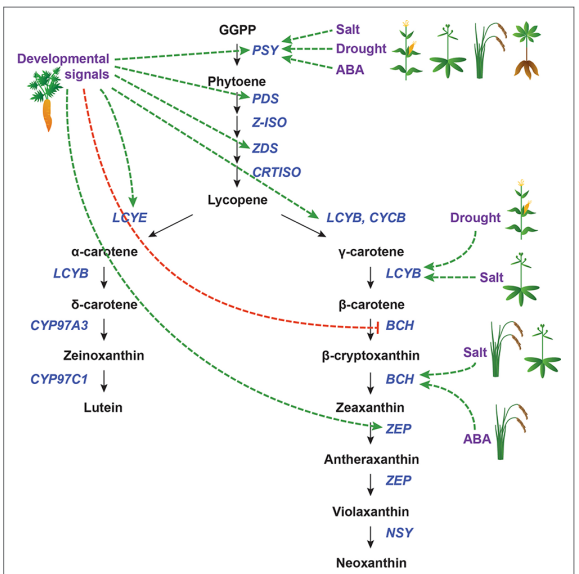

FIGURE 6 | Transcriptional regulation of CBP genes in roots. The regulation of CBP genes in root tissues. Icons indicate the species (carrot, cassava, maize, rice, and *Arabidopsis*). Developmental and environmental cues are shown in purple. The carotenoid biosynthesis pathway is shown in black, with carotenoid biosynthesis genes indicated in dark blue. Carotenoid regulators discussed in the paper are shown in light blue. Green arrows indicate positive regulation, while blunt red arrows indicate negative regulation. Dotted lines show indirect/unknown interactions.

bound by P-box binding factor (PBF) and GAMYB proteins, respectively. The *ZmBCH2* promoter contains both elements and is bound *in vitro* by PBF and GAMYB (Jin et al., 2019). A transient assay in maize showed that overexpression of each transcription factor alone increased *ZmBCH2* transcript levels, but together, the effect was not additive. This regulation of *ZmBCH2* is probably tied to ABA biosynthesis, and not carotenoid accumulation, as maize seeds accumulate lutein (a separate branch of the pathway).

It is perhaps surprising that so little is known about CBP transcriptional regulation in seeds, given the developmental and economic importance of seed carotenoids. This may be because many carotenoid-containing seeds primarily accumulate lutein (e.g., wheat, maize, millet, sunflower, pumpkin, canola), and the regulation of the α-carotene branch of the pathway is little understood (Howitt and Pogson, 2006). Additionally, promoter screens for late pathway carotenoid biosynthesis genes are rarely performed and/or reported, perhaps due to a biased focus on early pathway genes like *PSY*.

Roots

Although most roots do not produce carotenoids in appreciable amounts, the CBP is active to provide the precursors for ABA biosynthesis (Rock and Zeevaart, 1991; Bartley and Scolnik, 1995). ABA induces expression change of stress-related genes in response to dehydration (reviewed in Shinozaki and Yamaguchi-Shinozaki, 2007). Thus, the transcriptional regulation of carotenoid biosynthesis is key to water stress responses in plants. Additionally, some crop plants (e.g., sweet potatoes and carrots) accumulate large amounts of carotenoids in storage roots, where developmental signals regulate CBP genes over the course of root maturation.

Abiotic Stress Responses

Because roots are responsible for water and nutrient acquisition, root tissues must be able to respond to environmental cues. Of particular relevance to carotenoid biosynthesis is the sensing of and response to drought and salt stress (**Figure 6**). These mechanisms are related and overlapping (Zhu, 2002) and will thus be considered together. Rice (*Oryza sativa*) and maize each have three *PSY* paralogues, one of which (*PSY3*) appears to be strongly inducible by drought, salt, and exogenous ABA application. *OsZEP* and *ZmBCH* are also moderately upregulated by these stressors in rice and maize, respectively (Welsch et al., 2008; Li et al., 2008b).

In cassava (*Manihot esculenta*), there are also three copies of *PSY*. However, *MePSY3* is expressed at extremely low levels, and its transcription is not affected by salt or drought stress. Instead, *MePSY1* and *MePSY2*, which are normally expressed in photosynthetic tissues, are upregulated in roots to mediate the salt/drought response (Arango et al., 2010).

In *Arabidopsis*, which has only one *PSY* gene, salt stress upregulates *AtPSY* in the root but not the shoot. There is also a root-specific increase in the transcript levels of *AtBCH1*, *AtBCH2*, and *AtZEP*, but not other CBP genes. It was speculated that ABA signaling transcription factors might bind the *AtPSY* promoter preferentially in the root (Ruiz-Sola et al., 2014).

It appears that the transcriptional regulation of *PSY* is a conserved mechanism for drought/salt stress response in plants. When multiple paralogues of *PSY* are present in a genome, there may be specialization in function, perhaps mediated by differences in *cis*-regulatory elements (CREs). In cases where no specialization is evident, *PSY* regulation is tissue-specific: in both cassava and *Arabidopsis*, salt/drought stress upregulates *PSY* specifically in the root, with leaves exhibiting no change in *PSY* mRNA levels. Some downstream genes in the β-carotene branch of the CBP (which leads to ABA) are also altered by drought/salt stress, but the affected genes appear to be species-specific, with no later pathway genes being consistently responsive.

Storage Roots

In carrots (*Daucus carota*), the expression levels of most CBP genes (*DcPSY1/2*, *DcPDS*, *DcZDS1/2*, *DcLCYE*, *DcLCYB*, and *DcZEP*) increase over root development in several different carrot cultivars, including white carrots, which ultimately do not sequester carotenoids (Clotault et al., 2008). White carrots overexpressing a bacterial orthologue of *PSY* (*crtB*) in roots had significantly increased carotenoid levels (though not nearly as much β-carotene as orange carrots, suggesting that other factors also mediate this process) (Maass et al., 2009). This demonstrated that transcriptional regulation could play an important role in carotenoid accumulation in carrot roots.

In Fuentes et al. (2012), carrot roots were grown either underground or in light, and the mRNA levels of multiple CBP genes were assessed. Light-grown carrots accumulated a carotenoid profile similar to that of leaves, while dark-grown carrots accumulated mostly β-carotene. The expression patterns of most CBP genes mirrored these changes, with the exception of *DcZDS1* and *DcLCYB2* (which were not affected by treatment) and *DcLCYE* (which actually increased in both treatments). As proposed before, transcriptional regulation alone cannot account for these differences. It is important to note that light induced the formation of chloroplasts instead of chromoplasts, which indicates that plastid-to-nucleus retrograde signaling may somehow regulate CBP gene expression.

So Many Regulators, So Little Consensus

A fairly large number of putative transcriptional regulators of carotenoid biosynthesis have been identified from various species and tissue types (**Table S1**), mostly in the past decade. A conundrum emerges from this otherwise exciting progress: why so many candidate regulators but so little consensus? Almost every tissue type in every species studied to date seems to utilize a different group of transcriptional regulators for carotenoid biosynthesis. Perhaps it is not too surprising that the CBP is differentially regulated in various tissue types, as carotenoids serve very different functions in different organs (e.g., in leaves as essential components of the photosynthetic apparatus vs. in flowers and fruits as secondary metabolites), but it is puzzling that each species seems to have evolved its own carotenoid regulators. In our opinion, this conundrum exists at least in part because of the following challenges:

(1) The endogenous functions of some of these putative transcriptional regulators have not been verified through knockout or knockdown experiments (e.g., *CpEIN3a*, *CpNAC1/2*, *CrMYB68*, *CsMADS6*, *CpbHLH1/2*, *AdMYB7*, *ZmPBF*, *ZmGAMYB*). These regulators were usually identified through transcriptome-based co-expression analyses or yeast one-hybrid screens using promoters of CBP genes. Interactions between these regulators and their DNA binding sites in the CBP gene promoters were often tested by *in vitro* gel shift assays and/or dual luciferase assays. Sometimes these regulators were further characterized by transient or stable overexpression in a heterologous host (e.g., tobacco). However, one should be cautious when interpreting these results, as heterologous expression can sometimes be uninformative or even misleading (Kramer, 2015). Before knockout or knockdown data become available, we think these genes should be regarded as "candidate" instead of *bona fide* carotenoid regulators.
(2) Most putative regulators were identified from ripening fruits, especially tomato (e.g., *TAGL1*, *RIN*, *FUL1*, *FUL2*, *SlMADS1*, *SlNAC4*, *SlAP2a*, *SGR1*, *SlHDA3*), making it very difficult to disentangle these regulators' influence on carotenoid biosynthesis from their other ripening roles, which are largely mediated through ethylene signaling. In fact, most of the putative carotenoid regulators identified in tomato are components of the ethylene signaling network (Li et al., 2019). Therefore, it would not be unexpected if these tomato fruit ripening genes do not regulate carotenoid biosynthesis in other tissue types or in non-climacteric fruits.
(3) Current major model systems for carotenoid regulation are somewhat unusual or at least not representative. For example, the best genetic model system, *Arabidopsis*, does not produce chromoplast-containing tissues. The foremost fruit model, tomato, accumulates lycopene and is climacteric, whereas fruits of many other plant species (e.g., orange, papaya) accumulate abundant downstream products (e.g., β-carotene and xanthophylls). These limitations raise the question whether the knowledge gained from these systems is widely applicable to other plant species.
(4) Minimal effort has been put into testing whether the function of a certain regulator identified from one species is conserved in another species. So far, only the PIF1/HY5 regulatory module has been shown to play a role in carotenoid biosynthesis during both *Arabidopsis* photomorphogenesis and the onset of tomato fruit ripening. Even in this case, it is unclear whether PIF1/HY5 function at the onset of tomato fruit ripening is an ancestral feature of all fleshy fruits or was accidentally co-opted from the photomorphogenesis network just in tomatoes.

In addition to these challenges, there are also many gaps in our understanding of transcriptional regulation of carotenoid biosynthesis. For example, we know very little about what regulates most CBP genes downstream of *PSY* in photosynthetic tissues, even in *Arabidopsis*; we know virtually nothing about the transcriptional regulators of CBP genes in the roots of any model systems; we know only three regulators in flowers (i.e., COI1/MYB305, RCP1, and RCP2), and even for these, we know nothing about their functional mechanisms; we know a variety of phytohormones affecting CBP gene expression, but we do not know which transcriptional regulators relay their signals to CBP genes.

FUTURE PERSPECTIVES

The challenges and knowledge gaps discussed above present wonderful opportunities for future carotenoid research. We think the following research directions will be fruitful in understanding how carotenoid biosynthesis is controlled at the transcriptional level:

(1) Testing the function of known putative carotenoid regulators (**Table S1**) across multiple species with well-developed genetic/genomic resources and functional tools. For example, generating knockdown transgenic lines or Clustered Regularly Interspaced Short Palindromic Repeats (CRISPR) mutants of the *SDG8* orthologue in readily transformable species like tomatoes or monkeyflowers would be a straightforward way to test whether the role of this gene in *CRTISO* regulation is conserved across angiosperms or just an oddity in *Arabidopsis*. Likewise, it would be interesting to generate knockdown/knockout lines of *RCP1* or *RCP2* in tomatoes to see whether tomato flower color changes.
(2) Identifying regulators of late pathway CBP genes using promoter screens. The recent study in maize (Jin et al., 2019) where two new regulators were identified using the *ZmBCH2* promoter is a good example. Besides traditional yeast one-hybrid screens, recently developed methods such as CAPTURE (CRISPR Affinity Purification *in siTU* of Regulatory Elements) can be used to identify both transcription factors and chromatin remodelers at a particular promoter site with high specificity (Liu et al., 2017).
(3) Discovering key CREs of the CBP genes in various species. Databases such as PLACE (Higo et al., 1999) and PlantCare (Lescot et al., 2002), in conjunction with phylogenetic shadowing methods (Blanchette and Tompa, 2002), are extremely useful in predicting CREs *in silico*. Additionally, for species that are transformable, a powerful new way to discover CREs *in vivo* is CRISPR/Cas9 genome editing with multiple guide RNAs targeted to a gene promoter (e.g., eight guide RNAs in Rodríguez-Leal et al., 2017). This method can generate a wide range of mutant alleles with deletions of various lengths within the promoter region; and because this method does not rely on *a priori* knowledge of sequence motifs, it allows the discovery of novel CREs.
(4) Integrating multi-omics data (genomics, transcriptomics, proteomics, metabolomics, etc.) towards a more comprehensive understanding of CBP gene expression. With the rapid advances in generating large quantities of high-quality data as well as sophisticated bioinformatics methods and analytical tools, the systems biology approach will allow us to uncover correlations between metabolome and transcriptome profiles,

to identify candidate transcriptional regulators of biosynthetic genes in co-expression modules, and to map regulatory network interactions (e.g., Amiour et al., 2012; Maruyama et al., 2014; Balazadeh et al., 2014; Larsen et al., 2016). We envision that this integrative approach will be particularly helpful in elucidating the "missing" regulators that relay various hormone cues to CBP genes. There are many "omics" resources and databases that could be used for these purposes (Mochida and Shinozaki, 2011; Rai et al., 2017), but there are also many challenges to integrating such data. Experimental design and data quality/curation must be taken into account when combining multiple omics resources (Cavill et al., 2016; Helmy et al., 2016).

(5) Broadening the diversity of "model" systems. For example, citrus would be an excellent system to complement the existing tomato fruit model because it is non-climacteric and accumulates various carotenoids beyond lycopene. In addition, carotenoid-containing, embryogenic citrus calli can be readily produced and transformed (Lu et al., 2018), making them a powerful tool for rigorous tests of gene function. As high-quality genome assemblies and genome editing technologies become more and more accessible, it is not difficult to envision the development of even brand-new model species with interesting/economically important carotenoid phenotypes in the near future.

We believe that these research avenues will lead to many more exciting discoveries in the coming years, which will not only contribute new knowledge on the transcriptional regulation of carotenoid biosynthesis but also likely have a significant impact on carotenoid biofortification of crop plants. So far, most of the efforts towards enhancing carotenoid biosynthesis or engineering novel carotenoid products in staple crops have focused on CBP genes (e.g., aSTARice; Zhu et al., 2018). However, effective biofortification often requires transferring multiple CBP genes simultaneously to the host plant and expressing these transgenes in a coordinated fashion, the latter being a particular challenge in metabolic engineering (Nielsen and Keasling, 2016). Building both transcriptional regulators and CBP genes into a synthetic biology framework will allow us to better coordinate the expression of multiple CBP genes, to make quantitative predictions of metabolic flux, and to rationally design optimal genetic circuits with maximal phenotypic outputs.

AUTHOR CONTRIBUTIONS

LS and Y-WY wrote the manuscript.

FUNDING

Our work on carotenoids is supported by the National Science Foundation (IOS-1558083, IOS-1827645).

ACKNOWLEDGMENTS

We thank members of our laboratory and Drs. Foen Peng, Pam Diggle, Jeff Seemann, and Qinlong Zhu for discussions.

SUPPLEMENTARY MATERIAL

The Supplementary Material for this article can be found online at: https://www.frontiersin.org/articles/10.3389/fpls.2019.01017/full#supplementary-material

REFERENCES

Alba, R., Payton, P., Fei, Z., McQuinn, R., Debbie, P., Martin, G. B., et al. (2005). Transcriptome and selected metabolite analyses reveal multiple points of ethylene control during tomato fruit development. *Plant Cell* 17 (11), 2954–2965. doi: 10.1105/tpc.105.036053

Alder, A., Jamil, M., Marzorati, M., Bruno, M., Vermathen, M., Bigler, P., et al. (2012). The path from β-carotene to carlactone, a strigolactone-like plant hormone. *Science* 335 (6074), 1348. doi: 10.1126/science.1218094

Amiour, N., Imbaud, S., Clément, G., Agier, N., Zivy, M., Valot, B., et al. (2012). The use of metabolomics integrated with transcriptomic and proteomic studies for identifying key steps involved in the control of nitrogen metabolism in crops such as maize. *J. Exp. Bot.* 63 (14), 5017–5033. doi: 10.1093/jxb/ers186

Ampomah-Dwamena, C., Thrimawithana, A. H., Dejnoprat, S., Lewis, D., Espley, R. V., and Allan, A. C. (2019). A kiwifruit (*Actinidia deliciosa*) R2R3-MYB transcription factor modulates chlorophyll and carotenoid accumulation. *New Phytol.* 221 (1), 309–325. doi: 10.1111/nph.15362

Andersson, A., Keskitalo, J., Sjödin, A., Bhalerao, R., Sterky, F., Wissel, K., et al. (2004). A transcriptional timetable of autumn senescence. *Genome Biol.* 5 (4), R24. doi: 10.1186/gb-2004-5-4-r24

Andrade, P., Caudepón, D., Altabella, T., Arró, M., Ferrer, A., and Manzano, D. (2017). Complex interplays between phytosterols and plastid development. *Plant Signal Behav.* 12 (11), e1387708. doi: 10.1080/15592324.2017.1387708

Arango, J., Wüst, F., Beyer, P., and Welsch, R. (2010). Characterization of phytoene synthases from cassava and their involvement in abiotic stress-mediated responses. *Planta* 232 (5), 1251–1262. doi: 10.1007/s00425-010-1250-6

Arango, J., Beltrán, J., Nuñez, J., and Chavarriaga, P. (2016). "Evidence of epigenetic mechanisms affecting carotenoids," in *Carotenoids in Nature* (Cham, Switzerland: Springer) 295–307.

Audran, C., Borel, C., Frey, A., Sotta, B., Meyer, C., Simonneau, T., et al. (1998). Expression studies of the zeaxanthin epoxidase gene in *Nicotiana plumbaginifolia*. *J. Plant Physiol.* 118 (3), 1021–1028. doi: 10.1104/pp.118.3.1021

Audran, C., Liotenberg, S., Gonneau, M., North, H., Frey, A., Tap-Waksman, K., et al. (2001). Localisation and expression of zeaxanthin epoxidase mRNA in *Arabidopsis* in response to drought stress and during seed development. *Funct. Plant Biol.* 28 (12), 1161–1173.

Auldridge, M. E., McCarty, D. R., and Klee, H. J. (2006). Plant carotenoid cleavage oxygenases and their apocarotenoid products. *Curr. Opin. Plant Biol.* 9 (3), 315–321. doi: 10.1016/j.pbi.2006.03.005

Avendaño-Vázquez, A., Cordoba, E., Llamas, E., San Román, C., Nisar, N., Torre, D. L., et al. (2014). An uncharacterized apocarotenoid-derived signal generated in ζ-carotene desaturase mutants regulates leaf development and the expression of chloroplast and nuclear genes in *Arabidopsis*. *Plant Cell* 26 (6), 2524–2537. doi: 10.1105/tpc.114.123349

Bae, G., and Choi, G. (2008). Decoding of light signals by plant phytochromes and their interacting proteins. *Annu. Rev. Plant Biol.* 59 (1), 281–311. doi: 10.1146/annurev.arplant.59.032607.092859

Balazadeh, S., Schildhauer, J., Araújo, W. L., Munné-Bosch, S., Fernie, A. R., Proost, S., et al. (2014). Reversal of senescence by N resupply to N-starved *Arabidopsis thaliana*: transcriptomic and metabolomic consequences. *J. Exp. Bot.* 65 (14), 3975–3992. doi: 10.1093/jxb/eru119

Baroli, I., and Niyogi, K. K. (2000). Molecular genetics of xanthophyll dependent photoprotection in green algae and plants. *Philos. Trans. R. Soc. Lond., B, Biol. Sci.* 355 (1402), 1385–1394. doi: 10.1098/rstb.2000.0700

Bartley, G. E., and Scolnik, P. A. (1995). Plant carotenoids: pigments for photoprotection, visual attraction, and human health. *Plant Cell* 7 (7), 1027–1038. doi: 10.1105/tpc.7.7.1027

Bemer, M., Karlova, R., Ballester, A. R., Tikunov, Y. M., Bovy, A. G., Wolters-Arts, M., et al. (2012). The tomato FRUITFULL homologs TDR4/FUL1 and MBP7/FUL2 regulate ethylene-independent aspects of fruit ripening. *Plant Cell* 24 (11), 4437–4451. doi: 10.1105/tpc.112.103283

Biswal, B. (1995). Carotenoid catabolism during leaf senescence and its control by light. *J. Photochem. Photobiol. B, Biol.* 30 (1), 3–13. doi: 10.1016/1011-1344(95)07197-A

Blanchette, M., and Tompa, M. (2002). Discovery of regulatory elements by a computational method for phylogenetic footprinting. *Genome Res.* 12 (5), 739–748. doi: 10.1101/gr.6902

Bou-Torrent, J., Toledo-Ortiz, G., Ortiz-Alcaide, M., Cifuentes-Esquivel, N., Halliday, K. J., Martinez-García, J., et al. (2015). Regulation of carotenoid biosynthesis by shade relies on specific subsets of antagonistic transcription factors and cofactors. *J. Plant Physiol.* 169 (3), 1584. doi: 10.1104/pp.15.00552

Bradshaw, H., Jr., and Schemske, D. W. (2003). Allele substitution at a flower colour locus produces a pollinator shift in monkeyflowers. *Nature* 426 (6963), 176. doi: 10.1038/nature02106

Breeze, E., Harrison, E., Mchattie, S., Hughes, L., Hickman, R., Hill, C., et al. (2011). High-resolution temporal profiling of transcripts during *Arabidopsis* leaf senescence reveals a distinct chronology of processes and regulation. *Plant Cell* 23 (3), 873–894. doi: 10.1105/tpc.111.083345

Britton, G., and Young, A. J. (1989). "Chloroplast carotenoids: function, biosynthesis and effects of stress and senescence," in *Trends in Photosynthesis Research*. Eds. U. C. Biswal and G. Britton (India: Agro Botanical Publishers), 303–319.

Brown, B. A., Cloix, C., Jiang, G. H., Kaiserli, E., Herzyk, P., Kliebenstein, D. J., et al. (2005). A UV-B–specific signaling component orchestrates plant UV protection. *Proc Natl Acad Sci* 102 (50), 18225–18230. doi: 10.1073/pnas.0507187102

Brown, B. A., and Jenkins, G. I. (2008). UV-B signaling pathways with different fluence-rate response profiles are distinguished in mature *Arabidopsis* leaf tissue by requirement for UVR8, HY5, and HYH. *J. Plant Physiol.* 146 (2), 576–588. doi: 10.1104/pp.107.108456

Catalá, R., Medina, J., and Salinas, J. (2011). Integration of low temperature and light signaling during cold acclimation response in *Arabidopsis*. *Proc. Natl. Acad. Sci. U. S. A.* 108 (39), 16475. doi: 10.1073/pnas.1107161108

Cavill, R., Jennen, D., Kleinjans, J., and Briedé, J. J. (2016). Transcriptomic and metabolomic data integration. *Brief. Bioinformatics* 17 (5), 891–901. doi: 10.1093/bib/bbv090

Cazzonelli, C. I., Cuttriss, A. J., Cossetto, S. B., Pye, W., Crisp, P., Whelan, J., et al. (2009). Regulation of carotenoid composition and shoot branching in *Arabidopsis* by a chromatin modifying histone methyltransferase, SDG8. *Plant Cell* 21 (1), 39–53. doi: 10.1105/tpc.108.063131

Cazzonelli, C. I., and Pogson, B. J. (2010). Source to sink: regulation of carotenoid biosynthesis in plants. *Trends Plant Sci.* 15 (5), 266–274. doi: 10.1016/j.tplants.2010.02.003

Cheminant, S., Wild, M., Bouvier, F., Pelletier, S., Renou, J., Erhardt, M., et al. (2011). DELLAs regulate chlorophyll and carotenoid biosynthesis to prevent photooxidative damage during seedling deetiolation in *Arabidopsis*. *Plant Cell* 23 (5), 1849. doi: 10.1105/tpc.111.085233

Chiou, C., Pan, H., Chuang, Y., and Yeh, K. (2010). Differential expression of carotenoid-related genes determines diversified carotenoid coloration in floral tissues of *Oncidium* cultivars. *Planta* 232 (4), 937–948. doi: 10.1007/s00425-010-1222-x

Chung, M., Vrebalov, J., Alba, R., Lee, J., McQuinn, R., Chung, J., et al. (2010). A tomato (*Solanum lycopersicum*) APETALA2/ERF gene, SlAP2a, is a negative regulator of fruit ripening. *Plant J.* 64 (6), 936–947. doi: 10.1111/j.1365-313X.2010.04384.x

Cloix, C., and Jenkins, G. I. (2008). Interaction of the Arabidopsis UV-B–specific signaling component UVR8 with chromatin. *Mol. Plant* 1 (1), 118–128. doi: 10.1093/mp/ssm012

Clotault, J., Peltier, D., Berruyer, R., Thomas, M., Briard, M., and Geoffriau, E. (2008). Expression of carotenoid biosynthesis genes during carrot root development. *J. Exp. Bot.* 59 (13), 3563–3573. doi: 10.1093/jxb/ern210

Corona, V., Aracri, B., Kosturkova, G., Bartley, G. E., Pitto, L., Giorgetti, L., et al. (1996). Regulation of a carotenoid biosynthesis gene promoter during plant development. *Plant J.* 9 (4), 505–512.

Cutler, S. R., Rodriguez, P. L., Finkelstein, R. R., and Abrams, S. R. (2010). Abscisic acid: emergence of a core signaling network. *Annu. Rev. Plant Biol.* 61, 651–679. doi: 10.1146/annurev-arplant-042809-112122

D'Andrea, L., Simon-Moya, M., Llorente, B., Llamas, E., Marro, M., Loza-Alvarez, P., et al. (2018). Interference with clp protease impairs carotenoid accumulation during tomato fruit ripening. *J. Exp. Bot.* 69 (7), 1557–1568. doi: 10.1093/jxb/erx491

Dalal, M., Chinnusamy, V., and Bansal, K. C. (2010). Isolation and functional characterization of lycopene β-cyclase (CYC-B) promoter from *Solanum habrochaites*. *BMC Plant Biol.* 10 (1), 61. doi: 10.1186/1471-2229-10-61

Dall'Osto, L., Cazzaniga, S., North, H., Marion-Poll, A., and Bassi, R. (2007). The *Arabidopsis* aba4-1 mutant reveals a specific function for neoxanthin in protection against photooxidative stress. *Plant Cell* 19 (3), 1048. doi: 10.1105/tpc.106.049114

Dall'Osto, L., Holt, N. E., Kaligotla, S., Fuciman, M., Cazzaniga, S., Carbonera, D., et al. (2012). Zeaxanthin protects plant photosynthesis by modulating chlorophyll triplet yield in specific light-harvesting antenna subunits. *J. Biol. Chem.* 287 (50), 41820–41834. doi: 10.1074/jbc.M112.405498

Delker, C., Sonntag, L., James, G., Janitza, P., Ibañez, C., Ziermann, H., et al. (2014). The DET1–COP1–HY5 pathway constitutes a multipurpose signaling module regulating plant photomorphogenesis and thermomorphogenesis. *Cell Rep.* 9 (6), 1983–1989. doi: 10.1016/j.celrep.2014.11.043

Demmig-Adams, B., and Adams, W. W., III (1996). The role of xanthophyll cycle carotenoids in the protection of photosynthesis. *Trends Plant Sci.* 1 (1), 21–26. doi: 10.1016/S1360-1385(96)80019-7

Dong, J., Tang, D., Gao, Z., Yu, R., Li, K., He, H., et al. (2014). *Arabidopsis* DE-ETIOLATED1 represses photomorphogenesis by positively regulating phytochrome-interacting factors in the dark. *Plant Cell* 26 (9), 3630. doi: 10.1105/tpc.114.130666

Dong, T., Hu, Z., Deng, L., Wang, Y., Zhu, M., Zhang, J., et al. (2013). A tomato MADS-box transcription factor, SlMADS1, acts as a negative regulator of fruit ripening. *J. Plant Physiol.* 163 (2), 1026–1036. doi: 10.1104/pp.113.224436

Dudareva, N., Negre, F., Nagegowda, D. A., and Orlova, I. (2006). Plant volatiles: recent advances and future perspectives. *Crit. Rev. Plant Sci.* 25 (5), 417–440. doi: 10.1080/07352680600899973

Emiliani, J., D'Andrea, L., Ferreyra, M. L. F., Maulión, E., Rodriguez, E., Rodriguez-Concepción, M., et al. (2018). A role for β, β-xanthophylls in *Arabidopsis* UV-B photoprotection. *J. Exp. Bot.* 69 (20), 4921–4933. doi: 10.1093/jxb/ery242

Enfissi, E. M. A., Nogueira, M., Bramley, P. M., and Fraser, P. D. (2017). The regulation of carotenoid formation in tomato fruit. *Plant J.* 89 (4), 774–788. doi: 10.1111/tpj.13428

Eriksson, E. M., Bovy, A., Manning, K., Harrison, L., Andrews, J., De Silva, J., et al. (2004). Effect of the colorless non-ripening mutation on cell wall biochemistry and gene expression during tomato fruit development and ripening. *J. Plant Physiol.* 136 (4), 4184–4197. doi: 10.1104/pp.104.045765

Favory, J. J., Stec, A., Gruber, H., Rizzini, L., Oravecz, A., Funk, M., et al. (2009). Interaction of COP1 and UVR8 regulates UV-B–induced photomorphogenesis and stress acclimation in *Arabidopsis*. *EMBO J.* 28 (5), 591–601. doi: 10.1038/emboj.2009.4

Frank, H. A., and Cogdell, R. J. (1996). Carotenoids in photosynthesis. *Photochem. Photobiol.* 63 (3), 257–264. doi: 10.1111/j.1751-1097.1996.tb03022.x

Fraser, P. D., Truesdale, M. R., Bird, C. R., Schuch, W., and Bramley, P. M. (1994). Carotenoid biosynthesis during tomato fruit development (evidence for tissue-specific gene expression). *J. Plant Physiol.* 105 (1), 405–413. doi: 10.1104/pp.105.1.405

Fu, C., Han, Y., Fan, Z., Chen, J., Chen, W., Lu, W., et al. (2016). The papaya transcription factor CpNAC1 modulates carotenoid biosynthesis through activating phytoene desaturase genes CpPDS2/4 during fruit ripening. *J. Agric. Food Chem.* 64 (27), 5454–5463. doi: 10.1021/acs.jafc.6b01020

Fu, C., Han, Y., Kuang, J., Chen, J., and Lu, W. (2017). Papaya CpEIN3a and CpNAC2 co-operatively regulate carotenoid biosynthesis-related genes CpPDS2/4, CpLCY-e and CpCHY-b during fruit ripening. *Plant Cell Physiol.* 58 (12), 2155–2165. doi: 10.1093/pcp/pcx149

Fuentes, P., Pizarro, L., Moreno, J. C., Handford, M., Rodriguez-Concepcion, M., and Stange, C. (2012). Light-dependent changes in plastid differentiation influence carotenoid gene expression and accumulation in carrot roots. *Plant Mol. Biol.* 79 (1–2), 47–59. doi: 10.1007/s11103-012-9893-2

Fujisawa, M., Nakano, T., and Ito, Y. (2011). Identification of potential target genes for the tomato fruit-ripening regulator RIN by chromatin immunoprecipitation. *BMC Plant Biol.* 11 (1), 26. doi: 10.1186/1471-2229-11-26

Fujisawa, M., Shima, Y., Higuchi, N., Nakano, T., Koyama, Y., Kasumi, T., et al. (2012). Direct targets of the tomato-ripening regulator RIN identified by transcriptome and chromatin immunoprecipitation analyses. *Planta* 235 (6), 1107–1122. doi: 10.1007/s00425-011-1561-2

Fujisawa, M., Nakano, T., Shima, Y., and Ito, Y. (2013). A large-scale identification of direct targets of the tomato MADS box transcription factor RIPENING INHIBITOR reveals the regulation of fruit ripening. *Plant Cell* 25 (2), 371–386. doi: 10.1105/tpc.112.108118

Fujisawa, M., Shima, Y., Nakagawa, H., Kitagawa, M., Kimbara, J., Nakano, T., et al. (2014). Transcriptional regulation of fruit ripening by tomato FRUITFULL homologs and associated MADS box proteins. *Plant Cell* 26 (1), 89–101. doi: 10.1105/tpc.113.119453

Galpaz, N., Ronen, G., Khalfa, Z., Zamir, D., and Hirschberg, J. (2006). A chromoplast-specific carotenoid biosynthesis pathway is revealed by cloning of the tomato white-flower locus. *Plant Cell* 18 (8), 1947–1960. doi: 10.1105/tpc.105.039966

Gan, S., and Amasino, R. M. (1997). Making sense of senescence (molecular genetic regulation and manipulation of leaf senescence). *J. Plant Physiol.* 113 (2), 313. doi: 10.1104/pp.113.2.313

Gandikota, M., Birkenbihl, R. P., Höhmann, S., Cardon, G. H., Saedler, H., and Huijser, P. (2007). The miRNA156/157 recognition element in the 3′ UTR of the *Arabidopsis* SBP box gene SPL3 prevents early flowering by translational inhibition in seedlings. *Plant J.* 49 (4), 683–693. doi: 10.1111/j.1365-313X.2006.02983.x

Giménez, E., Pineda, B., Capel, J., Antón, M. T., Atarés, A., Pérez-Martín, F., et al. (2010). Functional analysis of the Arlequin mutant corroborates the essential role of the Arlequin/TAGL1 gene during reproductive development of tomato. *PLoS One* 5 (12), e14427. doi: 10.1371/journal.pone.0014427

Giovannoni, J. J. (2007). Fruit ripening mutants yield insights into ripening control. *Curr. Opin. Plant Biol.* 10 (3), 283–289. doi: 10.1016/j.pbi.2007.04.008

Giovannoni, J., Nguyen, C., Ampofo, B., Zhong, S., and Fei, Z. (2017). The epigenome and transcriptional dynamics of fruit ripening. *Annu. Rev. Plant Biol.* 68, 61–84.

Giuliano, G., Bartley, G. E., and Scolnik, P. A. (1993). Regulation of carotenoid biosynthesis during tomato development. *Plant Cell* 5 (4), 379–387. doi: 10.1105/tpc.5.4.379

Goodwin, T., and Britton, G. W. (1988). "Distribution and analysis of carotenoids," in *Plant Pigments*. Ed. T. W. Goodwin (London: Academic Press), 62–132.

Grassi, S., Piro, G., Lee, J. M., Zheng, Y., Fei, Z., Dalessandro, G., et al. (2013). Comparative genomics reveals candidate carotenoid pathway regulators of ripening watermelon fruit. *BMC Genomics* 14 (1), 781. doi: 10.1186/1471-2164-14-781

Guo, J., Hu, Z., Yu, X., Li, A., Li, F., Wang, Y., et al. (2018). A histone deacetylase gene, SlHDA3, acts as a negative regulator of fruit ripening and carotenoid accumulation. *Plant Cell Rep.* 37 (1), 125–135. doi: 10.1007/s00299-017-2211-3

Ha, S., Kim, J., Park, J., Lee, S., and Cho, K. (2007). A comparison of the carotenoid accumulation in capsicum varieties that show different ripening colours: deletion of the capsanthin–capsorubin synthase gene is not a prerequisite for the formation of a yellow pepper. *J. Exp. Bot.* 58 (12), 3135–3144. doi: 10.1093/jxb/erm132

Hao, Y., Hu, G., Breitel, D., Liu, M., Mila, I., Frasse, P., et al. (2015). Auxin response factor SlARF2 is an essential component of the regulatory mechanism controlling fruit ripening in tomato. *PLoS Genetics* 11 (12), e1005649. doi: 10.1371/journal.pgen.1005649

Hashimoto, H., Uragami, C., and Cogdell, R. J. (2016). "Carotenoids and photosynthesis," in *Carotenoids in Nature* (Cham, Switzerland: Springer), 111–139.

Havaux, M. (1998). Carotenoids as membrane stabilizers in chloroplasts. *Trends Plant Sci.* 3 (4), 147–151. doi: 10.1016/S1360-1385(98)01200-X

Helmy, M., Crits-Christoph, A., and Bader, G. D. (2016). Ten simple rules for developing public biological databases. *PLoS Comput. Biol.* 12 (11), e1005128. doi: 10.1371/journal.pcbi.1005128

Higo, K., Ugawa, Y., Iwamoto, M., and Korenaga, T. (1999). Plant cis-acting regulatory DNA elements (PLACE) database: 1999. *Nucleic Acids Res.* 27 (1), 297–300. doi: 10.1093/nar/27.1.297

Hirschberg, J. (2001). Carotenoid biosynthesis in flowering plants. *Curr. Opin. Plant Biol.* 4 (3), 210–218. doi: 10.1016/S1369-5266(00)00163-1

Hou, X., Rivers, J., León, P., McQuinn, R. P., and Pogson, B. J. (2016). Synthesis and function of apocarotenoid signals in plants. *Trends Plant Sci.* 21 (9), 792–803. doi: 10.1016/j.tplants.2016.06.001

Howitt, C. A., and Pogson, B. J. (2006). Carotenoid accumulation and function in seeds and non-green tissues. *Plant Cell Environ.* 29 (3), 435–445. doi: 10.1111/j.1365-3040.2005.01492.x

Itkin, M., Seybold, H., Breitel, D., Rogachev, I., Meir, S., and Aharoni, A. (2009). TOMATO AGAMOUS-LIKE 1 is a component of the fruit ripening regulatory network. *Plant J.* 60 (6), 1081–1095. doi: 10.1111/j.1365-313X.2009.04064.x

Ito, Y., Kitagawa, M., Ihashi, N., Yabe, K., Kimbara, J., Yasuda, J., et al. (2008). DNA-binding specificity, transcriptional activation potential, and the rin mutation effect for the tomato fruit-ripening regulator RIN. *Plant J.* 55 (2), 212–223. doi: 10.1111/j.1365-313X.2008.03491.x

Jahns, P., and Holzwarth, A. R. (2012). The role of the xanthophyll cycle and of lutein in photoprotection of photosystem II. *BBA-Bioenergetics* 1817 (1), 182–193. doi: 10.1016/j.bbabio.2011.04.012

Jia, K., Baz, L., and Al-Babili, S. (2017). From carotenoids to strigolactones. *J. Exp. Bot.* 69 (9), 2189–2204. doi: 10.1093/jxb/erx476

Jiao, Y., Lau, O. S., and Deng, X. W. (2007). Light-regulated transcriptional networks in higher plants. *Nat. Rev. Genet.* 8 (3), 217. doi: 10.1038/nrg2049

Jin, X., Bai, C., Bassie, L., Nogareda, C., Romagosa, I., Twyman, R. M., et al. (2019). ZmPBF and ZmGAMYB transcription factors independently transactivate the promoter of the maize (*Zea mays*) β-carotene hydroxylase 2 gene. *New Phytol.* 222 (2), 793–804. doi: 10.1111/nph.15614

Karlova, R., Rosin, F. M., Busscher-Lange, J., Parapunova, V., Do, P. T., Fernie, A. R., et al. (2011). Transcriptome and metabolite profiling show that APETALA2a is a major regulator of tomato fruit ripening. *Plant Cell* 23 (3), 923–941. doi: 10.1105/tpc.110.081273

Kim, D. H., Yamaguchi, S., Lim, S., Oh, E., Park, J., Hanada, A., et al. (2008). SOMNUS, a CCCH-type zinc finger protein in *Arabidopsis*, negatively regulates light-dependent seed germination downstream of PIL5. *Plant Cell* 20 (5), 1260–1277. doi: 10.1105/tpc.108.058859

Kim, J., Kang, H., Park, J., Kim, W., Yoo, J., Lee, N., et al. (2016). PIF1-interacting transcription factors and their binding sequence elements determine the *in vivo* targeting sites of PIF1. *Plant Cell* 28 (6), 1388–1405. doi: 10.1105/tpc.16.00125

Kishimoto, S., Oda-Yamamizo, C., and Ohmiya, A. (2018). Regulation of carotenoid pigmentation in corollas of petunia. *Plant Mol. Biol. Rep.* 36 (4), 632–642. doi: 10.1007/s11105-018-1107-x

Klee, H. J., and Giovannoni, J. J. (2011). Genetics and control of tomato fruit ripening and quality attributes. *Annu. Rev. Genet.* 45 (1), 41–59. doi: 10.1146/annurev-genet-110410-132507

Kolotilin, I., Koltai, H., Tadmor, Y., Bar-Or, C., Reuveni, M., Meir, A., et al. (2007). Transcriptional profiling of high pigment-2^{dg} tomato mutant links early fruit plastid biogenesis with its overproduction of phytonutrients. *J. Plant Physiol.* 145 (2), 389–401. doi: 10.1104/pp.107.102962

Kramer, E. M. (2015). A stranger in a strange land: the utility and interpretation of heterologous expression. *Front. Plant Sci.* 6, 734. doi: 10.3389/fpls.2015.00734

Lau, O. S., and Deng, X. W. (2012). The photomorphogenic repressors COP1 and DET1: 20 years later. *Trends Plant Sci.* 17 (10), 584–593. doi: 10.1016/j.tplants.2012.05.004

Larsen, P. E., Sreedasyam, A., Trivedi, G., Desai, S., Dai, Y., Cseke, L. J., et al. (2016). Multi-omics approach identifies molecular mechanisms of plant–fungus mycorrhizal interaction. *Front. Plant Sci.* 6, 1061. doi: 10.3389/fpls.2015.01061

Lescot, M., Déhais, P., Thijs, G., Marchal, K., Moreau, Y., Van de Peer, Y., et al. (2002). PlantCARE, a database of plant cis-acting regulatory elements and a

portal to tools for in silico analysis of promoter sequences. *Nucleic Acids Res.* 30 (1), 325–327. doi: 10.1093/nar/30.1.325

Levin, I., Frankel, P., Gilboa, N., Tanny, S., and Lalazar, A. (2003). The tomato dark green mutation is a novel allele of the tomato homolog of the DEETIOLATED1 gene. *Theor. Appl. Genet.* 106 (3), 454–460. doi: 10.1007/s00122-002-1080-4

Li, F., Vallabhaneni, R., Yu, J., Rocheford, T., and Wurtzel, E. T. (2008a). The maize phytoene synthase gene family: overlapping roles for carotenogenesis in endosperm, photomorphogenesis, and thermal stress tolerance. *J. Plant Physiol.* 147 (3), 1334–1346. doi: 10.1104/pp.108.122119

Li, F., Vallabhaneni, R., and Wurtzel, E. T. (2008b). PSY3, a new member of the phytoene synthase gene family conserved in the Poaceae and regulator of abiotic stress–induced root carotenogenesis. *J. Plant Physiol.* 146 (3), 1333–1345. doi: 10.1104/pp.107.111120

Li, L., Yuan, H., Zeng, Y., and Xu, Q. (2016). "Plastids and carotenoid accumulation," in *Carotenoids in Nature* (Cham, Switzerland: Springer), 273–293.

Li, S., Chen, K., and Grierson, D. (2019). A critical evaluation of the role of ethylene and MADS transcription factors in the network controlling fleshy fruit ripening. *New Phytol.* 221 (4), 1724–1741. doi: 10.1111/nph.15545

Lieberman, M., Segev, O., Gilboa, N., Lalazar, A., and Levin, I. (2004). The tomato homolog of the gene encoding UV-damaged DNA binding protein 1 (DDB1) underlined as the gene that causes the high pigment-1 mutant phenotype. *Theor. Appl. Genet.* 108 (8), 1574–1581. doi: 10.1007/s00122-004-1584-1

Lim, P. O., Kim, H. J., and Gil Nam, H. (2007). Leaf senescence. *Annu. Rev. Plant Biol.*58, 115–136. doi: 10.1146/annurev.arplant.57.032905.105316

Lin, Z., Hong, Y., Yin, M., Li, C., Zhang, K., and Grierson, D. (2008). A tomato HD-Zip homeobox protein, LeHB-1, plays an important role in floral organogenesis and ripening. *Plant J.* 55 (2), 301–310. doi: 10.1111/j.1365-313X.2008.03505.x

Liu, G., Ren, G., Guirgis, A., and Thornburg, R. W. (2009). The MYB305 transcription factor regulates expression of nectarin genes in the ornamental tobacco floral nectary. *Plant Cell* 21 (9), 2672–2687. doi: 10.1105/tpc.108.060079

Liu, L., Jia, C., Zhang, M., Chen, D., Chen, S., Guo, R., et al. (2014). Ectopic expression of a BZR1-1D transcription factor in brassinosteroid signalling enhances carotenoid accumulation and fruit quality attributes in tomato. *Plant Biotechnol. J.* 12 (1), 105–115. doi: 10.1111/pbi.12121

Liu, L., Wei, J., Zhang, M., Zhang, L., Li, C., and Wang, Q. (2012). Ethylene independent induction of lycopene biosynthesis in tomato fruits by jasmonates. *J. Exp. Bot.* 63 (16), 5751–5761. doi: 10.1093/jxb/ers224

Liu, L., Shao, Z., Zhang, M., and Wang, Q. (2015a). Regulation of carotenoid metabolism in tomato. *Mol. Plant* 8 (1), 28–39. doi: 10.1016/j.molp.2014.11.006

Liu, M., Pirrello, J., Chervin, C., Roustan, J., and Bouzayen, M. (2015b). Ethylene control of fruit ripening: revisiting the complex network of transcriptional regulation. *J. Plant Physiol.* 169 (4), 2380. doi: 10.1104/pp.15.01361

Liu, X., Zhang, Y., Chen, Y., Li, M., Zhou, F., Li, K., et al. (2017). In situ capture of chromatin interactions by biotinylated dCas9. *Cell* 170 (5), 1028–1043. doi: 10.1016/j.cell.2017.08.003

Llorente, B., D'andrea, L., Ruiz-Sola, M. A., Botterweg, E., Pulido, P., Andilla, J., et al. (2016). Tomato fruit carotenoid biosynthesis is adjusted to actual ripening progression by a light-dependent mechanism. *Plant J.* 85 (1), 107–119. doi: 10.1111/tpj.13094

Llorente, B., Martinez-Garcia, J., Stange, C., and Rodriguez-Concepcion, M. (2017). Illuminating colors: regulation of carotenoid biosynthesis and accumulation by light. *Curr. Opin. Plant Biol.* 37, 49–55. doi: 10.1016/j.pbi.2017.03.011

López-Ráez, J. A., Charnikhova, T., Gómez-Roldán, V., Matusova, R., Kohlen, W., De Vos, R., et al. (2008). Tomato strigolactones are derived from carotenoids and their biosynthesis is promoted by phosphate starvation. *New Phytol.* 178 (4), 863–874. doi: 10.1111/j.1469-8137.2008.02406.x

Lu, S., Van Eck, J., Zhou, X., Lopez, A. B., O'Halloran, D. M., Cosman, K. M., et al. (2006). The cauliflower or gene encodes a DnaJ cysteine-rich domain–containing protein that mediates high levels of beta-carotene accumulation. *Plant Cell* 18 (12), 3594–3605. doi: 10.1105/tpc.106.046417

Lu, S., Zhang, Y., Zhu, K., Yang, W., Ye, J., Chai, L., et al. (2018). The citrus transcription factor CsMADS6 modulates carotenoid metabolism by directly regulating carotenogenic genes. *J. Plant Physiol.* 176 (4), 2657–2676. doi: 10.1104/pp.17.01830

Luo, Z., Zhang, J., Li, J., Yang, C., Wang, T., Ouyang, B., et al. (2013). A STAY-GREEN protein SlSGR1 regulates lycopene and β-carotene accumulation by interacting directly with SlPSY1 during ripening processes in tomato. *New Phytol.* 198 (2), 442–452. doi: 10.1111/nph.12175

Ma, N., Feng, H., Meng, X., Li, D., Yang, D., Wu, C., et al. (2014). Overexpression of tomato SlNAC1 transcription factor alters fruit pigmentation and softening. *BMC Plant Biol.* 14 (1), 351. doi: 10.1186/s12870-014-0351-y

Maass, D., Arango, J., Wüst, F., Beyer, P., and Welsch, R. (2009). Carotenoid crystal formation in *Arabidopsis* and carrot roots caused by increased phytoene synthase protein levels. *PloS One* 4 (7), e6373. doi: 10.1371/journal.pone.0006373

Manning, K., Tör, M., Poole, M., Hong, Y., Thompson, A. J., King, G. J., et al. (2006). A naturally occurring epigenetic mutation in a gene encoding an SBP-box transcription factor inhibits tomato fruit ripening. *Nat. Genet.* 38 (8), 948. doi: 10.1038/ng1841

Martel, C., Vrebalov, J., Tafelmeyer, P., and Giovannoni, J. J. (2011). The tomato MADS-box transcription factor RIPENING INHIBITOR interacts with promoters involved in numerous ripening processes in a COLORLESS NONRIPENING–dependent manner. *J. Plant Physiol.* 157 (3), 1568. doi: 10.1104/pp.111.181107

Maruyama, K., Urano, K., Yoshiwara, K., Morishita, Y., Sakurai, N., Suzuki, H., et al. (2014). Integrated analysis of the effects of cold and dehydration on rice metabolites, phytohormones, and gene transcripts. *J. Plant Physiol.* 164 (4), 1759–1771. doi: 10.1104/pp.113.231720

Meier, S., Tzfadia, O., Vallabhaneni, R., Gehring, C., and Wurtzel, E. T. (2011). A transcriptional analysis of carotenoid, chlorophyll and plastidial isoprenoid biosynthesis genes during development and osmotic stress responses in *Arabidopsis thaliana. BMC Syst. Biol.* 5 (1), 77. doi: 10.1186/1752-0509-5-77

Meng, C., Yang, D., Ma, X., Zhao, W., Liang, X., Ma, N., et al. (2016). Suppression of tomato SlNAC1 transcription factor delays fruit ripening. *J. Plant Physiol.* 193, 88–96. doi: 10.1016/j.jplph.2016.01.014

Middleton, E. M., and Teramura, A. H. (1993). The role of flavonol glycosides and carotenoids in protecting soybean from ultraviolet-B damage. *J. Plant Physiol.* 103 (3), 741–752. doi: 10.1104/pp.103.3.741

Mochida, K., and Shinozaki, K. (2011). Advances in omics and bioinformatics tools for systems analyses of plant functions. *Plant Cell Physiol.* 52 (12), 2017–2038. doi: 10.1093/pcp/pcr153

Moehs, C. P., Tian, L., Osteryoung, K. W., and DellaPenna, D. (2001). Analysis of carotenoid biosynthetic gene expression during marigold petal development. *Plant Mol. Biol.* 45 (3), 281–293. doi: 10.1023/A:1006417009203

Moon, J., Zhu, L., Shen, H., and Huq, E. (2008). PIF1 directly and indirectly regulates chlorophyll biosynthesis to optimize the greening process in *Arabidopsis. Proc. Natl. Acad. Sci. U. S. A.* 105 (27), 9433. doi: 10.1073/pnas.0803611105

Mou, W., Li, D., Bu, J., Jiang, Y., Khan, Z. U., Luo, Z., et al. (2016). Comprehensive analysis of ABA effects on ethylene biosynthesis and signaling during tomato fruit ripening. *PLoS One* 11 (4), e0154072. doi: 10.1371/journal.pone.0154072

Müller, P., Li, X. P., and Niyogi, K. K. (2001). Non-photochemical quenching. A response to excess light energy. *J. Plant Physiol.* 125 (4), 1558–1566. doi: 10.1104/pp.125.4.1558

Mustilli, A. C., Fenzi, F., Ciliento, R., Alfano, F., and Bowler, C. (1999). Phenotype of the tomato high pigment-2 mutant is caused by a mutation in the tomato homolog of DEETIOLATED1. *Plant Cell* 11 (2), 145–157. doi: 10.1105/tpc.11.2.145

Nambara, E., and Marion-Poll, A. (2005). Abscisic acid biosynthesis and catabolism. *Annu. Rev. Plant Biol.* 56, 165–185. doi: 10.1146/annurev.arplant.56.032604.144046

Nielsen, J., and Keasling, J. D. (2016). Engineering cellular metabolism. *Cell* 164 (6), 1185–1197. doi: 10.1016/j.cell.2016.02.004

Nielsen, K. M., Lewis, D. H., and Morgan, E. R. (2003). Characterization of carotenoid pigments and their biosynthesis in two yellow flowered lines of *Sandersonia aurantiaca* (Hook). *Euphytica* 130 (1), 25–34. doi: 10.1023/A:1022328828688

Nisar, N., Li, L., Lu, S., Khin, N., and Pogson, B. (2015). Carotenoid metabolism in plants. *Mol. Plant* 8 (1), 68–82. doi: 10.1016/j.molp.2014.12.007

Niyogi, K. K. (1999). Photoprotection Revisited: Genetic and molecular approaches. *Annu. Rev. Plant Biol.* 50 (1), 333–359. doi: 10.1146/annurev.arplant.50.1.333

Oh, E., Kang, H., Yamaguchi, S., Park, J., Lee, D., Kamiya, Y., et al. (2009). Genome-wide analysis of genes targeted by PHYTOCHROME INTERACTING FACTOR 3-LIKE5 during seed germination in *Arabidopsis. Plant Cell* 21 (2), 403–419. doi: 10.1105/tpc.108.064691

Ohmiya, A., Kishimoto, S., Aida, R., Yoshioka, S., and Sumitomo, K. (2006). Carotenoid cleavage dioxygenase (CmCCD4a) contributes to white color

formation in chrysanthemum petals. *J. Plant Physiol.* 142 (3), 1193–1201. doi: 10.1104/pp.106.087130

Ohmiya, A. (2011). Diversity of carotenoid composition in flower petals. *Jpn. Agric. Res. Q.* 45 (2), 163–171. doi: 10.6090/jarq.45.163

Ohmiya, A. (2013). Qualitative and quantitative control of carotenoid accumulation in flower petals. *Sci. Hortic.* 163, 10–19. doi: 10.1016/j.scienta.2013.06.018

Ohmiya, A., Kato, M., Shimada, T., Nashima, K., Kishimoto, S., and Nagata, M. (2019). Molecular basis of carotenoid accumulation in horticultural crops. *Hortic. J.* 88 (2), 135–149. doi: 10.2503/hortj.UTD-R003

Ougham, H. J., Morris, P., and Thomas, H. (2005). The colors of autumn leaves as symptoms of cellular recycling and defenses against environmental stresses. *Curr. Top. Dev. Biol.* 66, 136–161.

Pecker, I., Chamovitz, D., Linden, H., Sandmann, G., and Hirschberg, J. (1992). A single polypeptide catalyzing the conversion of phytoene to zeta-carotene is transcriptionally regulated during tomato fruit ripening. *Proc. Natl. Acad. Sci. U. S. A.* 89 (11), 4962–4966. doi: 10.1073/pnas.89.11.4962

Pfeiffer, A., Shi, H., Tepperman, J. M., Zhang, Y., and Quail, P. H. (2014). Combinatorial complexity in a transcriptionally centered signaling hub in *Arabidopsis*. *Mol. Plant* 7 (11), 1598–1618. doi: 10.1093/mp/ssu087

Pogson, B. J., Niyogi, K. K., Bjorkman, O., and Dellapenna, D. (1998). Altered xanthophyll compositions adversely affect chlorophyll accumulation and nonphotochemical quenching in *Arabidopsis* mutants. *Proc. Natl. Acad. Sci.* 95 (22), 13324–13329. doi: 10.1073/pnas.95.22.13324

Pospíšil, P. (2016). Production of reactive oxygen species by photosystem II as a response to light and temperature stress. *Front. Plant Sci.* 7, 1950. doi: 10.3389/fpls.2016.01950

Qin, G., Wang, Y., Cao, B., Wang, W., and Tian, S. (2012). Unraveling the regulatory network of the MADS box transcription factor RIN in fruit ripening. *Plant J.* 70 (2), 243–255. doi: 10.1111/j.1365-313X.2011.04861.x

Rai, A., Saito, K., and Yamazaki, M. (2017). Integrated omics analysis of specialized metabolism in medicinal plants. *Plant J.* 90 (4), 764–787. doi: 10.1111/tpj.13485

Rizzini, L., Favory, J. J., Cloix, C., Faggionato, D., O'Hara, A., Kaiserli, E., et al. (2011). Perception of UV-B by the *Arabidopsis* UVR8 protein. *Science* 332 (6025), 103–106. doi: 10.1126/science.1200660

Rock, C. D., and Zeevaart, J. A. (1991). The aba mutant of *Arabidopsis thaliana* is impaired in epoxy-carotenoid biosynthesis. *Proc. Natl. Acad. Sci. U. S. A.* 88 (17), 7496–7499. doi: 10.1073/pnas.88.17.7496

Rodríguez-Leal, D., Lemmon, Z. H., Man, J., Bartlett, M. E., and Lippman, Z. B. (2017). Engineering quantitative trait variation for crop improvement by genome editing. *Cell* 171 (2), 470–480. doi: 10.1016/j.cell.2017.08.030

Rodríguez-Villalón, A., Gas, E., and Rodríguez-Concepción, M. (2009). Phytoene synthase activity controls the biosynthesis of carotenoids and the supply of their metabolic precursors in dark-grown *Arabidopsis* seedlings. *Plant J.* 60 (3), 424–435. doi: 10.1111/j.1365-313X.2009.03966.x

Ronen, G., Cohen, M., Zamir, D., and Hirschberg, J. (1999). Regulation of carotenoid biosynthesis during tomato fruit development: expression of the gene for lycopene epsilon-cyclase is down-regulated during ripening and is elevated in the mutant delta. *Plant J.* 17 (4), 341–351. doi: 10.1046/j.1365-313X.1999.00381.x

Rossel, J. B., Wilson, I. W., and Pogson, B. J. (2002). Global changes in gene expression in response to high light in *Arabidopsis*. *J. Plant Physiol.* 130 (3), 1109–1120. doi: 10.1104/pp.005595

Ruiz-Sola, M. Á., Arbona, V., Gómez-Cadenas, A., Rodríguez-Concepción, M., and Rodríguez-Villalón, A. (2014). A root specific induction of carotenoid biosynthesis contributes to ABA production upon salt stress in *Arabidopsis*. *PLoS One* 9 (3), e90765. doi: 10.1371/journal.pone.0090765

Ruiz-Sola, M. A., and Rodríguez-Concepción, M. (2012). Carotenoid biosynthesis in *Arabidopsis*: a colorful pathway. *Arabidopsis Book* 10, e0158. doi: 10.1199/tab.0158

Sagawa, J. M., Stanley, L. E., LaFountain, A. M., Frank, H. A., Liu, C., and Yuan, Y. (2016). An R2R3-MYB transcription factor regulates carotenoid pigmentation in *Mimulus lewisii* flowers. *New Phytol.* 209 (3), 1049–1057. doi: 10.1111/nph.13647

Sakakibara, H. (2006). Cytokinins: activity, biosynthesis, and translocation. *Annu. Rev. Plant Biol.* 57, 431–449. doi: 10.1146/annurev.arplant.57.032905.105231

Shen, H., Zhu, L., Castillon, A., Majee, M., Downie, B., and Huq, E. (2008). Light-induced phosphorylation and degradation of the negative regulator PHYTOCHROME-INTERACTING FACTOR1 from *Arabidopsis* depend upon its direct physical interactions with photoactivated phytochromes. *Plant Cell* 20 (6), 1586. doi: 10.1105/tpc.108.060020

Shi, H., Wang, X., Mo, X., Tang, C., Zhong, S., and Deng, X. W. (2015). *Arabidopsis* DET1 degrades HFR1 but stabilizes PIF1 to precisely regulate seed germination. *Proc. Natl. Acad. Sci. U. S. A.* 112 (12), 3817. doi: 10.1073/pnas.1502405112

Shima, Y., Kitagawa, M., Fujisawa, M., Nakano, T., Kato, H., Kimbara, J., et al. (2013). Tomato FRUITFULL homologues act in fruit ripening *via* forming MADS-box transcription factor complexes with RIN. *Plant Mol. Biol.* 82 (4-5), 427–438. doi: 10.1007/s11103-013-0071-y

Shin, J., Kim, K., Kang, H., Zulfugarov, I. S., Bae, G., Lee, C., et al. (2009). Phytochromes promote seedling light responses by inhibiting four negatively-acting phytochrome-interacting factors. *Proc. Natl. Acad. Sci. U. S. A.* 106 (18), 7660. doi: 10.1073/pnas.0812219106

Shinozaki, K., and Yamaguchi-Shinozaki, K. (2007). Gene networks involved in drought stress response and tolerance. *J. Exp. Bot.* 58 (2), 221–227. doi: 10.1093/jxb/erl164

Snowden, K. C., Simkin, A. J., Janssen, B. J., Templeton, K. R., Loucas, H. M., Simons, J. L., et al. (2005). The Decreased apical dominance1/*Petunia hybrida* CAROTENOID CLEAVAGE DIOXYGENASE8 gene affects branch production and plays a role in leaf senescence, root growth, and flower development. *Plant Cell* 17 (3), 746. doi: 10.1105/tpc.104.027714

Stanley, L. E., Ding, B., Sun, W., Mou, F., Hill, C., Chen, S., et al. (2017). A tetratricopeptide repeat protein regulates carotenoid biosynthesis and chromoplast development in monkeyflowers (*Mimulus*). *Biorxiv* 171249. doi: 10.1101/171249

Su, L., Diretto, G., Purgatto, E., Danoun, S., Zouine, M., Li, Z., et al. (2015). Carotenoid accumulation during tomato fruit ripening is modulated by the auxin–ethylene balance. *BMC Plant Biol.* 15 (1), 114. doi: 10.1186/s12870-015-0495-4

Sun, T., Yuan, H., Cao, H., Yazdani, M., Tadmor, Y., and Li, L. (2018a). Carotenoid metabolism in plants: the role of plastids. *Mol. Plant* 11 (1), 58–74. doi: 10.1016/j.molp.2017.09.010

Sun, Y., Liang, B., Wang, J., Kai, W., Chen, P., Jiang, L., et al. (2018b). SlPti4 affects regulation of fruit ripening, seed germination and stress responses by modulating ABA signaling in tomato. *Plant Cell Physiol.* 59 (10), 1956–1965. doi: 10.1093/pcp/pcy111

Szymańska, R., Ślesak, I., Orzechowska, A., and Kruk, J. (2017). Physiological and biochemical responses to high light and temperature stress in plants. *Environ. Exp. Bot.* 139, 165–177. doi: 10.1016/j.envexpbot.2017.05.002

Thompson, A. J., Tor, M., Barry, C. S., Vrebalov, J., Orfila, C., Jarvis, M. C., et al. (1999). Molecular and genetic characterization of a novel pleiotropic tomato-ripening mutant. *J. Plant Physiol.* 120 (2), 383–390. doi: 10.1104/pp.120.2.383

Toledo-Ortiz, G., Huq, E., and Rodríguez-Concepción, M. (2010). Direct regulation of phytoene synthase gene expression and carotenoid biosynthesis by phytochrome-interacting factors. *Proc. Natl. Acad. Sci. U. S. A.* 107 (25), 11626. doi: 10.1073/pnas.0914428107

Toledo-Ortiz, G., Johansson, H., Lee, K. P., Bou-Torrent, J., Stewart, K., Steel, G., et al. (2014). The HY5–PIF regulatory module coordinates light and temperature control of photosynthetic gene transcription (light and temperature photosynthetic gene transcription regulation). *PLoS Genetics* 10 (6), e1004416. doi: 10.1371/journal.pgen.1004416

Ueda, H., and Kusaba, M. (2015). Strigolactone regulates leaf senescence in concert with ethylene in *Arabidopsis*. *J. Plant Physiol.* 169 (1), 138. doi: 10.1104/pp.15.00325

Vallabhaneni, R., Bradbury, L. M. T., and Wurtzel, E. T. (2010). The carotenoid dioxygenase gene family in maize, sorghum, and rice. *Arch. Biochem. Biophys.* 504 (1), 104–111. doi: 10.1016/j.abb.2010.07.019

Vardhini, B. V., and Rao, S. S. R. (2002). Acceleration of ripening of tomato pericarp discs by brassinosteroids. *Phytochemistry* 61 (7), 843–847. doi: 10.1016/S0031-9422(02)00223-6

Vrebalov, J., Ruezinsky, D., Padmanabhan, V., White, R., Medrano, D., Drake, R., et al. (2002). A MADS-box gene necessary for fruit ripening at the tomato ripening-inhibitor (rin) locus. *Science* 296 (5566), 343–346. doi: 10.1126/science.1068181

Vrebalov, J., Pan, I. L., Arroyo, A. J. M., Mcquinn, R., Chung, M., Poole, M., et al. (2009). Fleshy fruit expansion and ripening are regulated by the tomato SHATTERPROOF gene TAGL1. *Plant Cell* 21 (10), 3041–3062. doi: 10.1105/tpc.109.066936

Wang, J., Czech, B., and Weigel, D. (2009). miR156-regulated SPL transcription factors define an endogenous flowering pathway in *Arabidopsis thaliana*. *Cell* 138 (4), 738–749. doi: 10.1016/j.cell.2009.06.014

Wang, W., Liu, G., Niu, H., Timko, M. P., and Zhang, H. (2014). The F-box protein COI1 functions upstream of MYB305 to regulate primary carbohydrate metabolism in tobacco (*Nicotiana tabacum* L. cv. TN90). *J. Exp. Bot.* 65 (8), 2147–2160. doi: 10.1093/jxb/eru084

Wang, X., and Yamagishi, M. (2019). Mechanisms suppressing carotenoid accumulation in flowers differ depending on the hybrid groups of lilies (*Lilium* spp.). *Sci. Hortic.* 243, 159–168. doi: 10.1016/j.scienta.2018.08.025

Wei, S., Yu, B., Gruber, M. Y., Khachatourians, G. G., Hegedus, D. D., and Hannoufa, A. (2010). Enhanced seed carotenoid levels and branching in transgenic *Brassica napus* expressing the *Arabidopsis* miR156b gene. *J. Agric. Food Chem.* 58 (17), 9572–9578. doi: 10.1021/jf102635f

Welsch, R., Medina, J., Giuliano, G., Beyer, P., and von Lintig, J. (2003). Structural and functional characterization of the phytoene synthase promoter from *Arabidopsis* thaliana. *Planta* 216 (3), 523–534. doi: 10.1007/s00425-002-0885-3

Welsch, R., Maass, D., Voegel, T., Dellapenna, D., and Beyer, P. (2007). Transcription factor RAP2.2 and its interacting partner SINAT2: stable elements in the carotenogenesis of *Arabidopsis* leaves. *J. Plant Physiol.* 145 (3), 1073–1085. doi: 10.1104/pp.107.104828

Welsch, R., Wust, F., Bar, C., Al-Babili, S., and Beyer, P. (2008). A third phytoene synthase is devoted to abiotic stress–induced abscisic acid formation in rice and defines functional diversification of phytoene synthase genes. *J. Plant Physiol.* 147 (1), 367–380. doi: 10.1104/pp.108.117028

Weng, L., Zhao, F., Li, R., Xu, C., Chen, K., and Xiao, H. (2015). The zinc finger transcription factor SlZFP2 negatively regulates abscisic acid biosynthesis and fruit ripening in tomato. *J. Plant Physiol.* 167 (3), 931–949. doi: 10.1104/pp.114.255174

Wu, W., Liu, L. L., and Yan, Y. C. (2019). TERF1 regulates nuclear gene expression through chloroplast retrograde signals. *Russ. J. Plant Physiol.*, 66 (1), 22–28. doi: 10.1134/S1021443719010205

Xie, Q., Hu, Z., Zhu, Z., Dong, T., Zhao, Z., Cui, B., et al. (2014). Overexpression of a novel MADS-box gene SlFYFL delays senescence, fruit ripening and abscission in tomato. *Sci. Rep.* 4, 4367. doi: 10.1038/srep04367

Xiong, C., Luo, D., Lin, A., Zhang, C., Shan, L., He, P., et al. (2019). A tomato B-box protein SlBBX20 modulates carotenoid biosynthesis by directly activating PHYTOENE SYNTHASE 1, and is targeted for 26S proteasome–mediated degradation. *New Phytol.* 221 (1), 279–294. doi: 10.1111/nph.15373

Yamagishi, M., Kishimoto, S., and Nakayama, M. (2010). Carotenoid composition and changes in expression of carotenoid biosynthetic genes in tepals of Asiatic hybrid lily. *Plant Breed.* 129 (1), 100–107. doi: 10.1111/j.1439-0523.2009.01656.x

Yamamizo, C., Kishimoto, S., and Ohmiya, A. (2010). Carotenoid composition and carotenogenic gene expression during *Ipomoea* petal development. *J. Exp. Bot.* 61 (3), 709–719. doi: 10.1093/jxb/erp335

Yang, J. C., Zhang, J. H., Wang, Z. Q., Zhu, Q. S., and Liu, L. J. (2003). Involvement of abscisic acid and cytokinins in the senescence and remobilization of carbon reserves in wheat subjected to water stress during grain filling. *Plant Cell Environ.* 26 (10), 1621–1631. doi: 10.1046/j.1365-3040.2003.01081.x

Yuan, H., Zhang, J., Nageswaran, D., and Li, L. (2015). Carotenoid metabolism and regulation in horticultural crops. *Hortic Res.* 2, 15036. doi: 10.1038/hortres.2015.36

Zhang, B., Liu, C., Wang, Y., Yao, X., Wang, F., Wu, J., et al. (2015). Disruption of a CAROTENOID CLEAVAGE DIOXYGENASE 4 gene converts flower colour from white to yellow in *Brassica* species. *New Phytol.* 206 (4), 1513–1526. doi: 10.1111/nph.13335

Zhang, J., Hu, Z., Yao, Q., Guo, X., Nguyen, V., Li, F., et al. (2018a). A tomato MADS-box protein, SlCMB1, regulates ethylene biosynthesis and carotenoid accumulation during fruit ripening. *Sci. Rep.* 8 (1), 3413. doi: 10.1038/s41598-018-21672-8

Zhang, M., Yuan, B., and Leng, P. (2009). The role of ABA in triggering ethylene biosynthesis and ripening of tomato fruit. *J. Exp. Bot.* 60 (6), 1579–1588. doi: 10.1093/jxb/erp026

Zhang, Y., Li, Z., Tu, Y., Cheng, W., and Yang, Y. (2018b). Tomato (*Solanum lycopersicum*) SlIPT4, encoding an isopentenyltransferase, is involved in leaf senescence and lycopene biosynthesis during fruit ripening. *BMC Plant Biol.* 18 (1), 107. doi: 10.1186/s12870-018-1327-0

Zhong, S., Fei, Z., Yun-Ru, C., Zheng, Y., Huang, M., Vrebalov, J., et al. (2013). Single-base resolution methylomes of tomato fruit development reveal epigenome modifications associated with ripening. *Nat. Biotechnol.* 31 (2), 154. doi: 10.1038/nbt.2462

Zhou, X., Welsch, R., Yang, Y., Alvarez, D., Riediger, M., Yuan, H., et al. (2015). *Arabidopsis* OR proteins are the major posttranscriptional regulators of phytoene synthase in controlling carotenoid biosynthesis. *Proc. Natl. Acad. Sci. U. S. A.* 112 (11), 3558–3563. doi: 10.1073/pnas.1420831112

Zhou, D., Shen, Y., Zhou, P., Fatima, M., Lin, J., Yue, J., et al. (2019). Papaya CpbHLH1/2 regulate carotenoid biosynthesis-related genes during papaya fruit ripening. *Hortic Res.* 6 (1), 80. doi: 10.1038/s41438-019-0162-2

Zhu, F., Luo, T., Liu, C., Wang, Y., Yang, H., Yang, W., et al. (2017a). An R2R3-MYB transcription factor represses the transformation of α- and β-branch carotenoids by negatively regulating expression of CrBCH2 and CrNCED5 in flavedo of citrus reticulate. *New Phytol.* 216 (1), 178–192. doi: 10.1111/nph.14684

Zhu, J. (2002). Salt and drought stress signal transduction in plants. *Annu. Rev. Plant Biol.* 53 (1), 247–273. doi: 10.1146/annurev.arplant.53.091401.143329

Zhu, L., Bu, Q., Xu, X., Paik, I., Huang, X., Hoecker, U., et al. (2015). CUL4 forms an E3 ligase with COP1 and SPA to promote light-induced degradation of PIF1. *Nat. Commun.* 6, 7245. doi: 10.1038/ncomms8245

Zhu, M., Chen, G., Zhou, S., Tu, Y., Wang, Y., Dong, T., et al. (2014). A new tomato NAC (NAM/ATAF1/2/CUC2) transcription factor, SlNAC4, functions as a positive regulator of fruit ripening and carotenoid accumulation. *Plant Cell Physiol.* 55 (1), 119–135. doi: 10.1093/pcp/pct162

Zhu, Q., Zeng, D., Yu, S., Cui, C., Li, J., Li, H., et al. (2018). From Golden Rice to aSTARice: bioengineering astaxanthin biosynthesis in rice endosperm. *Mol. Plant* 11 (12), 1440–1448. doi: 10.1016/j.molp.2018.09.007

Zhu, Z., Chen, G., Guo, X., Yin, W., Yu, X., Hu, J., et al. (2017b). Overexpression of SlPRE2, an atypical bHLH transcription factor, affects plant morphology and fruit pigment accumulation in tomato. *Sci. Rep.* 7 (1), 5786. doi: 10.1038/s41598-017-04092-y

Zhu, Z., Li, G., Yan, C., Liu, L., Zhang, Q., Han, Z., et al. (2019). DRL1, encoding a NAC transcription factor, is involved in leaf senescence in grapevine. *Int. J. Mole. Sci.* 20 (11), 2678. doi: 10.3390/ijms20112678

Conflict of Interest Statement: The authors declare that the research was conducted in the absence of any commercial or financial relationships that could be construed as a potential conflict of interest.

Table S1. Transcriptional regulators of carotenoid biosynthesis. A summary of regulators discussed in this review, giving protein name, class, system, and carotenoid biosynthesis pathway (CBP) genes positively/negatively regulated. Information about regulatory mechanisms is provided in the D/I/U, T/V, E/H, and Interacting factors columns. References for each regulator are provided. Regulators whose mechanisms are direct and have been demonstrated *in vivo* in their endogenous systems are bolded. Note: if a regulator affects some CBP genes directly and others indirectly/unknown, indirect/unknown regulation is shown in parentheses.

Regulator	Class	Endogenous system	CBP genes positively regulated	CBP genes negatively regulated	D/I/U*	T/V†	E/H‡	Interacting factors	Reference
PIF1	bHLH	*Arabidopsis*	-	*PSY*	D	V	E	DET1, DDB1, CUL4, PAR1, DELLAs	Toledo-Ortiz et al., 2010; Llorente et al., 2017; Rodriguez-Villalon et al., 2009; Cheminant et al., 2011
SlPIF1a	bHLH	Tomato	-	*PSY1*	D	V	E	-	Llorente et al., 2015
HY5	bZIP	*Arabidopsis*	*PSY*	-	D	V	E	COP1, DDB1, CUL4, DELLAs	Toledo-Ortiz et al., 2014; Llorente et al., 2017; Rodriguez-Villalon et al., 2009; Cheminant et al., 2011
DRL1	NAC	*Vitis*	-	*ZEP*	U	-	-	-	Zhu et al., 2019
RAP2.2	AP2/ERF	*Arabidopsis*	*PSY, PDS*	-	D	T	-	-	Welsch et al., 2007
SlAP2a	AP2/ERF	Tomato	*PSY1, CRTISO, BCH, PDS1*	*ZEP1, CYCB*	U	-	-	SlCMB1	Chung et al., 2010, Karlova et al., 2011
SDG8	HMT	*Arabidopsis*	*CRTISO, LCYE*	-	D	V	E	-	Cazzonelli et al., 2009
TAGL1	MADS-box	Tomato	*PSY1*	*LCYB, CYCB*	U	-	-	RIN, FUL2, SlCMB1	Vrebalov et al., 2009; Fujisawa et al., 2014
CsMADS6	MADS-box	*Citrus*	*PSY, PDS (CRTISO, LCYB2, BCH)*	*(LCYE)*	D+(I)	V	H	-	Lu et al., 2018
RIN	MADS-box	Tomato	*PSY1, Z-ISO, CRTISO (PSY2, ZDS)*	*LCYE, LCYB, ZEP*	D+(I)	V	E	FUL1, FUL2, TAGL1, SlCMB1, SlMADS1, SlFYFL	Fujisawa et al., 2011, 2012, 2013, 2014; Martel et al., 2011; Zhong et al., 2013

FUL1	MADS-box	Tomato	*PSY1, Z-ISO, CRTISO, BCH*	*LCYB, ZEP*	D	V	E	RIN	Shima et al., 2013; Fujisawa et al., 2014
FUL2	MADS-box	Tomato	*Z-ISO, CRTISO, BCH*	*LCYB, ZEP*	D	V	E	TAGL1, RIN	Fujisawa et al., 2014
SlMADS1	MADS-box	Tomato	-	*PSY1*	U	-	-	RIN, SlFYFL, SlCMB1	Dong et al., 2013
SlFYFL	MADS-box	Tomato	-	*PSY1, PDS, ZDS*	U	-	-	RIN, SlMADS1, SlJOINTLESS	Xie et al., 2014
SlCMB1	MADS-box	Tomato	*PSY1, PDS*	*CYCB, LCYE, LCYB*	U	-	-	RIN, SlMADS1, TAGL1, AP2a	Zhang et al., 2018
TERF1	AP2/ERF	Tomato	*ZDS*	-	U	-	-	-	Wu et al., 2019
SlPti4	AP2/ERF	Tomato	-	*CYCB*	U	-	-	-	Sun et al., 2018
SlBZR1	BR response TF	Tomato	*PSY1, ZDS*	-	U	-	-	-	Liu et al., 2014
SlNAC4	NAC	Tomato	*PSY1*	*CYCB, LCYE, LCYB*	U	-	-	RIN, NOR	Zhu et al., 2013
SlNAC1	NAC	Tomato	*(CYCB, LCYE, LCYB)*	*PSY1*	D+(U)	T	-	-	Ma et al., 2014; Meng et al., 2016
SlARF2	ARF	Tomato	*PSY1, PDS, ZDS*	*LCYB1, LCYB1, CYCB*	U	-	-	-	Hao et al., 2015
SlPRE2	bHLH (atypical)	Tomato	-	*PSY1, PDS, ZDS*	U	-	-	-	Zhu et al., 2017
SlBBX20	B-box	Tomato	*PSY1, VDE*	-	D	T	-	DET1	Xiong et al., 2019
ClpR1	Clp protease	Tomato	*LCYB, CYCB, CYP97C11*	-	U	-	-	-	D'Andrea et al., 2018
SGR1	STAY-GREEN	Tomato	-	*PSY1*	U	-	-	PSY1	Luo et al., 2013
SlIPT4	IPT	Tomato	*Z-ISO, ZDS*	*PSY1, PDS, CRTISO, LCYB, LCYE*	U	-	-	-	Zhang et al., 2018
CNR	SPL	Tomato	*PSY1*	-	U	-	-	-	Zhong et al., 2013
SlHDA3	HDA	Tomato	*CYCB, LCYB, LCYE*	*PSY1*	U	-	-	-	Guo et al., 2018
CpEIN3a	EIN3/EIL	Papaya	*PDS4, BCH*	-	D	V	H	CpNAC2	Fu et al., 2017

CpNAC2	NAC	Papaya	*PDS2, PDS4, ZDS, LCYE, BCH*	-	D	V	H	CpEIN3a	Fu et al., 2017
CpNAC1	NAC	Papaya	*PDS2, PDS4*	-	D	V	H	-	Fu et al., 2016
CpbHLH1	bHLH	Papaya	-	*CYCB, LCYB*	D	V	H	-	Zhou et al., 2019
CpbHLH2	bHLH	Papaya	*CYCB, LCYB*	-	D	V	H	-	Zhou et al., 2019
AdMYB7	MYB	Kiwifruit	*LCYB (PSY, PDS, ZDS, LCYE)*	-	D+(U)	T	-	-	Ampomah-Dwamena et al., 2018
CrMYB68	MYB	*Citrus*	*BCH2*	-	D	V	H	-	Zhu et al., 2017
COI1	F-box	*Nicotiana*	*PSY, ZDS, LCY*	-	U	-	-	-	Wang et al., 2014
RCP1	MYB	*Mimulus*	*PSY1, PDS1, PDS2, Z-ISO, ZDS1, ZDS2, CRTISO, LCYB1, BCH1, ZEP1, ZEP2, NSY1*	-	U	-	-	-	Sagawa et al., 2016
RCP2	TPR	*Mimulus*	*PSY1, PDS1, PDS2, Z-ISO, ZDS1, ZDS2, CRTISO, LCYB1, BCH1, ZEP1, ZEP2, NSY1*	-	U	-	-	-	Stanley et al., 2017
PBF	P-box	Maize	*BCH2*	-	D	T	-	-	Jin et al., 2018
GAMYB	MYB	Maize	*BCH2*	-	D	T	-	-	Jin et al., 2018

*D/I/U refers to the regulatory mechanism (Direct/Indirect/Unknown)
†T/V indicates whether the regulatory mechanism has been shown to function *in vitro* (T) or *in vivo* (V)
‡E/H designates whether the regulatory mechanism has been shown to function in an endogenous (E) or heterologous (H) system
Note: LeHB-1 and SlZFP2 from the main text are not included in this table because their effects on the transcription of CBP genes have not been reported.

Frontiers Copyright Statement

All content included on Frontiers websites (including Loop), such as text, graphics, logos, button icons, images, video/audio clips, downloads, data compilations and software, is the property of Frontiers if created by Frontiers, or of the person or entity who or which owned it prior to submission to Frontiers. If not owned by Frontiers, it is licensed to Frontiers Media SA (Frontiers) or its licensees and/or subcontractors.

The copyright in the text of individual articles (including research articles, opinion articles, book reviews, conference proceedings and abstracts) is not the property of Frontiers, and its ownership is not affected by its submission to or publication by Frontiers. Frontiers benefits from a general licence over all content submitted to it, and both Frontiers and its users benefit from a Creative Commons CC-BY licence over all content, as specified below.

Images and graphics not forming part of user-contributed materials are the property of or are licensed to Frontiers may not be downloaded or copied without Frontiers' explicit and specific permission or in accordance with any specific copyright notice attached to that material.

The combination of all content on Frontiers websites, as well as the design and the look and feel of the Frontiers websites, and the copyright and all other rights in such content and combination, are the sole property of Frontiers.

As an author or contributor you grant permission to others to reproduce your articles, **including any graphics and third-party materials supplied by you**, in accordance with the Frontiers Terms and Conditions. The licence granted to third parties over all contents of each article, **including third-party elements**, is a Creative Commons Attribution ("CC BY") licence. The current version is CC-BY, version 4.0, and the licence will automatically be updated as and when updated by the Creative Commons organisation.

You may include a requirement to reproduce copyright notices in materials contributed by you, but you may not restrict the right to reproduce the entire article, including third-party graphics. This means that you must obtain any necessary third-party consents and permissions to reproduce third-party materials in your articles submitted to Frontiers.

E-books are subject to the same licensing conditions as the articles within them.

Articles published prior to the effective date of this notice: Please note that reproduction of third-party graphics and other third-party materials contained in articles published prior to the effective date of this notice may be subject to third-party notices prohibiting their reproduction without permission. You must comply with those notices.

Articles published prior to July 2012: The licence granted for these articles may be different and you should check the pdf version of any article to establish what licence was granted. If an article, dating from before July 2012, carries only a non-commercial licence and you wish to obtain a commercial licence, please contact Frontiers at editorial.office@frontiersin.org.

All software used on this website, and the copyright in the code constituting such software, is the property of or is licensed to Frontiers and its use is restricted in accordance with the Frontiers Terms and Conditions. All copyright, and all rights therein, are protected by national and international copyright laws.

This Copyright Statement comes into effect on **25th May, 2018**.

UCONN
UNIVERSITY OF CONNECTICUT

Lauren Stanley <lauren.stanley@uconn.edu>

RE: Permission to reprint
1 message

Frontiers in Plant Science - Peer Review <plantscience.editorial.office@frontiersin.org> Tue, May 5, 2020 at 11:57 AM
To: "lauren.stanley@uconn.edu" <lauren.stanley@uconn.edu>

Dear Lauren,

Many thanks for your email. If I may, I direct you to our copyright statement "The copyright in the text of individual articles (including research articles, opinion articles, book reviews, conference proceedings and abstracts) is not the property of Frontiers... As an author or contributor you grant permission to others to reproduce your articles, including any graphics and third-party materials supplied by you, in accordance with the Frontiers Terms and Conditions. The licence granted to third parties over all contents of each article, including third-party elements, is a Creative Commons Attribution ("CC BY") licence."

I believe this means you can reprint away.

Best wishes,

Eleanor Adams
Research Integrity Specialist

Research Integrity Manager: Gearóid Ó Faoleán, PhD
Frontiers | London Office
www.frontiersin.org

---------- Original Message ----------
From: Lauren Stanley [lauren.stanley@uconn.edu]
Sent: 22.04.2020 17:51
To: plantscience.editorial.office@frontiersin.org
Subject: Permission to reprint

Dear Managing Editor,

I am writing to request permission to reprint the following material from Frontiers in Plant Science: Stanley, Lauren, & Yuan, Yao-Wu (2019). Transcriptional regulation of carotenoid biosynthesis in plants: So many regulators, so little consensus. *Frontiers in Plant Science*, *10*, 1017. DOI: 10.3389/fpls.2019.01017

In accordance with the journal's copyright statement, the original publication will be fully cited, with copyright notices displayed prominently. This material is to appear in my dissertation at the University of Connecticut, entitled: The genetic regulation of carotenoid pigmentation in monkeyflowers (Mimulus), which will be published in 2020.

Thank you very much,

Lauren Stanley

ref:_00D58JetR._5004H10bSUS:ref

The Plant Cell, Vol. 32: 1536–1555, May 2020, www.plantcell.org © 2020 ASPB.

A Tetratricopeptide Repeat Protein Regulates Carotenoid Biosynthesis and Chromoplast Development in Monkeyflowers (*Mimulus*)[OPEN]

Lauren E. Stanley,[a,1] Baoqing Ding,[a] Wei Sun,[b] Fengjuan Mou,[a,c] Connor Hill,[a] Shilin Chen,[b] and Yao-Wu Yuan[a,d,1]

[a] Department of Ecology and Evolutionary Biology, University of Connecticut, Storrs, Connecticut 06269
[b] Institute of Chinese Materia Medica, China Academy of Chinese Medical Sciences, Beijing 100700, China
[c] Faculty of Forestry, Southwest Forestry University, Kunming, Yunnan 650224, China
[d] Institute for Systems Genomics, University of Connecticut, Storrs, Connecticut 06269

ORCID IDs: 0000-0001-9579-0639 (L.E.S.); 0000-0001-7183-9653 (B.D.); 0000-0001-5675-0466 (W.S.); 0000-0002-4134-3128 (F.M.); 0000-0003-4114-4513 (C.H.); 0000-0002-0449-236X (S.C.); 0000-0003-1376-0028 (Y.-W.Y.)

Little is known about the factors regulating carotenoid biosynthesis in flowers. Here, we characterized the *REDUCED CAROTENOID PIGMENTATION2* (*RCP2*) locus from two monkeyflower (*Mimulus*) species, the bumblebee-pollinated species *Mimulus lewisii* and the hummingbird-pollinated species *Mimulus verbenaceus*. We show that loss-of-function mutations of *RCP2* cause drastic down-regulation of the entire carotenoid biosynthetic pathway. The causal gene underlying *RCP2* encodes a tetratricopeptide repeat protein that is closely related to the Arabidopsis (*Arabidopsis thaliana*) REDUCED CHLOROPLAST COVERAGE proteins. RCP2 appears to regulate carotenoid biosynthesis independently of RCP1, a previously identified R2R3-MYB master regulator of carotenoid biosynthesis. We show that RCP2 is necessary and sufficient for chromoplast development and carotenoid accumulation in floral tissues. Simultaneous down-regulation of *RCP2* and two closely related paralogs, *RCP2-L1* and *RCP2-L2*, yielded plants with pale leaves deficient in chlorophyll and carotenoids and with reduced chloroplast compartment size. Finally, we demonstrate that *M. verbenaceus* is just as amenable to chemical mutagenesis and in planta transformation as the more extensively studied *M. lewisii*, making these two species an excellent platform for comparative developmental genetics studies of closely related species with dramatic phenotypic divergence.

INTRODUCTION

The colors of most flowers can be attributed to two classes of pigments: the red, pink, purple, or blue anthocyanins and the yellow, orange, or red carotenoids. The hydrophilic anthocyanins are usually stored in the vacuoles of petal cells, whereas the hydrophobic carotenoids accumulate in chromoplasts as various lipoprotein structures (e.g., plastoglobules, crystals, fibrils; Grotewold and Davies, 2008; Egea et al., 2010; Li and Yuan, 2013). A plant can frequently produce both pigment types in the same flower, forming contrasting spatial patterns that serve as nectar guides for animal pollinators (Glover, 2014). Common examples among horticultural plants include pansies (*Viola tricolor*), primroses (*Primula vulgaris*), lantanas (*Lantana camara*), and hibiscus (*Hibiscus rosa-sinensis*), to name but a few. As an example in nature, the vast majority of the ~160 species of monkeyflowers (*Mimulus*; Barker et al., 2012) produce both anthocyanins and carotenoids in their petals with striking patterns. While most plant genomes contain the genes encoding both anthocyanin and carotenoid biosynthetic pathways, the diversity of floral pigmentation patterns is largely due to when and where these pathway genes are expressed. As such, identifying the transcriptional regulators of these pigment biosynthetic pathways is critically important to understanding the developmental mechanisms of pigment pattern formation and the molecular bases of natural flower color variation.

The transcriptional control of anthocyanin biosynthesis is well understood. A highly conserved MYB-bHLH-WD40 (MBW) protein complex has been shown to coordinately activate all or some of the anthocyanin biosynthetic pathway genes in multiple plant systems (Paz-Ares et al., 1987; Ludwig et al., 1989; Martin et al., 1991; Goodrich et al., 1992; de Vetten et al., 1997; Quattrocchio et al., 1998; Borevitz et al., 2000; Spelt et al., 2000; Schwinn et al., 2006; reviewed by Davies et al., 2012; Xu et al., 2015). Among the three components, members of the R2R3-MYB transcription factor family often display tissue-specific expression patterns and cause spatial patterning of anthocyanin deposition in flower petals (Shang et al., 2011; Albert et al., 2011; Yuan et al., 2014; Martins et al., 2017).

By contrast, little is known about the transcriptional regulators of the carotenoid biosynthetic pathway (CBP) in flowers (Ruiz-Sola and Rodríguez-Concepción, 2012; Yuan et al., 2015), although many putative transcriptional regulators have been identified in other tissues. For example, in Arabidopsis leaves, PHYTOCHROME-INTERACTING FACTOR1 (PIF1) and ELONGATED HYPOCOTYL5 (HY5) operate as a regulatory switch during

[1] Address correspondence to lauren.stanley@uconn.edu and yuan.colreeze@gmail.com.
The authors responsible for distribution of materials integral to the findings presented in this article in accordance with the policy described in the Instructions for Authors (www.plantcell.org) are: Lauren E. Stanley (lauren.stanley@uconn.edu) and Yao-Wu Yuan (yuan.colreeze@gmail.com).
[OPEN]Articles can be viewed without a subscription.
www.plantcell.org/cgi/doi/10.1105/tpc.19.00755

IN A NUTSHELL

Background: Carotenoids are yellow, orange, or red pigments that give many flowers and fruits their brilliant colors. In order to make and accumulate carotenoids in these organs, plants must (i) switch on the genes for carotenoid-producing enzymes and (ii) build specialized storage organelles called chromoplasts. However, very few regulatory genes controlling these two processes in flowers have been identified.

Question: We wanted to discover new regulators of carotenoid production and storage in flowers. We did this by chemically mutating the DNA of two species of *Mimulus* (monkeyflower) and searching for mutants lacking yellow pigmentation in their flowers. We sequenced the DNA of one mutant with a dramatic decrease in carotenoid accumulation to identify which gene was impaired and did experiments to characterize how this gene contributes to flower coloration.

Findings: We found a gene that we named *REDUCED CAROTENOID PIGMENTATION2* (*RCP2*), because disruption of this gene causes *Mimulus* flowers to lose most of their carotenoids. *rcp2* mutant plants cannot switch on carotenoid enzyme genes to the same degree as wild-type plants and do not make normal chromoplast storage organelles. When we engineered plants to make extra RCP2 proteins, the normally whitish floral reproductive organs turned yellow. Together, these results show that RCP2 is necessary and sufficient for carotenoid pigmentation in *Mimulus* flowers. Interestingly, although *RCP2* by itself has no effect on carotenoid accumulation in leaves, simultaneously turning down the expression of *RCP2* and two closely related genes (*RCP2-like* genes) resulted in pale leaves that were deficient in both carotenoid and chlorophyll pigments and with a smaller cell volume occupied by chloroplasts. This indicates that the original function of *RCP2-like* genes might have been to regulate essential chlorophyll and carotenoid pigments in vegetative tissues and that *RCP2* has evolved specialized function in the regulation of carotenoid accumulation in reproductive organs for pollinator attraction.

Next steps: Moving forward, we want to learn more about the functional mechanism of RCP2 by identifying proteins that physically interact with RCP2 and to discover additional carotenoid regulators in the monkeyflower system by analyzing chemically induced mutants and natural variation.

photomorphogenesis, binding to the promoter of the phytoene synthase gene *PSY* to repress and activate carotenoid biosynthesis, respectively (Toledo-Ortiz et al., 2010, 2014). Another regulator, RELATED TO AP2 2 (RAP2.2), binds the promoters of *PSY* and the phytoene desaturase gene *PDS* in vitro, although its endogenous function in leaf carotenoid regulation remains unclear (Welsch et al.,2007). In addition, the histone methyltransferase SET DOMAIN GROUP8 (SDG8) activates the transcription of the carotenoid isomerase gene *CRTISO* by altering the methylation status around the transcription start site of this gene (Cazzonelli et al., 2009).

Numerous putative transcriptional regulators of carotenoid biosynthesis have also been described in fruits, particularly tomatoes (*Solanum lycopersicum*). For example, the MADS-box proteins RIPENING INHIBITOR (RIN), FRUITFULL1 (FUL1) and FUL2, TOMATO AGAMOUS LIKE1 (TAGL1), and SlMADS1 are master regulators of fruit ripening. Each protein regulates a subset of CBP genes, cooperatively promoting the production of lycopene, the major carotenoid in tomato fruits (Vrebalov et al., 2002; Ito et al., 2008; Itkin et al., 2009; Vrebalov et al., 2009; Giménez et al., 2010; Fujisawa et al., 2011, 2012, 2013, 2014; Martel et al., 2011; Bemer et al., 2012; Qin et al., 2012; Dong et al., 2013; Shima et al., 2013; Zhong et al., 2013). However, as these master regulators are involved in other aspects of fruit ripening (e.g., softening, aroma, and sugar production), it is difficult to decipher their specific functions in carotenoid regulation. Other classes of carotenoid regulators during tomato fruit ripening include SlNAC1/4, SlAP2a, and SlBBX20 (Chung et al., 2010; Karlova et al., 2011; Ma et al., 2014; Zhu et al., 2014; Meng et al., 2016; Xiong et al., 2019). Interestingly, SlPIF1a appears to play a similar role in carotenoid regulation at the onset of fruit ripening as its Arabidopsis homolog AtPIF1 does in photomorphogenesis by repressing the expression of *SlPSY1* until chlorophyll degradation (Llorente et al., 2016). Putative carotenoid transcriptional regulators have also been identified in other fruits, including CsMADS6 and CrMYB68 in orange (*Citrus* spp; Zhu et al., 2017; Lu et al., 2018), CpEIN3a, CpNAC1, CpNAC2, CpbHLH1, and CpbHLH2 in papaya (*Carica papaya*; Fu et al., 2016, 2017; Zhou et al., 2019), and AdMYB7 in kiwifruit (*Actinidia deliciosa*; Ampomah-Dwamena et al., 2019).

However, whether these leaf or fruit carotenoid regulators play a role in flower pigmentation is unknown. To date, only two transcriptional regulators have been implicated in carotenoid pigmentation in flower petals. *REDUCED CAROTENOID PIGMENTATION1* (*RCP1*), identified from the monkeyflower species *Mimulus lewisii*, encodes a subgroup-21 R2R3-MYB (Sagawa et al., 2016). The ventral (lower) petal of *M. lewisii* flowers contains two yellow ridges that are pigmented by carotenoids (Figure 1A), which serve as nectar guides for bumblebee pollinators (Owen and Bradshaw, 2011). Loss-of-function mutations in *RCP1* reduce the expression of the entire CBP and decrease the carotenoid content in the nectar guides (Figure 1B; Sagawa et al., 2016). *WHITE PETAL1* (*WP1*), identified from *Medicago truncatula*, encodes a subgroup-6 R2R3-MYB (Meng et al., 2019). Loss-of-function *wp1* mutants show dramatically reduced carotenoid contents and down-regulation of multiple carotenoid biosynthetic genes in flower petals. Since subgroup-6 R2R3-MYBs typically activate anthocyanin biosynthesis in plants (Davies et al., 2012; Glover, 2014; Xu et al., 2015), *WP1* represents an intriguing case where an anthocyanin activator

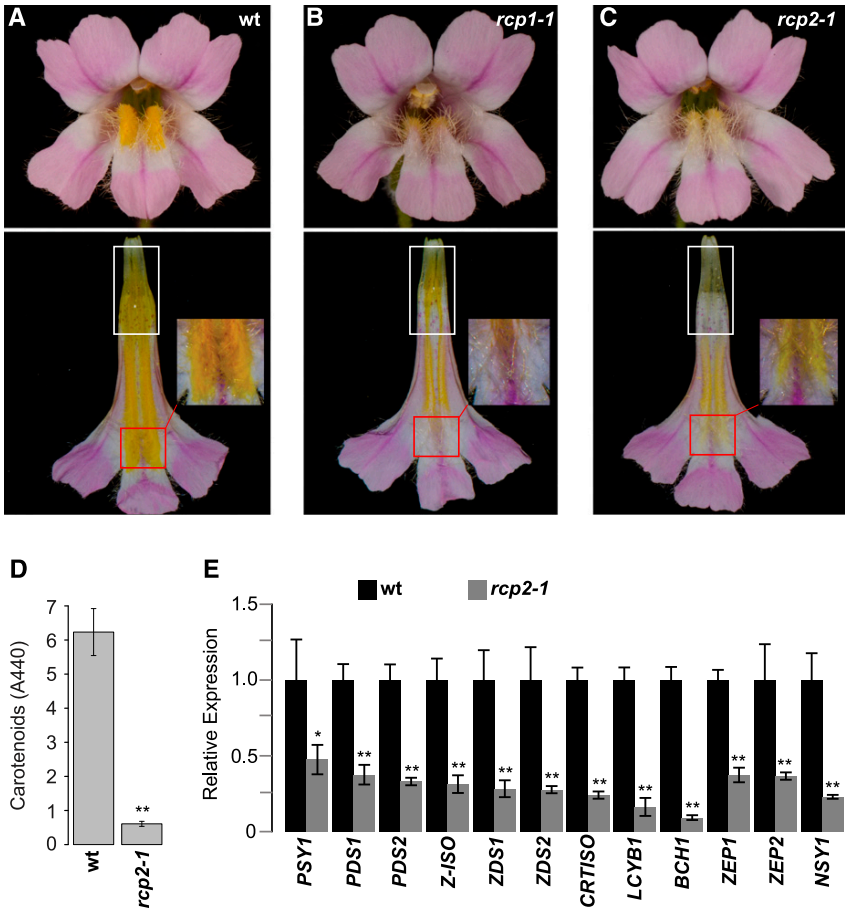

Figure 1. Reduced Carotenoid Pigmentation Phenotypes in *M. lewisii*.

Front view (top) and nectar guide view (bottom) of wild-type **(A)**, *rcp1-1* **(B)**, and *rcp2-1* **(C)** flowers. White and red boxes indicate the base and throat of the corolla tube, respectively.

(D) Carotenoid concentrations in wild-type and *rcp2-1* nectar guides, approximated based on absorbance measurements at 440 nm. Error bars are 1 SD ($n = 8$ individual flowers from the same plant).

(E) Relative transcript levels of the CBP genes in 15-mm nectar guides of wild-type and *rcp2-1* flowers, as determined by qRT-PCR. Error bars are 1 SD ($n = 3$ biological replicates, each consisting of pooled 15-mm nectar guides from a distinct plant). Asterisks indicate differences from the wild type (*$P < 0.05$, **$P < 0.01$, Student's *t* test).

might have been co-opted to regulate carotenoid pigmentation in some exceptional lineages. Besides these R2R3-MYBs, the carotenoid cleavage dioxygenases (particularly CCD1 and CCD4s) are well-known contributors to flower color variation among species or horticultural varieties that modulate carotenoid turnover (Ohmiya et al., 2006; Chiou et al., 2010; Zhang et al., 2015), although they are not involved in transcriptional regulation of the CBP per se.

In this study, to identify additional transcriptional regulators of floral carotenoid pigmentation, we characterized *reduced carotenoid pigmentation 2* (*rcp2*) mutants in *Mimulus*. Through bulk segregant analysis and transgenic experiments, we identified the causal gene of *RCP2*, encoding a tetratricopeptide repeat (TPR) protein homologous to the REDUCED CHLOROPLAST COVERAGE (REC) proteins in Arabidopsis. Loss-of-function *REC* mutants have reduced chlorophyll contents and smaller chloroplast compartment size compared with wild type (Larkin et al., 2016). Our analyses showed that *RCP2* is required for chromoplast development and carotenoid biosynthesis in *Mimulus* flowers and that overexpression of *RCP2* in pale or colorless floral tissues (e.g., filaments, style) promotes chromoplast formation and carotenoid accumulation. Additionally, we demonstrate that simultaneous down-regulation of *RCP2* and its two closely related paralogs reduces leaf chlorophyll and carotenoid contents as well as chloroplast coverage in *Mimulus*, suggesting that this small family of TPR genes plays conserved roles in regulating chlorophyll accumulation and chloroplast compartment size in eudicots.

RESULTS

rcp2-1 Displays a Distinct and Stronger Phenotype Than *rcp1-1*

We recovered three independent *rcp2* alleles from an ethyl methanesulfonate (EMS) mutant screen in the *M. lewisii* LF10 background. *rcp2-1* and *rcp2-2* are very similar phenotypically, whereas *rcp2-3* displays a slightly weaker phenotype (Figure 1C; Supplemental Figure 1). Like the *rcp1-1* mutant, *rcp2-1* has reduced carotenoid contents in the nectar guides compared to the wild type. However, *rcp2-1* can be readily distinguished from *rcp1-1* in two ways. First, the total carotenoid content in the nectar guides of *rcp2-1* is ~10-fold lower than the wild type (Figure 1D), whereas that of *rcp1-1* is only ~4.4-fold lower (Sagawa et al., 2016). Second, the residual carotenoid pigments in *rcp1-1* and *rcp2-1* show distinct spatial distributions. At the base of the corolla tube (white boxes in Figures 1A to 1C), carotenoid pigments are completely lacking in *rcp2-1* but present in *rcp1-1*. By contrast, at the throat of the corolla tube (red boxes in Figures 1A to 1C), carotenoid pigments are completely lacking in *rcp1-1* but present at low concentrations in *rcp2-1*, giving a cream instead of bright yellow color. These spatial distribution patterns of residual pigments are consistent among allelic mutants within each complementation group (Supplemental Figure 1).

To test whether RCP2 regulates CBP genes at the transcriptional level, we performed qRT-PCR experiments on nectar guide tissue at the 15-mm corolla developmental stage (same stage as in the previous study on *RCP1*; Sagawa et al., 2016). Compared with wild type, the *rcp2-1* mutant showed a coordinated down-regulation of the entire CBP (Figure 1E), with a 3- to 4-fold decrease in expression of most CBP genes and ~10-fold decrease in *BETA CAROTENOID HYDROXYLASE1* (*BCH1*) expression. These results suggest that RCP2 is involved in the transcriptional regulation of CBP genes in the nectar guides. Consistent with the more severe reduction in total carotenoid content, the extent of CBP gene down-regulation is stronger in *rcp2-1* than in *rcp1-1* (Sagawa et al., 2016).

In contrast to the wholesale CBP down-regulation in the nectar guides, only two CBP genes (*ZDS2* and *ZEP1*) showed >1.5-fold down-regulation (with $P < 0.05$) in *rcp2-1* leaf tissue (Supplemental Figure 1; Supplemental Data Set 1).

Two Additional *rcp2* Mutants Are Recovered from *Mimulus verbenaceus*

Coincidentally, we found two additional *rcp2* mutants in *M. verbenaceus*, a hummingbird-pollinated species that is closely related to *M. lewisii* (Beardsley et al., 2003). We performed a pilot EMS mutagenesis experiment using the *M. verbenaceus* inbred line MvBL as part of our effort to develop these two species as a platform for comparative developmental genetics studies. We screened 460 M2 families (~20 M2 plants per family) and recovered more than 100 floral mutants. While wild-type *M. verbenaceus* (MvBL) produces bright red corollas with high concentrations of yellow carotenoids and magenta anthocyanins (Figure 2A), two recessive mutants (*MV00025* and *MV00051*) lack

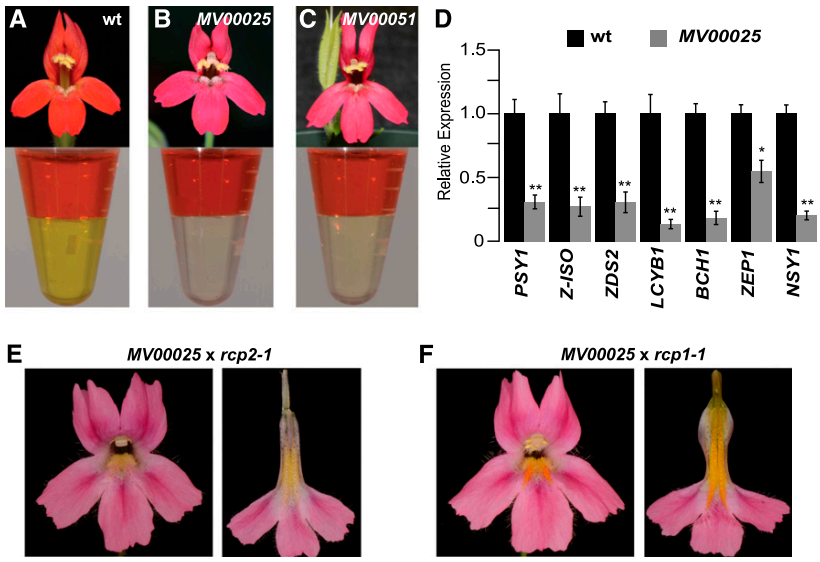

Figure 2. *rcp2* Phenotypes in *M. verbenaceus* Flowers.

Phenotypes of wild-type **(A)**, *MV00025* **(B)**, and *MV00051* **(C)** flowers. Top row, Front view of the flower. Bottom row, Separation of anthocyanins (top aqueous layer) and carotenoids (bottom organic layer).

(D) qRT-PCR of a subset of the CBP genes in wild-type *M. verbenaceus* and *MV00025*. Error bars are 1 SD ($n = 3$ biological replicates, each consisting of pooled 15-mm corollas from a distinct plant); asterisks indicate differences from the wild type (*$P < 0.05$, **$P < 0.01$, Student's *t* test).

(E) and **(F)** Complementation crosses between *MV00025* and *M. lewisii rcp2* and *rcp1* mutants.

carotenoids in the entire corolla (Figures 2B and 2C). Similar to *M. lewisii rcp2-1*, the *M. verbenaceus* mutants show coordinated down-regulation of CBP genes compared with wild-type MvBL (Figure 2D).

Crossing these two mutants with each other and with *M. lewisii rcp2-1* produced plants bearing flowers with very little carotenoid pigmentation in the nectar guides (Figure 2E). By contrast, crosses between the *M. verbenaceus* mutants and *rcp1-1* produced plants with intense yellow color in the nectar guides (Figure 2F). These complementation crosses suggest that *MV00025* and *MV00051* represent two additional *rcp2* alleles. Note that the F1 hybrids between *M. lewisii* and *M. verbenaceus* have pink petal lobes without carotenoids because they are heterozygous for *YELLOW UPPER* (*YUP*), a dominant repressor known to prevent carotenoid

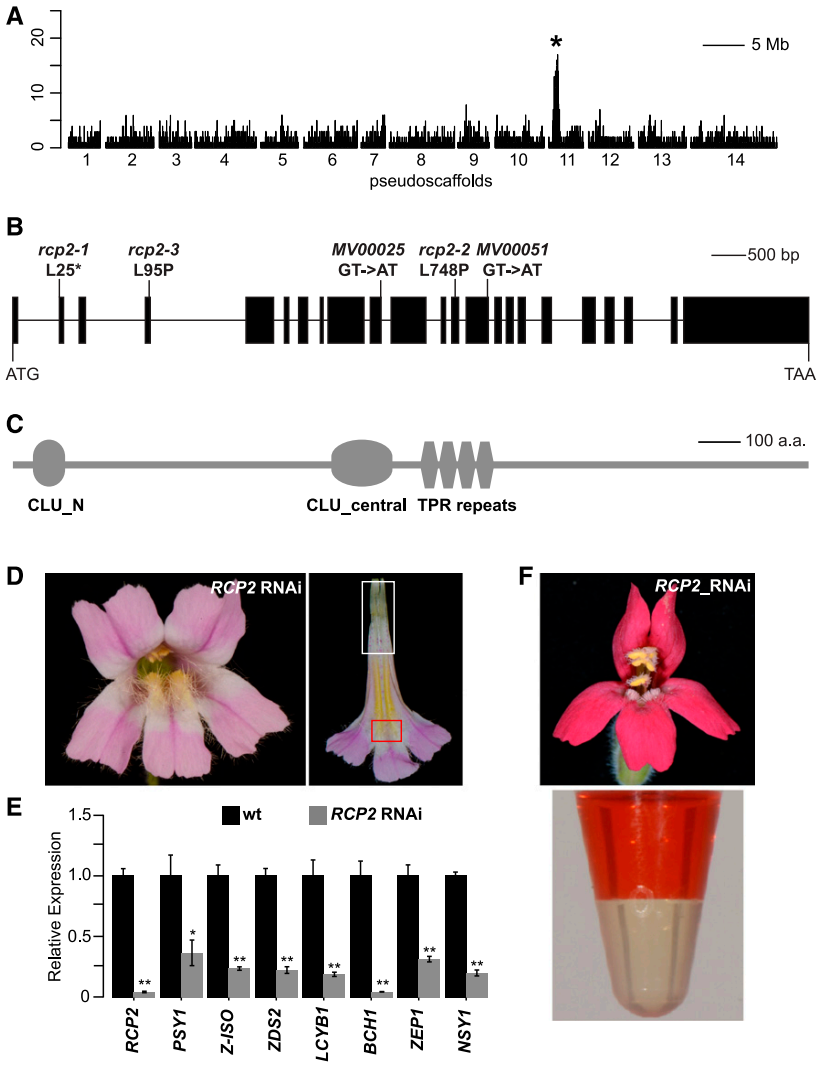

Figure 3. Identification of *RCP2*.

(A) Whole-genome scan for regions enriched in homozygous SNPs.

(B) Schematic *RCP2* gene map highlighting mutations from *M. lewisii (rcp2-1*, *rcp2-2*, *and rcp2-3)* and *M. verbenaceus* (*MV00025* and *MV00051*). Black boxes, exons; lines, introns.

(C) RCP2 protein schematic showing the key domains.

(D) Front view and nectar guide view of a representative *M. lewisii RCP2* RNAi line. White and red boxes indicate the base and throat of the corolla tube, respectively.

(E) Relative transcript levels of a subset of CBP genes in 15-mm nectar guides of *M. lewisii RCP2* RNAi lines compared to the wild type, as determined by qRT-PCR. Error bars are 1 SD ($n = 3$ biological replicates, each consisting of pooled 15-mm nectar guides from an independent RNAi line); asterisks indicate differences from the wild type (*$P < 0.05$, **$P < 0.01$, Student's t test).

(F) Front view (top) and pigment separation (bottom) of a representative *RCP2* RNAi flower in *M. verbenaceus*.

accumulation in the petal lobes (Hiesey et al., 1971): *M. lewisii* is homozygous for the dominant allele and *M. verbenaceus* is homozygous recessive.

RCP2 Encodes a TPR Protein

To identify *RCP2*, we performed bulk segregant analysis by Illumina sequencing of an F2 population, which was derived from a cross between *rcp2-1* (in the LF10 background) and the mapping line SL9 (see Methods). A conspicuous peak was detected on pseudoscaffold 11 (Figure 3A), corresponding to a 70-kb region in the LF10 genome (LF10g_v1.8 scaffold 278, 1,215,000 to 1,285,000). Remapping the Illumina reads to this 70-kb interval of the LF10 genome revealed only one mutation in the entire region. This mutation causes a premature stop codon at the beginning of the second exon of a gene encoding a TPR protein of 1794 amino acids (Figure 3B), with a calculated mass of 196 kD. Sequencing the independent *rcp2-2* and *rcp2-3* alleles showed that both contain nonsynonymous amino acid replacements at highly conserved sites (Figure 3B; Supplemental Figure 2) of this TPR protein. Additionally, *MV00025* and *MV00051* each contain an intron splicing mutation in this gene (Figure 3B), corroborating the results of the complementation test.

To further verify that this *TPR* gene is *RCP2*, we knocked down its expression in both species, expecting to recapitulate the mutant phenotypes. To this end, we constructed an RNA interference (RNAi) plasmid using a 408-bp fragment in the last exon of the *M. lewisii TPR* gene, which has a unique nucleotide sequence, as determined by BLAST analysis against the LF10 genome assembly, and transformed it into wild-type LF10. We

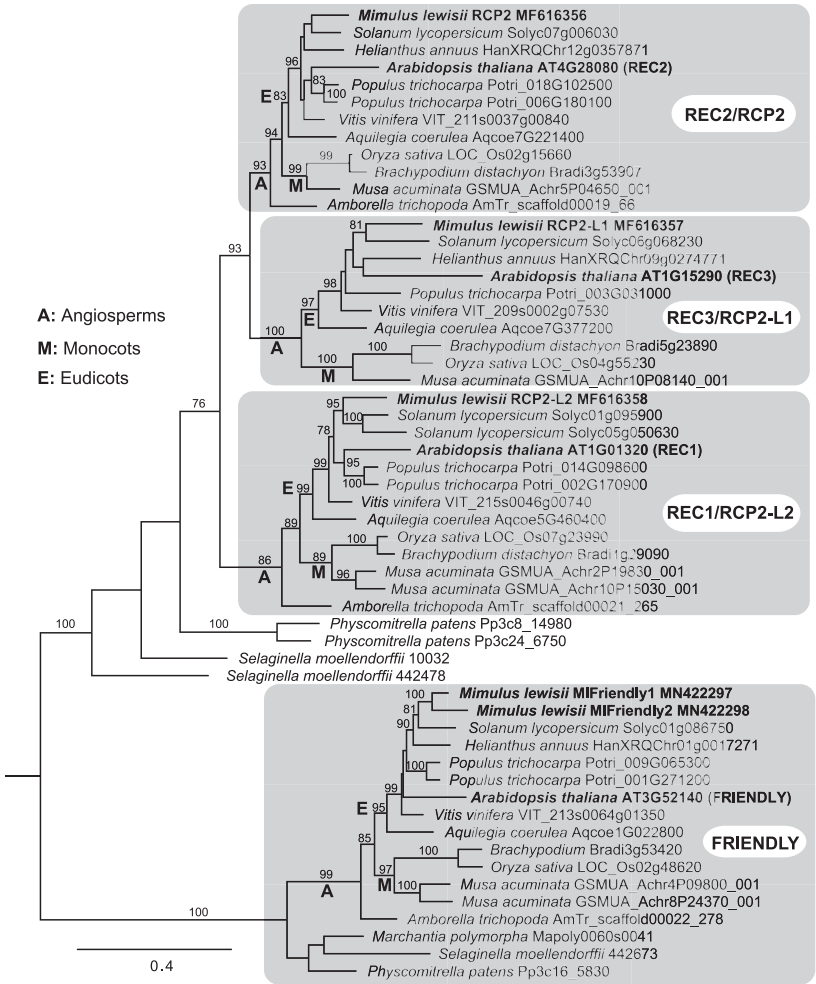

Figure 4. Maximum Likelihood (ML) Phylogenic Tree of RCP2 and Related Proteins.

GenBank accession numbers for the *Mimulus* sequences are provided after each gene name. The Arabidopsis sequences were retrieved from TAIR (https://www.arabidopsis.org/). All other sequences were retrieved from Phytozome v13 (https://phytozome-next.jgi.doe.gov/), with locus name following the species name. Bootstrap values higher than 75 are shown along the branches. The tree was rooted by midpoint rooting. "A," "M," and "E" indicate the clades containing all angiosperms, monocots, and eudicots, respectively.

obtained 127 stable transgenic plants, 96% of which closely resemble the *rcp2-1* mutant, including the complete lack of yellow pigments at the base of the corolla tube and the creamy yellow color at the throat of the corolla tube (Figure 3D). Evaluation of the expression level of this *TPR* gene in three of the RNAi lines showed ~95% knockdown, and qRT-PCR confirms that the CBP genes are also down-regulated in the RNAi lines to a similar degree as in the *rcp2-1* mutant (Figure 3E). Transforming the same RNAi construct into MvBL (the RNAi fragment has 95% sequence identity between the two species) yielded 40 independent transgenic lines, 37 of which recapitulated the mutant phenotype (Figure 3F). Based on the bulk segregant analysis, five independent allelic mutants, and the RNAi results, we conclude that this *TPR* gene is indeed *RCP2* and that *rcp2-1* is likely to be a null allele, as the translated protein would contain only 24 of the 1794 amino acids (Figure 3B).

BLAST analysis of the RCP2 protein sequence against the NCBI Conserved Domain Database (Marchler-Bauer et al., 2015) revealed three conserved domains—a TPR domain with four TPR repeats, a CLUstered mitochondria protein N-terminal domain (CLU_N), and a CLU central domain (CLU_central; Figure 3C)—but no recognizable DNA binding domain. TPR repeats, which are found in a wide range of proteins, function as scaffolds to mediate protein-protein interactions (D'Andrea and Regan, 2003; Zeytuni and Zarivach, 2012; Bohne et al., 2016). By contrast, no specific functions have been assigned to the CLU domains to date. There are two closely related paralogs of *RCP2* in the *M. lewisii* genome, *RCP2-L1* and *RCP2-L2* (Figure 4; Supplemental Figure 2). Phylogenetic analysis indicates that the divergence of these three paralogs predated the origin of angiosperms: there is a corresponding ortholog for each of the three genes in both eudicots and monocots as well as the most basal angiosperm lineage, *Amborella* (note that the lack of *RCP2-L1/REC3* ortholog in *Amborella* is most likely due to secondary loss; Figure 4). The Arabidopsis homologs (*REC1*, *AT1G01320*; *REC2*, *AT4G28080*; *REC3*, *AT1G15290*) help establish the size of the chloroplast compartment in Arabidopsis leaf cells (Larkin et al., 2016). All the *REC* genes together are sister to the *FRIENDLY* clade (Figure 4), as shown in Larkin et al. (2016).

The existence of three closely related paralogs with potentially redundant functions raised the question as to why mutations in a single gene, *RCP2*, result in such a strong phenotype in floral carotenoid pigmentation. We hypothesized that *RCP2* and the *RCP2*-like genes have evolved different expression patterns. To test this, we performed RT-PCR at different stages of LF10 corolla development and in different tissues. *RCP2* is primarily expressed in the corolla (both nectar guides and petal lobes) and its expression gets progressively stronger as the corolla grows larger and the yellow color in the nectar guides becomes more intense (Figures 5A to 5C). By contrast, *RCP2-L1* and *RCP2-L2* are only expressed in the early stages of corolla development before the yellow color becomes conspicuous, suggesting these genes play a relatively minor role in floral carotenoid pigmentation compared to *RCP2*. On the other hand, these two genes are strongly expressed in the leaf, where *RCP2* is expressed relatively weakly.

RCP2 Is Required for Chromoplast Development

The *RCP2* homologs in Arabidopsis, *REC1* to *REC3*, are involved in controlling the chloroplast compartment size (Larkin et al., 2016), and the gene that is sister to the *REC* clade, *FRIENDLY* (Larkin et al., 2016), controls mitochondrial morphology and intracellular distribution (Logan et al., 2003; El Zawily et al., 2014). These observations prompted us to investigate the possibility that *RCP2* is involved in the development of another organelle, the chromoplast, in *Mimulus* flowers. This supposition seemed promising because chromoplasts and chloroplasts are known to be interconvertible (Egea et al., 2010; Li and Yuan, 2013), and chromoplast development is known to play an important role in carotenoid accumulation, although not necessarily in the global

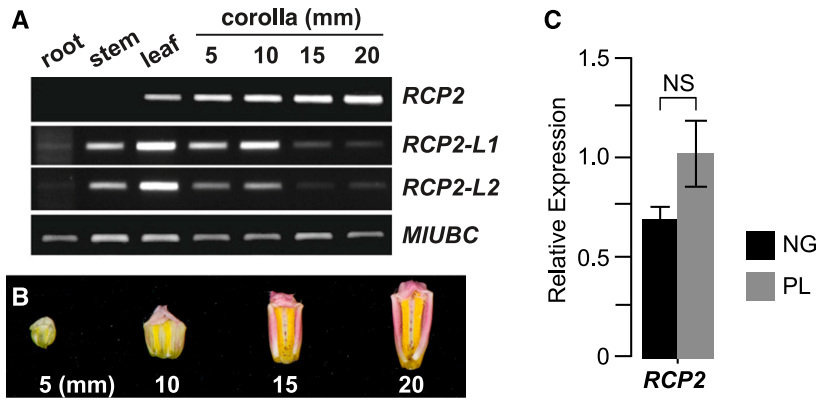

Figure 5. Expression Patterns of *RCP2*, *RCP2-L1*, and *RCP2-L2*.

(A) Qualitative RT-PCR (28 cycles) of *RCP2* and *RCP2-like* genes in various tissues and corollas at different developmental stages in wild-type *M. lewisii.* Root, stem, and leaf tissues were collected from 4-week old seedlings. *MIUBC* was used as the reference gene.

(B) Carotenoid accumulation in the nectar guides of wild-type *M. lewisii* across developmental stages.

(C) qRT-PCR measurement of relative *RCP2* expression level in *M. lewisii* nectar guides (NG) and petal lobes (PL). Error bars are 1 SD ($n = 3$ biological replicates, each consisting of pooled 15-mm nectar guides (NG) or petal lobes (PL) from a distinct plant. NS, non-significant; Student's *t* test).

transcriptional regulation of CBP genes (Mustilli et al., 1999; Liu et al., 2004a; Lu, 2006; Galpaz et al., 2008; Lopez et al., 2008; Chayut, 2017). To test this possibility, we examined the ultrastructure of flower epidermal cells by transmission electron microscopy (TEM). In wild-type *M. lewisii* nectar guide epidermal cells, numerous rounded chromoplasts are pushed to the periphery of the cell by the vacuole (Figure 6A), and each chromoplast contains several electron-dense plastoglobuli, the main carotenoid-sequestering structures (Figure 6B). In sharp contrast, in the *rcp2* mutant, the chromoplasts on the cell periphery are skinny, irregularly shaped, and usually contain few plastoglobuli (Figures 6C and 6D). Similar differences can be observed in *MV00025* petal lobe epidermal cells compared with wild-type MvBL (Figures 6E and 6F). These results suggest that *RCP2* is required for proper chromoplast development.

Because carotenoid accumulation is concomitant with chromoplast formation, it is difficult to distinguish whether the malformation of chromoplasts disrupts the transcription of the carotenoid biosynthesis genes or whether a lack of carotenoids due to the down-regulation of the CBP genes leads to the improper development of chromoplasts. We reasoned that if decreased carotenoid biosynthesis causes the chromoplast malformation,

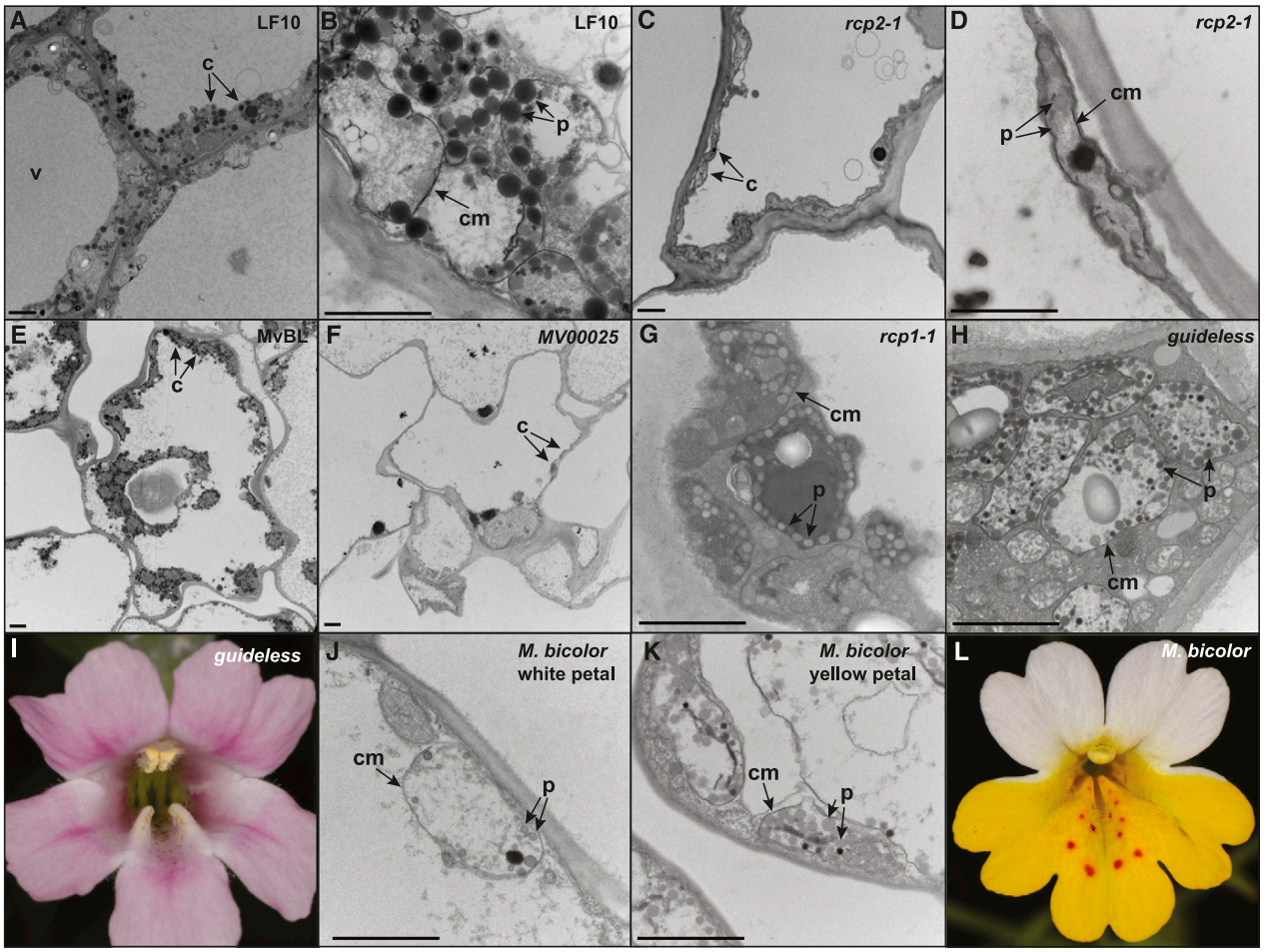

Figure 6. Transmission Electron Micrographs of Chromoplasts.

(A) and **(B)** Micrographs of *M. lewisii* wild-type LF10 nectar guide upper epidermal cells (section from the center of the nectar guide): whole-cell view **(A)** and detailed view of chromoplasts **(B)**.
(C) and **(D)** Micrographs of *M. lewisii rcp2-1* mutant nectar guide upper epidermal cells, sampled and presented in the same fashion as in **(A)** and **(B)**, respectively.
(E) and **(F)** Whole-cell view of petal lobe upper epidermal cells of *M. verbenaceus* wild-type MvBL **(C)** and *MV00025* **(D)**.
(G) and **(H)** Detailed view of chromoplasts from nectar guide upper epidermal cells of the *M. lewisii* mutants *rcp1-1* **(G)** and *guideless* **(H)**.
(I) Front view of *M. lewisii guideless* flower.
(J) and **(K)** Detailed view of plastids from the upper epidermis of the white dorsal petal **(J)** and the yellow ventral petal **(K)** of *M. bicolor.*
(L) Front view of *M. bicolor* flower. v, Vacuole; c, chromoplast; P, plastoglobule; cm, chromoplast membrane. Scale bars are 2 μm.

both *rcp1-1* and another mutant with greatly reduced carotenoid pigmentation in the nectar guides, *guideless* (Figure 6I; Yuan et al. 2013a), should also exhibit abnormal chromoplast development. However, in these mutants, chromoplasts appear normal in shape (Figures 6G and 6H), unlike the skinny, abnormally shaped chromoplasts in *rcp2* petals. The plastoglobuli are smaller and less electron-dense in *rcp1* and *guideless* than in the wild type, as one would expect if carotenoids are less abundant. Furthermore, we compared the plastids in the completely white upper petals of another *Mimulus* species, *Mimulus bicolor*, to its yellow lower petals (Figures 6J to 6L). We found that the white petals, though lacking carotenoids, make plastids similar in appearance to the chromoplasts made in the yellow petals of the same flower. These observations suggest that the defective chromoplast development in *rcp2* mutants is not due to the lack of carotenoid pigments per se but is a more direct consequence of *RCP2* malfunction.

RCP2 Regulates Carotenoid Biosynthesis Independently of *RCP1*

To test potential genetic interactions between *RCP1* and *RCP2*, we created the *rcp1-1 rcp2-1* double mutant. The double mutant shows an additive phenotype regarding the spatial distribution of residual carotenoids, which are completely absent at both the base (as in *rcp2-1*) and the throat (as in *rcp1-1*) of the corolla tube (Figure 7A). The additive phenotype suggests that *RCP1* and *RCP2* most likely act independently in the regulation of carotenoid biosynthesis. Consistent with this inference, neither of these genes regulates the other at the transcriptional level. qRT-PCR assays showed no significant difference in the transcript level of *RCP2* between the *rcp1-1* mutant and the wild type. Likewise, *RCP1* transcript level did not differ between the *rcp2-1* mutant and the wild type (Figure 7B). In addition, a yeast two-hybrid assay showed no direct interaction between the RCP1 and RCP2 proteins (Supplemental Figure 3). Furthermore, *RCP1* and *RCP2* have very different spatiotemporal expression patterns: while *RCP1* expression is restricted to the nectar guides (Sagawa et al., 2016) and peaks at the 10-mm corolla developmental stage, *RCP2* is expressed in both nectar guides and petal lobes and gets stronger over the course of flower development (Figure 5C).

RCP2 Overexpression Promotes Ectopic Carotenoid Biosynthesis and Potentially Chromoplast Proliferation

To further characterize the function of *RCP2*, we generated transgenic plants overexpressing this gene. Because the dominant *YUP* allele represses carotenoid accumulation in the *M. lewisii* flower (except the nectar guides; Hiesey et al. 1971), we performed the overexpression experiment in *M. verbenaceus*, which is homozygous for the recessive *yup* allele. We transformed MvBL with a *35S:RCP2-yellow fluorescent protein* (*YFP*) construct and obtained seven stable transgenic lines, five of which showed a similar overexpression phenotype, with increased carotenoid contents in the flower, particularly the style and filaments (Figures 8A, 8B, and 8I). Correspondingly, the expression levels of CBP genes increased substantially in these tissues (Figures 8A and 8B; Supplemental Figure 4). Cells at the upper, middle, and the lower portions of both style and filaments appear to have not only yellower, but potentially more numerous chromoplasts in the *35S:RCP2-YFP* plants than in the wild type (Figures 8C to 8H). Because the exact number of chromoplasts per cell is difficult to quantify, we assayed relative expression levels of the plastid division genes *MvFtsZ1*, *MvFtsZ2*, *MvARC1*, and *MvARC6* in developing flower buds as a proxy. We found that *MvARC1* and *MvARC6* were slightly, but significantly, up-regulated (~1.5-fold) in the overexpression plants (Figure 8J). Although the function of these plastid division genes in chloroplast division has been well characterized (Osteryoung and Pyke, 2014), their role in chromoplast division is still largely hypothetical. As such, we can only tentatively conclude that *RCP2* overexpression promotes chromoplast proliferation in filaments and styles.

It should be noted that *RCP2* overexpression does not appear to cause carotenoid accumulation in colorless plastids in the roots (i.e., amyloplasts; Supplemental Figure 5), indicating that not all tissue types are competent to produce carotenoids upon *RCP2* expression.

Subcellular Localization of RCP2 Does Not Change upon Amitrole Treatment

To gain insight into the functional mechanism of RCP2, we attempted to determine the subcellular localization of the protein

Figure 7. Lack of Genetic Interaction between *RCP1* and *RCP2*.

(A) Front view and nectar guide view of the *rcp1-1 rcp2-1* double mutant. White and red boxes indicate the base and throat of the corolla tube, respectively.
(B) qRT-PCR experiments showing the relative expression of *RCP2* in the 15-mm nectar guides of the *rcp1* mutant compared to the wild type and *RCP1* in the 10-mm nectar guides of the *rcp2* mutant compared to the wild type. Error bars are 1 SD ($n = 3$ biological replicates, each consisting of pooled 15 [for *RCP2*]- or 10-mm (for *RCP1*) nectar guides from a distinct plant; NS, non-significant; Student's *t* test).

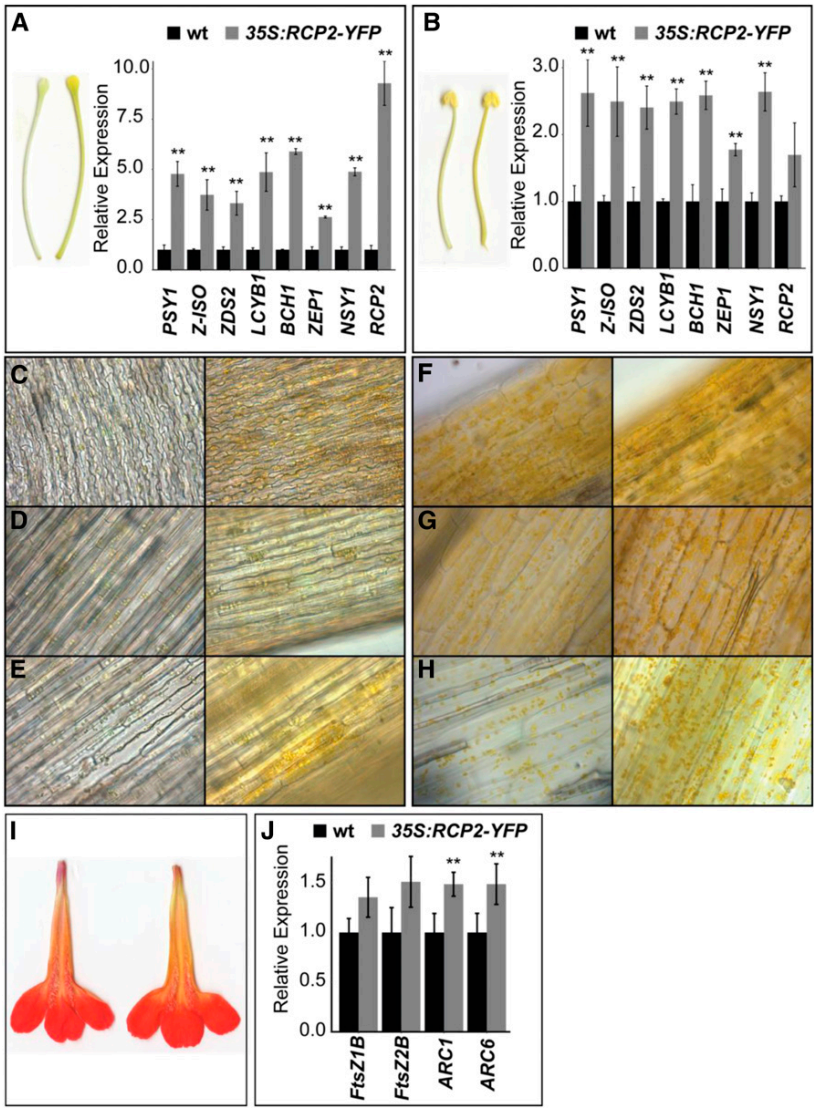

Figure 8. Overexpression of *RCP2* in *M. verbenaceus*.

(A) The phenotypes of wild-type (left) and *35S:RCP2-YFP* (right) styles, and the relative transcript levels of *RCP2* and a subset of CBP genes in the style tissue of 15-mm corollas. Error bars are 1 SD ($n = 3$ biological replicates, each consisting of pooled 15-mm stage styles from a distinct T2 plant of transgenic line 6).
(B) Filament phenotypes and relative gene expression levels shown in the same fashion as in **(A)**.
(**C**) to **(E)** Light microscopy of wild-type (left) and *35S:RCP2-YFP* (right) styles, showing the top **(C)**, middle **(D)**, and base **(E)** of the style.
(**F**) to **(H)** Light microscopy of filaments, shown in the same manner as in **(C)** to **(E)**.
(I) The lower petals of wild-type (left) and *35S:RCP2-YFP* (right) corollas.
(J) Relative expression of the plastid division genes in the 2-mm flower buds of *35S:RCP2-YFP* compared to wild-type plants. Error bars are 1 SD ($n = 3$ biological replicates, each consisting of pooled 2-mm flower buds from a distinct T2 plant of transgenic line 6). Asterisks indicate differences from the wild type (**$P < 0.01$, Student's *t* test).

using the *35S:RCP2-YFP* plants. Unexpectedly, no fluorescence was observed, which was surprising because (1) the same YFP tag fused to the C termini of other proteins have been previously shown to emit strong fluorescence in *Mimulus* (Ding and Yuan, 2016); (2) the chimeric RCP2-YFP protein was clearly functional, as it produced overexpression phenotypes in the wild-type background (Figure 8) and resulted in phenotypic rescue when the *35S:RCP2-YFP* transgene was crossed into the *rcp2* mutant background (Supplemental Figure 4); and (3) REC1-YFP (chimeric protein of the Arabidopsis ortholog of RCP2-L2) showed fluorescence signal in a transient assay in *Nicotiana benthamiana* (Larkin et al., 2016). We therefore performed a transient assay by

agroinfiltrating the *35S:RCP2-YFP* plasmid into *N. benthamiana* leaves, using *35S:RCP1-YFP* as a positive control. While the RCP1-YFP was nuclear localized in *N. benthamiana* pavement cells (Figure 9A), RCP2-YFP still produced no detectable fluorescence signal. We therefore constructed a second overexpression plasmid (*35S:YFP-RCP2*) with the YFP tag fused to the N terminus of RCP2 and tested its localization in *N. benthamiana* leaves. This experiment showed cytonuclear localization (Figure 9B; Supplemental Figure 3), which is consistent with that of REC1-YFP (Larkin et al., 2016).

Larkin et al. (2016) showed that the blockage of carotenoid and chlorophyll biosynthesis by amitrole treatment in *N. benthamiana* leaves caused REC1 to be excluded from the nucleus. To test whether RCP2 has the same behavior, we treated *N. benthamiana* plants with 125 μM amitrole solution and performed transient assays using the *35S:YFP-RCP2* construct. The white leaves of amitrole-treated plants showed no change in protein localization compared to the leaves of mock-treated plants: fluorescence was still localized to both the nucleus and cytosol (Figure 9C). These results differ from those of Arabidopsis REC1 (Larkin et al., 2016), indicating functional divergence of these proteins.

RCP2-like Genes Affect Chlorophyll Accumulation and Chloroplast Coverage in Leaves

The *RCP2* homologs in Arabidopsis (*REC1*/*REC2*/*REC3*) regulate chlorophyll accumulation and the chloroplast compartment size in leaf mesophyll cells. Some of the Arabidopsis combinatorial mutants show clear chlorophyll deficiency (Larkin et al., 2016).

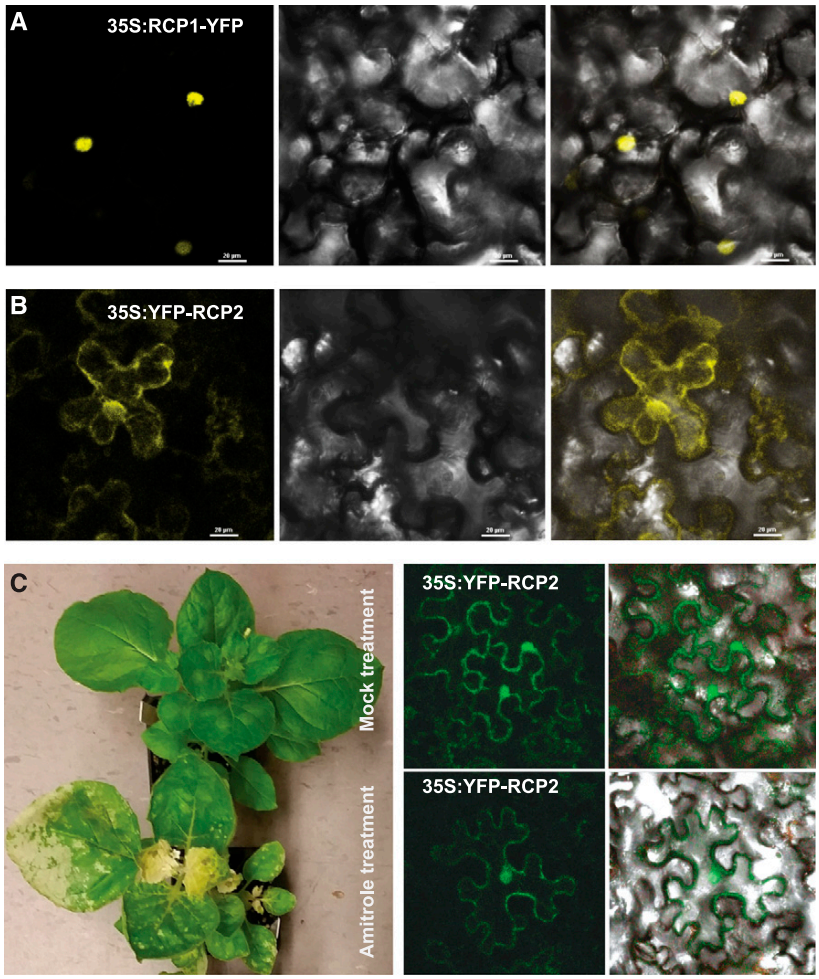

Figure 9. Protein Localization in *Nicotiana benthamiana*.

(A) and **(B)** Confocal microscopy of leaves transiently infiltrated with the plasmid *35S:RCP1-YFP* **(A)** and *35S:YFP-RCP2* **(B)**. Left, Green channel; middle, transmitted light; right, merged. Scale bars are 20 μm.

(C) RCP2 localization does not change after amitrole treatment (bottom) compared to mock-treated plants (top). For each transient assay, five patches of ~50 cells near injection sites were examined. Localization patterns were all the same as those shown in the figure.

rcp2 mutants in both *M. lewisii* (not shown) and *M. verbenaceus* have leaves similar in appearance to wild-type plants (Figure 10A). Pigment extractions from *M. verbenaceus* leaves showed that the chlorophyll content of the mutant *MV00025* is not significantly different from that of the wild type (Figure 10B). However, carotenoid content is slightly lower in *MV00025* than the wild type (Figure 10C).

If the function of *RCP2*-like genes in the regulation of chlorophyll accumulation and chloroplast compartment size is conserved between Arabidopsis and *Mimulus*, we expect that disrupting the function of *RCP2*, *RCP2-L1*, and *RCP2-L2* simultaneously would cause chlorophyll deficiency in photosynthetic tissues. To test this hypothesis, we attempted to induce a dominant-negative effect by overexpressing only the TPR domain of RCP2. The rationale is that

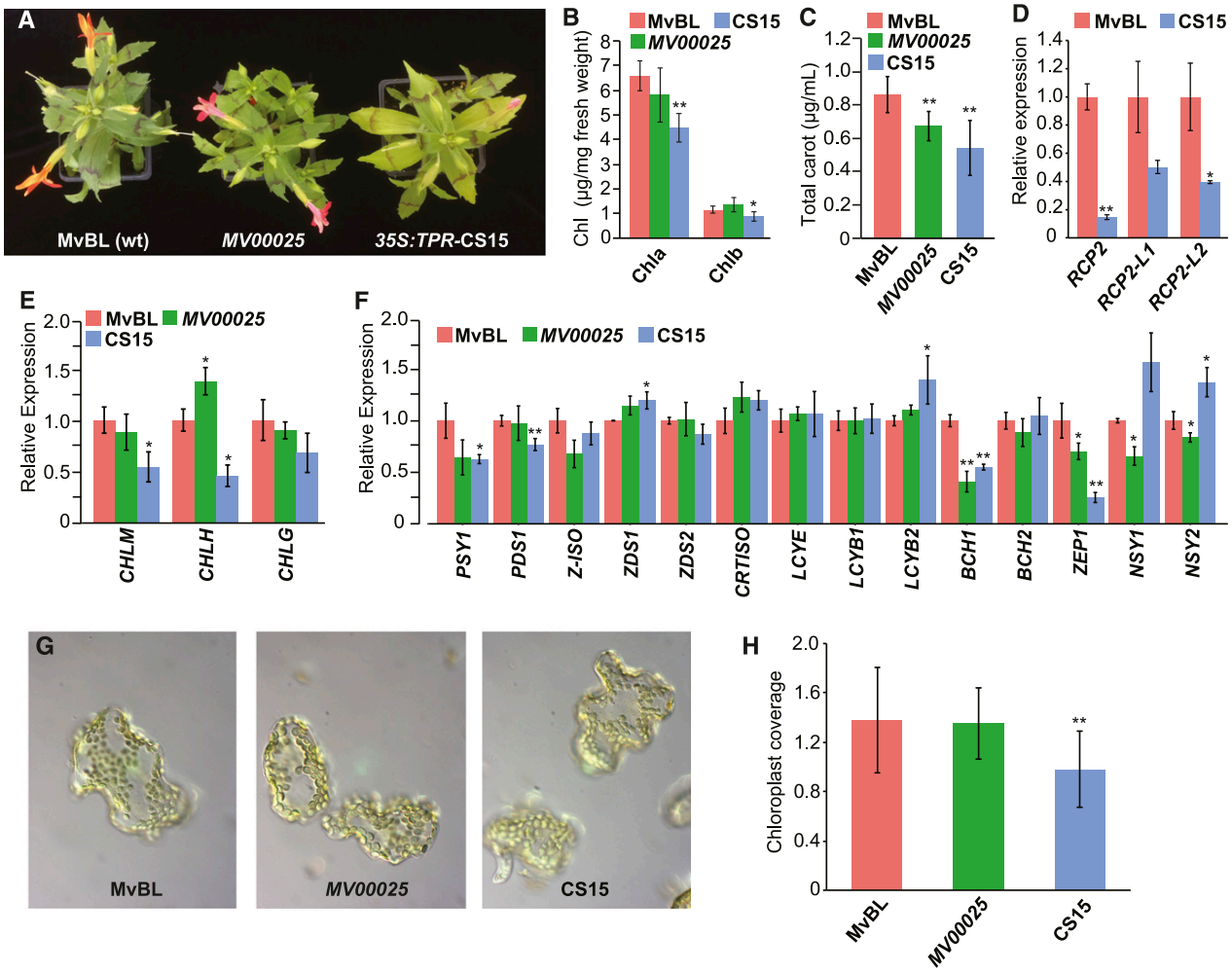

Figure 10. Phenotypic Effects of Simultaneous Down-Regulation of *RCP2*, *RCP2-L1*, and *RCP2-L2* in *Mimulus verbenaceus*.

(A) Left to right, wild-type (MvBL), *rcp2* mutant, and *35S:TPR* cosuppression line 15.

(B) Chlorophyll a and b concentrations in the distal half of 30-mm leaves. Error bars are 1 SD ($n = 6$ different leaves from the same plant).

(C) Total carotenoid content of the distal half of leaves, calculated by measuring carotenoid absorption at 470 nm and subtracting the concentrations of chlorophylls a and b. Error bars are 1 SD ($n = 10$ different leaves from the same plant).

(D) Relative transcript levels of *RCP2*, *RCP2-L1*, and *RCP2-L2* in 10-mm leaves of cosuppression line 15 (CS15) compared to the wild type. Error bars represent 1 SD ($n = 3$ biological replicates, each consisting of pooled 10-mm leaves from a distinct T2 plant of cosuppression line 15).

(E) and **(F)** Relative transcript levels of chlorophyll **(E)** and carotenoid **(F)** biosynthesis genes in 10-mm leaves of the *rcp2* mutant and cosuppression plants compared to the wild type. Error bars represent 1 SD ($n = 3$ biological replicates, each consisting of pooled 10-mm leaves from a distinct MvBL, *MV00025*, or T2 plant of cosuppression line 15).

(G) Representative mesophyll cells of 30-mm leaves from the wild type, *rcp2* mutant, and cosuppression plants.

(H) Chloroplast coverage in MvBL, *MV00025*, and CS15 mesophyll cells. Error bars are 1 SD ($n = 18$ cells for MvBL, $n = 17$ cells for *MV00025* and $n = 13$ cells for CS15). Asterisks indicate differences from the wild type (*$P < 0.05$, **$P < 0.01$, Student's *t* test).

the TPR domain is known to mediate protein-protein interactions, and overexpression of the TPR domain alone has been demonstrated to phenocopy loss-of-function mutations in other TPR genes (Chen et al., 1996; Tseng et al. 2001). Assuming that RCP2, RCP2-L1, and RCP2-L2 function redundantly in photosynthetic tissues by interacting with the same partners, overexpression of the RCP2 TPR domain should interfere with the function of all three proteins. To this end, we transformed wild-type *M. verbenaceus* (MvBL) with a *35S:TPR* construct and generated 36 stable transgenic lines. Somewhat surprisingly, only four of the 36 lines have a pale-leaf phenotype (Figure 10A) resembling the combinatorial *rec* mutants in Arabidopsis, as one would expect from a dominant-negative effect. The flowers of these four lines are also completely pink without carotenoids. Upon further examination, we determined that these phenotypes are actually caused by cosuppression rather than a dominant-negative effect, as all three genes are down-regulated at the transcript level (Figure 10D). The DNA sequence encoding the RCP2 TPR domain has ~80% identity to that of *RCP2-L1/L2*, which explains the relatively weak down-regulation of these two genes (~50% knock-down) compared with *RCP2* itself (~85% knock-down).

Both chlorophyll and carotenoid contents in the leaf are significantly reduced in the cosuppression plants compared with wild type (Figures 10B and 10C), although the relative compositions of individual chlorophyll or carotenoid species show no obvious differences (Supplemental Figure 6; Supplemental Table 1). Correspondingly, the chlorophyll biosynthesis genes *CHLM* and *CHLH* (but not *CHLG*) are modestly but significantly down-regulated (~50%) in the leaves of cosuppression plants but not in the *rcp2* mutant (*MV00025*; Figure 10E). These results indicate that either *RCP2* is not involved, or its function is redundant with that of *RCP2*-like genes, in the regulation of chlorophyll biosynthesis. The expression changes of CBP genes in the leaf, on the other hand, are more complex. For instance, *PSY1* and *BCH1* were down-regulated in both the *rcp2* mutant and cosuppression line to a similar degree; *ZEP1* expression showed a ~30% reduction in the *rcp2* mutant, but ~75% reduction in the cosuppression line; both *NSY* paralogs showed slightly lower expression in the *rcp2* mutant but higher expression in the cosuppression line; and several other genes showed no expression change between the wild type and either *rcp2* or the cosuppression plants (Figure 10F).

Similar to the *rec* mutants in Arabidopsis, our cosuppression plants show no obvious differences in chloroplast morphology but have reduced chloroplast compartment size compared with the wild type (Figures 10G and 10H; Supplemental Figure 7). The decrease in chloroplast coverage is less dramatic in our cosuppression plants (~28%) than in some of the combinatorial *rec* mutants (~50%). This is likely because the down-regulation of *RCP2-L1* and *RCP2-L2* was relatively weak in the cosuppression plants (Figure 10D), in contrast to the null alleles of *REC1/2/3* characterized in Arabidopsis (Larkin et al., 2016). This interpretation is also consistent with our observation that chlorophyll content in the cosuppression plants decreased by only ~30% compared with wild-type plants (Figure 10B), whereas *Arabidopsis rec1 rec2 rec3* triple mutants showed ~80% decrease in chlorophyll content. Taken together, these results demonstrate that the function of this small family of TPR genes in regulating chlorophyll accumulation and chloroplast compartment size in photosynthetic tissues is conserved between Arabidopsis and *Mimulus*.

DISCUSSION

In this study, we characterized the *RCP2* locus in *M. lewisii* and its close relative *M. verbenaceus*. Based on genetic mapping, multiple independent mutant alleles, transgenic experiments, and TEM analyses, we demonstrated that *RCP2* encodes a TPR protein that is necessary and sufficient for chromoplast development and CBP gene expression in *Mimulus* floral tissues. We also showed that simultaneous down-regulation of *RCP2* and its two paralogs, *RCP2-L1* and *RCP2-L2*, leads to reduced chlorophyll and carotenoid content as well as chloroplast compartment size in leaves.

RCP2 Positively Regulates Both Chromoplast Development and CBP Gene Expression in *Mimulus* Flowers

Our TEM results (Figure 6) suggest that one of the primary functions of *RCP2* is in the regulation of chromoplast development, independently of carotenoid biosynthesis, as other *Mimulus* flowers with reduced carotenoid accumulation produce petal plastids with the typical rounded shape (Figures 6G to 6L). Gene expression analyses of the *rcp2* mutants and *RCP2* overexpression lines showed that *RCP2* is also a positive regulator of CBP gene expression (Figures 1E, 2D, 8A, and 8B). However, our current data cannot distinguish whether the role of *RCP2* in CBP gene activation is independent of, or secondary to, chromoplast development.

The phenotypic effect of *RCP2* overexpression in *Mimulus* floral tissues is superficially similar to that of the gain-of-function mutations in the cauliflower and melon *Orange* (*Or*) gene and loss-of-function mutations in tomato *High Pigment-1*, *High Pigment-2*, and *High Pigment-3* genes (encoding DDB1, DET1, and ZEP, respectively), in terms of increased carotenoid content and altered chromoplast biogenesis. However, there are key differences. While RCP2 positively regulates the entire CBP at the transcriptional level, OR and HP-1/HP-2/HP-3 do not affect steady-state mRNA levels of CBP genes in general (Li et al., 2001; Cookson et al., 2003; Kolotilin et al., 2007; Galpaz et al., 2008; Yuan et al., 2015). The cauliflower mutant OR allele ($BoOR^{MUT}$) and the melon OR "golden SNP" ($CmOR^{His}$) enhance carotenoid accumulation in nonphotosynthetic tissues by stabilizing the PSY protein, triggering the formation of membranous chromoplasts and inhibiting β-carotene turnover (Lu et al., 2006; Tzuri et al., 2015; Yuan et al., 2015; Zhou et al., 2015; Chayut et al., 2017). Loss-of-function mutations in the *HP* genes produce tomato fruits with increased chlorophyll and carotenoid content due to increased plastid size and/or number (Cookson et al., 2003; Kolotilin et al., 2007; Galpaz et al., 2008), with no effect on CBP gene transcription. These differences suggest that *RCP2* has a distinct function from these previously characterized genes involved in plastid development and carotenoid regulation.

The biochemical functions of RCP2 and RCP2-like proteins are still poorly understood. Larkin et al. (2016) conducted an extensive genetic characterization of all four members of this small TPR gene family in Arabidopsis (i.e., *REC1/2/3* and *FRIENDLY*). They demonstrated that the REC1 protein (ortholog of RCP2-L2;

Figure 4) localizes to both the cytosol and the nucleus but is excluded from the nucleus upon amitrole treatment, which blocks chloroplast biogenesis. They suggested that this trafficking of REC1 between the nucleus and the cytosol might be important for the function of REC1 in maintaining a proper chloroplast compartment size. Beyond protein localization, very little information is available about the functional mechanisms of this small family of TPR proteins. Given that the TPR repeats are well known to serve as scaffolds mediating protein-protein interactions (D'Andrea and Regan, 2003; Zeytuni and Zarivach, 2012; Bohne et al., 2016), identifying the putative interacting partners of RCP2 and RCP2-like proteins may help elucidate their functional mechanisms in regulating plastid development and pigment biosynthesis.

Although carotenoid content decreased in the leaves of our cosuppression plants compared to the wild type (Figure 10C), there is no clear pattern of wholesale CBP gene down-regulation (Figure 10F), as observed in the flowers. These results indicate that the regulation of carotenoid accumulation in leaf tissue is more complex than in floral tissue, likely involving regulators in addition to *RCP2* or *RCP2*-like genes. This is not surprising, given that carotenoids in leaves are essential components of the photosynthetic apparatus (Liu et al., 2004b; Amunts et al., 2010), and their content and composition are tightly coregulated with other components of photosynthesis by both transcriptional and posttranslational mechanisms (Meier et al., 2011; Ruiz-Sola and Rodríguez-Concepción, 2012; Nisar et al., 2015; Sun and Li, 2020). By contrast, in flower petals, carotenoids are stored in chromoplasts as dispensable, secondary metabolites, and the regulation of carotenoid accumulation is decoupled from photosynthesis.

While the molecular mechanism of RCP2 remains to be elucidated, the finding that *RCP2* overexpression can increase both the biosynthetic activity and storage capacity of carotenoids, through coordinated CBP gene up-regulation and chromoplast development, respectively (Figure 8), suggests that *RCP2* represents an attractive target for carotenoid biofortification in crops.

Functional Conservation and Divergence of the *REC*/*RCP2* Gene Family Members

Our phylogenetic analysis shows that the *REC*/*RCP2*-like TPR genes in angiosperms fall into three well-supported clades (i.e., *REC1*/*RCP2-L2*, *REC2*/*RCP2*, and *REC3*/*RCP2-L1*; Figure 4), which is consistent with the results reported in Larkin et al. (2016). The three paralogs had already evolved in the common ancestor of all angiosperms. While the closely related *FRIENDLY* gene has a highly conserved function in regulating the intracellular distribution of mitochondria in a wide range of eukaryotes (Zhu et al., 1997; Fields et al., 1998; Logan et al., 2003; Cox and Spradling, 2009; Gao et al., 2014), whether the *REC* genes have a conserved role in regulating chlorophyll biosynthesis and chloroplast compartment size has been unclear. The simultaneous down-regulation of *RCP2*, *RCP2-L1*, and *RCP2-L2* in our cosuppression plants resulted in significant decrease in chlorophyll content and chloroplast compartment size (Figures 10B and 10H), suggesting that the role of these TPR genes in regulating chlorophyll accumulation and chloroplast compartment size is conserved between Arabidopsis and *Mimulus*.

The existence of three paralogs provides opportunities for functional divergence. For example, while the *Arabidopsis rec1* mutant is a *genomes uncoupled* (*gun*) mutant with disrupted chloroplast-to-nucleus signaling, *rec2* and *rec3* appear to have intact retrograde signaling (Larkin et al., 2016). Arabidopsis REC1 shows altered protein localization upon amitrole treatment (i.e., from cytonuclear to exclusively cytoplasmic), but the REC2 ortholog in *Mimulus*, RCP2, does not seem to have this behavior (Figure 9C). Furthermore, the FRIENDLY protein is exclusively localized to the cytosol in wild-type Arabidopsis (Logan et al., 2003; El Zawily et al., 2014), indicating that this nucleus-to-cytosol trafficking behavior might be specific to REC1 (and potentially its orthologs in other plants).

In addition to protein function, the expression patterns of these three genes have also diverged. In *Mimulus*, while *RCP2-L1* and *RCP2-L2* are primarily expressed in photosynthetic tissues, *RCP2* is expressed only weakly in leaves (and is not expressed in stems). Instead, this gene is strongly expressed in the corolla throughout flower development (Figure 5A). The evolution of the diverged *RCP2* paralog may allow for pigment/plastid innovation in non-green tissues such as flowers, while the *RCP2*-like genes continue to perform essential functions in photosynthetic tissues. *RCP2* and its orthologs in other species may therefore have great potential for generating natural variation in floral carotenoid pigmentation.

Mimulus verbenaceus Is an Excellent Developmental Genetics Model System Complementary to *M. lewisii*

Our results also demonstrate that the hummingbird-pollinated *M. verbenaceus* is just as amenable to chemical mutagenesis and in planta transformation as the more extensively studied, bumblebee-pollinated *M. lewisii*. This is significant because *M. verbenaceus* provides an excellent study system complementary to *M. lewisii*, allowing us to carry out experiments that might be challenging to interpret in *M. lewisii*. For example, *RCP2* overexpression produces clear phenotypes in *M. verbenaceus* floral tissues that might otherwise be masked in *M. lewisii* by the dominant *YUP* allele (Hiesey et al., 1971). In addition, despite being genetically very similar (Beardsley et al., 2003), these two species differ drastically in terms of many pollinator-associated floral traits. Given the ease of chemical mutagenesis in *M. verbenaceus* (e.g., recovery of more than 100 floral mutants from 460 M2 families), it is not difficult to envision that *M. verbenaceus* could become a key model system to dissect the genetic networks underpinning the evolution of hummingbird pollination syndromes (e.g., long stamen and pistil length, copious nectar production). Together, these two species provide an excellent platform for comparative developmental genetics studies of two closely related species with dramatic phenotypic divergence.

METHODS

Plant Materials

The *Mimulus lewisii* Pursh inbred line LF10 (wild type) and the mapping line SL9 were described in Yuan et al. (2013a, 2013b). Seeds of wild *Mimulus verbenaceus* were collected from Oak Creek Canyon (Sedona, Arizona)

and the inbred line MvBL was generated by single seed descent for >10 generations. EMS mutants were generated using LF10 and MvBL for *M. lewisii* and *M. verbenaceus*, respectively, following Owen and Bradshaw (2011). All plants were grown with FAFARD soil mix no. 2 (Sun Gro Horticulture) in the University of Connecticut EEB Research Greenhouses, under natural light either supplemented with sodium vapor lamps or shaded with greenhouse curtain systems, to provide a 16 h daylength with a light intensity of 110 to 160 $\mu mol \cdot m^{-2} \cdot s^{-1}$. Plants were watered by subirrigation and fertilized three times a week.

Carotenoid and Chlorophyll Analyses

To estimate relative carotenoid concentration in *M. lewisii* corollas, carotenoid pigments were extracted from the nectar guides of fresh flowers as described in Sagawa et al. (2016). Carotenoid concentration was estimated based on absorbance measurement at 440 nm and normalized to 100 mg tissue.

To determine chlorophyll concentration in *M. verbenaceus* leaf tissue, carotenoids and chlorophylls were extracted together from the distal half of 30-mm leaves in 1 mL methanol. Chlorophyll concentration was estimated using the following equations (Lichtenthaler, 1987):

$$[Chlorophyll\ a] = 16.72 \times A665 - 9.16 \times A652$$

$$[Chlorophyll\ b] = 34.09 \times A652 - 15.28 \times A665$$

The relative carotenoid concentration and composition in *M. verbenaceus* leaves were determined using ultraviolet–visible spectroscopy and high-performance liquid chromatography (HPLC). Leaves were collected from wild-type MvBL, *MV00025*, and CS15 plants, and tissue weighing 30 mg was trimmed from the distal tip of each leaf. Pigments were extracted by grinding tissue in 1 mL of methanol, pelleting the leaf tissue by centrifugation, and isolating the supernatant. Absorption spectra of extracts from 10 leaves of each line were measured using a Varian Cary 50 ultraviolet–visible spectrometer. A 200-μL aliquot of each sample was diluted 1:9 (v/v) with fresh methanol and measured in a 1-cm quartz cuvette. Total carotenoid content was calculated (g/mL of total extract) by measuring the carotenoid absorption at 470 nm and subtracting the concentrations of chlorophylls a and b, as described by Lichtenthaler (1987).

HPLC analysis was conducted for two leaves per line using a Waters 600 multisolvent delivery system equipped with a Waters 2996 photodiode array detector and a Waters Atlantis T3 column (5 particle size, 4.6 × 250 mm). A 400-μL aliquot of each sample was diluted with 600 μL of acetonitrile and filtered through a Millipore 0.2 m Millex-FG syringe filter. The mobile phase consisted of solvent A, 87:10:3 (v/v/v) acetonitrile:methanol:water; and solvent B, ethyl acetate. Chromatography was performed using the following gradient: 0 to 20 min, 99% A, 1% B (v/v); 20 to 40 min, linear gradient to 60% A, 40% B; 40 to 60 min, 60% A, 40% B. All solvents were purchased from Fisher Scientific and were HPLC-grade quality. The mobile phase flow rate was 1.2 mL/min, and the injection volume was 200 μL. The percent molar composition of each carotenoid was determined from the chromatograms as described in Lunch et al. (2013).

Separation of Anthocyanins and Carotenoids in *M. verbenaceus* Flowers

The red color of *M. verbenaceus* flowers is due to a combination of high concentrations of carotenoids and anthocyanins. To help visualize the relative carotenoid content in wild-type flowers versus the *rcp2* mutants or transgenic lines, we separated anthocyanins and carotenoids. This was accomplished by grinding two petal lobes in 200 μL methanol, which dissolves both carotenoids and anthocyanins. After 2 min of centrifugation at 13,000 rpm, 150 μL of the clear pigment extract was transferred to a new tube and thoroughly mixed with 150 μL of water and 150 μL of dichloromethane. The pigments were separated by centrifugation (13,000 rpm for 2 min): water-soluble anthocyanins were suspended in the aqueous phase, while hydrophobic carotenoids remained in the organic phase (Figures 2A to 2C and 3F).

Bulk Segregant Analysis

Genetic mapping of *RCP2* followed the protocol laid out in Yuan et al. (2013a). In short, we crossed *rcp2-1* (which was produced in the LF10 background) with the mapping line, SL9, and selfed an F1 individual to produce an F2 population. We extracted DNA from 120 F2 individuals displaying the mutant phenotype and pooled the samples for deep sequencing on an Illumina HiSeq 2500 platform. We mapped the ~196 million reads (Bioproject: PRJNA326848) to the SL9 genome using CLC Genomics Workbench 7.0 (Qiagen) and then scanned for regions enriched in homozygous single nucleotide polymorphisms. This allowed us to identify a 70-kb candidate region.

qRT-PCR

We extracted RNA and synthesized cDNA according to Yuan et al. (2013b). The relative transcript levels of carotenoid biosynthetic genes, chlorophyll biosynthetic genes, plastid division genes, as well as *RCP1* and *RCP2*, were assessed by qRT-PCR (primers are listed in Supplemental Table 2). qRT-PCR was performed using Power SYBR Green PCR master mix (Applied Biosystems) on a CFX96 touch real-time PCR detection system (Bio-Rad). Samples were amplified for 40 cycles of 95°C for 15 s and 60°C for 30 s. Amplification efficiencies for each primer pair were determined using critical threshold values obtained from a dilution series (1:4, 1:8, 1:16, 1:32) of pooled cDNAs. *MIUBC*, the *Mimulus* ortholog of the Arabidopsis ubiquitin-conjugating enzyme gene (AT5G25760), was used as the reference gene as described in Yuan et al. (2013b). Three biological replicates, with a single technical replicate for each sample, were used for all qRT-PCR experiments; see the figure legends for details. Relative expression of each target gene compared to the reference gene was calculated using the formula $(E_{ref})^{CP(ref)}/(E_{target})^{CP(target)}$.

Phylogenetic Analysis

Multiple sequence alignment of RCP2 and related proteins was performed using MUSCLE (Edgar, 2004). Only the three conserved domains (CLU_N, CLU_central, and TPR domain) that could be confidently aligned across all sequences (Supplemental Data Set 2) were used for phylogenetic analysis. Maximum likelihood analysis was conducted using the RAxML web server (https://raxml-ng.vital-it.ch/#/; Kozlov et al., 2019), with the Jones-Taylor-Thornton amino acid substitution matrix and the GAMMA model of rate heterogeneity. Clade support was estimated by 100 bootstrap replicates. The tree (Supplemental Data Set 3) was rooted by midpoint rooting.

RNAi Plasmid Construction

We built an RNAi construct by cloning a 408-bp fragment of exon 23 of the *M. lewisii RCP2* gene into the pFGC5941 vector (Kerschen et al., 2004) in both the sense and antisense directions, following Yuan et al. (2013b; primers are listed in Supplemental Table 3). This fragment, and every 12-bp block within it, matched only a single region of the *M. lewisii* (100% identity) and *M. verbenaceus* genomes (95% identity), indicating target specificity. The plasmid was verified by sequencing and transformed into *Agrobacterium tumefaciens* (strain GV3101), before being transformed into wild-type LF10 and MvBL plants by vacuum infiltration following the protocol described in Yuan et al. (2013b).

Overexpression Constructs and Protein subcellular localization

To characterize the phenotypes caused by overexpression of *RCP2* and to visualize the subcellular localization of RCP2 proteins, the 5382-bp full-length *RCP2* coding DNA sequence (CDS) was cloned into two different Gateway vectors: pEarleyGate 101 and pEarleyGate 104 (Earley et al., 2006), as previously described (Yuan et al., 2014). These vectors drive expression of the transgene by the cauliflower mosaic virus *35S* promoter. In pEarleyGate 101 and pEarleyGate 104, the YFP CDS is fused in frame with the 3′ end and 5′ end of the *RCP2* CDS, respectively (i.e., *35S:RCP2-YFP* and *35S:YFP-RCP2*, respectively). In an attempt to generate a dominant-negative effect by overexpressing only the RCP2 TPR domain, we amplified a 1227-bp fragment of the *RCP2* CDS that encodes the TPR domain and cloned it into pEarleyGate 100 (i.e., *35S:TPR*), the same destination vector as pEarleyGate 101 without the YFP tag. All overexpression plasmids were sequence verified before being transformed into *Agrobacterium tumefaciens* (strain GV3101). The *35S:RCP2-YFP* and *35S:TPR* constructs were transformed into MvBL plants to generate stable transgenic lines.

For transient protein expression, Agrobacterium solutions containing either the *35S:YFP-RCP2* or *35S:RCP2-YFP* plasmid were injected to the abaxial side of *Nicotiana benthamiana* leaves, following Ding and Yuan (2016). Fluorescence images were acquired using a Nikon A1R confocal laser scanning microscope equipped with a 60× water immersion objective. We performed immunoblot analysis to test whether the transiently expressed YFP-RCP2 protein was intact. *N. benthamiana* leaf tissue transfected with the *35S:YFP-RCP2* plasmid was harvested 6 d after inoculation. Total plant protein was extracted using the plant total protein extraction kit (Sigma) according to the manufacturer's instructions. Extracts were boiled in SDS sample buffer and loaded on 10% mini-PROTEAN TGX gels (Bio-Rad), prior to transfer onto polyvinylidene difluoride membranes (Millipore) and immunoblotting with the GFP tag monoclonal antibody (GF28R, Thermo Fisher Scientific) following standard protocols.

Yeast Two-Hybrid Assay

Yeast two-hybrid constructs were built using the Matchmaker Gold yeast two-hybrid system (Clontech). The full-length *RCP2* CDS was recombined into the pGBKT7-BD bait vector using an In-Fusion cloning kit (Clontech) and transformed into the Y2H Gold yeast strain by polyethylene glycol transformation, according to manufacturer's instructions. The *RCP1* CDS was recombined in vivo into the pGADT7-AD prey plasmid in the Y187 yeast strain (primers listed in Supplemental Table 3). Both plasmids were brought together in individual yeast cells by mating between the two yeast strains and screened on DDO, QDO, and QDO/X/A plates to test for protein-protein interactions.

TEM

Pieces of nectar guide tissue of *M. lewisii* or petal lobe tissue of *M. verbenaceus* were prefixed in 2.5% glutaraldehyde and 2.0% paraformaldehyde with 0.05 M Pipes buffer. The samples were postfixed with 1% osmium tetroxide and 0.8% $K_3Fe(CN)_6$ and then dehydrated in ethanol. The samples were embedded in Spurr's resin and sectioned tangentially. The sections were counterstained with 2% aqueous uranyl acetate and 2.5% Sato's lead citrate. The sections were examined and photographed under a Tecnai 12 G2 Spirit BioTWIN transmission electron microscope (FEI) at UConn's Bioscience Electron Microscopy Laboratory.

Mesophyll Cell Microscopy and Chloroplast Coverage

Leaf mesophyll cells of wild-type *M. verbenaceus* (MvBL), the *rcp2* mutant MV00025, and the cosuppression line *35S:TPR-CS15* were isolated following Pyke (2011) to examine chloroplast morphology and compartment size. In brief, 35-mm leaves were cut into strips and fixed in 4% glutaraldehyde. The middle lamella was weakened by heating the leaf tissue at 60°C for 4 h in 0.1 M EDTA. Prior to light microscopy, leaf strips were macerated with forceps to separate cells. To consistently count chloroplasts in leaf cells, light microscopy images were taken at different depths, and manual counts were made by marking all chloroplasts in each image and removing any chloroplasts that appeared in multiple images. The cell plan area and average chloroplast plan area (10 chloroplasts/cell) were determined using ImageJ, and chloroplast coverage was calculated using the following equation: (chloroplast number per cell × mean chloroplast plan area per cell)/mesophyll cell plan area (Pyke, 2011). The chloroplast coverage was determined for 13 to 18 mesophyll cells per genotype.

Root Plastid Microscopy

Seeds of wild-type MvBL and *35S:RCP2-YFP* overexpression plants were sown on wet paper towels in Petri dishes sealed with Parafilm. After 7 d, eight seedlings of each genotype were removed from the dish and whole-mounted in water. Root tips were examined and imaged under a light microscope.

Accession Numbers

Sequence data from this article can be found in the GenBank/EMBL libraries under the following accession numbers: *MlRCP2* (MF616356), *MlRCP2-L1* (MF616357), *MlRCP2-L2* (MF616358), *MvRCP2* (MF616359), *MlFRIENDLY1* (MN422297), and *MlFRIENDLY2* (MN422298). Illumina short read data have been deposited in NCBI SRA (accession number PRJNA326848).

Supplemental Data

Supplemental Figure 1. Additional characterization of the *M. lewisii rcp2* and *rcp1* mutants.

Supplemental Figure 2. Alignment of RCP2 and RCP2-like proteins in *M. lewisii* and their homologues in Arabidopsis and *Brachypodium*.

Supplemental Figure 3. Further characterization of the RCP2 protein.

Supplemental Figure 4. Characterization of additional *35S:RCP2-YFP* transgenic plants.

Supplemental Figure 5. Light micrographs of root plastids.

Supplemental Figure 6. HPLC analysis of *M. verbenaceus* leaf pigment composition.

Supplemental Figure 7. Correlations of cell plan area with chloroplast number and plan area.

Supplemental Table 1. Mole percentages of carotenoids in *M. verbenaceus* leaves.

Supplemental Table 2. qRT-PCR primers.

Supplemental Table 3. Primers used for plasmid construction.

Supplemental Data Set 1. Summary of statistical tests.

Supplemental Data Set 2. Sequence alignments for phylogenetic analysis.

Supplemental Data Set 3. Phylogenetic tree file.

ACKNOWLEDGMENTS

We thank Clinton Morse, Matt Opel, and Adam Histen for plant care in the UConn EEB Research Greenhouses, Maritza Abril and Xuanhao Sun at the

UConn Bioscience Electron Microscopy Laboratory for assistance in the TEM experiments, Amy LaFountain (University of Connecticut) for performing the HPLC analysis, and Yuan Gao (Boston University) for assistance in the immunoblot experiment. We thank the editor and three anonymous reviewers for their constructive criticism, which greatly improved the article. This work was supported by the National Science Foundation (grants IOS-1558083 and IOS-1827645 to Y.-W.Y.)

AUTHOR CONTRIBUTIONS

L.E.S. and Y.-W.Y. designed the research; L.E.S., B.D., F.M., C.H., and Y.-W.Y. performed the experiments; W.S. and S.C. contributed Illumina sequencing data; all authors analyzed the data; L.E.S. and Y.-W.Y. drafted the article.

Received September 27, 2019; revised February 3, 2020; accepted February 26, 2020; published March 4, 2020.

REFERENCES

Albert, N.W., Lewis, D.H., Zhang, H., Schwinn, K.E., Jameson, P.E., and Davies, K.M. (2011). Members of an R2R3-MYB transcription factor family in Petunia are developmentally and environmentally regulated to control complex floral and vegetative pigmentation patterning. Plant J. **65:** 771–784.

Ampomah-Dwamena, C., Thrimawithana, A.H., Dejnoprat, S., Lewis, D., Espley, R.V., and Allan, A.C. (2019). A kiwifruit (*Actinidia deliciosa*) R2R3-MYB transcription factor modulates chlorophyll and carotenoid accumulation. New Phytol. **221:** 309–325.

Amunts, A., Toporik, H., Borovikova, A., and Nelson, N. (2010). Structure determination and improved model of plant photosystem I. J. Biol. Chem. **285:** 3478–3486.

Barker, W., Nesom, G., Beardsley, P.M., and Fraga, N.S. (2012). A taxonomic conspectus of Phrymaceae: A narrowed circumscription for *Mimulus*, new and resurrected genera, and new names and combinations. Phytoneuron **39:** 1–60.

Beardsley, P.M., Yen, A., and Olmstead, R.G. (2003). AFLP phylogeny of *Mimulus* section *Erythranthe* and the evolution of hummingbird pollination. Evolution **57:** 1397–1410.

Bemer, M., Karlova, R., Ballester, A.R., Tikunov, Y.M., Bovy, A.G., Wolters-Arts, M., Rossetto, P., Angenent, G.C., and de Maagd, R.A. (2012). The tomato FRUITFULL homologs TDR4/FUL1 and MBP7/FUL2 regulate ethylene-independent aspects of fruit ripening. Plant Cell **24:** 4437–4451.

Bohne, A.-V., Schwenkert, S., Grimm, B., and Nickelsen, J. (2016). Roles of tetratricopeptide repeat proteins in biogenesis of the photosynthetic apparatus. Int. Rev. Cell Mol. Biol. **324:** 187–227.

Borevitz, J.O., Xia, Y., Blount, J., Dixon, R.A., and Lamb, C. (2000). Activation tagging identifies a conserved MYB regulator of phenylpropanoid biosynthesis. Plant Cell **12:** 2383–2394.

Cazzonelli, C.I., Cuttriss, A.J., Cossetto, S.B., Pye, W., Crisp, P., Whelan, J., Finnegan, E.J., Turnbull, C., and Pogson, B.J. (2009). Regulation of carotenoid composition and shoot branching in *Arabidopsis* by a chromatin modifying histone methyltransferase, SDG8. Plant Cell **21:** 39–53.

Chayut, N., et al. (2017). Distinct mechanisms of the ORANGE protein in controlling carotenoid flux. Plant Physiol. **173:** 376–389.

Chen, M.S., Silverstein, A.M., Pratt, W.B., and Chinkers, M. (1996). The tetratricopeptide repeat domain of protein phosphatase 5 mediates binding to glucocorticoid receptor heterocomplexes and acts as a dominant negative mutant. J. Biol. Chem. **271:** 32315–32320.

Chiou, C.-Y., Pan, H.-A., Chuang, Y.-N., and Yeh, K.-W. (2010). Differential expression of carotenoid-related genes determines diversified carotenoid coloration in floral tissues of *Oncidium* cultivars. Planta **232:** 937–948.

Chung, M.Y., Vrebalov, J., Alba, R., Lee, J., McQuinn, R., Chung, J.D., Klein, P., and Giovannoni, J. (2010). A tomato (*Solanum lycopersicum*) APETALA2/ERF gene, SlAP2a, is a negative regulator of fruit ripening. Plant J. **64:** 936–947.

Cookson, P.J., Kiano, J.W., Shipton, C.A., Fraser, P.D., Romer, S., Schuch, W., Bramley, P.M., and Pyke, K.A. (2003). Increases in cell elongation, plastid compartment size and phytoene synthase activity underlie the phenotype of the *high pigment-1* mutant of tomato. Planta **217:** 896–903.

Cox, R.T., and Spradling, A.C. (2009). *Clueless*, a conserved *Drosophila* gene required for mitochondrial subcellular localization, interacts genetically with *parkin*. Dis. Model. Mech. **2:** 490–499.

D'Andrea, L.D., and Regan, L. (2003). TPR proteins: The versatile helix. Trends Biochem. Sci. **28:** 655–662.

Davies, K.M., Albert, N.W., and Schwinn, K.E. (2012). From landing lights to mimicry: The molecular regulation of flower colouration and mechanisms for pigmentation patterning. Funct. Plant Biol. **39:** 619–638.

de Vetten, N., Quattrocchio, F., Mol, J., and Koes, R. (1997). The *an11* locus controlling flower pigmentation in petunia encodes a novel WD-repeat protein conserved in yeast, plants, and animals. Genes Dev. **11:** 1422–1434.

Ding, B., and Yuan, Y.-W. (2016). Testing the utility of fluorescent proteins in *Mimulus lewisii* by an Agrobacterium-mediated transient assay. Plant Cell Rep. **35:** 771–777.

Dong, T., Hu, Z., Deng, L., Wang, Y., Zhu, M., Zhang, J., and Chen, G. (2013). A tomato MADS-box transcription factor, SlMADS1, acts as a negative regulator of fruit ripening. Plant Physiol. **163:** 1026–1036.

Earley, K.W., Haag, J.R., Pontes, O., Opper, K., Juehne, T., Song, K., and Pikaard, C.S. (2006). Gateway-compatible vectors for plant functional genomics and proteomics. Plant J. **45:** 616–629.

Edgar, R.C. (2004). MUSCLE: Multiple sequence alignment with high accuracy and high throughput. Nucleic Acids Res. **32:** 1792–1797.

Egea, I., Barsan, C., Bian, W., Purgatto, E., Latché, A., Chervin, C., Bouzayen, M., and Pech, J.-C. (2010). Chromoplast differentiation: current status and perspectives. Plant Cell Physiol. **51:** 1601–1611.

El Zawily, A.M., et al. (2014). FRIENDLY regulates mitochondrial distribution, fusion, and quality control in *Arabidopsis*. Plant Physiol. **166:** 808–828.

Fields, S.D., Conrad, M.N., and Clarke, M. (1998). The *S. cerevisiae CLU1* and *D. discoideum cluA* genes are functional homologues that influence mitochondrial morphology and distribution. J. Cell Sci. **111:** 1717–1727.

Fu, C.C., Han, Y.C., Fan, Z.Q., Chen, J.Y., Chen, W.X., Lu, W.J., and Kuang, J.F. (2016). The papaya transcription factor CpNAC1 modulates carotenoid biosynthesis through activating phytoene desaturase genes *CpPDS2/4* during fruit ripening. J. Agric. Food Chem. **64:** 5454–5463.

Fu, C.C., Han, Y.C., Kuang, J.F., Chen, J.Y., and Lu, W.J. (2017). Papaya CpEIN3a and CpNAC2 co-operatively regulate carotenoid biosynthesis-related genes *CpPDS2/4, CpLCY-e* and *CpCHY-b* during fruit ripening. Plant Cell Physiol. **58:** 2155–2165.

Fujisawa, M., Nakano, T., and Ito, Y. (2011). Identification of potential target genes for the tomato fruit-ripening regulator RIN by chromatin immunoprecipitation. BMC Plant Biol. **11:** 26.

Fujisawa, M., Nakano, T., Shima, Y., and Ito, Y. (2013). A large-scale identification of direct targets of the tomato MADS box transcription factor RIPENING INHIBITOR reveals the regulation of fruit ripening. Plant Cell **25:** 371–386.

Fujisawa, M., Shima, Y., Higuchi, N., Nakano, T., Koyama, Y., Kasumi, T., and Ito, Y. (2012). Direct targets of the tomato-ripening regulator RIN identified by transcriptome and chromatin immunoprecipitation analyses. Planta **235:** 1107–1122.

Fujisawa, M., Shima, Y., Nakagawa, H., Kitagawa, M., Kimbara, J., Nakano, T., Kasumi, T., and Ito, Y. (2014). Transcriptional regulation of fruit ripening by tomato FRUITFULL homologs and associated MADS box proteins. Plant Cell **26:** 89–101.

Galpaz, N., Wang, Q., Menda, N., Zamir, D., and Hirschberg, J. (2008). Abscisic acid deficiency in the tomato mutant *high-pigment 3* leading to increased plastid number and higher fruit lycopene content. Plant J. **53:** 717–730.

Gao, J., Schatton, D., Martinelli, P., Hansen, H., Pla-Martin, D., Barth, E., Becker, C., Altmueller, J., Frommolt, P., Sardiello, M., and Rugarli, E.I. (2014). CLUH regulates mitochondrial biogenesis by binding mRNAs of nuclear-encoded mitochondrial proteins. J. Cell Biol. **207:** 213–223.

Giménez, E., Pineda, B., Capel, J., Antón, M.T., Atarés, A., Pérez-Martín, F., García-Sogo, B., Angosto, T., Moreno, V., and Lozano, R. (2010). Functional analysis of the *Arlequin* mutant corroborates the essential role of the *Arlequin/TAGL1* gene during reproductive development of tomato. PLoS One **5:** e14427.

Glover, B.J. (2014). Understanding Flowers and Flowering: An Integrated Approach. (Oxford: Oxford University Press).

Goodrich, J., Carpenter, R., and Coen, E.S. (1992). A common gene regulates pigmentation pattern in diverse plant species. Cell **68:** 955–964.

Grotewold, E., and Davies, K. (2008). Trafficking and sequestration of anthocyanins. Nat. Prod. Commun. **3:** 1251–1258.

Hiesey, W.M., Nobs, M.A., and Björkman, O. (1971). Experimental studies on the nature of species. V. Biosystematics, genetics, and physiological ecology of the Erythranthe section of Mimulus. In Carnegie Institute of Washington Publication, Volume **628, pp.** 1–213.

Itkin, M., Seybold, H., Breitel, D., Rogachev, I., Meir, S., and Aharoni, A. (2009). TOMATO AGAMOUS-LIKE 1 is a component of the fruit ripening regulatory network. Plant J. **60:** 1081–1095.

Ito, Y., Kitagawa, M., Ihashi, N., Yabe, K., Kimbara, J., Yasuda, J., Ito, H., Inakuma, T., Hiroi, S., and Kasumi, T. (2008). DNA-binding specificity, transcriptional activation potential, and the *rin* mutation effect for the tomato fruit-ripening regulator RIN. Plant J. **55:** 212–223.

Karlova, R., Rosin, F.M., Busscher-Lange, J., Parapunova, V., Do, P.T., Fernie, A.R., Fraser, P.D., Baxter, C., Angenent, G.C., and de Maagd, R.A. (2011). Transcriptome and metabolite profiling show that APETALA2a is a major regulator of tomato fruit ripening. Plant Cell **23:** 923–941.

Kerschen, A., Napoli, C.A., Jorgensen, R.A., and Müller, A.E. (2004). Effectiveness of RNA interference in transgenic plants. FEBS Lett. **566:** 223–228.

Kolotilin, I., Koltai, H., Tadmor, Y., Bar-Or, C., Reuveni, M., Meir, A., Nahon, S., Shlomo, H., Chen, L., and Levin, I. (2007). Transcriptional profiling of high pigment-2dg tomato mutant links early fruit plastid biogenesis with its overproduction of phytonutrients. Plant Physiol. **145:** 389–401.

Kozlov, A.M., Darriba, D., Flouri, T., Morel, B., and Stamatakis, A. (2019). RAxML-NG: A fast, scalable and user-friendly tool for maximum likelihood phylogenetic inference. Bioinformatics **35:** 4453–4455.

Larkin, R.M., Stefano, G., Ruckle, M.E., Stavoe, A.K., Sinkler, C.A., Brandizzi, F., Malmstrom, C.M., and Osteryoung, K.W. (2016). *REDUCED CHLOROPLAST COVERAGE* genes from *Arabidopsis thaliana* help to establish the size of the chloroplast compartment. Proc. Natl. Acad. Sci. USA **113:** E1116–E1125.

Li, L., Paolillo, D.J., Parthasarathy, M.V., Dimuzio, E.M., and Garvin, D.F. (2001). A novel gene mutation that confers abnormal patterns of β-carotene accumulation in cauliflower (*Brassica oleracea* var. *botrytis*). Plant J. **26:** 59–67.

Li, L., and Yuan, H. (2013). Chromoplast biogenesis and carotenoid accumulation. Arch. Biochem. Biophys. **539:** 102–109.

Lichtenthaler, H.K. (1987). Chlorophyll and carotenoids: Pigments of photosynthetic biomembranes. Methods Enzymol. **148:** 350–382.

Liu, Y., Roof, S., Ye, Z., Barry, C., van Tuinen, A., Vrebalov, J., Bowler, C., and Giovannoni, J. (2004a). Manipulation of light signal transduction as a means of modifying fruit nutritional quality in tomato. Proc. Natl. Acad. Sci. USA **101:** 9897–9902.

Liu, Z., Yan, H., Wang, K., Kuang, T., Zhang, J., Gui, L., An, X., and Chang, W. (2004b). Crystal structure of spinach major light-harvesting complex at 2.72 A resolution. Nature **428:** 287–292.

Llorente, B., D'Andrea, L., Ruiz-Sola, M.A., Botterweg, E., Pulido, P., Andilla, J., Loza-Alvarez, P., and Rodriguez-Concepcion, M. (2016). Tomato fruit carotenoid biosynthesis is adjusted to actual ripening progression by a light-dependent mechanism. Plant J. **85:** 107–119.

Logan, D.C., Scott, I., and Tobin, A.K. (2003). The genetic control of plant mitochondrial morphology and dynamics. Plant J. **36:** 500–509.

Lopez, A.B., Van Eck, J., Conlin, B.J., Paolillo, D.J., O'Neill, J., and Li, L. (2008). Effect of the cauliflower *Or* transgene on carotenoid accumulation and chromoplast formation in transgenic potato tubers. J. Exp. Bot. **59:** 213–223.

Lu, S., et al. (2006). The cauliflower Or gene encodes a DnaJ cysteine-rich domain-containing protein that mediates high levels of β-carotene accumulation. Plant Cell **18:** 3594–3605.

Lu, S., Zhang, Y., Zhu, K., Yang, W., Ye, J., Chai, L., Xu, Q., and Deng, X. (2018). The citrus transcription factor CsMADS6 modulates carotenoid metabolism by directly regulating carotenogenic genes. Plant Physiol. **176:** 2657–2676.

Ludwig, S.R., Habera, L.F., Dellaporta, S.L., and Wessler, S.R. (1989). Lc, a member of the maize R gene family responsible for tissue-specific anthocyanin production, encodes a protein similar to transcriptional activators and contains the myc-homology region. Proc. Natl. Acad. Sci. USA **86:** 7092–7096.

Lunch, C.K., Lafountain, A.M., Thomas, S., Frank, H.A., Lewis, L.A., and Cardon, Z.G. (2013). The xanthophyll cycle and NPQ in diverse desert and aquatic green algae. Photosynth. Res. **115:** 139–151.

Ma, N., Feng, H., Meng, X., Li, D., Yang, D., Wu, C., and Meng, Q. (2014). Overexpression of tomato SlNAC1 transcription factor alters fruit pigmentation and softening. BMC Plant Biol. **14:** 351.

Marchler-Bauer, A., et al. (2015). CDD: NCBI's conserved domain database. Nucleic Acids Res. **43:** D222–D226.

Martel, C., Vrebalov, J., Tafelmeyer, P., and Giovannoni, J.J. (2011). The tomato MADS-box transcription factor RIPENING INHIBITOR interacts with promoters involved in numerous ripening processes in a COLORLESS NONRIPENING-dependent manner. Plant Physiol. **157:** 1568–1579.

Martin, C., Prescott, A., Mackay, S., Bartlett, J., and Vrijlandt, E. (1991). Control of anthocyanin biosynthesis in flowers of *Antirrhinum majus*. Plant J. **1:** 37–49.

Martins, T.R., Jiang, P., and Rausher, M.D. (2017). How petals change their spots: cis-regulatory re-wiring in *Clarkia* (Onagraceae). New Phytol. **216:** 510–518.

Meier, S., Tzfadia, O., Vallabhaneni, R., Gehring, C., and Wurtzel, E.T. (2011). A transcriptional analysis of carotenoid, chlorophyll and plastidial isoprenoid biosynthesis genes during development and osmotic stress responses in *Arabidopsis thaliana*. BMC Syst. Biol. **5:** 77.

Meng, C., Yang, D., Ma, X., Zhao, W., Liang, X., Ma, N., and Meng, Q. (2016). Suppression of tomato SlNAC1 transcription factor delays fruit ripening. J. Plant Physiol. **193:** 88–96.

Meng, Y., Wang, Z., Wang, Y., Wang, C., Zhu, B., Liu, H., Ji, W., Wen, J., Chu, C., Tadege, M., Niu, L., and Lin, H. (2019). The MYB activator WHITE PETAL1 associates with MtTT8 and MtWD40–1 to regulate carotenoid-derived flower pigmentation in *Medicago truncatula*. Plant Cell **31:** 2751–2767.

Mustilli, A.C., Fenzi, F., Ciliento, R., Alfano, F., and Bowler, C. (1999). Phenotype of the tomato *high pigment-2* mutant is caused by a mutation in the tomato homolog of *DEETIOLATED1*. Plant Cell **11:** 145–157.

Nisar, N., Li, L., Lu, S., Khin, N.C., and Pogson, B.J. (2015). Carotenoid metabolism in plants. Mol. Plant **8:** 68–82.

Ohmiya, A., Kishimoto, S., Aida, R., Yoshioka, S., and Sumitomo, K. (2006). Carotenoid cleavage dioxygenase (CmCCD4a) contributes to white color formation in chrysanthemum petals. Plant Physiol. **142:** 1193–1201.

Osteryoung, K.W., and Pyke, K.A. (2014). Division and dynamic morphology of plastids. Annu. Rev. Plant Biol. **65:** 443–472.

Owen, C.R., and Bradshaw, H.D. (2011). Induced mutations affecting pollinator choice in *Mimulus lewisii* (Phrymaceae). Arthropod Plant Interact. **5:** 235–244.

Paz-Ares, J., Ghosal, D., Wienand, U., Peterson, P.A., and Saedler, H. (1987). The regulatory c1 locus of *Zea mays* encodes a protein with homology to myb proto-oncogene products and with structural similarities to transcriptional activators. EMBO J. **6:** 3553–3558.

Pyke, K. (2011). Analysis of plastid number, size, and distribution in Arabidopsis plants by light and fluorescence microscopy. In Methods Mol. Biol., Volume **774, pp.** 19–32.

Qin, G., Wang, Y., Cao, B., Wang, W., and Tian, S. (2012). Unraveling the regulatory network of the MADS box transcription factor RIN in fruit ripening. Plant J. **70:** 243–255.

Quattrocchio, F., Wing, J.F., van der Woude, K., Mol, J.N.M., and Koes, R. (1998). Analysis of bHLH and MYB domain proteins: Species-specific regulatory differences are caused by divergent evolution of target anthocyanin genes. Plant J. **13:** 475–488.

Ruiz-Sola, M., and Rodríguez-Concepción, M. (2012). Carotenoid biosynthesis in Arabidopsis: A colorful pathway. Arabidopsis Book **10:** e0158.

Sagawa, J.M., Stanley, L.E., LaFountain, A.M., Frank, H.A., Liu, C., and Yuan, Y.-W. (2016). An R2R3-MYB transcription factor regulates carotenoid pigmentation in *Mimulus lewisii* flowers. New Phytol. **209:** 1049–1057.

Schwinn, K., Venail, J., Shang, Y., Mackay, S., Alm, V., Butelli, E., Oyama, R., Bailey, P., Davies, K., and Martin, C. (2006). A small family of MYB-regulatory genes controls floral pigmentation intensity and patterning in the genus *Antirrhinum*. Plant Cell **18:** 831–851.

Shang, Y., Venail, J., Mackay, S., Bailey, P.C., Schwinn, K.E., Jameson, P.E., Martin, C.R., and Davies, K.M. (2011). The molecular basis for venation patterning of pigmentation and its effect on pollinator attraction in flowers of *Antirrhinum*. New Phytol. **189:** 602–615.

Shima, Y., Kitagawa, M., Fujisawa, M., Nakano, T., Kato, H., Kimbara, J., Kasumi, T., and Ito, Y. (2013). Tomato FRUITFULL homologues act in fruit ripening via forming MADS-box transcription factor complexes with RIN. Plant Mol. Biol. **82:** 427–438.

Spelt, C., Quattrocchio, F., Mol, J.N.M., and Koes, R. (2000). anthocyanin1 of petunia encodes a basic helix-loop-helix protein that directly activates transcription of structural anthocyanin genes. Plant Cell **12:** 1619–1632.

Sun, T., and Li, L. (2020). Toward the 'golden' era: The status in uncovering the regulatory control of carotenoid accumulation in plants. Plant Sci. **290:** 110331.

Toledo-Ortiz, G., Huq, E., and Rodríguez-Concepción, M. (2010). Direct regulation of phytoene synthase gene expression and carotenoid biosynthesis by phytochrome-interacting factors. Proc. Natl. Acad. Sci. USA **107:** 11626–11631.

Toledo-Ortiz, G., Johansson, H., Lee, K.P., Bou-Torrent, J., Stewart, K., Steel, G., Rodríguez-Concepción, M., and Halliday, K.J. (2014). The HY5-PIF regulatory module coordinates light and temperature control of photosynthetic gene transcription. PLoS Genet. **10:** e1004416.

Tseng, T.S., Swain, S.M., and Olszewski, N.E. (2001). Ectopic expression of the tetratricopeptide repeat domain of SPINDLY causes defects in gibberellin response. Plant Physiol. **126:** 1250–1258.

Tzuri, G., et al. (2015). A 'golden' SNP in *CmOr* governs the fruit flesh color of melon (*Cucumis melo*). Plant J. **82:** 267–279.

Vrebalov, J., Pan, I.L., Arroyo, A.J.M., McQuinn, R., Chung, M., Poole, M., Rose, J., Seymour, G., Grandillo, S., Giovannoni, J., and Irish, V.F. (2009). Fleshy fruit expansion and ripening are regulated by the Tomato SHATTERPROOF gene TAGL1. Plant Cell **21:** 3041–3062.

Vrebalov, J., Ruezinsky, D., Padmanabhan, V., White, R., Medrano, D., Drake, R., Schuch, W., and Giovannoni, J. (2002). A MADS-box gene necessary for fruit ripening at the tomato *ripening-inhibitor* (*rin*) locus. Science **296:** 343–346.

Welsch, R., Maass, D., Voegel, T., Dellapenna, D., and Beyer, P. (2007). Transcription factor RAP2.2 and its interacting partner SINAT2: stable elements in the carotenogenesis of *Arabidopsis* leaves. Plant Physiol. **145:** 1073–1085.

Xiong, C., et al. (2019). A tomato B-box protein SlBBX20 modulates carotenoid biosynthesis by directly activating PHYTOENE SYNTHASE 1, and is targeted for 26S proteasome-mediated degradation. New Phytol. **221:** 279–294.

Xu, W., Dubos, C., and Lepiniec, L. (2015). Transcriptional control of flavonoid biosynthesis by MYB-bHLH-WDR complexes. Trends Plant Sci. **20:** 176–185.

Yuan, H., Zhang, J., Nageswaran, D., and Li, L. (2015). Carotenoid metabolism and regulation in horticultural crops. Hortic. Res. **2:** 15036.

Yuan, Y.-W., Sagawa, J.M., Di Stilio, V.S., and Bradshaw, H.D., Jr. (2013a). Bulk segregant analysis of an induced floral mutant identifies a MIXTA-like R2R3 MYB controlling nectar guide formation in *Mimulus lewisii*. Genetics **194:** 523–528.

Yuan, Y.-W., Sagawa, J.M., Frost, L., Vela, J.P., and Bradshaw, H.D., Jr. (2014). Transcriptional control of floral anthocyanin pigmentation in monkeyflowers (*Mimulus*). New Phytol. **204:** 1013–1027.

Yuan, Y.-W., Sagawa, J.M., Young, R.C., Christensen, B.J., and Bradshaw, H.D., Jr. (2013b). Genetic dissection of a major anthocyanin QTL contributing to pollinator-mediated reproductive isolation between sister species of *Mimulus*. Genetics **194:** 255–263.

Zeytuni, N., and Zarivach, R. (2012). Structural and functional discussion of the tetra-trico-peptide repeat, a protein interaction module. Structure **20:** 397–405.

Zhang, B., Liu, C., Wang, Y., Yao, X., Wang, F., Wu, J., King, G.J., and Liu, K. (2015). Disruption of a CAROTENOID CLEAVAGE

DIOXYGENASE 4 gene converts flower colour from white to yellow in *Brassica* species. New Phytol. **206:** 1513–1526.

Zhong, S., Fei, Z., Chen, Y.R., Zheng, Y., Huang, M., Vrebalov, J., McQuinn, R., Gapper, N., Liu, B., Xiang, J., Shao, Y., and Giovannoni, J.J. (2013). Single-base resolution methylomes of tomato fruit development reveal epigenome modifications associated with ripening. Nat. Biotechnol. **31:** 154–159.

Zhou, D., Shen, Y., Zhou, P., Fatima, M., Lin, J., Yue, J., Zhang, X., Chen, L.Y., and Ming, R. (2019). Papaya *CpbHLH1/2* regulate carotenoid biosynthesis-related genes during papaya fruit ripening. Hortic. Res. **6:** 80.

Zhou, X., Welsch, R., Yang, Y., Álvarez, D., Riediger, M., Yuan, H., Fish, T., Liu, J., Thannhauser, T.W., and Li, L. (2015). Arabidopsis OR proteins are the major posttranscriptional regulators of phytoene synthase in controlling carotenoid biosynthesis. Proc. Natl. Acad. Sci. USA **112:** 3558–3563.

Zhu, F., et al. (2017). An R2R3-MYB transcription factor represses the transformation of α- and β-branch carotenoids by negatively regulating expression of *CrBCH2* and *CrNCED5* in flavedo of *Citrus reticulate*. New Phytol. **216:** 178–192.

Zhu, M., Chen, G., Zhang, J., Zhang, Y., Xie, Q., Zhao, Z., Pan, Y., and Hu, Z. (2014). The abiotic stress-responsive NAC-type transcription factor SlNAC4 regulates salt and drought tolerance and stress-related genes in tomato (*Solanum lycopersicum*). Plant Cell Rep. **33:** 1851–1863.

Zhu, Q., Hulen, D., Liu, T., and Clarke, M. (1997). The *cluA*- mutant of *Dictyostelium* identifies a novel class of proteins required for dispersion of mitochondria. Proc. Natl. Acad. Sci. USA **94:** 7308–7313.

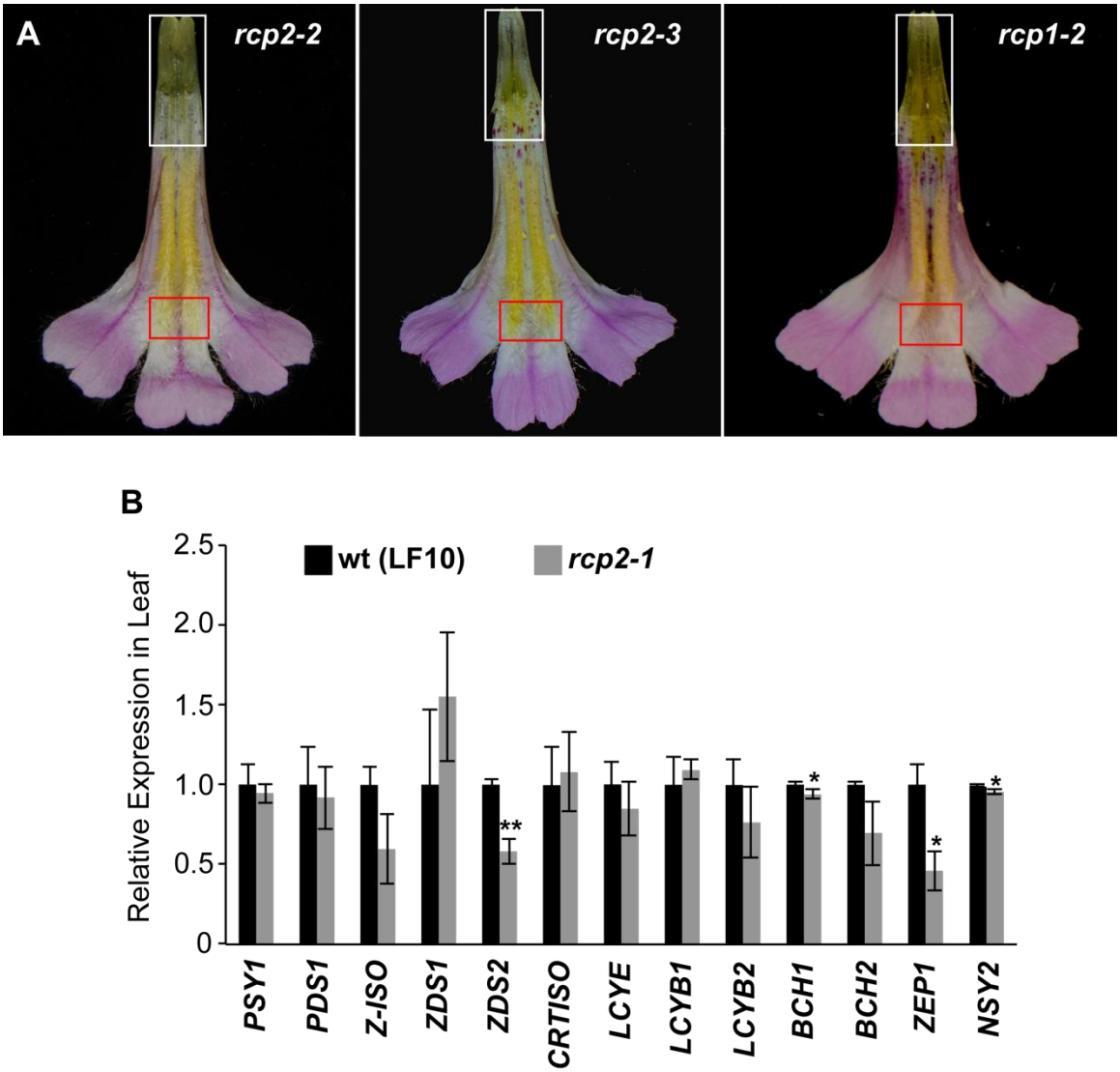

Supplemental Figure 1. Additional characterization of the *Mimulus lewisii rcp2* and *rcp1* mutants. (Supports Figure 1).

(**A**) Phenotypes of additional *rcp2* and *rcp1* mutant alleles.
(**B**) Relative transcript levels of carotenoid biosynthetic genes in leaves of the *rcp2-1* mutant compared to wild-type, determined by qRT-PCR. Error bars are 1 SD (n = 3 biological replicates, each consisting of pooled 10-mm leaves from one distinct plant). Asterisks indicate differences from the wild type (*$P < 0.05$, **$P < 0.01$, Student's *t* test).

Supplemental Figure 2 (continued on next page)

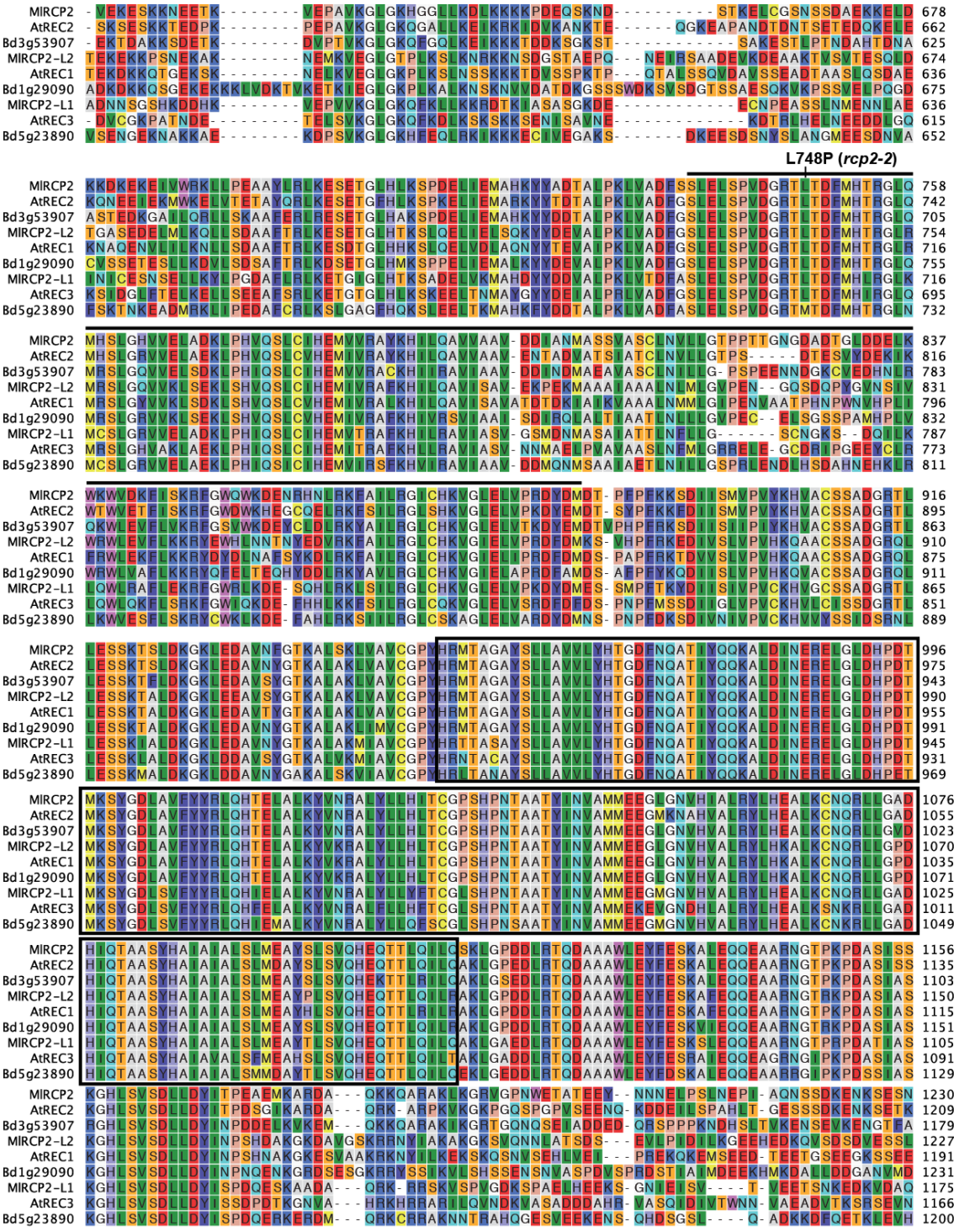

Supplemental Figure 2 (continued on next page)

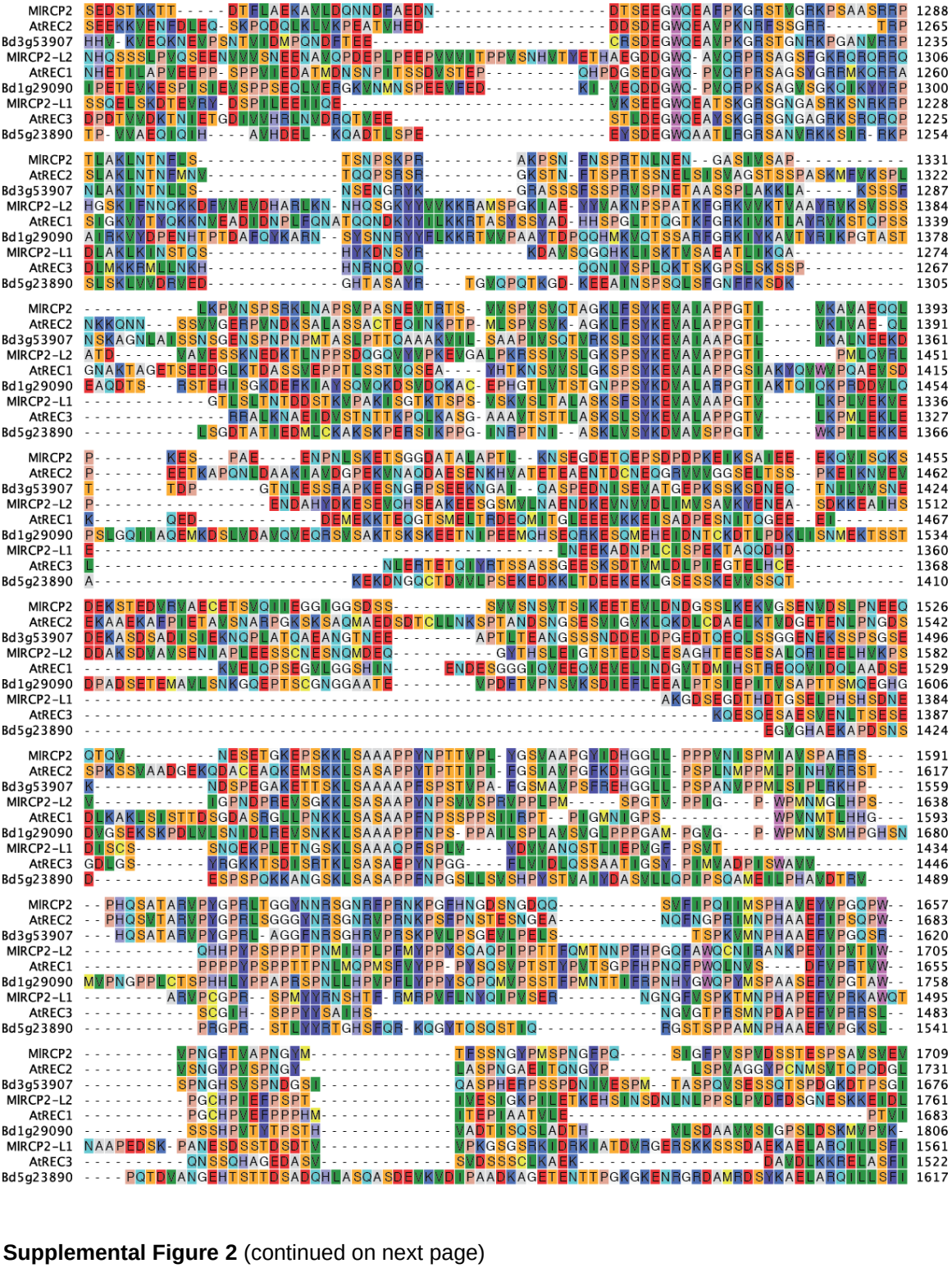

Supplemental Figure 2 (continued on next page)

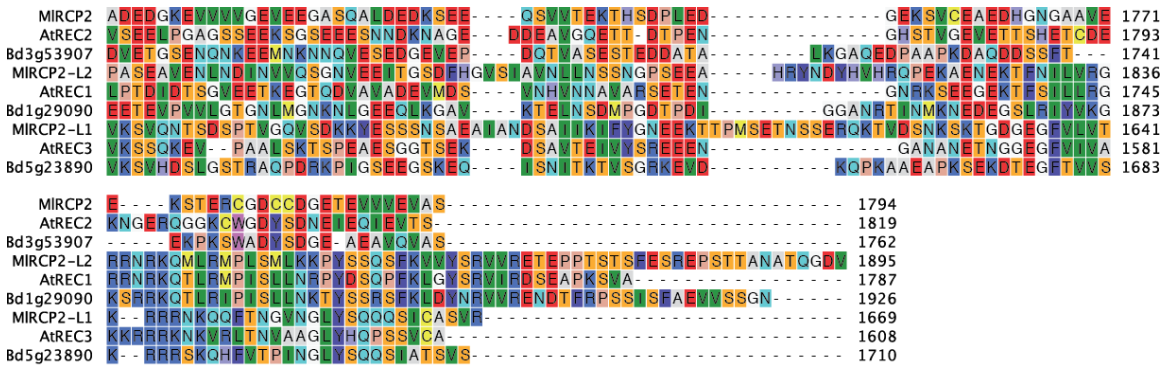

Supplemental Figure 2. Alignment of RCP2 and RCP2-like proteins in *Mimulus lewisii* and their homologues in *Arabidopsis* and *Brachypodium*. (Supports Figure 3).

The black lines above the sequences mark the CLU_N and CLU-central domains; the box marks the TPR domain. Mutations of the three independent alleles in *M. lewisii* are also indicated at the corresponding sites.

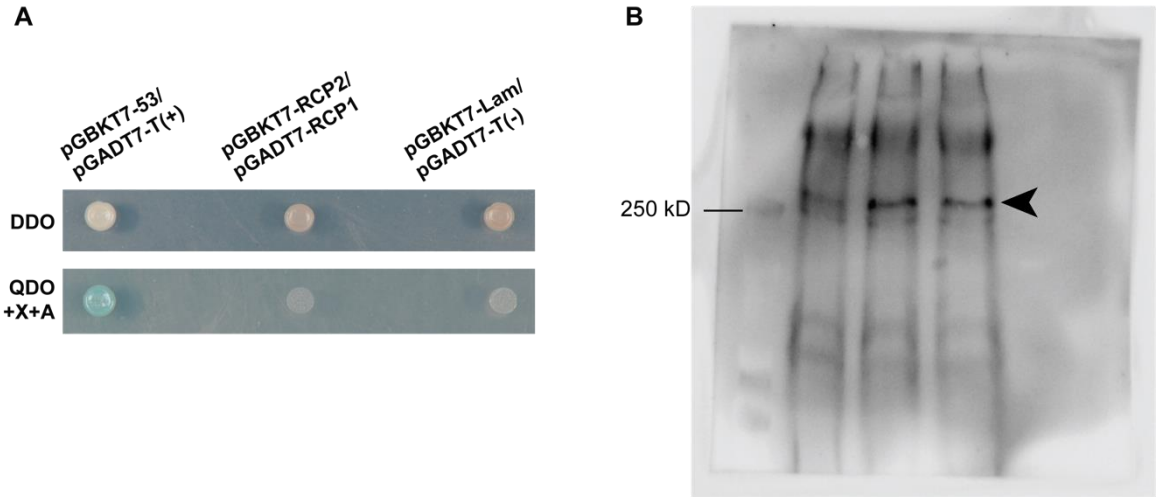

Supplemental Figure 3. Further characterization of the RCP2 protein. (Supports Figures 7 and 9).

(**A**) Yeast two-hybrid positive control (pGBKT7-53/pGADT7-T), experimental (pGBKT7-RCP2/pGADT7-RCP1), and negative control (pGBKT7-Lam/pGADT7-T) colonies growing on double dropout and quadruple dropout + X-α-gal + AbA medium.
(**B**) Immunoblot of total protein extracts from *Nicotiana benthamiana* leaves transiently expressing YFP-RCP2 (harvested six days after inoculation). GFP Tag monoclonal antibody was used for immunoblotting. The mass of the standard protein closest in size to the recovered band (black arrowhead) is indicated on the left. Three biological replicates are shown, each consisting of an individual leaf.

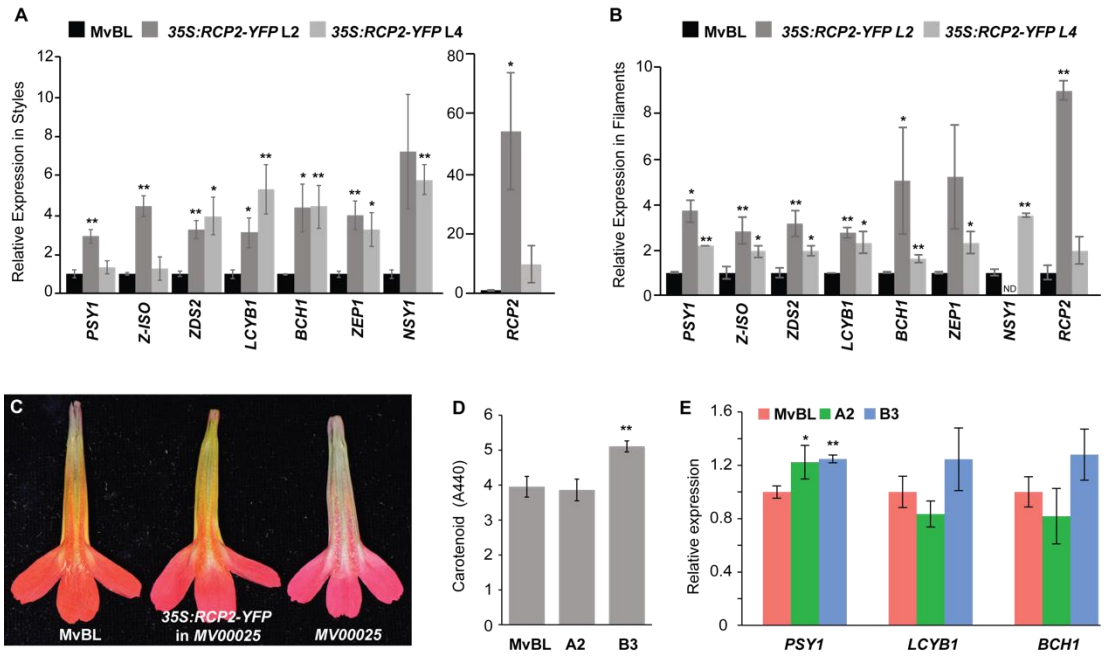

Supplemental Figure 4. Characterization of additional *35S:RCP2-YFP* transgenic plants. (Supports Figure 8).

(**A**) The relative transcript levels of *RCP2* and a subset of CBP genes in the style tissue of 15-mm corollas of two additional *35S:RCP2-YFP* lines compared to wild-type. Error bars are 1 SD (n = 3 biological replicates, each consisting of pooled 15-mm stage styles from one distinct T2 plant of transgenic line 2 or 4).
(**B**) Relative CBP gene expression levels in the filament tissue of 15-mm corollas of two additional *35S:RCP2-YFP* lines compared to wild-type. Error bars are 1 SD (n = 3 biological replicates, each consisting of pooled 15-mm stage filaments from one distinct T2 plant of transgenic line 2 or 4).
(**C**) Flower images of the wild-type *M. verbenaceus* (MvBL; left), transgenic in the homozygous *rcp2* mutant background (middle), and the homozygous mutant (right).
(**D**) Carotenoid concentration of corollas of the wild-type (MvBL) and two independent rescue lines (A2 and B3) recovered by screening F2 populations between *35S:RCP2-YFP* transgenics and *MV00025*. A2 and B3 are both homozygous for the *rcp2* mutation but contain the transgene. Error bars are 1 SD (n = 5 corollas from one plant of each genotype).
(**E**) Relative transcript levels of three arbitrarily selected CBP genes in 15-mm corolla, as measured by qRT-PCR. Error bars are 1 SD (n = 3 biological replicates, each consisting of pooled 15-mm corollas from different branches of the same plant).
Asterisks indicate differences from the wild type (*P < 0.05, **P < 0.01, Student's *t* test).

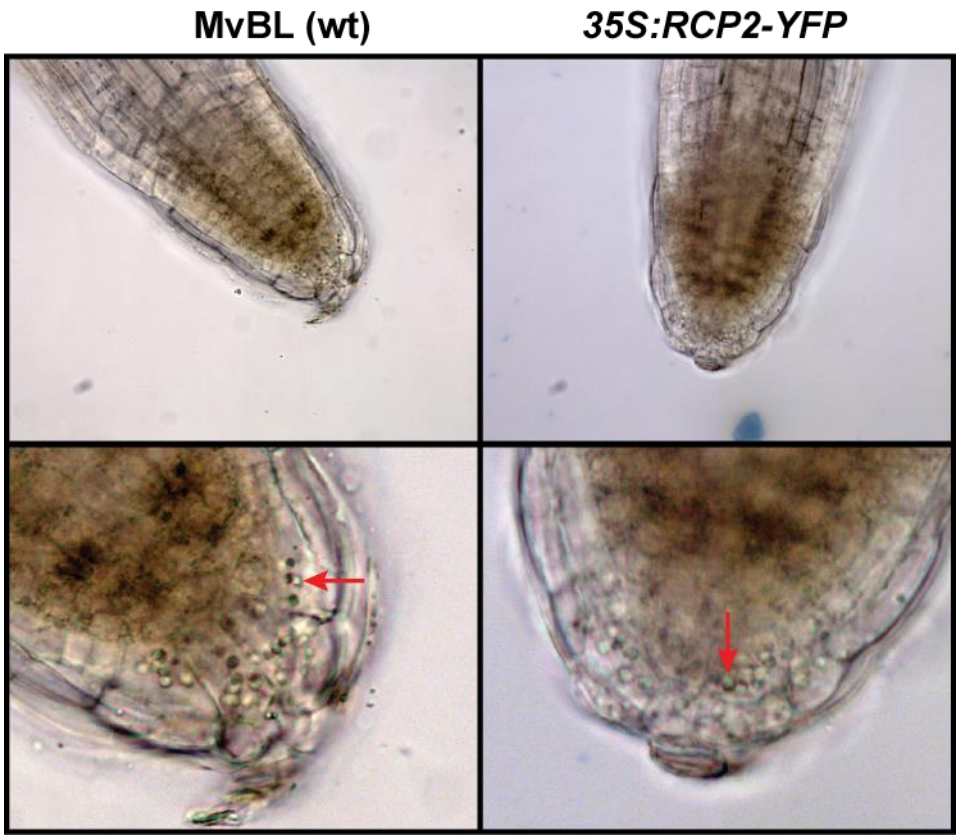

Supplemental Figure 5. Light micrographs of root plastids. (Supports Figure 8).

Representative images of the root tips of wild-type MvBL (left) and *35S:RCP2-YFP* (right) 7-day-old seedlings. Red arrows point to typical plastids.

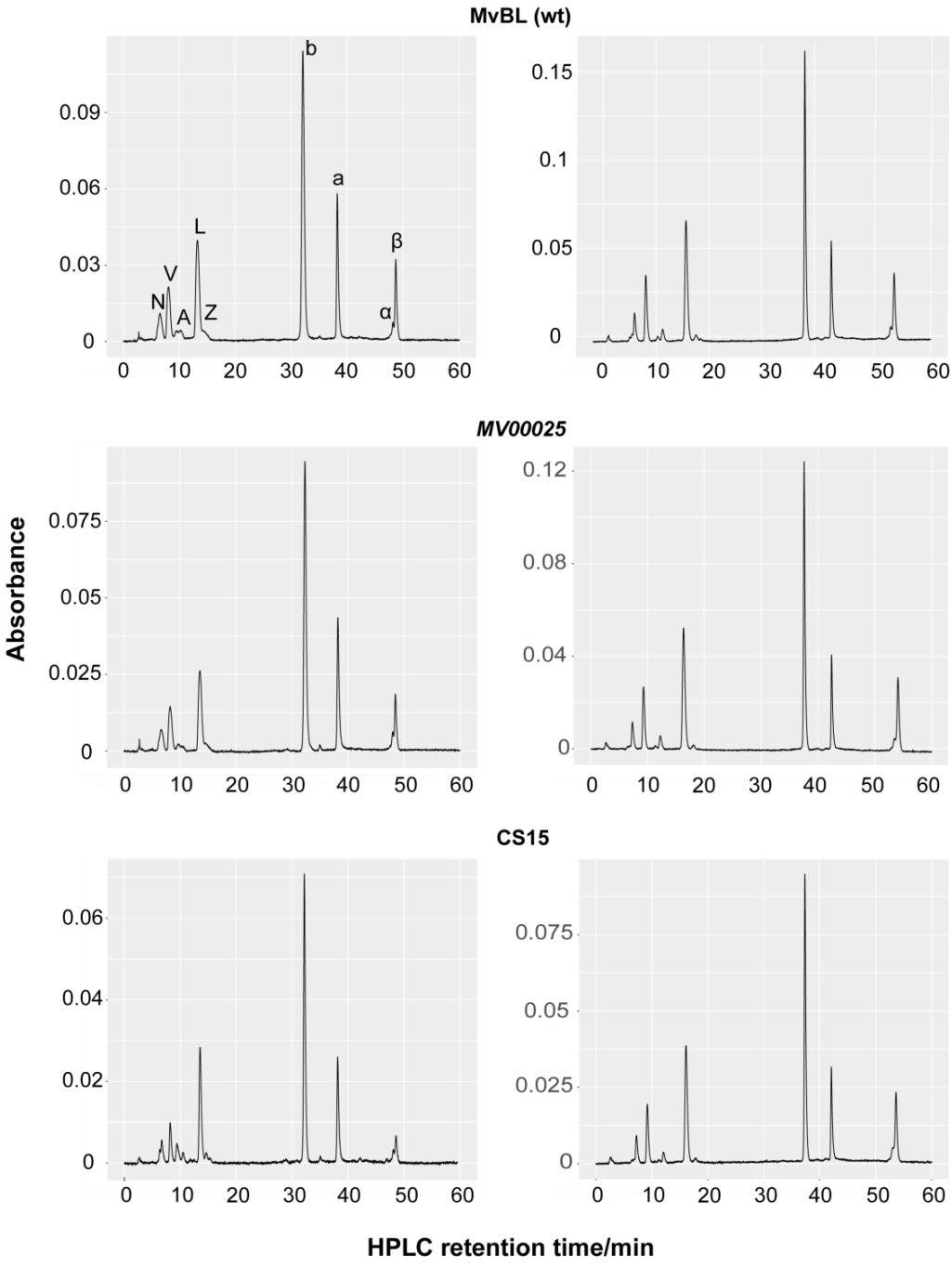

Supplemental Figure 6. HPLC analysis of *Mimulus verbenaceus* leaf pigment composition. (Supports Figure 10).

HPLC chromatograms for two 30-mg samples of wild-type MvBL (top), *MV00025* (middle), and CS15 (bottom) leaves. Detection wavelength is 450 nm. Abbreviations are as follows: N, neoxanthin; V, violaxanthin; A, antheraxanthin; L, lutein; Z, zeaxanthin; b, chlorophyll b; a, chlorophyll a; α, α-carotene; β, β−carotene.

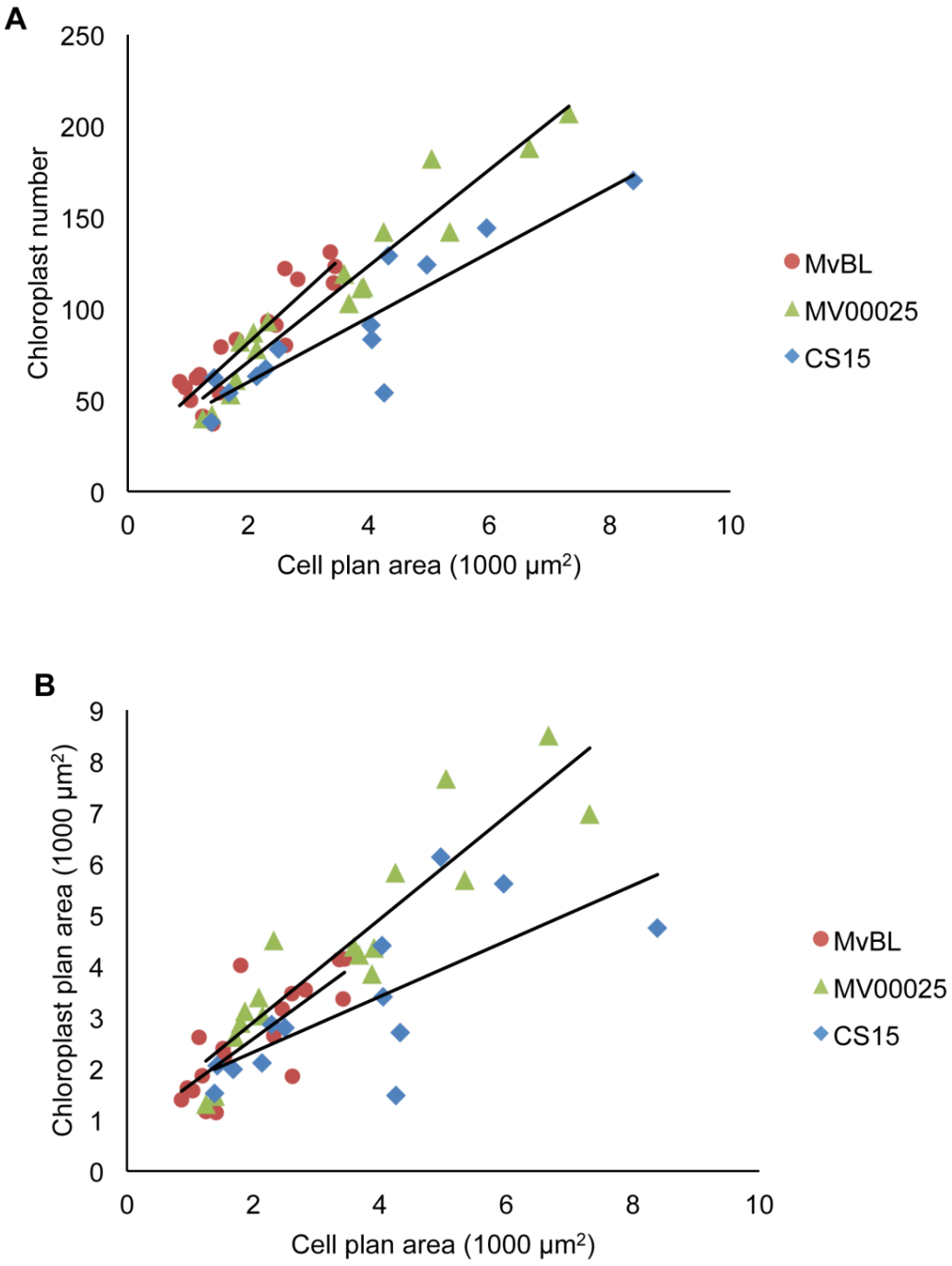

Supplemental Figure 7. Correlations of cell plan area with chloroplast number and plan area. (Supports Figure 10).

Correlations between cell plan area and chloroplast number (A) or total chloroplast plan area per cell (B) in wild-type MvBL, *MV00025*, and CS15 plants. 13-18 cells were analyzed for each genotype, and 10 chloroplasts were analyzed per cell. R^2 values fall between 0.73 and 0.93.

Supplemental Data. Stanley et al. (2020). Plant Cell 10.1105/tpc.19.00755

Supplemental Table 1. Mole percentages of carotenoids in *Mimulus verbenaceus* leaves. Percentages were calculated based on HPLC analysis shown in Supplemental Figure 6. Each genotype is represented by two samples from different leaves.

Carotenoid	**MvBL**		***MV00025***		**CS15**	
Neoxanthin	14.6	11.1	15.5	10.3	12.6	11.3
Violaxanthin	21.6	21.0	23.5	19.0	18.0	19.0
Antheraxanthin	2.3	3.2	1.5	4.9	3.2	3.3
Lutein	37.6	38.8	36.4	38.2	45.2	39.1
Zeaxanthin	1.4	1.8	1.3	2.1	5.3	1.2
α-carotene	4.1	3.8	4.6	4.0	2.9	3.4
β-carotene	18.5	20.3	17.2	21.6	12.8	22.8

Supplemental Table 2. (q)RT-PCR primers.

Gene	Forward (5'-3')	Reverse (5'-3')
RCP2	CTTGGACTTGATCACCCGGATA	CTGAAGAGTGGTTTGTTCATGC
RCP2-L1	GCTCTCAGATATTTGCATGAAGC	TTGCTGGCAATGGTTGCATCTGG
RCP2-L2	ATCAGACCAAGGGCAGGTTTATG	CATCACTCTTTGCATCATCTGAG
RCP1	ATGGCGAGCAAAAATTGCAGT	CGCCTGCATATCACATTCTTGA
PSY1	GATGATGCAGAGAGCGGTGTCA	GGAGGAACAAGAGACTTTGCAA
PDS1	CGACCGTTACAAAGATCTCCAT	TCCGCCAACTTCTTCTGCTCTC
PDS2	AAACTACACCTGGCACCGAGC	ATGCAACAATTGCCTTGCCCAA
Z-ISO	TTGCAGCGGTCGATAAGCCTAA	GCTGCTAATGTAACTGAGTTCC
ZDS1	CGACCAGAAGACACCTGTTAC	GTGTCAATTCAGCGACAGCAAC
ZDS2	TGACCAGAAGACCCCGGTCAA	ATAGGCACGTGATGAATTGYGAA
CRTISO	GCGATAAATGGTCTGTACTGTG	AAGGAGACCGGTATCGAGAACT
LCYE	ACAACTGGATACCGAGGGCATA	GCACCAGTGGGATCAGATATGA
LCYB1	TATCGGCTCGTGTTTGGAAGGA	GGAAGTGTGCCCTTTGCCATGA
LCYB2	TATCGGCTCGTGTTTGGAAGGA	GGAAGTGTGCCCTTTGCCATGA
BCH1	TAATGCTGTTCCCGCAATTGCC	TTTCCCTATCCAGCTCTTCCAA
BCH2	TAATGCTGTTCCAGCGATAGCT	TTTCCTTCTCCAACTCCTCTAG
ZEP1	GTGTCGATAGCTATACCTTCGC	ACGGAATCGCTTGTCTTCGTTG
ZEP2	TCCGGGAGTAGTATCGATAACA	GGTGATACACGATGTTGCCTTC
NSY1	ATCATGGACTCCCGATACCATG	TTCTCTGGTTCTGCTTAGAGC
NSY2	GTCTTGGACTCCAGAGACGGTT	CTTAGCTGCTTGTGGTTACAGA
FtsZ1B	ATACCAGGGCTAGTGAATGTGA	CGTTGTAGCCTTTGGATCGGTGA
FtsZ2B	GTGGATCCATCTCTAAGTGGTCA	ACGTTTGAATCTGCCTGTACCG
ARC1	GATACTTCAACAGCATCAGTCG	TTCGTACATATCGTGCATCA
ARC6	ATGTCAAGTCCCTAGCTCTTGG	AGGTTGTACTATACGAGTCGTT
CHLM	GACGTTAATAAGGTGCAGAGGA	TCACTTCGAATTTCGGCAGTACA
CHLH	CTGTCGAGAACTCGACTTGGAAC	GAACGGTCTCAGATAGTGTACGA
CHLG	CACTGCTCTACAGTATAGCTGGT	AAGCCTACAAGTGCTAATGCGTA
UBC	GGCTTGGACTCTGCAGTCTGT	TCTTCGGCATGGCAGCAAGTC

Supplemental Table 3. Primers used for plasmid construction. Nucleotides in red are necessary for integration into corresponding vectors.

Primer	Sequence (5'-3')	Utility
*RCP2*_cdsF	CACCATGGCTCCTAAAAATGGAAAGAC	*35S:RCP2-YFP* and *35S:YFP-RCP2*
*RCP2*_cdsR	TTAACTAGCTACCTCAACAACCAC	*35S:RCP2-YFP* and *35S:YFP-RCP2*
*RCP2*_RNAi_F	GTTCTAGACCATGGAGACCAACCCTTGCGAAATTGA	RNAi
*RCP2*_RNAi_R	GTGGATCCGGCGCGCCCTTCAATGTTGGTGCTAGTGCT	RNAi
Y2H_b_*RCP2*_cdsF	CATGGAGGCCGAATTCATGGCTCCTAAAAATGGAAAGAC	Y2H
Y2H_b_*RCP2*_cdsR	GCAGGTCGACGGATCCTTAACTAGCTACCTCAACAACCAC	Y2H
Y2H_p_*RCP1*_cdsF	TTCCACCCAAGCAGTGGTATCAACGCAGAGTGGCCATTATGGCCATGGCGAGCAAAAATTGCAGT	Y2H
Y2H_p_*RCP1*_cdsR	GTATCGATGCCCACCCTCTAGAGGCCGAGGCGGCCGACATGCAAAGCTCCAACACCAAGAAAG	Y2H
*RCP2_TPR*_F	CACCATGAATGGTGATGCAGATACGGGT	*35S:TPR*
*RCP2_TPR*_R	TTAGTCCTCAGAATTTGACTCAGA	*35S:TPR*

Permission to Reprint

Permission to Use Content from Plant Physiology® and The Plant Cell

Permission to make digital or hard copies of part or all of a work published in ***Plant Physiology*** or ***The Plant Cell*** is granted without fee for personal or classroom use, provided that copies are not made or distributed for profit or commercial advantage. Please include a citation in any standard format and a notice that the material is copyright by the American Society of Plant Biologists. If the use is commercial or if you wish to make multiple copies other than for educational purposes, please process your request through the Copyright Clearance Center at

Copyright Clearance Center Inc.
Re: *Plant Physiology®/The Plant Cell*
222 Rosewood Drive
Danvers, MA 01923 USA
Voice: 978-750-8400
Fax: 978-750-4470
Internet: **http://www.copyright.com/**

To Our Authors:
ASPB grants to authors whose work has been published in ***Plant Physiology***® or ***The Plant Cell*** the royalty-free right to reuse images, portions of an article, or full articles in any book, book chapter, or journal article of which the author is the author or editor. Reproductions must bear the full citation, the journal URL (www.plantphysiol.org or www.plantcell.org), and the following notice: "Copyright American Society of Plant Biologists." ASPB further grants to authors the permission to make digital or hard copies of part or all of a work published in ***Plant Physiology***® or ***The Plant Cell*** without fee for personal or classroom use.

Order Number: 1030124
Order Date: 22 Apr 2020

Payment Information

Lauren Stanley
lauren.stanley@uconn.edu
Payment method: Invoice

Billing Address:
Ms. Lauren Stanley
75 North Eagleville Road
Storrs Mansfield, CT 06269
United States

+1 (724) 841-5555
lauren.stanley@uconn.edu

Customer Location:
Ms. Lauren Stanley
75 North Eagleville Road
Storrs Mansfield, CT 06269
United States

Order Details

1. The plant cell

Billing Status: Open

Article: A Tetratricopeptide Repeat Protein Regulates Carotenoid Biosynthesis and Chromoplast Development in Monkeyflower (Mimulus)

Order license ID	1030124-1
Order detail status	Completed
ISSN	1040-4651
Type of use	Republish in a thesis/dissertation
Publisher	AMERICAN SOCIETY OF PLANT PHYSIOLOGISTS,
Portion	Chapter/article

0.00 USD
Republication Permission

LICENSED CONTENT

Publication Title	The plant cell	**Language**	English
Article Title	A Tetratricopeptide Repeat Protein Regulates Carotenoid Biosynthesis and Chromoplast Development in Monkeyflower (Mimulus)	**Country**	United States of America
		Rightsholder	American Society of Plant Biologists
		Publication Type	Journal
Author/Editor	AMERICAN SOCIETY OF PLANT PHYSIOLOGISTS.		
Date	01/01/1989		

REQUEST DETAILS

Portion Type	Chapter/article	**Rights Requested**	Main product
Page range(s)	1-45	**Distribution**	Worldwide
Total number of pages	45	**Translation**	Original language of publication
Format (select all that apply)	Electronic	**Copies for the disabled?**	No
Who will republish the content?	Author of requested content	**Minor editing privileges?**	No
		Incidental promotional use?	No
Duration of Use	Life of current edition	**Currency**	USD
Lifetime Unit Quantity	Up to 499		

NEW WORK DETAILS

Title	The genetic regulation of carotenoid pigmentation in monkeyflowers (Mimulus)	**Institution name**	University of Connecticut
		Expected presentation date	2020-05-08
Instructor name	Lauren Stanley		

ADDITIONAL DETAILS

The requesting person / organization to appear on the license	Lauren Stanley

REUSE CONTENT DETAILS

Title, description or numeric reference of the portion(s)	A Tetratricopeptide Repeat Protein Regulates Carotenoid Biosynthesis and Chromoplast Development in Monkeyflower (Mimulus)	**Title of the article/chapter the portion is from**	A Tetratricopeptide Repeat Protein Regulates Carotenoid Biosynthesis and Chromoplast Development in Monkeyflower (Mimulus)
Editor of portion(s)	Yuan, Yao-Wu; Chen, Shilin; Hill, Connor; Mou, Feng-Juan; Sun, Wei; Ding, Baoqing; Stanley, Lauren E	**Author of portion(s)**	Yuan, Yao-Wu; Chen, Shilin; Hill, Connor; Mou, Feng-Juan; Sun, Wei; Ding, Baoqing; Stanley, Lauren E
Volume of serial or monograph	N/A	**Publication date of portion**	2020-03-04
Page or page range of portion	tpc.00755.2019		

American Society of Plant Biologists Terms and Conditions

Permission is granted for the life of the current edition and all future editions, in all languages and in all media.

Total Items: 1

Subtotal: 0.00 USD
Order Total: 0.00 USD

Accumulation and Replication of Chloroplasts 6 (ARC6) regulates chromoplast biogenesis in monkeyflowers (*Mimulus*)

Lauren E. Stanley[1] and Yao-Wu Yuan[1,2]

[1]Department of Ecology and Evolutionary Biology, University of Connecticut, Storrs, CT 06269, USA; [2]Institute for Systems Genomics, University of Connecticut, Storrs, CT 06269, USA

INTRODUCTION

Carotenoid pigments are deposited as secondary metabolites in non-photosynthetic tissues, contributing to the vibrant red, orange, and yellow colors of many flowers and fruits. For carotenoids to accumulate in these tissues, plants must (1) enhance pigment production by activating carotenoid biosynthesis pathway (CBP) genes and (2) build specialized storage organelles, chromoplasts, to act as carotenoid sinks. Considerable research effort has gone into identifying the transcriptional regulators of CBP genes. Although much uncertainty remains, numerous potential CBP transcriptional regulators have been identified (reviewed in Chapter 1, Stanley and Yuan, 2019). By contrast, the genetic control of chromoplast biogenesis has received much less attention.

Chromoplasts are non-photosynthetic plastids that accumulate large quantities of carotenoids. These organelles differentiate from proplastids or from pre-existing chloroplasts, leucoplasts, or amyloplasts (Egea et al., 2010; Li and Yuan, 2013), and are categorized into many

different types based on the morphology of their carotenoid storage substructures (e.g., crystalline, reticular-tubular, membranous, fibrillar, globular) (Camara et al., 1995). Chromoplast biogenesis has primarily been studied from structural and metabolic perspectives, and the majority of previous studies focused on the most common type of development, chloroplast-to-chromoplast conversion. This conversion involves the breakdown of chlorophyll, disassembly of grana and thylakoid membranes, rapid turnover of starch, production of storage substructures, and accumulation of carotenoid pigments (Forth and Pyke, 2006; Simkin et al., 2007; Egea et al., 2010; Li and Yuan, 2013). Recently, transcriptomic and proteomic approaches in tomato, pepper, and *Citrus* fruits have provided more details on the metabolic shifts that occur during chloroplast-to-chromoplast conversion, such as the loss of proteins involved in photosynthesis and plastid division, the arrest of plastid translation, and the production of storage and stress response proteins (e.g., fibrillin, ACCD, heat shock proteins) (Siddique et al., 2006; Kahlau and Bock, 2008; Barsan et al., 2012). Beyond chloroplast-to-chromoplast conversion, very little is known about the genetic control of chromoplast biogenesis in general. This knowledge gap is at least partly due to the lack of chromoplasts in the foremost plant genetic model system, *Arabidopsis thaliana*.

Very few genes regulating chromoplast biogenesis have been identified to date. These include the *High Pigment (HP)-1, -2,* and *-3* genes from tomato, the *Orange* gene, originally isolated from cauliflower, and *Reduced Carotenoid Pigmentation 2* (*RCP2*) from *Mimulus* (monkeyflowers). Mutations in the *HP* genes, which encode DDB1, DET1, and ZEP, produce an increased number and/or size of chloroplasts in developing tomato fruits, which then differentiate into chromoplasts (Cookson et al., 2003; Kolotilin et al., 2007; Galpaz et al., 2008). Mutation in the *Orange* gene leads to the conversion of colorless leucoplasts to chromoplasts, promoting

carotenoid accumulation in typically white or pale yellow tissues (Lu et al., 2006). Interestingly, this mutation also disrupts the division of plastids: most cells only contain a single, enlarged plastid (Li et al., 2001; Paolillo et al., 2004). Orange has been shown to stabilize phytoene synthase, a carotenoid biosynthesis enzyme, and to channel the flux of the carotenoid pathway toward β-carotene, but its exact role in chromoplast development is still unknown (Zhou et al., 2015; Chayut et al., 2017). RCP2 is a tetratricopeptide repeat protein that enhances both the transcription of the CBP genes and chromoplast development in flowers (Chapter 2, Stanley et al., 2020). Overexpression of this gene causes the conversion of pale or colorless plastids to chromoplasts in floral tissues, but the functional mechanisms underlying this conversion remain elusive.

To identify additional regulators of chromoplast biogenesis, we took advantage of a new genetic model system, the crimson monkeyflower *Mimulus verbenaceus*. This species bears bright red flowers whose color results from a combination of yellow carotenoids and magenta anthocyanins, and is amenable to ethyl methanesulfonate (EMS) mutagenesis and *in planta* stable transformation (Figure 1A; Chapter 2, Stanley et al., 2020). Here we characterized *MV00160*, an EMS mutant bearing pinkish flowers (Figure 1B). We show that *MV00160* flowers accumulate a lower concentration of carotenoids than their wild-type counterparts, but this is not due to mutation in or reduced expression of carotenoid biosynthesis genes. Examination of mutant flowers under light and transmission electron microscopy revealed the presence of many fewer, larger, chromoplasts than in the wild-type, whose reduced coverage explains the observed reduced carotenoid accumulation. Using bulk segregant analysis, we mapped the *MV00160* mutation to the *Mimulus* homologue of *ACCUMULATION AND REPLICATION OF CHLOROPLASTS 6* (*ARC6*), an essential chloroplast division gene in *Arabidopsis*. Examination

of photosynthetic tissues revealed that *MV00160* also produces fewer, larger chloroplasts. This study provides the first evidence that ARC6 affects chromoplast biogenesis, highlighting the importance of studying diverse model systems.

RESULTS

MV00160 flowers have reduced carotenoid accumulation and abnormally large chromoplasts

Our EMS mutagenesis screen in the wild-type MvBL background recovered a pink-flowered mutant, *MV00160* (Figures 1A and 1B). We examined the pigment content of wild-type and mutant flowers by extracting all corolla pigments in methanol and then separating them into layers with polar and non-polar solvents. We found that, in *MV00160* flowers, both the anthocyanins in the upper polar layer and the carotenoids in the lower non-polar layer appeared less concentrated than in wild-type (Figure 1C). We then quantified these differences by extracting anthocyanin and carotenoid pigments separately from weighed corollas and estimating their concentrations by UV/Vis spectroscopy. We confirmed that the content of both anthocyanins and carotenoids decreased in mutant corollas (by 1.2-fold and 1.8-fold, respectively), with a stronger effect on carotenoids (Figures 1D and 1E).

To determine whether this decrease in carotenoid pigmentation was correlated with the down-regulation of CBP gene expression, we performed quantitative reverse transcriptase (qRT-PCR) assays. We found that none of the CBP genes was differentially expressed in *MV00160* flowers compared to wild-type (Figure 1F). This indicates that the carotenoid phenotype in mutant plants is not caused by a transcriptional regulator of CBP genes. To determine if any of

the CBP genes were mutated, we performed an HPLC analysis on *MV00160* flower petal lobes. We found that the carotenoid composition was unaltered in the mutant compared to wild-type, suggesting that all of the carotenoid biosynthesis genes were functional (Figure 1G).

Because neither CBP gene expression nor carotenoid composition were altered in *MV00160*, we hypothesized that this mutant might be defective in chromoplast biogenesis. To test this, we examined flower petal cells under light microscopy. We found that wild-type petals produce many small chromoplasts that, though they tend to cluster, produce a fairly even chromoplast "envelope" surrounding the central vacuole filled with magenta anthocyanins (Figure 2A). By contrast, *MV00160* flowers have few (~8-15), abnormally large chromoplasts (Figure 2D). These chromoplasts are heterogeneous in size, and appear to have extremely long stroma-filled tubules (stromules) (indicated by arrows in Figure 2D). To confirm that mutant chromoplasts were properly differentiated, we performed transmission electron microscopy (TEM). We observed that, despite their large size, internal structure of *MV00160* chromoplasts is very similar to that of the wild-type, with no apparent structural defects (Figures 2B, 2C, 2E, and 2F). The flowers of *MV00160* may appear pink because the scattered, abnormally large chromoplasts leave "gaps" where anthocyanin pigments in the vacuole are not overlain by carotenoids in a dispersed, even chromoplast envelope. Alternatively, altered light scattering or the reduced ratio of carotenoids to anthocyanins in *MV00160* mutants could account for this difference.

To better understand how chromoplasts normally develop in the wild-type *M. verbenaceus*, we examined plastid biogenesis in wild-type MvBL flowers. In the petals of 2-mm corollas, there are several (approximately 15-20) relatively large, colorless plastids. As the flower

develops, these remain colorless and appear to decrease in size while increasing in number (Supplementary Figure 1). Finally, plastids begin to accumulate carotenoids in 15-mm flowers.

MV00160 plants have a mutation in ARC6

To determine the causal mutation in *MV00160*, we employed a hybrid strategy that combines bulk segregant analysis of a *MV00160* x MvBL F2 population and genome comparisons between multiple EMS mutants generated using the same MvBL inbred line, as described in LaFountain et al. (2017). This analysis produced five candidate single nucleotide polymorphisms (SNPs). One of these is an intron splicing mutation (Figure 3A) in the gene orthologous to AT5G42480, the *Arabidopsis thaliana ACCUMULATION AND REPLICATION OF CHLOROPLASTS 6 (ARC6)* gene. AtARC6 is an essential component of the plastid division machinery in plant cells (Pyke et al., 1994; Robertson et al., 1995; Vitha et al., 2003; Glynn et al., 2008).

To examine the expression pattern of the candidate *ARC6* gene, we performed RT-PCR on RNA extracted from multiple tissues at multiple developmental stages of wild-type MvBL plants. While *ARC6* is expressed in all organs examined (very weakly in root), its expression is especially strong in 10-mm corollas (Figure 3B).

Because the candidate mutation was in an intron-exon boundary, we performed an RT-PCR on MvBL and *MV00160* leaf and corolla samples to determine whether proper splicing was occurring in mutant plants. In the wild-type, as expected, there was only one splice variant which excises the entire intron. By contrast, the *MV00160* mutant produces *ARC6* transcripts of three different lengths (Figure 3C). Based on observations of size alone, one appears to contain the full

intron, one appears to excise the full intron, and one contains a partial intron. These splice variants have not been sequence verified, so even the "properly" spliced variant may be improperly spliced. Although these splice variants are detectable when the RT-PCR is saturated (34 total cycles), their expression is quite weak compared to the correctly spliced transcript in wild-type plants. Additionally, despite several attempts, full-length *ARC6* transcripts could not be amplified from *MV00160* cDNA (data not shown). These results suggest that *MV00160* most likely represents a null *arc6* allele.

MV00160 has abnormal chloroplasts in leaves and calyces

In addition to the chromoplast phenotype in flowers, *MV00160* plants have several other visible phenotypes. As early as the development of the first pair of leaves, it becomes apparent that stems are entirely white, lacking both the chlorophyll and anthocyanin pigments present in wild-type. Later in development, stems turn deep purple. Plants are also slow-growing, with drooping stems and pedicels. *MV00160* leaves are pale compared to wild-type, and the bases of *MV00160* calyces appear entirely white rather than green (Figures 4A and 4C). To test whether leaves and calyces have reduced chlorophyll and carotenoid content, we extracted these pigments in methanol and performed UV/Vis spectroscopy. In leaves, chlorophyll a and carotenoid content were similar in wild-type and *MV00160* plants, but the amount of chlorophyll b was significantly reduced ($P << 0.01$, Student's t-test) (Figure 4B). In calyces, chlorophyll a and carotenoid concentrations are both reduced in mutant plants ($P << 0.01$ and $P < 0.06$, respectively), while chlorophyll b concentration is unaffected (Figure 4D).

Because *arc6* mutants have been shown to produce large plastids in all tissues in *Arabidopsis* (Pyke et al., 1994; Robertson et al., 1995), we examined the leaves and calyces of our *MV00160* mutant by light and transmission electron microscopy. We found that, in both of these tissues, *MV00160* produces abnormal plastids. In leaf mesophyll cells, *MV00160* mutants make large, elongated chloroplasts, typically just one or two per cell (Figure 5). This is a severe reduction in number compared to the wild-type, which we previously showed to contain ~90 chloroplasts on average (Stanley et al., 2020), and appears to affect chromoplast coverage. Transmission electron microscopy reveals that the large plastids of *MV00160* mesophyll cells have typical chloroplast morphology, with numerous grana thylakoids and small plastoglobules (Figures 5E and 5F). In the leaf epidermis, some *MV00160* stomatal guard cells have few, large plastids, but others have numerous, small plastids resembling those of the wild-type (Figure 5G-I). Occasionally, one guard cell lacks chloroplasts altogether, possibly indicating a failure in segregation of plastids between daughter cells in the guard mother cell (Figure 5J). TEM of the white calyx base also shows few, greatly enlarged plastids compared to wild-type. ULtrastructurally, some of these resemble wild-type chloroplasts with typical grana thylakoids, while others are vacuolated and lack thylakoids (Figure 6).

DISCUSSION

In this study, we characterized a pink-flowered mutant of the crimson monkeyflower, *Mimulus verbenaceus*. We demonstrated that *MV00160* flowers produce reduced carotenoid levels. This is not due to altered expression of, or mutation in, the carotenoid biosynthetic genes, but rather to abnormal chromoplast biogenesis. Compared to wild-type, mutant flowers had

fewer, larger chromoplasts, accounting for the color difference, but unaltered internal structure. Using a bulk segregant approach, we mapped the *MV00160* mutation to the *ACCUMULATION AND REPLICATION OF CHLOROPLASTS 6* (ARC6) locus, and showed that this mutation may result in a null allele. We further demonstrated that the pale leaves and white calyces of the mutant also have reduced pigment content, and contain just one or two abnormally large plastids. Although the enlarged leaf chloroplasts have typical internal anatomy, many calyx plastids were improperly differentiated, indicating a function for this gene in not only plastid division but plastid differentiation in certain tissues.

Mimulus arc6 mutants are generally similar to *Arabidopsis arc6* mutants in their leaf phenotypes. Both have few, enlarged, abnormally shaped chloroplasts in leaf mesophyll cells as well as occasional aplastidic guard cells in the leaf epidermis (Pyke et al., 1994; Robertson et al., 1995). Additionally, though *Arabidopsis arc6* mutants do not have obvious leaf color phenotypes, they have been shown to accumulate less chlorophyll compared to wild-type plants. This is correlated with reduced efficiency of photosynthesis and altered composition of the photosynthetic apparatus in high light conditions (Austin II and Webber, 2005). Photosystem composition is likely also altered in *Mimulus arc6* mutants, which have reduced chlorophyll b content (and therefore a much higher ratio of chlorophyll a:b) in leaves (Figure 4A and 4B).

One difference in leaf phenotype between *Mimulus* and *Arabidopsis arc6* mutants is the twisted and curled leaves of *Atarc6*, which are correlated with mesophyll cell irregularities (Pyke et al., 1994). Abnormal chloroplast development has been shown to correlate with defective leaf development in other mutants and in other species (e.g., Chatterjee et al., 1996; Keddie et al., 1996), so it is curious that *Mimulus* leaves do not show obvious leaf defects other than the pale color.

In petals, the comparison between *Arabidopsis* and *Mimulus arc6* mutants is less straightforward. *Arabidopsis* flowers do not produce chromoplasts; the colorless plastids in wild-type petals de-differentiate from chloroplasts into leucoplasts. Therefore, the few enlarged leucoplasts in *Arabidopsis arc6* mutants are derived from an already small number of enlarged chloroplasts (Pyke and Page, 1998). In *Mimulus*, we have shown that colorless plastids directly give rise to chromoplasts (Supplementary Figure 1). Unlike the leaf and calyx, which have only one or two chloroplasts per cell, *MV00160* flower petals have multiple chromoplasts (~8-15 per cell). This is somewhat difficult to explain, given that all plastids are derived from the same proplastid precursors. In *Arabidopsis arc6* mutants, cells of the apical meristems only have two large proplastids; these divide by some mechanism independent of ARC6 during cell division, producing at least one plastid in each daughter cell (Robertson et al., 1995). We hypothesize that, in *Mimulus arc6* mutant flowers, there must be several plastid divisions as petal epidermal cells differentiate and divide (i.e., late-stage proplastid division or chromoplast division). It cannot be ruled out based on our current data that these divisions occur because at least some properly spliced transcripts of *ARC6* are present in petals. However, we do not think that this is the case because plastids of leaf mesophyll cells and calyces, which have the same splice variants, do not divide (Figure 3C).

Although plastids divide by binary fission like their cyanobacterial progenitors, the process is under nuclear control. During plastid division, concentric contractile rings form at the center of the plastid: a bacteria-derived FtsZ ring on the stromal side of the inner envelope membrane, and a plant-derived ARC5 ring on the cytosolic side of the outer envelope membrane. In order to successfully assemble and coordinate the plastid division machinery, many proteins are required. Min proteins (ARC3, MCD1, MinD, and MinE) position the FtsZ ring at the center

of the plastid, while transmembrane proteins mediate the interactions between the two contractile rings (ARC6 and PARC6 across the inner envelope and PDV1 and PDV2 across the outer envelope) (Wang et al., 2017; Chen et al., 2018). ARC6 spans the inner envelope membrane. Its N-terminus recruits and interacts with FtsZ2 in the stroma while its C-terminus interacts with PDV2 (which recruits ARC5) in the intermembrane space. ARC6 therefore mediates the connection of the Z-ring and the ARC5 ring (Vitha et al., 2003; Glynn et al., 2008; Wang et al., 2017). *Arabidopsis arc6* mutants do not form an FtsZ ring (Vitha et al., 2003), and therefore the plastid division necessary to prevent production of aplastidic cells must proceed via another mechanism. Robertson et al. (1995) speculate that cell division itself could partition plastids into daughter cells, as the large plastid is wrapped around the nucleus.

It has long been ambiguous whether differentiated chromoplasts can divide, and, if so, whether these divisions are governed by the chloroplast division machinery or other/additional factors. In most systems for which we have detailed morphological data, precursor plastids, typically chloroplasts, complete all necessary divisions before chromoplasts develop. In tomato fruits, for example, it has been determined that all chromoplasts develop from existing chloroplasts (Egea et al., 2011). However, potential chromoplast divisions have been observed in some systems: images of apparently dividing chromoplasts in carrot roots, *Capsicum annuum* fruits, and *Forsythia suspensa* flower petals have been captured (Wrischer, 1972; Sitte, 1987; Leech and Pyke, K. A., 1988; Camara et al., 1995).

Genetic studies of mutants have also provided evidence that differentiated chromoplasts divide. For example, the apical meristematic cells of the cauliflower *Orange* mutant have just one or two large chromoplasts instead of colorless proplastids. These cells divide to give rise to daughter cells with few, large chromoplasts. As in *MV00160* mutants, this phenotype persists

only in some tissues: *Orange* plants maintain large chromoplasts in normally unpigmented tissues such as curd, pith, leaf bases, and roots, but not in leaves or even in flower petals, which develop typical numbers of properly sized and differentiated chloroplasts or chromoplasts, respectively (Li et al., 2001; Paolillo et al., 2004). Perhaps the most similar reported mutant to *MV00160* plants is the tomato *suffulta* mutant, for which the causal gene has not been identified. These plants have pale stems and leaves, reduced growth, few, greatly enlarged leaf and stem chloroplasts, and occasional aplastidic guard cells. Interestingly, *suffulta* mutants have a normal population of chromoplasts in fruits that form by chromoplast budding and fragmentation (Forth and Pyke, 2006). Something similar to this method of plastid division does occur normally in developing tomato fruits by the breakage of stromules, and it has been shown that inhibiting chloroplast development produces more stromules (Waters et al., 2004). Perhaps when normal chromoplast division is inhibited, the budding/fragmentation method increases in frequency in chromoplast-containing tissues.

One phenotype not reported in *Arabidopsis arc6* mutants is the improper differentiation of plastids in the calyx (Pyke and Page, 1998). MV00160 calyx cells contain plastids resembling the abnormal plastids in white sectors of variegated *Arabidopsis* mutants such as *immutans* (Wetzel et al., 1994). Atypical plastids in both *MV00160* mutant calyces and the white sectors of *immutans* leaves most resemble proplastids, as they lack thylakoids, prolamellar bodies, and large starch grains. This may indicate that plastid identity in certain tissues is somewhat reliant on plastid division.

Our study demonstrates that chromoplast biogenesis, as well as chloroplast biogenesis, requires *ARC6* in *Mimulus*. While chromoplast division is certainly affected by *arc6* mutation, it appears that chromoplast division is not as reliant on the plastid division machinery as

chloroplast division in photosynthetic tissues. To our knowledge, there are no other reported *arc6* mutants from other species, and this is the first description of a plastid division mutant affecting chromoplasts that are not derived from chloroplast precursors. This study demonstrates the value of mutagenesis screens in diverse model systems.

METHODS

Plant materials

MvBL, the wild-type *Mimulus verbenaceus* inbred line, was developed as described in Chapter 2, Stanley et al. (2020). Ethyl methanesulfonate (EMS) mutagenesis was performed in the MvBL background following Owen and Bradshaw (2011). The plants used in this study were grown in the University of Connecticut EEB Research Greenhouses in FAFARD soil mix #2 (Sun Gro Horticulture), watered by subirrigation and fertilized by top-watering 3 times per week. Plants were exposed to a 16-hr day length (natural light supplemented with ~110-160 μmol $m^{-2}s^{-1}$ sodium vapor lamps) to ensure continuous flowering.

Pigment analysis

To visualize the differences in pigment content between wild-type MvBL and mutant *MV00160* plants, we performed a pigment separation as described in Yuan et al. (2013). In brief, corollas of two open flowers from each line were ground in 150 μl methanol. Equal volumes of water and dichloromethane were promptly added and mixed thoroughly with the extracts.

Anthocyanin and carotenoid pigments were separated by centrifugation into the upper aqueous and lower organic phases, respectively.

To quantify the pigmentation phenotypes of *MV00160* mutants, both anthocyanin and carotenoid pigments were extracted from the corollas of weighed mutant and wild-type open flowers. For anthocyanin extraction, all pigments were extracted by grinding weighed corollas in 600 µL methanol/0.1% HCl. Extracts were left overnight in the dark at -20 ºC to break down carotenoid pigments, which are degraded in acidic solutions. Extracts were then centrifuged to pellet tissue, and 100 µL of supernatant was diluted in 1 mL methanol/0.1% HCl. Absorption spectra were measured on a Varian Cary 50 UV/Vis spectrometer in a 1 cm quartz cuvette. The absorbance peak at 515 nm was used to approximate anthocyanin concentration, and was normalized to 100 mg of tissue. Six samples were collected from MvBL or *MV00160* plants on the same day. Any samples collected from the same individual plants were considered biological replicates because these lines are highly inbred and variation in flower pigment content between individual plants is not greater than the variation within individual plants.

To extract carotenoid pigments, weighed corollas were ground in 600 µL of 100% methanol. Extracts were left overnight at -20 ºC in the dark to degrade anthocyanin pigments, which are only stable in acidic conditions, and then centrifuged to pellet the tissue. 100 µL of the supernatant was diluted in 1 mL 100% methanol, and measured in a 1 cm quartz cuvette on the Varian Cary 50 UV/Vis spectrometer. Absorbance at 440 nm was measured as a proxy of carotenoid concentration, and normalized to 100 mg of tissue. Six samples were collected from MvBL or *MV00160* plants on the same day. High performance liquid chromatography (HPLC) was conducted for petal lobe tissue samples of MvBL and *MV00160* as described in (LaFountain et al., 2015).

We also examined the chlorophyll and carotenoid content of photosynthetic tissues. For calyx samples, 30 mg of 15-mm stage calyx tissue was used; for leaves, 30 mg of tissue from the distal half of 5-cm leaves was used. Pigments were extracted by grinding tissue in 1 mL of methanol, pelleting tissue, and recovering the supernatant. A 200 µL aliquot of each sample was diluted 1:9 with fresh methanol, and then measured in a 1 cm quartz cuvette on a Varian Cary 50 UV/Vis spectrometer. The absorption at 652, 665, and 470 nm were used to determine the concentrations (g/ml of total extract) of chlorophyll a, chlorophyll b, and total carotenoids as described by Lichtenthaler (1987). Five leaf and five calyx samples were collected from MvBL and *MV00160* plants on the same day.

(q)RT-PCR

To determine the expression levels of relevant genes, we extracted RNA, synthesized cDNA, and performed qualitative and quantitative reverse transcriptase PCR (RT-PCR and qRT-PCR, respectively). Total RNA was extracted with the Spectrum Plant Total RNA Kit (Sigma) and cDNA was synthesized with the Superscript III First Strand Synthesis Kit (Invitrogen), following kit manuals. All qRT-PCR assays were conducted using Power SYBR Green PCR Master Mix (Applied Biosystems). qRT-PCR samples were run for 40 cycles of 95 °C for 15 s and 60 °C for 30 s on a CFX96 Touch Real-Time PCR Detection System (Bio-Rad). We confirmed from melt curves that each primer pair yielded only a single product. To determine amplification efficiencies for each primer pair, we used a dilution series of pooled cDNA samples (1:4, 1:8, 1:16, and 1:32). We used *MlUBC* as the reference gene, following Yuan et al. (2013b). Unless otherwise indicated, independent tissue samples collected from MvBL or

MV00160 plants constituted three biological replicates. Each gene of interest was compared to *MlUBC* to determine relative expression using the following formula: $(E_{ref})^{CP(ref)} / (E_{target})^{CP(target)}$ (Pfaffl, 2001). All (q)RT-PCR primers are listed in Supplemental Table 1.

Genetic mapping

To determine the identity of the causal gene, we performed a bulk segregant analysis followed by mutant library SNP filtering, as detailed in LaFountain et al. (2017). Briefly, we grew an MvBL x *MV00160* F2 population (91 individuals) to flower and extracted the DNA of the 19 plants showing the mutant phenotype. DNA samples were pooled with equal representation, and used to prepare a small-insert library. ~400 million paired-end, 100-bp reads were generated on an Illumina HiSeq 4000. We mapped these short reads to the MvBL genome assembly version 1.92 (http://monkeyflower.uconn.edu/resources/) using CLC Genomics Workbench 7.0 (QIAGEN).

To identify the causal SNP, we scanned the genome for SNPs occurring at 100% frequency in the sequenced pool (other SNPs unrelated to the locus of interest should segregate at about 50% frequency). We removed "false positive" SNPs resulting from non-specific mapping (those with >200-fold coverage, likely associated with repetitive regions) and from genome assembly errors (those which appeared in mapping analyses from other *M. verbenaceus* mutants). After SNP filtering, we were left with only five 100% SNPs.

Microscopy

To visualize plastids in different plant tissues, we performed light and transmission electron microscopy (TEM). For flower tissues, live tissue of open flowers was imaged on a light microscope. For calyx and leaf tissues, both live tissue cross sections and fixed, isolated mesophyll cells were imaged by light microscopy. Mesophyll cells were isolated following Pyke (2011). In short, we cut 35-mm leaves into strips and fixed them in 4% glutaraldehyde. Samples were washed with water, placed in 0.1 M EDTA at pH 9.0, and heated at 60 °C for 4 hours to weaken the middle lamella. Prior to imaging on a light microscope, cells were separated by macerating the tissue with forceps.

TEM was conducted at UConn's Bioscience Electron Microscopy Laboratory. Pieces of open flower petal lobe, 15 mm calyx, and 20 mm leaf of wild-type MvBL and *MV00160* were pre-fixed in 2.0% paraformaldehyde and 2.5% glutaraldehyde with 0.05 M PIPES buffer. Samples were then post-fixed with 0.8 % $K_3Fe(CN)_6$ and 1% osmium tetroxide and dehydrated in ethanol. The samples were embedded in Spurr's resin and sectioned: petal lobe and calyx samples were cut longitudinally, while leaf samples were cut transversely. Sections were counterstained with 2% aqueous uranyl acetate and 2.5% Sato's lead citrate. We photographed the sections on a FEI Tecnai 12 G2 Spirit BioTWIN transmission electron microscope.

ACKNOWLEDGEMENTS

We thank Clinton Morse, Matt Opel, and Adam Histen for plant care in the UConn EEB Research Greenhouses, Amy LaFountain for performing HPLC analyses, Qiaoshan Lin for mapping of the candidate gene interval, and Maritza Abril and Xuanhao Sun at the UConn Bioscience Electron Microscopy Laboratory for assistance in the TEM experiments.

AUTHOR CONTRIBUTIONS

L.E.S. and Y-W.Y. planned and designed the research. L.E.S. performed experiments. L.E.S and Y-W.Y analyzed the data, and L.E.S. and Y-W.Y wrote the manuscript.

REFERENCES

Austin II, Jotham and Webber, A.N. (2005). Photosynthesis in *Arabidopsis thaliana* mutants with reduced chloroplast number. Photosynth. Res. **85**: 373–384.

Barsan, C., Zouine, M., Maza, E., Bian, W., Egea, I., Rossignol, M., Bouyssie, D., Pichereaux, C., Purgatto, E., Bouzayen, M., Latché, A., and Pech, J.-C. (2012). Proteomic analysis of chloroplast-to-chromoplast transition in tomato reveals metabolic shifts coupled with disrupted thylakoid biogenesis machinery and elevated energy-production components. Plant Physiol. **160**: 708–725.

Camara, B., Hugueney, P., Bouvier, F., Kuntz, M., and Monéger, R. (1995). Biochemistry and molecular biology of chromoplast development. In International Review of Cytology, K.W. Jeon and J. Jarvik, eds (Academic Press), pp. 175–247.

Chatterjee, M., Sparvoli, S., Edmunds, C., Garosi, P., Findlay, K., and Martin, C. (1996). *DAG*, a gene required for chloroplast differentiation and palisade development in *Antirrhinum majus*. EMBO J. **15**: 4194–4207.

Chayut, N., Yuan, H., Ohali, S., Meir, A., Sa'ar, U., Tzuri, G., Zheng, Y., Mazourek, M., Gepstein, S., Zhou, X. and Portnoy, V. (2017). Distinct mechanisms of the ORANGE protein in controlling carotenoid flux. Plant Physiol. **173**: 376–389.

Chen, C., MacCready, J.S., Ducat, D.C., and Osteryoung, K.W. (2018). The molecular machinery of chloroplast division. Plant Physiol. **176**: 138–151.

Cookson, P.J., Kiano, J.W., Shipton, C.A., Fraser, P.D., Romer, S., Schuch, W., Bramley, P.M., and Pyke, K.A. (2003). Increases in cell elongation, plastid compartment size and phytoene synthase activity underlie the phenotype of the *high pigment-1* mutant of tomato. Planta **217**: 896–903.

Egea, I., Barsan, C., Bian, W., Purgatto, E., Latché, A., Chervin, C., Bouzayen, M., and Pech, J.-C. (2010). Chromoplast differentiation: Current status and perspectives. Plant Cell Physiol. **51**: 1601–1611.

Egea, I., Bian, W., Barsan, C., Jauneau, A., Pech, J.-C., Latché, A., Li, Z., and Chervin, C. (2011). Chloroplast to chromoplast transition in tomato fruit: spectral confocal microscopy analyses of carotenoids and chlorophylls in isolated plastids and time-lapse recording on intact live tissue. Ann. Bot. **108**: 291–297.

Forth, D. and Pyke, K.A. (2006). The *suffulta* mutation in tomato reveals a novel method of plastid replication during fruit ripening. J. Exp. Bot. **57**: 1971–1979.

Galpaz, N., Wang, Q., Menda, N., Zamir, D., and Hirschberg, J. (2008). Abscisic acid deficiency in the tomato mutant *high-pigment 3* leading to increased plastid number and higher fruit lycopene content. Plant J. **53**: 717–730.

Glynn, J.M., Froehlich, J.E., and Osteryoung, K.W. (2008). *Arabidopsis* ARC6 coordinates the division machineries of the inner and outer chloroplast membranes through interaction with PDV2 in the intermembrane space. Plant Cell **20**: 2460–2470.

Kahlau, S. and Bock, R. (2008). Plastid transcriptomics and translatomics of tomato fruit

development and chloroplast-to-chromoplast differentiation: chromoplast gene expression largely serves the production of a single protein. Plant Cell **20**: 856–874.

Keddie, J.S., Carroll, B., Jones, J.D., and Gruissem, W. (1996). The DCL gene of tomato is required for chloroplast development and palisade cell morphogenesis in leaves. EMBO J. **15**: 4208–4217.

Kolotilin, I., Koltai, H., Tadmor, Y., Bar-Or, C., Reuveni, M., Meir, A., Nahon, S., Shlomo, H., Chen, L., and Levin, I. (2007). Transcriptional profiling of *high pigment-2^{dg}* tomato mutant links early fruit plastid biogenesis with its overproduction of phytonutrients. Plant Physiol. **145**: 389–401.

LaFountain, A.M., Chen, W., Sun, W., Chen, S., Frank, H.A., Ding, B., and Yuan, Y.-W. (2017). Molecular basis of overdominance at a flower color locus. G3 Genes Genomes Genet. **7**:3947–3954.

LaFountain, A.M., Frank, H.A., and Yuan, Y.-W. (2015). Carotenoid composition of the flowers of *Mimulus lewisii* and related species: Implications regarding the prevalence and origin of two unique, allenic pigments. Arch. Biochem. Biophys. **573**: 32–39.

Leech, R.M. and Pyke, K. A. (1988). Chloroplast division in higher plants with particular reference to wheat. S.A. Boffey and D. Lloyd, eds (Cambridge University Press).

Li, L., Paolillo, D.J., Parthasarathy, M.V., DiMuzio, E.M., and Garvin, D.F. (2001). A novel gene mutation that confers abnormal patterns of β-carotene accumulation in cauliflower (*Brassica oleracea* var. *botrytis*). Plant J. **26**: 59–67.

Li, L. and Yuan, H. (2013). Chromoplast biogenesis and carotenoid accumulation. Arch. Biochem. Biophys. **539**: 102–109.

Lichtenthaler, H.K. (1987). [34] Chlorophylls and carotenoids: Pigments of photosynthetic

biomembranes. In Methods in Enzymology, Plant Cell Membranes. (Academic Press), pp. 350–382.

Lu, S. et al. (2006). The cauliflower *Or* gene encodes a DnaJ cysteine-rich domain-containing protein that mediates high levels of β-carotene accumulation. Plant Cell **18**: 3594–3605.

Owen, C.R. and Bradshaw, H.D. (2011). Induced mutations affecting pollinator choice in *Mimulus lewisii* (Phrymaceae). Arthropod-Plant Interact. **5**: 235.

Paolillo, D.J., Garvin, D.F., and Parthasarathy, M.V. (2004). The chromoplasts of *Or* mutants of cauliflower (*Brassica oleracea* L. var. *botrytis*). Protoplasma **224**: 245–253.

Pfaffl, M.W. (2001). A new mathematical model for relative quantification in real-time RT–PCR. Nucleic Acids Res. **29**: e45–e45.

Pyke, K. (2011). Analysis of plastid number, size, and distribution in *Arabidopsis* plants by light and fluorescence microscopy. In Chloroplast Research in Arabidopsis: Methods and Protocols, Volume I, R.P. Jarvis, ed, Methods in Molecular Biology. (Humana Press: Totowa, NJ), pp. 19–32.

Pyke, K.A. and Page, A.M. (1998). Plastid ontogeny during petal development in *Arabidopsis*. Plant Physiol. **116**: 797–803.

Pyke, K.A., Rutherford, S.M., Robertson, E.J., and Leech, R.M. (1994). *arc6*, a fertile *Arabidopsis* mutant with only two mesophyll cell chloroplasts. Plant Physiol. **106**: 1169–1177.

Robertson, E.J., Pyke, K.A., and Leech, R.M. (1995). *arc6*, an extreme chloroplast division mutant of *Arabidopsis* also alters proplastid proliferation and morphology in shoot and root apices. J. Cell Sci. **108**: 2937–2944.

Siddique, M.A., Grossmann, J., Gruissem, W., and Baginsky, S. (2006). Proteome Analysis of

Bell Pepper (Capsicum annuum L.) Chromoplasts. Plant Cell Physiol. **47**: 1663–1673.

Simkin, A.J., Gaffé, J., Alcaraz, J.-P., Carde, J.-P., Bramley, P.M., Fraser, P.D., and Kuntz, M. (2007). Fibrillin influence on plastid ultrastructure and pigment content in tomato fruit. Phytochemistry **68**: 1545–1556.

Sitte, P. (1987). Development and division of chromoplasts in petals of *Forsythia*. Cellule **74**: 59–77.

Stanley, L. and Yuan, Y.-W. (2019). Transcriptional regulation of carotenoid biosynthesis in plants: so many regulators, so little consensus. Front. Plant Sci. **10**.

Stanley, L.E., Ding, B., Sun, W., Mou, F.-J., Hill, C., Chen, S., and Yuan, Y.-W. (2020). A tetratricopeptide repeat protein regulates carotenoid biosynthesis and chromoplast development in monkeyflowers (*Mimulus*). Plant Cell. **32**:1536-1555.

Vitha, S., Froehlich, J.E., Koksharova, O., Pyke, K.A., Erp, H. van, and Osteryoung, K.W. (2003). ARC6 Is a J-domain plastid division protein and an evolutionary descendant of the cyanobacterial cell division protein Ftn2. Plant Cell **15**: 1918–1933.

Wang, W., Li, J., Sun, Q., Yu, X., Zhang, W., Jia, N., An, C., Li, Y., Dong, Y., Han, F. and Chang, N. (2017). Structural insights into the coordination of plastid division by the ARC6–PDV2 complex. Nat. Plants **3**: 1–9.

Waters, M.T., Fray, R.G., and Pyke, K.A. (2004). Stromule formation is dependent upon plastid size, plastid differentiation status and the density of plastids within the cell. Plant J. **39**: 655–667.

Wetzel, C.M., Jiang, C.-Z., Meehan, L.J., Voytas, D.F., and Rodermel, S.R. (1994). Nuclear—organelle interactions: the *immutans* variegation mutant of *Arabidopsis* is plastid autonomous and impaired in carotenoid biosynthesis. Plant J. **6**: 161–175.

Wrischer, M. (1972). Transformation of plastids in young carrot callus. Acta Bot. Croat. **31**: 41–46.

Yuan, Y.-W., Sagawa, J.M., Stilio, V.S.D., and Bradshaw, H.D. (2013a). Bulk segregant analysis of an induced floral mutant identifies a MIXTA-like R2R3-MYB controlling nectar guide formation in *Mimulus lewisii*. Genetics **194**: 523–528.

Yuan, Y.-W., Sagawa, J.M., Young, R.C., Christensen, B.J., and Bradshaw, H.D. (2013b). Genetic dissection of a major anthocyanin QTL contributing to pollinator-mediated reproductive isolation between sister species of *Mimulus*. Genetics **194**: 255–263.

Zhou, X., Welsch, R., Yang, Y., Álvarez, D., Riediger, M., Yuan, H., Fish, T., Liu, J., Thannhauser, T.W., and Li, L. (2015). *Arabidopsis* OR proteins are the major posttranscriptional regulators of phytoene synthase in controlling carotenoid biosynthesis. Proc. Natl. Acad. Sci. **112**: 3558–3563.

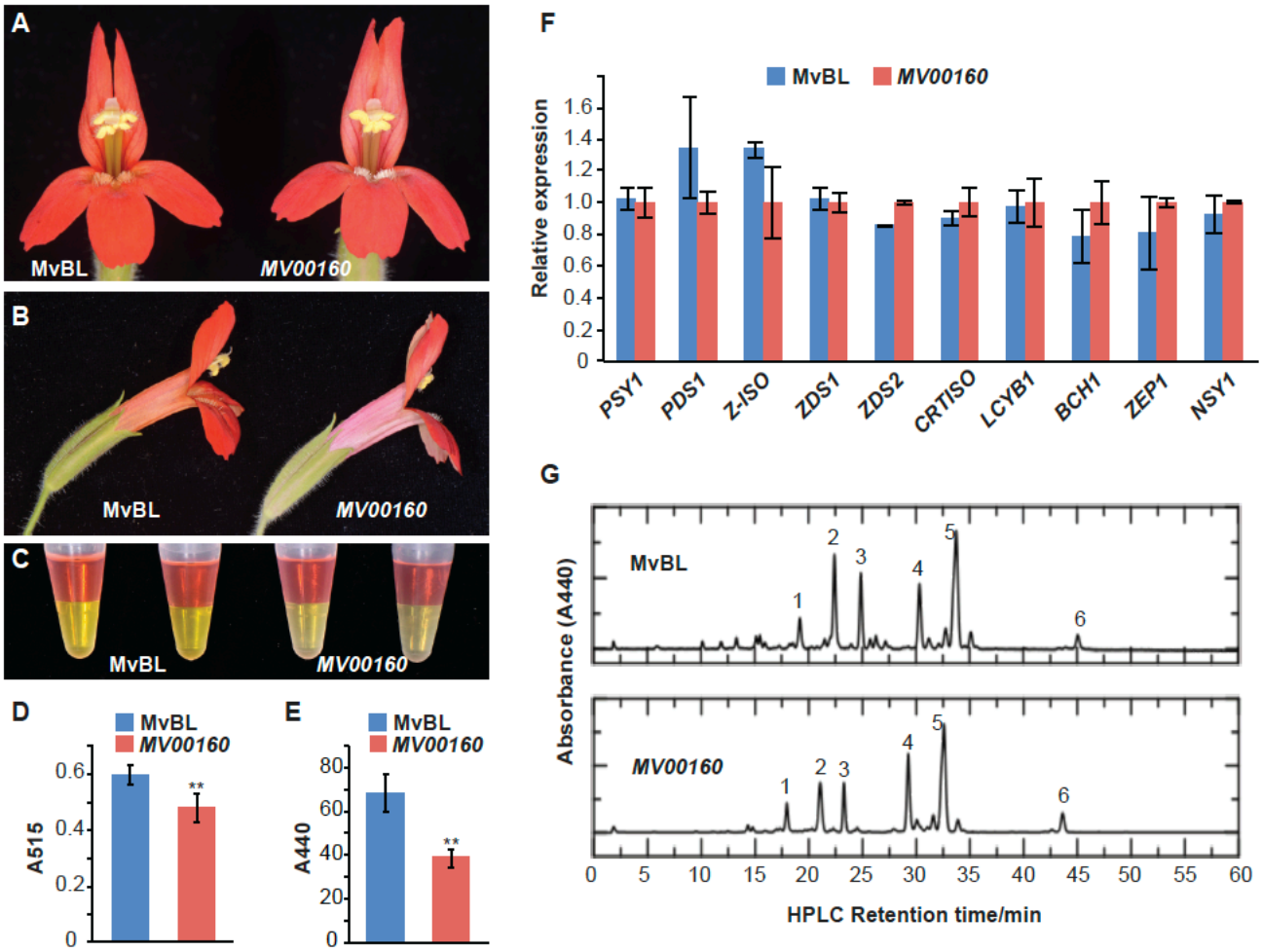

Figure 1. Floral phenotypes of *MV00160* mutants. (A) Front view of wild-type MvBL and *MV00160* flowers. **(B)** Side view of MvBL and *MV00160* flowers, showing corolla tube. **(C)** Pigment extractions from MvBL and *MV00160* petal lobes showing the anthocyanin-pigmented aqueous layer (top) and the carotenoid-pigmented organic layer (bottom). **(D)** Anthocyanin concentration of MvBL and *MV00160* corollas, estimated by absorbance at 515 nm. Error bars are 1 SD (n = 6 individual flowers from MvBL or *MV00160* plants). Asterisks indicate differences from the wild type (*P < 0.05, **P < 0.01, Student's t-test). **(E)** Carotenoid concentration of MvBL and *MV00160* corollas, estimated by absorbance at 440 nm. Error bars are 1 SD (n = 6 individual flowers from MvBL or *MV00160* plants). Asterisks indicate differences from the wild type (*P < 0.05, **P < 0.01, Student's t-test). **(F)** Transcript levels of carotenoid biosynthetic pathway genes in wild-type MvBL and *MV00160* 15-mm corollas as estimated by qRT-PCR. Error bars are 1 SD (n = 3 individual samples from MvBL or *MV00160* plants). **(G)** HPLC chromatograms for wild-type MvBL (top) and *MV00160* (bottom). Detection wavelength is 440 nm. Peaks are as follows: 1, all-trans antheraxanthin; 2, all-trans violaxanthin; 3, cis-violaxanthin; 4, deepoxyneoxanthin; 5, neoxanthin (all-trans and/or cis); 6, mimulaxanthin.

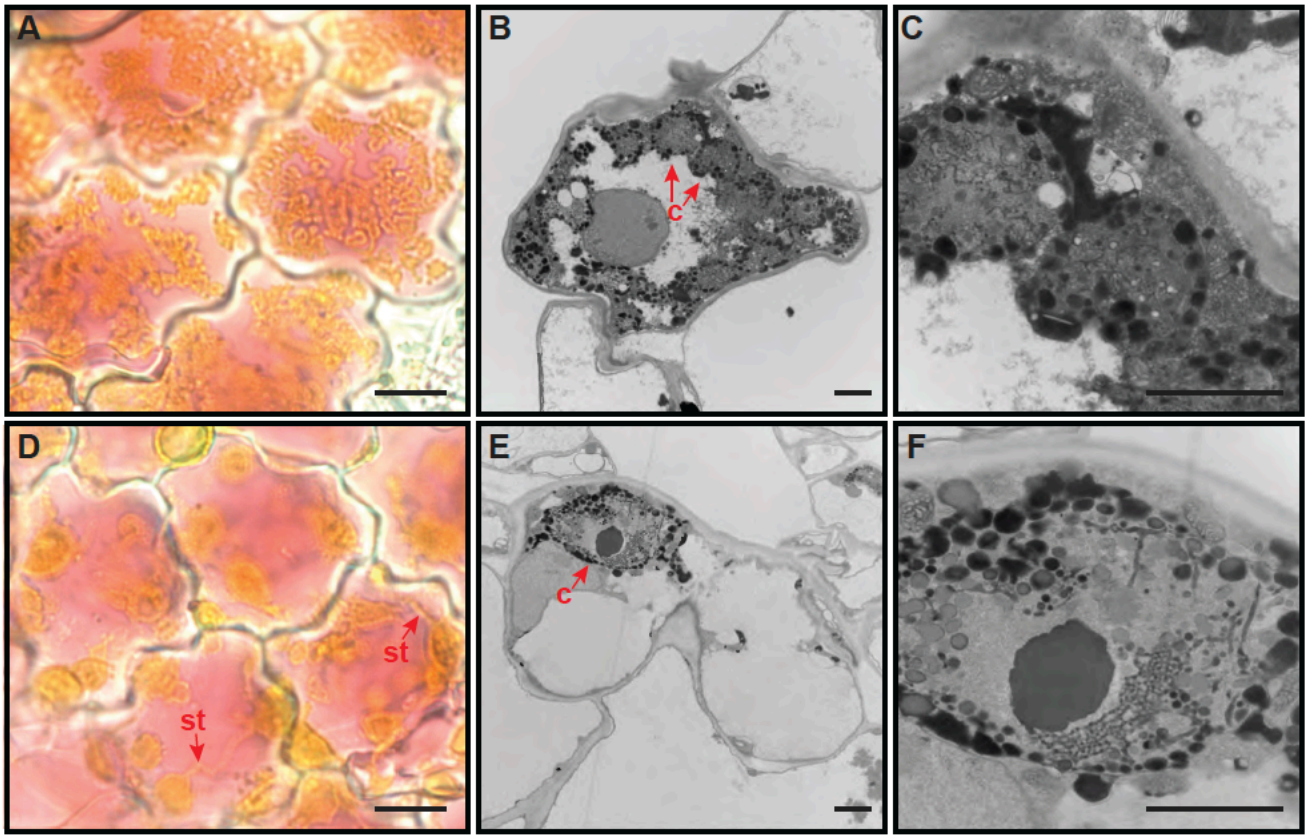

Figure 2. Light and transmission electron micrographs of *MV00160* petals. (A) Light micrograph of wild-type MvBL petal lobe epidermal cells. Scale bar = 5 microns. **(B)** Transmission electron micrograph of an MvBL petal lobe epidermal cell. Scale bar = 2 microns. **(C)** TEM image of MvBL chromoplasts. Scale bar = 500 nm. **(D)** Light micrograph of *MV00160* petal lobe epidermal cells. Scale bar = 5 microns. **(E)** TEM image of an *MV00160* petal lobe epidermal cell. Scale bar = 2 microns. **(F)** TEM image of an *MV00160* chromoplast. Scale bar = 500 nm. Abbreviations are as follows: c, chromoplast; st, stromule.

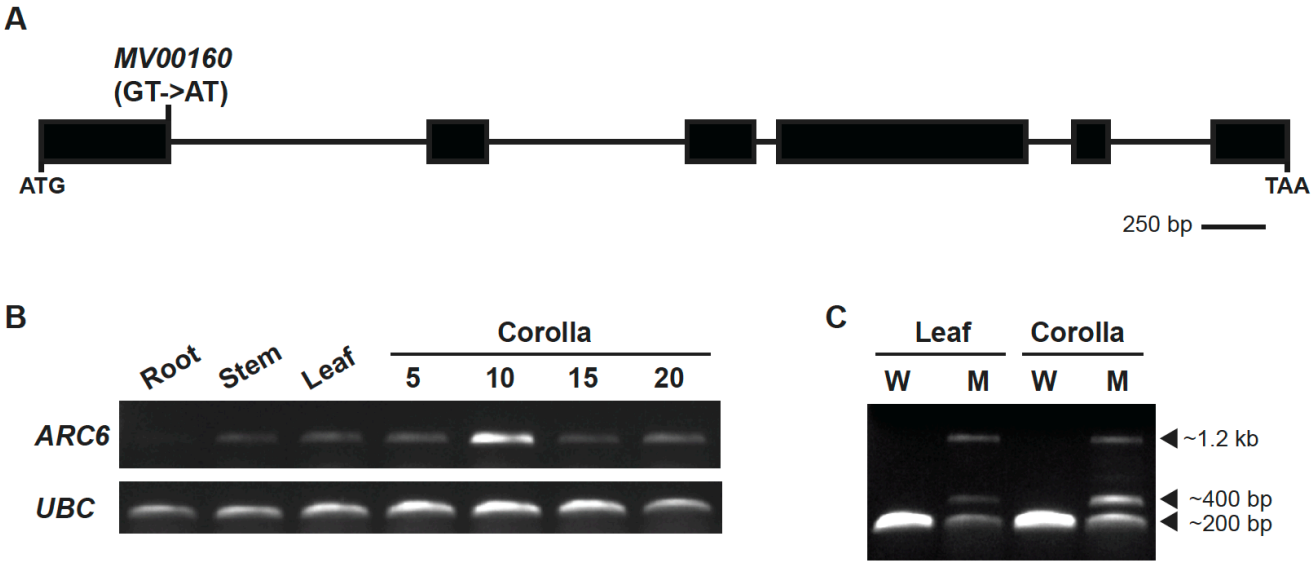

Figure 3. Identification of *MV00160*. (A) Schematic of the *Mimulus verbenaceus* homologue of *ACCUMULATION AND REPLICATION OF CHLOROPLASTS 6* (*ARC6*) showing *MV00160* mutation. Black boxes: exons; lines: introns. **(B)** Qualitative RT-PCR of *ARC6* expression in the tissues of mature wild-type MvBL plants and developing flowers. *UBC* was used as the reference gene. Cycle numbers: *ARC6*, 34 cycles; *UBC*, 28 cycles). **(C)** Qualitative RT-PCR across first *ARC6* intron in wild-type MvBL (W) and *MV00160* (M) leaf and 15-mm corolla cDNA. Band sizes are indicated at right. Asterisks indicate differences from the wild type (*P < 0.05, **P < 0.01, Student's t-test).

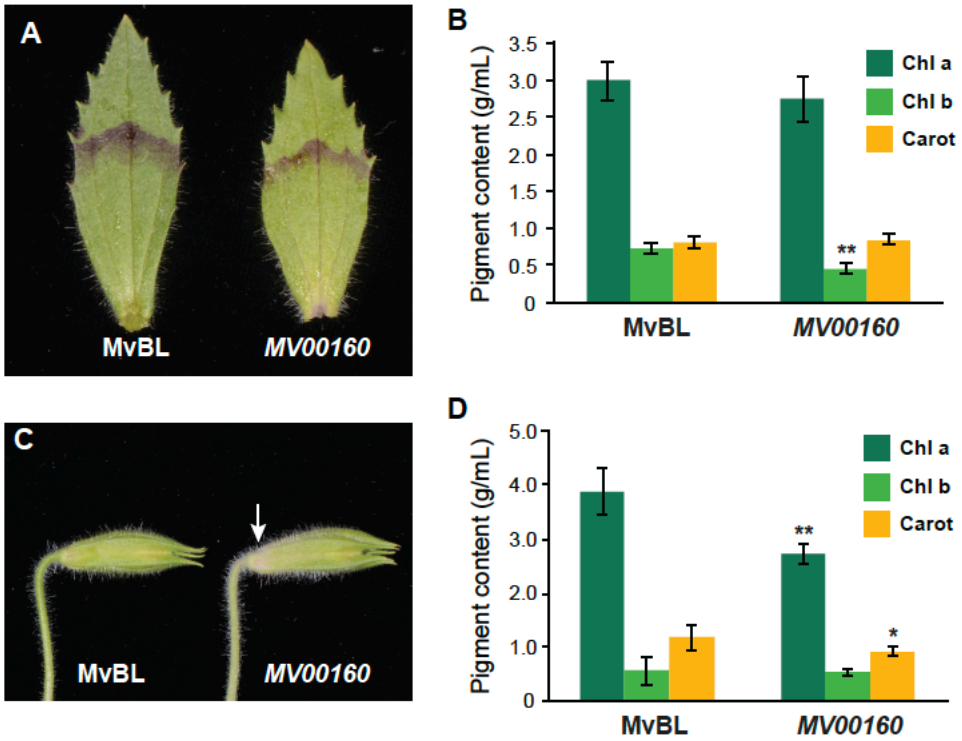

Figure 4. Phenotypes of *MV00160* calyces and leaves. (**A**) Leaves of wild-type MvBL (left) and *MV00160* (right) leaves. (**B**) Chlorophyll a, chlorophyll b, and carotenoid content of 5-cm leaves. (**C**) 15-mm calyces of MvBL and *MV00160*. (**D**) Chlorophyll and carotenoid content of 15-mm calyces. Error bars are one standard deviation (n = 6 leaves/calyces from MvBL or *MV00160* plants). Asterisks indicate differences from the wild-type (*P < 0.05, **P < 0.01, Student's t-test).

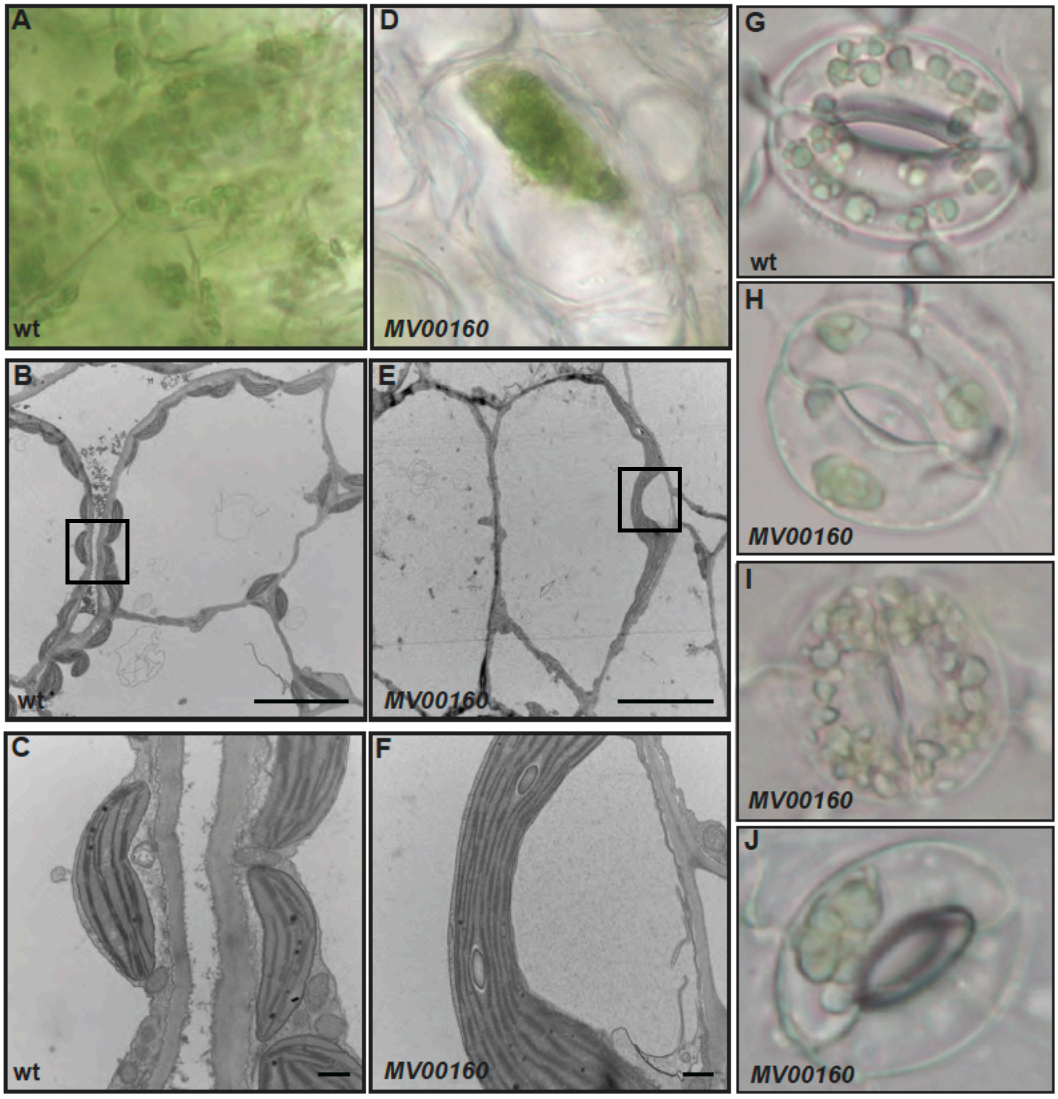

Figure 5. Light and transmission electron micrographs of *MV00160* leaves. (A) Wild-type MvBL mesophyll cell chloroplasts under light microscopy. **(B** and **C)** TEM images of MvBL leaf mesophyll cells with chloroplasts in whole cell (B) and close-up (C) views. Box in (B) indicates area enlarged in (A). Scale bars = 10 microns and 500 nm, respectively. **(D)** *MV00160* mesophyll cell chloroplast under light microscopy. **(E** and **F)** TEM images of *MV00160* leaf mesophyll cells with a chloroplast in whole cell (E) and close-up (F) views. Box in (E) indicates area enlarged in (F). Scale bars = 10 microns and 500 nm, respectively. (**G**) Light microscope image of guard cells on MvBL lower leaf epidermis. **(H** through **J)** *MV00160* guard cells showing a range of chloroplast phenotypes.

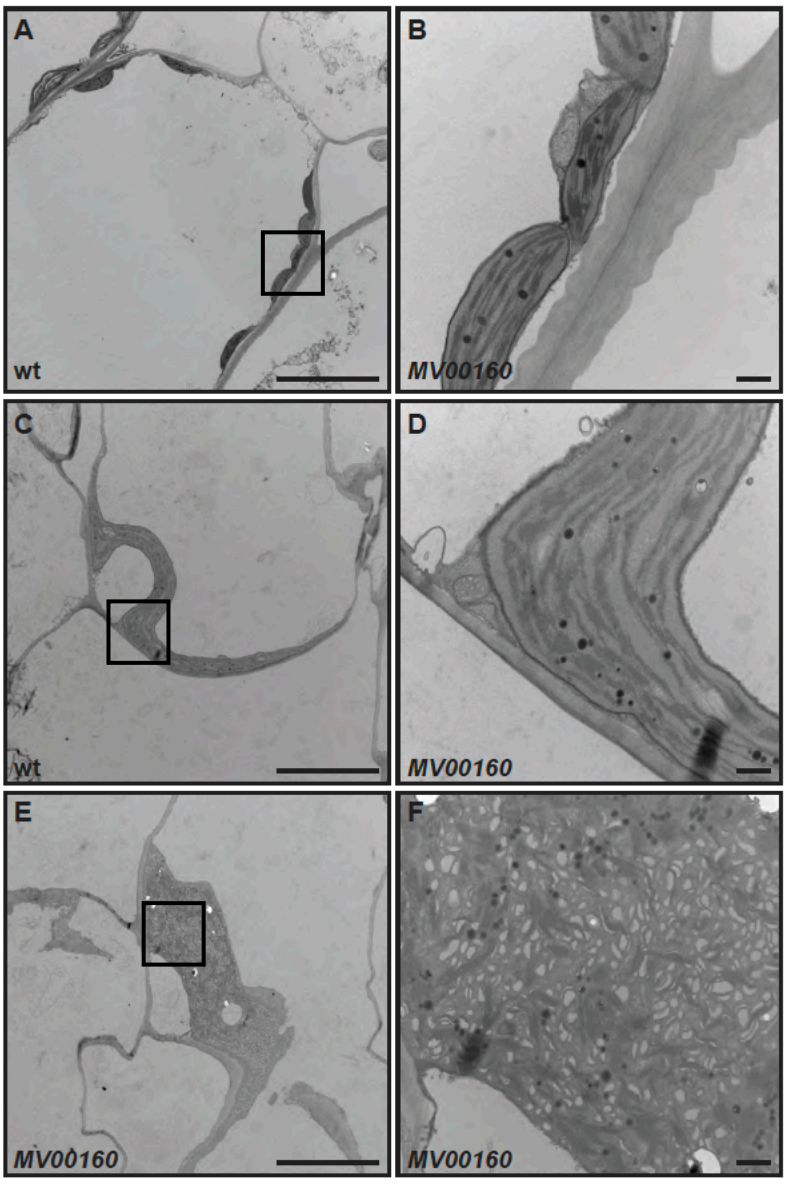

Figure 6. Transmission electron micrographs of *MV00160* calyx base. (A and **B)** Wild-type MvBL calyx base chloroplasts. **(C** through **F)** Plastids of *MV00160* calyx base. Boxes in (A), (C), and (E) show area enlarged in (B), (D), and (F), respectively. Scale bars for (A), (C), and (E): 10 microns; (B), (D), and (F): 500 nm.

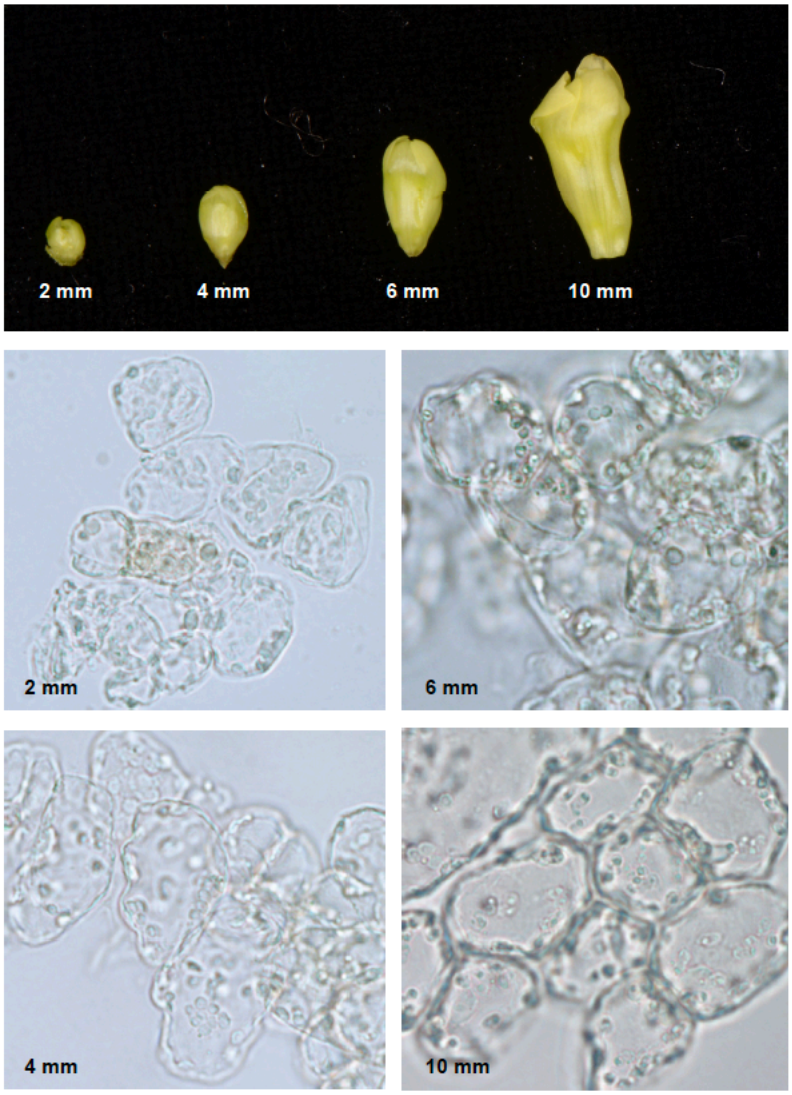

Supplementary Figure 1. Plastid development in MvBL corollas. Developmental series of MvBL flowers (top) and light microscope images of fixed petal lobe epidermal cells (bottom).

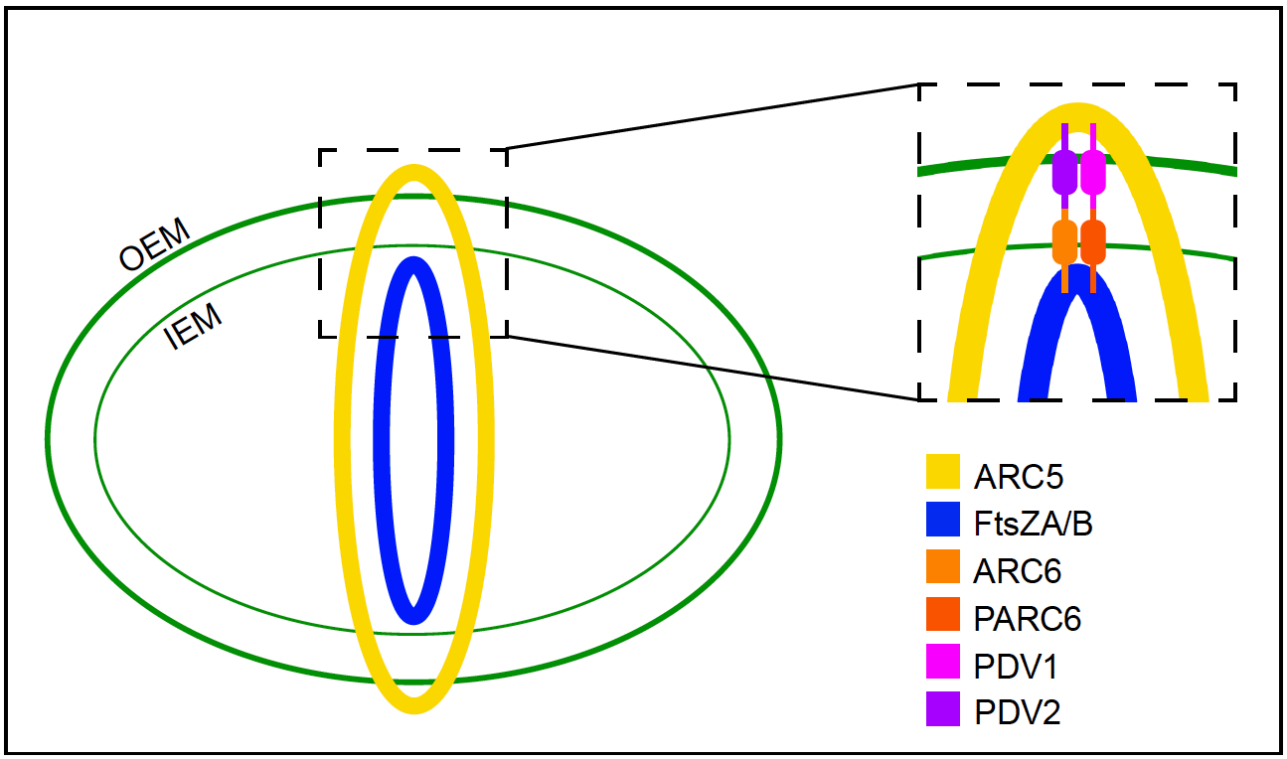

Supplementary Figure 2. Plastid division machinery of *Arabidopsis*. Diagrammatic representation of the proteins involved in plastid division, based on Chen et al. (2018).

Supplementary Table 1. (q)RT-PCR primers.

Gene	Forward (5'-3')	Reverse (5'-3')
PSY1	GATGATGCAGAGAGCGGTGTCA	GGAGGAACAAGAGACTTTGCATA
PDS1	CGACCGTTACAAAGATCTCCAT	TCCGCCAACTTCTTCTGCTCTC
Z-ISO	TTGCAGCGGTCGATAAGCCTAA	GCTGCTAATGTAACTGAGTTCC
ZDS1	CGACCAGAAGACACCTGTTAC	GTGTCAATTCAGCGACAGCAAC
ZDS2	TGACCAGAAGACCCCGGTCAA	ATAGGCACGTGATGAATTGYGAA
CRTISO	GCGATAAATGGTCTGTACTGTG	AAGGAGACCGGTATCGAGAACT
LCYB1	TATCGGCTCGTGTTTGGAAGGA	GGAAGTGTGCCCTTTGCCATGA
BCH1	TAATGCTGTTCCCGCAATTGCC	TTTCCCTATCCAGCTCTTCCAA
ZEP1	GTGTCGATAGCTATACCTTCGC	ACGGAATCGCTTGTCTTCGTTG
NSY1	ATCATGGACTCCCGATACCATG	TTCTCTGGTTCTGCTTAGAGC
UBC	GGCTTGGACTCTGCAGTCTGT	TCTTCGGCATGGCAGCAAGTC
ARC6	GCAAGACATCCTGTTGTCGATGG	CCTCCAGCAATAGCAGCTGCACC
ARC6_splice	CTTGTGAAACATTGGCGAACCC	GAACCAACTCTGTCTCACCTG

Potential role for small RNAs in carotenoid patterning of *Mimulus* flowers

Lauren E. Stanley[1] and Yao-Wu Yuan[1,2]

[1]Department of Ecology and Evolutionary Biology, University of Connecticut, Storrs, CT 06269, USA; [2]Institute for Systems Genomics, University of Connecticut, Storrs, CT 06269, USA

INTRODUCTION

Flowers display a tremendous diversity of colors and patterns typically resulting from the distribution of anthocyanin and carotenoid pigments. These pigments are often spatially restricted to particular petals, or arranged within petals to produce colored veins, spots, or stripes. Such contrasting patterns can serve as nectar guides for animal pollinators, enhancing the efficiency of pollination (e.g., Waser and Price, 1983; Leonard and Papaj, 2011; Hansen et al., 2012; de Jager et al., 2017). Nectar guides are common and phylogenetically widespread in angiosperms (Weiss, 1995), and it is therefore of great interest to elucidate the genetic underpinnings of nectar guide pigmentation.

Most pigmentation pattern studies to date have focused on the transcriptional regulation of pigment biosynthesis genes. For anthocyanins, a regulatory complex composed of R2R3-**M**YB, **b**HLH, and **W**D40 (MBW) proteins directly binds the promoters of all or a subset of anthocyanin biosynthesis genes to activate their transcription, giving rise to many floral patterns (Schwinn et al., 2006; Albert et al., 2011; Yamagishi et al., 2010; Shang et al., 2011; Davies et al., 2012; Xu et al., 2015; Yuan et al., 2016; Ding et al., 2020). For carotenoids, there have been

reports of floral transcriptional regulators such as the R2R3-MYB WHITE PETAL1 from *Medicago* and the tetratricopeptide repeat protein Reduced Carotenoid Pigmentation 2 (RCP2) from *Mimulus*, but the universality of these regulators and their potential role in patterning are unknown (Chapter 2, Stanley et al., 2020; Meng et al., 2019). Thus far, the only transcriptional regulator shown to contribute to carotenoid pigment patterning in multiple species is Reduced Carotenoid Pigmentation 1 (RCP1), an R2R3-MYB which activates the expression of carotenoid biosynthesis genes in the ventral petal of *Mimulus* and the hypochile of ornamental orchids to produce bright yellow nectar guides (Sagawa et al., 2016; Li et al., 2020).

Although a more complete understanding of transcriptional regulation, particularly for carotenoids, would advance the study of floral pigment patterning, there are other layers of regulation about which even less is known. One of these is post-transcriptional regulation of pigment biosynthesis genes by endogenous small RNAs (sRNAs). sRNAs have previously been shown to restrict the expression of flavonoid pigment biosynthesis genes in flowers to produce contrasting patterns. For instance, in snapdragon (*Antirrhinum major*), the *SULF* locus suppresses aurone pigmentation in the petal lobes, constraining the bright yellow aurones to a small area at the entrance of the corolla tube that serves as a nectar guide. This locus contains an inverted repeat with sequence homology to the aurone biosynthesis gene *Am4'CGT*, and produces 21-22 nt sRNAs that target its transcripts for degradation (Bradley et al., 2017). Another example is the “Picotee” and “Star” cultivars of horticultural petunias (*Petunia hybrida*), which have bullseye and petal-margin-restricted anthocyanin patterns, respectively. Both of these cultivars have tandem head-to-tail copies of the anthocyanin biosynthesis gene *CHS-A*. These loci produce 21-nt siRNAs in white petal regions, and the accumulation of these siRNAs is negatively correlated with *CHS* transcript levels (Morita et al., 2012). To our

knowledge, post-transcriptional regulation of carotenoid biosynthesis by endogenous sRNAs has not been reported.

In this study, we characterized the *Mimulus lewisii* mutant *yellow expanded* (*yex*). *yex* mutant flowers have an altered nectar guide pattern with carotenoid pigmentation expanded towards the distal end of the ventral petal. Through bulk segregant analysis and CRISPR/Cas9-mediated gene editing, we demonstrated that the *YEX* locus encodes the *Mimulus* orthologue of *Arabidopsis* Dicer-like 4, an endoribonuclease involved in sRNA biogenesis. Further, we show that *Mimulus lewisii* DCL4 (MlDCL4) negatively regulates the expression of the carotenoid activator *RCP1*. Based on our findings, we propose a model for nectar guide pattern formation in *Mimulus lewisii* flowers.

RESULTS

The yex *mutant has extended nectar guides and vegetative phenotypes*

In order to identify genes regulating carotenoid biosynthesis and patterning in *Mimulus lewisii* flowers, we performed a chemical mutagenesis screen in the wild-type LF10 background. We recovered several recessive carotenoid mutants, one of which produces yellow pigmentation extending beyond the boundaries of the nectar guides (Figures 1A and 1B). We named this mutant *yellow expanded* (*yex*). The severity of the carotenoid phenotype differs from flower to flower; while all mutant flowers have carotenoid pigmentation extending into the region between the two yellow ridges and the white patch (i.e., light area) of the ventral petal, some also produce carotenoids at the junction between the dorsal and lateral petal (Figure 1B).

To quantify the carotenoid phenotype, we extracted carotenoids from the lower three petals (i.e., the ventral and lateral petals) of 15-mm corollas. *yex* flowers produce ~2-fold more carotenoids than wild-type flowers (Figure 1D). As expected, the variation in carotenoid content is much greater in *yex* than in the wild-type, due to variable presence of carotenoids in lateral petals. To assess whether this difference in carotenoid pigmentation is associated with differential expression of carotenoid biosynthesis genes, we performed a quantitative reverse transcriptase PCR (qRT-PCR) in the light areas of 12-mm ventral petals. The transcript levels of all the genes we assessed were ~2-2.5 fold higher in *yex* mutants than in wild-type (Figure 1E). This indicates that *YEX* affects carotenoid biosynthesis at the transcriptional or post-transcriptional level.

The *yex* mutant also produces flowers with split corolla tubes: the dorsal petals are often partially or completely separated from the lateral and ventral petals (Figure 1C), and the degree of separation is correlated with the intensity of carotenoid pigmentation at the petal junction (Figure 1B). Similarly, the stigma lobes are sometimes split, giving a serrated appearance (Figure 1F). In addition to floral phenotypes, y*ex* plants also have vegetative phenotypes, including short internodes and accelerated senescence of leaves (Figure 1G).

YEX *encodes the homologue of* Arabidopsis *Dicer-like 4*

To identify *YEX*, we utilized a strategy that combines bulk segregant analysis and comparison of multiple mutants (LaFountain et al., 2017). Briefly, we produced an F2 population by crossing *yex* to the wild-type LF10 and sequenced a pooled sample of DNA from those F2 plants displaying a *yex* phenotype using the Illumina HiSeq4000 platform. We mapped the

resulting reads to the LF10 reference genome, searching for SNPs occurring at ~100% frequency. To remove "false positive" SNPs resulting from non-specific mapping, we discarded any SNPs with >200-fold coverage (assumed to be from highly repetitive regions). To remove 100% SNPs resulting from genome assembly errors, we compared the SNP profile of the *yex* F2 sample to the profiles of our previously sequenced mutants and eliminated any SNPs that were shared between them. This narrowed the 100% SNPs unique to *yex* mutants to only 11 mutations.

Among these 11 candidate mutations, only one could obviously disrupt gene function. This mutation results in a premature stop codon in the eighth exon of a gene encoding a protein with 1,516 amino acids (Figure 2A). BLASTing against the *Arabidopsis* proteome and phylogenetic analysis revealed that this protein is the orthologue of Arabidopsis Dicer-like 4 (Figures 2B and 2C). Dicer-like 4 is a type III restriction endonuclease that produces several types of small interfering RNAs (siRNAs) required for development, defense, and stress responses (Xie et al., 2005). Because the premature stop codon in the *yex* mutant would result in the loss of all protein domains except the DEAD-box helicase domain, this is probably a null allele.

To better understand the expression pattern of *MlDCL4*, we performed RT-PCR in multiple wild-type LF10 tissues and different floral developmental stages (Figure 2D). As expected, *DCL4* is expressed in all tissues sampled: root, stem, leaf, and corolla. In the flower, *DCL4* expression peaks when corollas reach 10 mm in size and declines thereafter.

To verify the identity of the candidate gene, we generated mutant *dcl4* alleles via CRISPR/Cas9 gene editing in the LF10 background. We constructed a pYLCRISPR/Cas9P35S-B plasmid containing four sgRNAs targeting two sites in exon 2 and two sites in exon 14 of *DCL4* (Supplementary Figure 1). In total, 42 transgenic lines were obtained, four of which were

successfully edited (9.5% efficiency). One line, DCL4 CRISPR-33, presented with a mosaic phenotype in the T1 generation, with some branches resembling wild-type and others resembling the *yex* mutant (Supplementary Figure 2). This mutant phenotype could not be recovered from selfed seeds in the T2 generation. Three other lines displayed stable phenotypes closely resembling the *yex* mutant in the T2 generation: DCL4 CRISPR-4, -6, and -24 (Figure 3). Editing was confirmed by sequencing around the target sites, which showed indels of various sizes (Figure 3). These mutant alleles were named $dcl4^{CR4}$, $dcl4^{CR6}$, and $dcl4^{CR24}$. Individuals found to be homozygous for $dcl4^{CR4}$ or $dcl4^{CR24}$ and lacking the transgene were selected for further analysis. We made complementation crosses between the *yex* mutant and these plants. All F1 plants recovered from these crosses displayed the *yex* mutant phenotype, confirming that *yex* is a *dcl4* allele (Figure 3). We will therefore refer to the *yex* allele as *dcl4-1* in the remaining text.

dcl4-1 *mutants have ectopic expression of the carotenoid regulatory gene* RCP1

Based on the known function of DCL4 in the production of sRNAs, we hypothesized that this gene could contribute to the patterning of the nectar guide in two ways. sRNA(s) produced by DCL4 could target the transcripts of either (1) carotenoid biosynthesis gene(s) or (2) their positive regulator(s) for degradation in the light area. Because a suite of carotenoid biosynthesis genes is upregulated in *dcl4-1* light areas, it is more likely that a small RNA produced by DCL4 targets a carotenoid transcriptional activator. Therefore, we assayed the expression levels of *RCP1* in the light areas of 12-mm corollas of LF10 and *dcl4-1* plants by RT-PCR. We found that while *RCP1* is not expressed in the light area of wild-type plants, it is weakly expressed in mutant light area (Figure 4A). In our previous study on RCP1, we found that this transcription

factor is normally expressed at a very low level for only a short developmental window in the nectar guides (Sagawa et al., 2016). Therefore even the weak expression we detected in the light area of *dcl4-1* is likely to be biologically significant. Correspondingly, flowers overexpressing *RCP1* show similar phenotypes to *dcl4-1* mutants: they have carotenoid pigmentation expanded into the space between the two yellow ridges, the light area, and the junction between the dorsal and lateral petals (Sagawa et al., 2016; Figure 4B). These observations suggest that MlDCL4 is required for the biogenesis of a sRNA that targets *RCP1*, and that ectopic *RCP1* expression in the *dcl4-1* mutant is sufficient to alter carotenoid pigmentation pattern in the flower.

DISCUSSION

In this study, we used the *yex* mutant of *Mimulus lewisii* to examine the genetic underpinnings of floral carotenoid patterning. We found that *yex* flowers, which have distally expanded nectar guides, produce two-fold more carotenoids than those of wild-type, and that the increased pigment content was correlated with upregulation of a suite of carotenoid biosynthesis genes. Based on genetic mapping and CRISPR/Cas9 gene editing, we demonstrated that the causal mutation in *yex* plants is in the *Dicer-like 4* (*DCL4*) gene encoding an endoribonuclease which produces regulatory sRNAs. Finally, we demonstrated that *dcl4-1* mutants have ectopic expression of the carotenoid activator *RCP1,* which provides a proximate explanation for the expanded carotenoid phenotype.

In plants, sRNAs are necessary for development, environmental and stress responses, and defense against viruses and transposons. The biogenesis of these small RNAs requires Dicer-like endoribonucleases, of which angiosperms have at least four paralogues (DCL1-4) (Margis et al.,

2006; Wang et al., 2016). DCL1 converts precursor RNA hairpins to 21-nt microRNAs (miRNAs), while DCL2-4 primarily function in the processing of dsRNAs to generate several types of small interfering RNAs (siRNAs) (reviewed in Borges and Martienssen, 2015). DCL4 processes the majority of 21-nt siRNAs, including endogenous trans-acting small interfering RNAs (tasiRNAs) (e.g., Allen et al., 2004; Gasciolli et al., 2005; Xie et al., 2005; Blevins et al., 2006; Henderson et al., 2006; Creasey et al., 2014).

Defects in the tasiRNA pathway can explain several of the other phenotypes observed in *yex*. Our previous study on the *flayed1* and *flayed2* mutants of *Mimulus lewisii*, which encode defective alleles of the tasiRNA biogenesis pathway genes *AGO7* and *SGS3*, respectively, share several of the phenotypes we observed in our *dcl4-1* and DCL4 CRISPR/Cas9 mutants (Ding et al., 2018). These include the lateral petal "nectar guides" as well as split corolla tubes and stigmas (Figures 1B, 1C, and 2A). In the *dcl4-1* mutant, these phenotypes are much less severe, which could be explained by partial compensation of the *dcl4-1* mutation by other Dicer-like genes, a phenomenon that has been observed in *Arabidopsis* (Gasciolli et al., 2005; Henderson et al., 2006; Parent et al., 2015). The accelerated senescence that we observed in our study is apparently unrelated to the tasiRNA pathway, but is shared with *dcl4* mutants in other systems. *Arabidopsis dcl4* mutants show an early transition from vegetative to reproductive growth (Xie et al., 2005), and tomato *dcl4* mutants show advanced leaf necrosis (Yifhar et al., 2012), resulting in premature plant death. Both of these phenotypes are fairly similar to the accelerated aging of *yex*, though these plants do not die soon after flowering.

The only *dcl4-1* phenotype that is not present in tasiRNA mutants or *dcl4* mutants in other systems is the extended nectar guide. To produce this unique phenotype, DCL4 must function independently of AGO7-1 and SGS3-1 (and perhaps of the tasiRNA pathway altogether)

to regulate carotenoid patterning. This was confirmed by double mutant analysis; *dcl4-1 sgs3-1* plants show additive phenotypes (Supplementary Figure 3). DCL4 clearly serves a non-redundant, non-canonical function in carotenoid pigmentation patterning. This is not entirely unexpected, as both DCL4 and DCL2 have been shown to produce unique endogenous miRNAs via non-canonical pathways (Rajagopalan et al., 2006; Amor et al., 2009; Wang et al., 2018), and DCL4 has also been shown to participate in transcriptional regulation (Liu et al., 2012). There is clearly much more to discover about the many regulatory roles Dicer-like proteins play in plants.

In *Mimulus lewisii*, DCL4 negatively regulates carotenoid pigmentation, restricting it to the ridges of the ventral petal. We have shown that *dcl4-1* mutants have ectopic carotenoids in the ventral petal light area, and that this correlates with ectopic expression of the positive carotenoid regulator *RCP1*. The similarly extended nectar guides of *dcl4-1* mutants and *RCP1* overexpression plants may indicate that DCL4 has some role in the regulation of this gene. We hypothesize that DCL4 processes a small RNA that targets the transcripts of either *RCP1* or its upstream activator(s) for degradation. We anticipate that this small RNA is not a tasiRNA, as neither *ago7* nor *sgs3* mutants have extended nectar guides. To test this hypothesis, the small RNA libraries of wild-type and *dcl4-1* developing corollas should be compared in a future study. If small RNA sequences with complementarity to *RCP1* are present in the mutant but not the wild-type, *RCP1* is subject to post-transcriptional regulation by DCL4-processed sRNA. If no such small RNA is found, it is likely that this approach would lead to the discovery of a new carotenoid regulator.

It should be noted that, in both *dcl4-1* mutants and *RCP1* overexpression plants, carotenoid expression is still restricted to the nectar guide and light areas of the ventral and sometimes lateral petals. This is due to the presence of a dominant carotenoid repressor,

YELLOW UPPER (YUP) (Hiesey, et al., 1971; Bradshaw and Schemske, 2003), for which the causal gene remains unidentified. YUP is clearly epistatic to *RCP1*, and therefore DCL4-mediated regulation of carotenoid biosynthesis is certainly not the only nectar guide patterning mechanism in *Mimulus.*

To our knowledge, this study represents the first potential example of sRNA-mediated regulation of carotenoid patterning. It demonstrates a novel role for DCL4 in the regulation of floral carotenoid biosynthesis, making it one of just four known genes contributing to this important and ubiquitous floral phenotype.

MATERIALS AND METHODS

Plant materials

The wild-type *Mimulus lewisii* LF10 inbred line was developed as described in Yuan et al. (2013b). Ethyl methanesulfonate (EMS) mutants were produced in the LF10 background following Owen and Bradshaw (2011). All plants were grown in FAFARD soil mix #2 (Sun Gro Horticulture) in the University of Connecticut EEB Research Greenhouses. The plants were provided a 16-hour day length, supplementing natural light with sodium vapor lamps (~110-160 μmol $m^{-2}s^{-1}$). Plants were subirrigated and fertilized three times a week.

Carotenoid extractions

To estimate the total carotenoid content of flowers, we collected and weighed the ventral and lateral petals from 15 mm corollas. Five samples were collected on the same day from LF10 or *yex* plants. Any samples collected from the same individual plants were considered biological replicates because these lines are highly inbred and variation in flower pigment content between individual plants is not greater than the variation within individual plants. We extracted carotenoid pigments in 1.3 mL of 100% methanol by grinding tissue with a nylon pestle and pelleting the debris. 200 µL of the extract was diluted in 900 µL of 100% methanol and absorption spectra were measured in a 1 cm quartz cuvette with a Varian Cary 50 UV/Vis spectrometer. Total carotenoid content was then estimated by absorption at 440 nm and normalized to 1 g of tissue.

Genetic mapping

To map the causal gene underlying the *yex* phenotype, we employed the hybrid bulk segregant/mutant genome comparison method used in LaFountain et al., (2017). In brief, an LF10 x *yex* (Ml14453) F2 population (203 individuals) was grown to flower. DNA samples were collected from 35 plants displaying the *yex* phenotype and pooled with equal representation. A small-insert library was prepared and ~400 million paired-end, 100-bp reads were generated by an Illumina HiSeq 4000. We mapped the short reads to the LF10 genome assembly version 1.8 (http://monkeyflower.uconn.edu/resources/) using CLC Genomics Workbench 7.0 (QIAGEN). In order to identify the causal mutation, which should have a 100% SNP frequency in the pooled sample (compared to ~50% frequency expected for unrelated EMS mutations), we had to remove "false positive" 100% SNPs resulting from genome assembly error or non-specific mapping. To

that end, we compared the SNP profile of our bulk sample to the profiles of previously published mutants (Yuan et al., 2013a; Sagawa et al., 2016; Ding et al., 2017, 2018; Stanley et al., 2017), removing any SNPs which appeared in multiple profiles. Our script for bulk segregant analysis is available on GitHub (https://github.com/qslin/Bulk-Segregation-Analysis).

Protein domain prediction and gene tree building

In order to predict protein domains, we used the NCBI conserved domain database (https://www.ncbi.nlm.nih.gov/Structure/cdd/wrpsb.cgi) and ScanProsite (https://prosite.expasy.org/scanprosite/) (de Castro et al., 2006; Lu et al., 2020). We built a maximum likelihood (ML) phylogeny of the *Mimulus lewisii* Dicer-like proteins and the Dicer-like proteins from *Arabidopsis* and rice (*Oryza sativa*). The *Arabidopsis* sequences were retrieved from TAIR (https://www.arabidopsis.org/), and the rice sequences were retrieved from Phytozome v13 (https://phytozome-next.jgi.doe.gov/). Only the conserved domains that could be confidently aligned across all sequences were used for phylogenetic analysis. ML analysis was conducted using the RAxML web-server (http://embnet.vital-it.ch/raxml-bb/), with the JTT amino acid substitution matrix and the GAMMA model of rate heterogeneity. Clade support was estimated by 100 bootstrap replicates.

(q)RT-PCR and 5'RACE PCR

In order to estimate the expression levels of relevant genes, we performed qualitative and quantitative reverse transcriptase PCR (RT-PCR). We extracted total RNA using the Spectrum

Plant Total RNA Kit (Sigma) and synthesized cDNA using the Superscript III First Strand Synthesis Kit (Invitrogen), according to the manufacturers' instructions. The relative transcript levels of genes of interest were assessed qualitatively (RT-PCR) or quantitatively (qRT-PCR). All (q)RT-PCR primers are listed in Supplementary Table 1. For qRT-PCR experiments, we used Power SYBR Green PCR Master Mix (Applied Biosystems) and a CFX96 Touch Real-Time PCR Detection System (Bio-Rad). The protocol was as follows: 40 cycles of 95 °C for 15 s and 60 °C for 30 s. After confirming from melt curves that each primer pair yielded only a single product, we used a dilution series of pooled cDNA samples (1:4, 1:8, 1:16, and 1:32) to determine amplification efficiencies for each primer pair. As described in Yuan et al. (2013b), *MlUBC* was used as the reference gene. Three independent tissue samples collected from LF10 or *dcl4* plants were used for all qRT-PCR experiments unless otherwise indicated (lines are highly inbred and variation in gene expression between individual plants is not greater than the variation within individual plants). Relative expression of each target gene compared to the reference gene was calculated using the formula $(E_{\text{ref}})^{\text{CP(ref)}} / (E_{\text{target}})^{\text{CP(target)}}$ (Pfaffl, 2001).

CRISPR/Cas9 gene editing

Four 20-nt target sequences were chosen, two in exon 2 and in exon 14, intended to induce large deletions in each exon. These target sequences were unique in the genome, and immediately adjacent to Protospacer Adjacent Motifs (PAMs). Four sgRNA cassettes were prepared by cloning target sequences (Supplementary Figure 1) into intermediate plasmids containing gRNA scaffolds and one of the *Arabidopsis* U3 or U6 promoters: pYLsgRNA_AtU3d, pYLsgRNA_AtU3b, pYLsgRNA_AtU6-1, and pYLsgRNA_AtU6-29 (Ma

et al., 2015; Addgene Plasmids #66200, 66198, 66202, 66203). sgRNA cassettes from each intermediate plasmid were amplified by nested PCR and linked together via Golden Gate ligation (Engler et al., 2008). The full expression cassette containing four sgRNAs was cloned into the pYLCRISPR/Cas9P35S-B plasmid (Ma et al., 2015; Addgene Plasmid #66190). Primers for cloning can be found in Supplementary Table 2. The DCL4 pYLCRISPR/Cas9P35S-B plasmid was verified by sequencing and subsequently stably transformed into wild-type LF10 plants by *Agrobacterium*-mediated vacuum infiltration, following the protocol described in Yuan et al. (2013a).

ACKNOWLEDGEMENTS

We thank Clinton Morse, Matt Opel, and Adam Histen for plant care in the UConn EEB Research Greenhouses, Amy LaFountain for performing HPLC analyses, and Qiaoshan Lin for mapping of the candidate gene interval.

AUTHOR CONTRIBUTIONS

L.E.S. and Y-W.Y. planned and designed the research. L.E.S. performed experiments. L.E.S and Y-W.Y analyzed the data, and L.E.S. and Y-W.Y wrote the manuscript.

REFERENCES

Albert, N.W., Lewis, D.H., Zhang, H., Schwinn, K.E., Jameson, P.E., and Davies, K.M. (2011). Members of an R2R3-MYB transcription factor family in *Petunia* are developmentally and environmentally regulated to control complex floral and vegetative pigmentation patterning. Plant J. **65**: 771–784.

Allen, E., Xie, Z., Gustafson, A.M., Sung, G.-H., Spatafora, J.W., and Carrington, J.C. (2004). Evolution of microRNA genes by inverted duplication of target gene sequences in *Arabidopsis thaliana*. Nat. Genet. **36**: 1282–1290.

Amor, B.B. et al. (2009). Novel long non-protein coding RNAs involved in *Arabidopsis* differentiation and stress responses. Genome Res. **19**: 57–69.

Blevins, T., Rajeswaran, R., Shivaprasad, P.V., Beknazariants, D., Si-Ammour, A., Park, H.-S., Vazquez, F., Robertson, D., Meins, F., Hohn, T., and Pooggin, M.M. (2006). Four plant Dicers mediate viral small RNA biogenesis and DNA virus induced silencing. Nucleic Acids Res. **34**: 6233–6246.

Borges, F. and Martienssen, R.A. (2015). The expanding world of small RNAs in plants. Nat. Rev. Mol. Cell Biol. **16**: 727–741.

Bradley, D. et al. (2017). Evolution of flower color pattern through selection on regulatory small RNAs. Science **358**: 925–928.

Bradshaw, H.D. and Schemske, D.W. (2003). Allele substitution at a flower colour locus produces a pollinator shift in monkeyflowers. Nature **426**: 176–178.

de Castro, E., Sigrist, C.J.A., Gattiker, A., Bulliard, V., Langendijk-Genevaux, P.S., Gasteiger, E., Bairoch, A., and Hulo, N. (2006). ScanProsite: detection of PROSITE signature matches and ProRule-associated functional and structural residues in proteins. Nucleic Acids Res. **34**: W362–W365.

Creasey, K.M., Zhai, J., Borges, F., Ex, F.V., Regulski, M., Meyers, B.C., and Martienssen, R.A. (2014). miRNAs trigger widespread epigenetically activated siRNAs from transposons in *Arabidopsis*. Nature **508**: 411–415.

Davies, K.M., Albert, N.W., and Schwinn, K.E. (2012). From landing lights to mimicry: the molecular regulation of flower colouration and mechanisms for pigmentation patterning. Funct. Plant Biol. **39**: 619.

Ding, B., Mou, F., Sun, W., Chen, S., Peng, F., Bradshaw, H.D., and Yuan, Y.-W. (2017). A dominant-negative actin mutation alters corolla tube width and pollinator visitation in *Mimulus lewisii*. New Phytol. **213**: 1936–1944.

Ding, B., Patterson, E.L., Holalu, S.V., Li, J., Johnson, G.A., Stanley, L.E., Greenlee, A.B., Peng, F., Bradshaw, H.D., Blinov, M.L., Blackman, B.K., and Yuan, Y.-W. (2020). Two MYB proteins in a self-organizing activator-inhibitor system produce spotted pigmentation patterns. Curr. Biol. **30**: 802-814.

Ding, B., Xia, R., Lin, Q., Gurung, V., Sagawa, J.M., Stanley, L.E., Strobel, M., Diggle, P.K., Meyers, B.C., and Yuan, Y.-W. (2018). Developmental genetics of corolla tube formation: role of the tasiRNA-ARF pathway and a conceptual model. bioRxiv: 253112.

Engler, C., Kandzia, R., and Marillonnet, S. (2008). A one pot, one step, precision cloning method with high throughput capability. PLoS ONE **3**.

Gasciolli, V., Mallory, A.C., Bartel, D.P., and Vaucheret, H. (2005). Partially redundant functions of *Arabidopsis* DICER-like enzymes and a role for DCL4 in producing trans-acting siRNAs. Curr. Biol. **15**: 1494–1500.

Hansen, D.M., Van der Niet, T., and Johnson, S.D. (2012). Floral signposts: testing the significance of visual 'nectar guides' for pollinator behaviour and plant fitness. Proc. R. Soc. B Biol. Sci. **279**: 634–639.

Henderson, I.R., Zhang, X., Lu, C., Johnson, L., Meyers, B.C., Green, P.J., and Jacobsen, S.E. (2006). Dissecting *Arabidopsis thaliana* DICER function in small RNA processing, gene silencing and DNA methylation patterning. Nat. Genet. **38**: 721–725.

Hiesey, William M., Nobs, M.A., and Björkman, O. (1971). Experimental studies on the nature of species (Carnegie Institution of Washington: Washington, D.C.).

de Jager, M.L., Willis-Jones, E., Critchley, S., and Glover, B.J. (2017). The impact of floral spot and ring markings on pollinator foraging dynamics. Evol. Ecol. **31**: 193–204.

LaFountain, A.M., Chen, W., Sun, W., Chen, S., Frank, H.A., Ding, B., and Yuan, Y.-W. (2017). Molecular basis of overdominance at a flower color locus. G3 Genes Genomes Genet. **7**: 3947–3954.

Leonard, A.S. and Papaj, D.R. (2011). 'X' marks the spot: The possible benefits of nectar guides to bees and plants. Funct. Ecol. **25**: 1293–1301.

Li, B.-J., Zheng, B.-Q., Wang, J.-Y., Tsai, W.-C., Lu, H.-C., Zou, L.-H., Wan, X., Zhang, D.-Y., Qiao, H.-J., Liu, Z.-J., and Wang, Y. (2020). New insight into the molecular mechanism of colour differentiation among floral segments in orchids. Commun. Biol. **3**: 1–13.

Liu, B., Chen, Z., Song, X., Liu, C., Cui, X., Zhao, X., Fang, J., Xu, W., Zhang, H., Wang, X. and Chu, C. (2007). *Oryza sativa* Dicer-like4 reveals a key role for small interfering RNA silencing in plant development. Plant Cell **19**: 2705–2718.

Liu, F., Bakht, S., and Dean, C. (2012). Cotranscriptional Role for *Arabidopsis* DICER-LIKE 4 in transcription termination. Science **335**: 1621–1623.

Lu, S., Wang, J., Chitsaz, F., Derbyshire, M.K., Geer, R.C., Gonzales, N.R., Gwadz, M., Hurwitz, D.I., Marchler, G.H., Song, J.S. and Thanki, N. (2020). CDD/SPARCLE: the conserved domain database in 2020. Nucleic Acids Res. **48**: D265–D268.

Ma, X., Zhang, Q., Zhu, Q., Liu, W., Chen, Y., Qiu, R., Wang, B., Yang, Z., Li, H., Lin, Y. and Xie, Y. (2015). A robust CRISPR/Cas9 system for convenient, high-efficiency multiplex genome editing in monocot and dicot plants. Mol. Plant **8**: 1274–1284.

Margis, R., Fusaro, A.F., Smith, N.A., Curtin, S.J., Watson, J.M., Finnegan, E.J., and Waterhouse, P.M. (2006). The evolution and diversification of Dicers in plants. FEBS Lett. **580**: 2442–2450.

Meng, Y., Wang, Z., Wang, Y., Wang, C., Zhu, B., Liu, H., Ji, W., Wen, J., Chu, C., Tadege, M., Niu, L., and Lin, H. (2019). The MYB activator WHITE PETAL1 associates with

MtTT8 and MtWD40-1 to regulate carotenoid-derived flower pigmentation in *Medicago truncatula*. Plant Cell **31**: 2751–2767.

Morita, Y., Saito, R., Ban, Y., Tanikawa, N., Kuchitsu, K., Ando, T., Yoshikawa, M., Habu, Y., Ozeki, Y., and Nakayama, M. (2012). Tandemly arranged *Chalcone Synthase A* genes contribute to the spatially regulated expression of siRNA and the natural bicolor floral phenotype in *Petunia hybrida*. Plant J. **70**: 739–749.

Owen, C.R. and Bradshaw, H.D. (2011). Induced mutations affecting pollinator choice in *Mimulus lewisii* (Phrymaceae). Arthropod-Plant Interact. **5**: 235.

Parent, J.-S., Bouteiller, N., Elmayan, T., and Vaucheret, H. (2015). Respective contributions of *Arabidopsis* DCL2 and DCL4 to RNA silencing. Plant J. **81**: 223–232.

Pfaffl, M.W. (2001). A new mathematical model for relative quantification in real-time RT–PCR. Nucleic Acids Res. **29**: e45–e45.

Rajagopalan, R., Vaucheret, H., Trejo, J., and Bartel, D.P. (2006). A diverse and evolutionarily fluid set of microRNAs in *Arabidopsis thaliana*. Genes Dev. **20**: 3407–3425.

Sagawa, J.M., Stanley, L.E., LaFountain, A.M., Frank, H.A., Liu, C., and Yuan, Y.-W. (2016). An R2R3-MYB transcription factor regulates carotenoid pigmentation in *Mimulus lewisii* flowers. New Phytol. **209**: 1049–1057.

Schwinn, K., Venail, J., Shang, Y., Mackay, S., Alm, V., Butelli, E., Oyama, R., Bailey, P., Davies, K., and Martin, C. (2006). A small family of MYB-regulatory genes controls

floral pigmentation intensity and patterning in the genus *Antirrhinum*. Plant Cell **18**: 831–851.

Shang, Y., Venail, J., Mackay, S., Bailey, P.C., Schwinn, K.E., Jameson, P.E., Martin, C.R., and Davies, K.M. (2011). The molecular basis for venation patterning of pigmentation and its effect on pollinator attraction in flowers of *Antirrhinum*. New Phytol. **189**: 602–615.

Stanley, L.E., Ding, B., Sun, W., Mou, F.-J., Hill, C., Chen, S., and Yuan, Y.-W. (2020). A tetratricopeptide repeat protein regulates carotenoid biosynthesis and chromoplast development in monkeyflower (*Mimulus*). Plant Cell. tpc.00755.2019. 10.1105/tpc.19.00755.

Wang, T., You, L., Li, R., Fu, D.-Q., Zhu, B.-Z., Luo, Y.-B., and Zhu, H.-L. (2016). Cloning, identification, and expression analysis of a Dicer-Like gene family from *Solanum lycopersicum*. Biol. Plant. **60**: 410–418.

Wang, Z., Hardcastle, T.J., Canto Pastor, A., Yip, W.H., Tang, S., and Baulcombe, D.C. (2018). A novel DCL2-dependent miRNA pathway in tomato affects susceptibility to RNA viruses. Genes Dev. **32**: 1155–1160.

Waser, N.M. and Price, M.V. (1983). Pollinator behaviour and natural selection for flower colour in *Delphinium nelsonii*. Nature **302**: 422–424.

Weiss, M.R. (1995). Floral color change: A widespread functional convergence. Am. J. Bot. **82**: 167–185.

Xie, Z., Allen, E., Wilken, A., and Carrington, J.C. (2005). DICER-LIKE 4 functions in trans-acting small interfering RNA biogenesis and vegetative phase change in *Arabidopsis thaliana*. Proc. Natl. Acad. Sci. **102**: 12984–12989.

Xu, W., Dubos, C., and Lepiniec, L. (2015). Transcriptional control of flavonoid biosynthesis by MYB–bHLH–WDR complexes. Trends Plant Sci. **20**: 176–185.

Yamagishi, M., Shimoyamada, Y., Nakatsuka, T., and Masuda, K. (2010). Two R2R3-MYB genes, homologs of *Petunia AN2*, regulate anthocyanin biosynthesis in flower tepals, tepal spots and leaves of Asiatic hybrid lily. Plant Cell Physiol. **51**: 463–474.

Yifhar, T., Pekker, I., Peled, D., Friedlander, G., Pistunov, A., Sabban, M., Wachsman, G., Alvarez, J.P., Amsellem, Z., and Eshed, Y. (2012). Failure of the tomato trans-acting short interfering RNA program to regulate AUXIN RESPONSE FACTOR3 and ARF4 underlies the wiry leaf syndrome. Plant Cell **24**: 3575–3589.

Yuan, Y.-W., Rebocho, A.B., Sagawa, J.M., Stanley, L.E., and Bradshaw, H.D. (2016). Competition between anthocyanin and flavonol biosynthesis produces spatial pattern variation of floral pigments between *Mimulus* species. Proc. Natl. Acad. Sci. **113**: 2448–2453.

Yuan, Y.-W., Sagawa, J.M., Stilio, V.S.D., and Bradshaw, H.D. (2013a). Bulk segregant analysis of an induced floral mutant identifies a MIXTA-like R2R3-MYB controlling nectar guide formation in *Mimulus lewisii*. Genetics **194**: 523–528.

Yuan, Y.-W., Sagawa, J.M., Young, R.C., Christensen, B.J., and Bradshaw, H.D. (2013b). Genetic dissection of a major anthocyanin QTL contributing to pollinator-mediated reproductive isolation between sister species of *Mimulus*. Genetics **194**: 255–263.

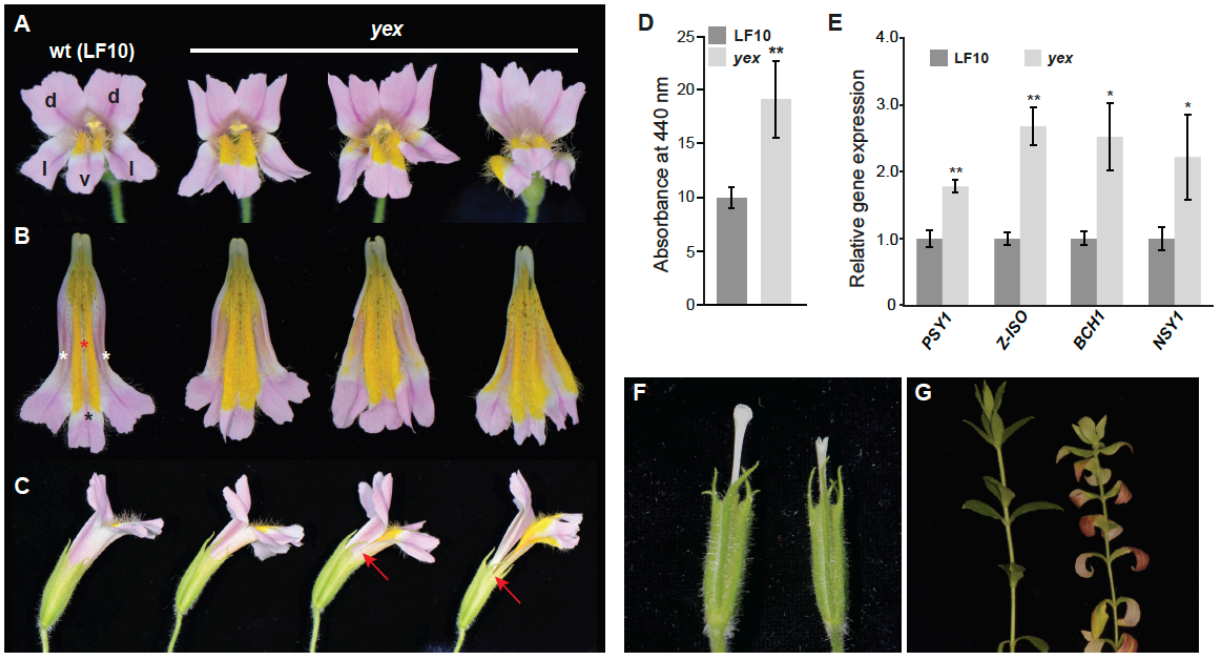

Figure 1. Phenotypes of *yex* mutants. (A through **C)** Corollas of wild-type LF10 (left) and *yex* mutants with weak to strong phenotypes (right three images). (**A**) Front view with dorsal (d) lateral (l) and ventral (v) petals indicated. (**B**) Nectar guide view. Key areas are marked with asterisks (white = lateral/dorsal petal junction; red = region between nectar guide ridges; black = light area). (**C**) Side view. Red arrows indicate the separation of dorsal and lateral petals. **(D)** Carotenoid concentration of LF10 and *yex* corollas, estimated by absorbance at 440 nm. Error bars are one standard deviation (n = 5 flowers collected from LF10 or *yex* plants). Asterisks indicate differences from the wild type (*$P < 0.05$, **$P < 0.01$, Student's *t*-test). **(E)** Transcript levels of a subset of carotenoid biosynthesis genes in LF10 and *yex* 12-mm light areas. Error bars are one standard deviation (n = 3 samples of pooled light areas from 10 flowers of LF10 or *yex* plants). Asterisks indicate differences from the wild type (*$P < 0.05$, **$P < 0.01$, Student's *t*-test). **(F)** Stigmas of LF10 (left) and a severe *yex* mutant (right). **(G)** Stems of LF10 (left) and *yex* (right) plants of the same age with approximately the same number of nodes.

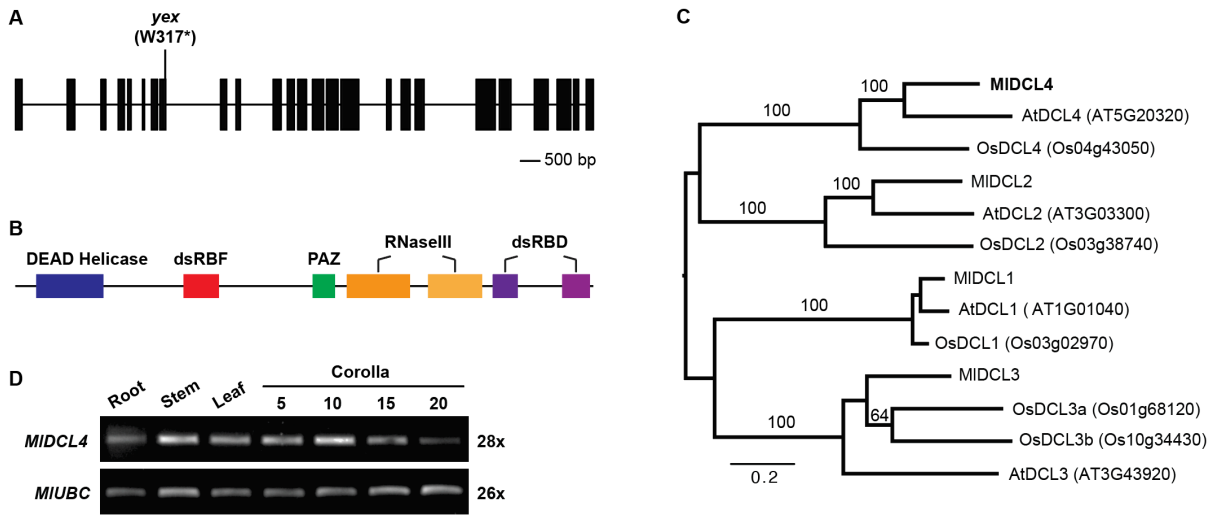

Figure 2. Identification of *YEX*. (A) A schematic of the *MlDCL4* gene showing the *yex* mutation. Black boxes indicate exons; lines indicate introns. **(B)** Protein schematic of MlDCL4 showing important domains: DEAD Helicase = DEAD-box helicase; dsRBF = double stranded RNA-binding fold; PAZ = Piwi Argonaut Zwille; RnaseIII = Ribonuclease III family; dsRBD = double stranded RNA-binding domain. **(C)** RAxML maximum likelihood tree of *Mimulus lewisii* Dicer-like proteins and Dicer-like proteins from *Arabidopsis* and rice. GenBank accession numbers for the sequences are provided after each gene name. Bootstrap values are shown along the branches. **(D)** Qualitative RT-PCR showing expression of *MlDCL4* in different tissues and developmental stages of wild-type LF10 plants. PCR cycle numbers are shown at right. *MlUBC* was used as the reference gene.

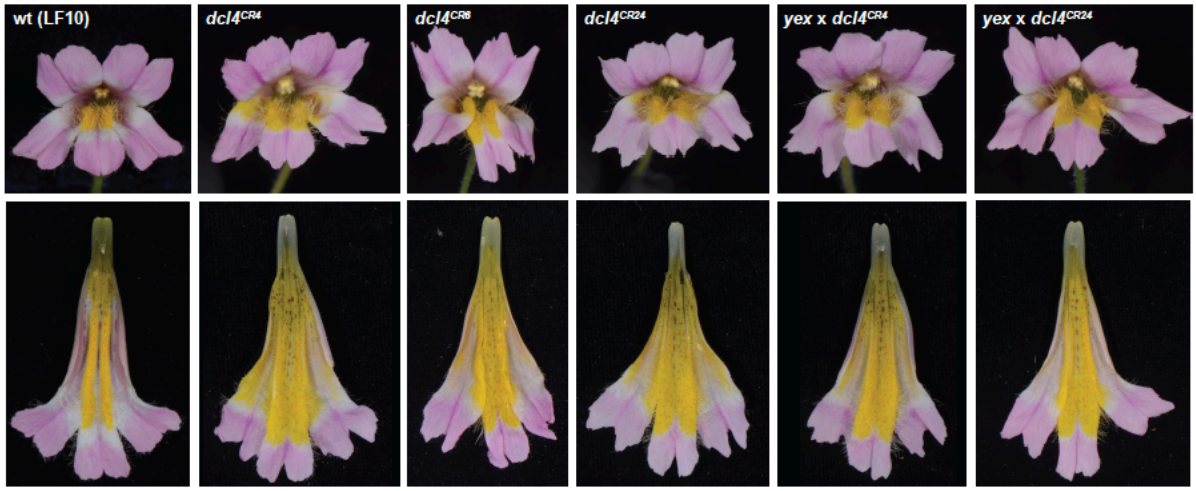

dcl4^{CR4}

AGGAGCAGTCACGAGCTGAACTATACGAGATGCTTGTTCCTGCTGCCCTTAGGAAAACATGGACAGAAGTGGAGCATTCCACTTCTTTTAGC

TCGTATTACATCAAAATTTGTCCAAATCCAGCGGATAGGATATACCAAAGATTTGGTCTTTTCGTGAAGGAGCCACTCTCGGAGGAGGCTGG

GAAAATGAAAGTTGATCTTTGTTTGGCCCGTGGTAGAATGGTGATGACAGAGATGATTCCATCTGGAGTTCTTAGAATGGATAAAAATGAGG

dcl4^{CR6}

AGGAGCAGTCACGAGCTGAACTATACGAGATGCTTGTTCCTGCTGC----

----TCGGAGGAGGCTGG

GAAAATGAAAGTTGATCTTTGTTTGGCCCGTGGTAGAATGGTGATGACAGAGATGATTCCATCTGGAGTTCTTAGAATGGATAAAAATGAGG

dcl4^{CR24}

AGGAGCAGTCACGAGCTGAACTATACGAGATGCTTGTTCCTGCTGCCCTTAGGAAAACATGGACAGAAGTGGAGCATTCCACTTCTTTTAGC

TCGTATTACATCAAAATTTGTCCAAATCCAGCGGATAGGATATACCAAAGATTTGGTCTTTTCGTGAAGGAGCCAC------

----CTGGAGTTCTTAGAATGGATAAAAATGAGG

Figure 3. Gene verification by CRISPR/Cas9 gene editing. Front view and nectar guide view of wild-type LF10 (left), *dcl4* CRISPR mutants, and complementation crosses (*yex* x *dcl4* CRISPR F1). The sequence for each mutant allele is provided below. Orange boxes indicate target sequences; the triangle indicates an insertion, and the dashes indicate deletions.

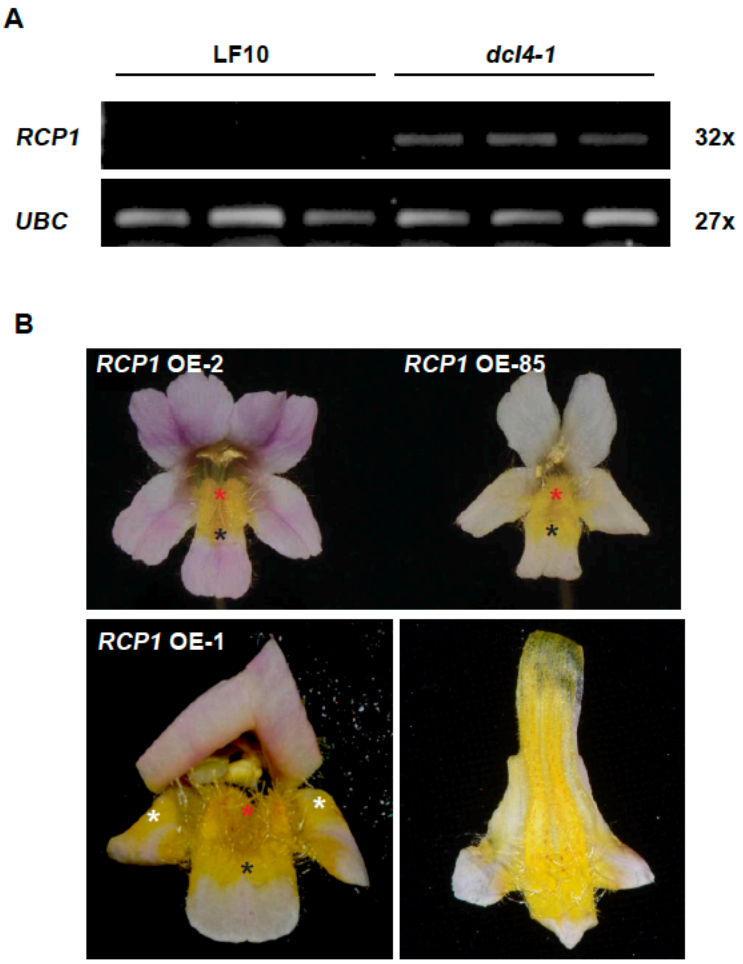

Figure 4. Ectopic RCP1 expression. (A) Qualitative RT-PCR of *RCP1* in LF10 and *dcl4-1* 12-mm corolla light areas. *MlUBC* was used as the reference gene. PCR cycle numbers are indicated at right. **(B)** Flower phenotypes of *RCP1* overexpression lines. Key areas are marked with asterisks (white = lateral/dorsal petal junction; red = region between nectar guide ridges; black = light area).

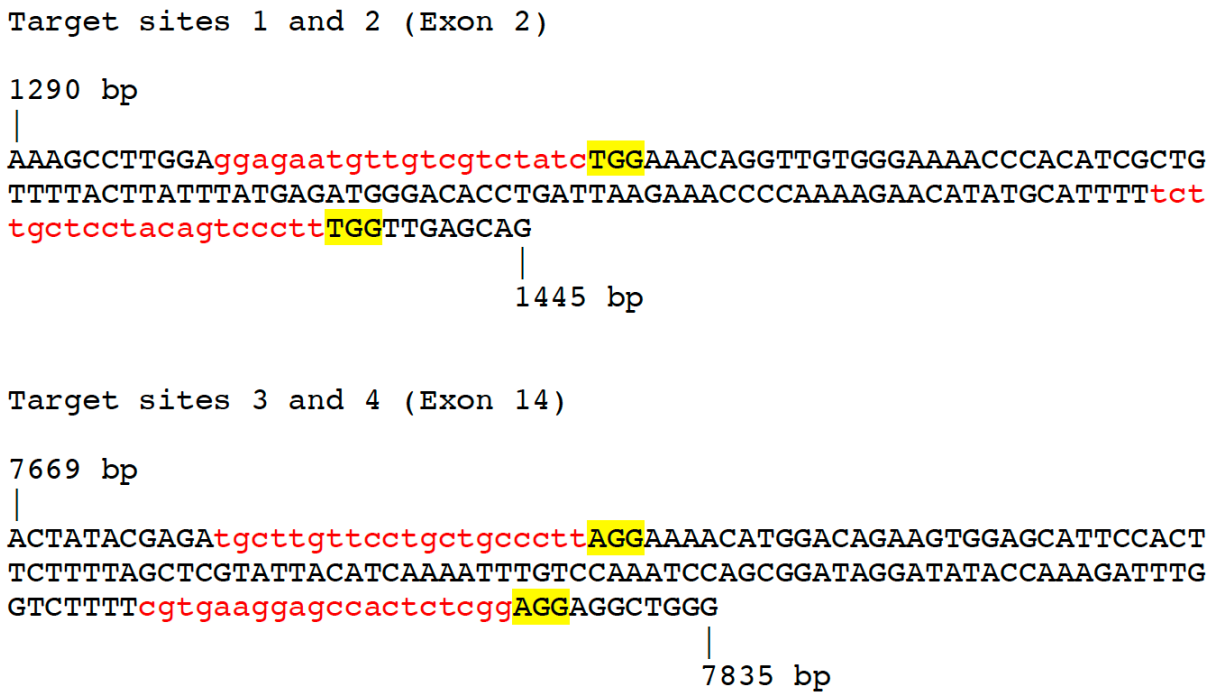

Supplementary Figure 1. sgRNA target sequences. The four target sites chosen for this study are shown: two in the second exon and two in the fourteenth exon (base pair positions are based on genomic DNA). Red, lower case letters indicate the target sites; yellow, highlighted text indicates the protospacer adjacent motifs (PAMs).

Supplementary Figure 2. DCL4 CRISPR-33. Front view (top) and nectar guide view (bottom) of LF10 and DCL4 CRISPR -33 T1 plants.

Supplementary Figure 3. *sgs3 dcl4* double mutant. Flower phenotypes of *sgs3-1* (left) and *sgs3-1 dcl4-1* double mutants. Key areas are marked with asterisks (red = region between nectar guide ridges; black = light area).

Supplementary Table 1. (q)RT-PCR primers.

Gene	Forward (5'-3')	Reverse (5'-3')
PSY1	GATGATGCAGAGAGCGGTGTCA	GGAGGAACAAGAGACTTTGCAA
Z-ISO	TTGCAGCGGTCGATAAGCCTAA	GCTGCTAATGTAACTGAGTTCC
BCH1	TAATGCTGTTCCCGCAATTGCC	TTTCCCTATCCAGCTCTTCCAA
NSY1	ATCATGGACTCCCGATACCATG	TTCTCTGGTTCTGCTTAGAGC
DCL4	CCTGAGGGAGCAGAAGTTACTG	CCACGGCATCGAGAGTGAATAC
RCP1	ATGGCGAGCAAAAATTGCAGT	CGCCTGCATATCACATTCTTGA
UBC	GGCTTGGACTCTGCAGTCTGT	TCTTCGGCATGGCAGCAAGTC

Supplementary Table 2. Primers for CRISPR/Cas9 construct building. Red text indicates nucleotides necessary for integration into pYLsgRNA vectors; black text indicates guide RNA sequence.

Primer	Sequence
DCL4_CRISPR_Ex2_F1	GTCAGGAGAATGTTGTCGTCTATC
DCL4_CRISPR_Ex2_R1	AAACGATAGACGACAACATTCTCC
DCL4_CRISPR_Ex2_F2	ATTGTCTTGCTCCTACAGTCCCTT
DCL4_CRISPR_Ex2_R2	AAACAAGGGACTGTAGGAGCAAGA
DCL4_CRISPR_Ex14_F1	GTCATGCTTGTTCCTGCTGCCCTT
DCL4_CRISPR_Ex14_R1	AAACAAGGGCAGCAGGAACAAGCA
DCL4_CRISPR_Ex14_F2	ATTGCGTGAAGGAGCCACTCTCGG
DCL4_CRISPR_Ex14_R2	AAACCCGAGAGTGGCTCCTTCACG